ADVERTIMENT. La consulta d'aquesta tesi queda condicionada a l'acceptació de les següents condicions d'ús: La difusió d'aquesta tesi per mitjà del servei TDX (www.tesisenxarxa.net) ha estat autoritzada pels titulars dels drets de propietat intel·lectual únicament per a usos privats emmarcats en activitats d'investigació i docència. No s'autoritza la seva reproducció amb finalitats de lucre ni la seva difusió i posada a disposició des d'un lloc aliè al servei TDX. No s'autoritza la presentació del seu contingut en una finestra o marc aliè a TDX (framing). Aquesta reserva de drets afecta tant al resum de presentació de la tesi com als seus continguts. En la utilització o cita de parts de la tesi és obligat indicar el nom de la persona autora.

ADVERTENCIA. La consulta de esta tesis queda condicionada a la aceptación de las siguientes condiciones de uso: La difusión de esta tesis por medio del servicio TDR (www.tesisenred.net) ha sido autorizada por los titulares de los derechos de propiedad intelectual únicamente para usos privados enmarcados en actividades de investigación y docencia. No se autoriza su reproducción con finalidades de lucro ni su difusión y puesta a disposición desde un sitio ajeno al servicio TDR. No se autoriza la presentación de su contenido en una ventana o marco ajeno a TDR (framing). Esta reserva de derechos afecta tanto al resumen de presentación de la tesis como a sus contenidos. En la utilización o cita de partes de la tesis es obligado indicar el nombre de la persona autora.

WARNING. On having consulted this thesis you're accepting the following use conditions: Spreading this thesis by the TDX (www.tesisenxarxa.net) service has been authorized by the titular of the intellectual property rights only for private uses placed in investigation and teaching activities. Reproduction with lucrative aims is not authorized neither its spreading and availability from a site foreign to the TDX service. Introducing its content in a window or frame foreign to the TDX service is not authorized (framing). This rights affect to the presentation summary of the thesis as well as to its contents. In the using or citation of parts of the thesis it's obliged to indicate the name of the author

UNIVERSITAT POLITÈCNICA DE CATALUNYA

Soft Error Mitigation Techniques For Future Chip Multiprocessors

by

Gaurang Upasani

A thesis submitted in partial fulfillment for the degree of Doctor of Philosophy

in the
Department of Computer Architecture

September 2015

Declaration of Authorship

I, Gaurang Upasani, declare that this thesis titled, 'Soft error mitigation techniques for future chip multiprocessors' and the work presented in it are my own. I confirm that:

- This work was done wholly or mainly while in candidature for a research degree at this University.
- Where any part of this thesis has previously been submitted for a degree or any other qualification at this University or any other institution, this has been clearly stated.
- Where I have consulted the published work of others, this is always clearly attributed.
- Where I have quoted from the work of others, the source is always given. With the exception of such quotations, this thesis is entirely my own work.
- I have acknowledged all main sources of help.
- Where the thesis is based on work done by myself jointly with others, I have made clear exactly what was done by others and what I have contributed myself.

Signed: ____________________________

Date: ____________________________

'Here's to the crazy ones. The misfits. The rebels. The troublemakers. The round pegs in the square holes.
The ones who see things differently. They're not fond of rules. And they have no respect for the status quo. You can quote them, disagree with them, glorify or vilify them.
But the only thing you can't do is ignore them. Because they change things. They invent. They imagine. They heal. They explore. They create. They inspire. They push the human race forward. Maybe they have to be crazy.
How else can you stare at an empty canvas and see a work of art? Or sit in silence and hear a song thats never been written? Or gaze at a red planet and see a laboratory on wheels?
We make tools for these kinds of people.
While some see them as the crazy ones, we see genius. Because the people who are crazy enough to think they can change the world, are the ones who do!'

Apple Computer, Inc. (Written by Rob Siltanen & Lee Clow)

Dedicated to my wife and family . . .

Abstract

The sustained drive to downsize the transistors has reached a point where device sensitivity against transient faults due to neutron and alpha particle strikes a.k.a *soft errors* has moved to the forefront of concerns for next-generation designs. Following Moore's law, the exponential growth in the number of transistors per chip has brought tremendous progress in the performance and functionality of processors. However, incorporating billions of transistors into a chip makes it more likely to encounter a soft *soft errors*. Moreover, aggressive voltage scaling and process variations make the processors even more vulnerable to *soft errors*.

Also, the number of cores on chip is growing exponentially fueling the multicore revolution. With increased core counts and larger memory arrays, the total failure-in-time (FIT) per chip (or package) increases. Our studies concluded that the shrinking technology required to match the power and performance demands for servers and future exa- and tera-scale systems impacts the FIT budget. New soft error mitigation techniques that allow meeting the failure rate target are important to keep harnessing the benefits of Moore's law.

Traditionally, reliability research has focused on providing circuit, microarchitecture and architectural solutions, which include device hardening, redundant execution, lock–step, error correcting codes, modular redundancy etc. In general, all these techniques are very effective in handling soft errors but expensive in terms of performance, power, and area overheads. Traditional solutions fail to scale in providing the required degree of reliability with increasing failure rates while maintaining low area, power and performance cost. Moreover, this family of solutions has hit the point of diminishing return, and simply achieving 2× improvement in the soft error rate may be impractical.

Instead of relying on some kind of redundancy, a new direction that is growing in interest by the research community is detecting the actual particle strike rather than its consequence. The proposed idea consists of deploying a set of detectors on silicon that would be in charge of perceiving the particle strikes that can potentially create a soft error. Upon detection, a hardware or software mechanism would trigger the appropriate recovery action.

This work proposes a lightweight and scalable soft error mitigation solution. As a part of our soft error mitigation technique, we show how to use acoustic wave

detectors for detecting and locating particle strikes. We use them to protect both the logic and the memory arrays, acting as *unified error detection* mechanism. We architect an error containment mechanism and a unique recovery mechanism based on checkpointing that works with acoustic wave detectors to effectively recover from soft errors.

Our results show that the proposed mechanism protects the whole processor (logic, flip-flop, latches and memory arrays) incurring minimum overheads.

Acknowledgements

My sincere thanks to:

Xavier Vera for his direct supervision and guidance throughout this work. Xavi is extremely approachable. Hes one of the smartest people I know. I hope that I could be as lively, enthusiastic, and energetic as him;

Antonio González for reviewing and providing his insights and experience in improvising my papers, tutoring this thesis work, providing the financial support during initial phase and for providing me with the required logistical support;

My parents for enrolling me into my first computer course at the age of 9 and buying the first computer (A BBC Micro with 32kB RAM by Acron Computers™) when I was a kid; and supporting me to take up the research in computer architecture. My wonderful sister for making me feel home even though I was away.

My beautiful and loving wife for her constant support and infinite patience...

My good friends, Rakesh Kumar, Amrit Kumar Panda and lab mates for numerous discussions on random topics of research in microarchitecture.

A special mention to Javier Carretero, Nicholas Axelos and Enric Herrero who generously gave of their time and assisted me with the part of research of this thesis and setting up the required infrastructure;

Lastly, thanks to everyone at ARCO, Intel Barcelona Research Center and DAC-UPC. Thanks to badminton group Manoj, Gaurav and Prashanth. Thanks to the Generalitat of Catalunya for awarding me the FI-AGAUR fellowship and funding my research and the DAC administration for arranging the numerous trips to the conferences and solving countless administrative problems.

Barcelona, April 2015

Contents

Declaration of Authorship ii

Abstract viii

Acknowledgements x

List of Figures xviii

List of Tables xxiii

Publications xxv

Glossary xxvi

Physical Constants xxx

1 Introduction **1**
- 1.1 Motivation . . . 2
  - 1.1.1 Soft Error Trends . . . 4
  - 1.1.2 Current Solutions and Challenges . . . 5
- 1.2 Problem Statement . . . 6
  - 1.2.1 Soft Error Rate Limits the Core Count . . . 7
  - 1.2.2 Soft Errors in the age of Dark Silicon . . . 8
  - 1.2.3 Soft Errors in Large Memories . . . 9
  - 1.2.4 Handling SDC & DUE . . . 10
  - 1.2.5 Protecting all Computing Segments . . . 11
- 1.3 Thesis Scope and Contributions . . . 12
- 1.4 Organization . . . 14

2 Soft Errors: Background and Overview **16**
- 2.1 Soft Error Terminologies . . . 16
  - 2.1.1 Faults, Errors and Failures . . . 17
  - 2.1.2 Metrics . . . 18

2.1.3 SDC and DUE . . . 19
2.2 Realizing Reliable Solution . . . 20
2.3 Soft Error Sources . . . 22
2.3.1 Alpha particles . . . 22
2.3.2 Neutron particles . . . 23
2.3.3 Neutron induced boron fission . . . 23
2.4 Interaction of Particles with Silicon . . . 24
2.4.1 Generation of Light, Sound and Heat! . . . 25
2.5 Computing Soft Error Rate . . . 26
2.6 Soft Error Manifestation in Electronics . . . 28
2.6.1 Soft Errors in SRAM . . . 28
2.6.2 Soft Errors in DRAM . . . 29
2.6.3 Soft Errors in Logic . . . 29
2.6.4 Evidence of Soft Errors . . . 31
2.7 Parameters Affecting Soft Error Rate . . . 32
2.8 Soft Errors and Future Processors . . . 35
2.8.1 Impact of Technology Scaling . . . 35
2.8.1.1 SRAM . . . 35
2.8.1.2 DRAM . . . 35
2.8.1.3 Logic Components . . . 36
2.8.2 Impact of New Technologies . . . 37
2.8.2.1 Silicon on Insulator (SOI) . . . 37
2.8.2.2 Multigate-FET Devices . . . 38
2.8.2.3 Non-Volatile Memories . . . 38
2.9 Calculating SER to Make Architectural Decisions . . . 39
2.9.1 Fault Injection: . . . 40
2.9.2 Architecture Vulnerability Factor (AVF) Analysis: . . . 40

3 Error Detection using Acoustic Wave Detectors 42
3.1 Particle Strike Detectors . . . 42
3.2 The Microelectromechanical Ears: Acoustic Wave Detectors . . . 46
3.2.1 Structure and Properties of Device . . . 47
3.2.2 Calibrating the Detector . . . 48
3.2.2.1 False Positives . . . 48
3.3 Soft Error Detection via Detecting Particle Strikes . . . 49
3.4 Location Estimation of a Particle Strike . . . 51
3.4.1 Example . . . 53
3.4.2 Obtaining TDOA . . . 54
3.4.3 Generating TDOA Equations . . . 55
3.4.4 Solving TDOA Equations . . . 56
3.5 Algorithms for TDOA Equations . . . 57
3.5.1 Deterministic Method . . . 57
3.5.2 Non-deterministic Method . . . 58
3.5.2.1 Non-iterative Algorithms . . . 58

3.5.2.2 Iterative Algorithm 60
3.5.3 Metrics for Evaluating Algorithms 61
3.5.3.1 Runtime 61
3.5.3.2 Complexity 61
3.5.3.3 Location Estimation Coverage 62
3.5.3.4 Accuracy 62
3.6 Assessing the Algorithms 63
3.6.1 Placement of Detectors 63
3.6.1.1 Accuracy 64
3.6.1.2 Location Estimation Coverage 65
3.6.2 Choosing Detectors for TDOA Equations 69
3.6.2.1 Accuracy 69
3.6.2.2 Location Estimation Coverage 69
3.6.3 Effect of Solving More TDOA Equations 69
3.6.3.1 Accuracy 70
3.6.3.2 Runtime 72
3.6.3.3 Complexity 74
3.6.4 Effect of Sampling Frequency on Accuracy 74
3.6.5 Detection Latency 77
3.6.6 Summary of Chosen Configuration 77
3.6.7 Summary of Results 79
3.7 Related Work 79
3.7.1 Current Glitch Detectors 80
3.7.1.1 Built-In Current Sensors (BICS) 80
3.7.1.2 Switching Current Detector 81
3.7.2 Voltage Glitch Detectors 81
3.7.3 Metastability Detectors 82
3.7.4 Deposited Charge Detectors 83
3.7.4.1 Thin film silicon detectors 83
3.7.4.2 Heavy-ion Sensing 83
3.7.5 Comparison of Detectors 83
3.7.5.1 Hardware cost/Area overhead 84
3.7.5.2 Power overhead and detection latency 85
3.7.5.3 False alarms 86
3.7.5.4 Detected particles/Fault types 87
3.7.5.5 Intrusiveness of the design 87
3.7.5.6 Fault coverage vs. Cost 88
3.8 Chapter Summary 89

4 Protecting Caches with Acoustic Wave Detectors 91
4.1 Error Detection and Localization in Cache 91
4.2 Providing Error Correction in Caches 93
4.2.1 Reaction upon a Particle Strike 94
4.2.2 Standalone Acoustic Wave Detectors 94

4.2.2.1 Error Area Granularity: Cache Lines 95
4.2.2.2 Error Area Granularity: Exact bit 95
4.3 Acoustic Wave Detectors with Error Codes 97
4.3.1 Error Area Granularity: Cache Lines 97
4.3.2 Error Area Granularity: Exact bit 100
4.3.2.1 Acoustic Wave Detectors + Parity per Block 102
4.3.2.2 Acoustic Wave Detectors + Parity per Byte 105
4.3.2.3 Acoustic Wave Detectors with Physical Interleaving 107
4.4 Handling Multi-bit Upsets in Caches 109
4.5 Cost of Protection 112
4.6 Related Work 112
4.6.1 Particle Strike Detection for Soft Errors 113
4.6.2 Soft Error Detection 113
4.6.2.1 Error Codes 113
4.6.3 Soft Error Mitigation 115
4.6.3.1 Physical Interleaving 116
4.6.3.2 Cache Scrubbing 116
4.6.3.3 Cache Flush 117
4.6.3.4 Early Writeback 117
4.6.4 Comparison of Techniques 117
4.7 Chapter Summary 122

5 Protecting Entire Core with Acoustic Wave Detectors 124
5.1 "SDC & DUE 0" Architecture 124
5.1.1 Effect of Detection Latency on SDC & DUE 125
5.1.2 Achieving SDC-& DUE 0 per Core 127
5.1.3 Divide and Conquer for SDC and DUE 0 129
5.1.4 Containment in Core: Recap 131
5.1.5 Proposed Architecture 131
5.2 Implementation of Proposed Architecture: Unicore Processor 133
5.2.1 Error Containment Mechanism 133
5.2.1.1 Dealing with Verified Cache. 134
5.2.1.2 Dealing with Not-Verified Cache. 134
5.2.2 Creating Checkpoints 136
5.2.2.1 Validating the Checkpoint. 138
5.2.3 Recovering from Error 139
5.2.4 Intrusiveness of Design 139
5.3 Implementation of Proposed Architecture: Multicore Processor . . . 140
5.3.1 Shared Memory Architecture 140
5.3.1.1 MOESI Protocol for Error Containment. 140
5.3.1.2 MOESI Protocol for Checkpointing. 142
5.3.1.3 Recovering from Error. 142
5.4 Managing System Calls, Interrupts and Exceptions 142
5.4.1 Handling Interrupts. 142

5.4.2 Dealing with Exceptions. 143
5.4.3 Context switching and Multi-programming. 144
5.5 Performance Evaluation of "SDC- & DUE 0" Architecture 144
5.5.1 Experimental Setup 144
5.5.1.1 Single core system. 144
5.5.1.2 Multicore system. 146
5.5.2 Error Detection Latency vs Containment Area 146
5.5.3 Checkpoint Length vs Checkpoint Area 147
5.5.4 Uniprocessor Performance 150
5.5.5 Performance of Multicore for Data Non-Sharing Applications 150
5.5.6 Multicore Shared Memory Performance 152
5.6 Related Work 152
5.6.1 Error Detection and Recovery in Core 152
5.6.1.1 Dual Modular Redundancy with Recovery 152
5.6.1.2 Lockstepping with Recovery 154
5.6.1.3 Redundant Multithreading (RMT) with Recovery . 156
5.6.1.4 Error Detection and Recovery using Checker Core . 158
5.7 Chapter Summary 159

6 Protecting Embedded Core with Acoustic Wave Detectors 161
6.1 Experimental Setup 161
6.2 Handling SDC & DUE in Embedded Core 163
6.2.1 Acoustic Wave Detectors and Error Detection Latency . . . 163
6.2.2 Error Containment Granularity 164
6.2.2.1 Error Containment Granularity: Core 165
6.2.2.2 Error Containment Granularity: Cache 166
6.2.3 Putting everything together 168
6.3 Selective Error Containment 168
6.3.1 Protecting Individual Data Paths & Latency Guard Bands . 168
6.3.1.1 Traversal of Instructions in Pipeline 169
6.3.1.2 Cost of Error Containment 170
6.4 Error Containment Coverage vs. Vulnerability 172
6.4.1 ACE Analysis 173
6.4.2 Reducing AVF using Acoustic Wave Detectors 175
6.5 Related Work 176
6.5.1 Soft Error Sensitivity Analysis 177
6.5.2 Soft Error Protection 178
6.5.2.1 Hardware Only Approach 178
6.5.2.2 Software Only Approach 179
6.5.2.3 Hybrid Approach 180
6.6 Chapter Summary 180

7 Related Work 182
7.1 Soft Error Protection Schemes 182

7.1.1 Device Enhancements 182
7.1.1.1 Triple-well technology 183
7.1.1.2 Silicon-on-insulator 183
7.1.1.3 Process techniques 184
7.1.2 Circuit Enhancements 184
7.1.2.1 Increasing nodal capacitance in the circuit 185
7.1.2.2 Radiation hardened cells 186
7.2 Soft Error Detection Schemes 186
7.2.1 Spatial Redundancy 187
7.2.1.1 Detectors for Error Detection 187
7.2.1.2 Error Detection via Monitoring Invariants 188
7.2.1.3 Error Detection via Dynamic Control/Data Flow Checks 190
7.2.1.4 Error Detection via Hardware Assertion 191
7.2.1.5 Error Detection via Symptom Checks 192
7.2.1.6 Error Detection via Selective Protection 193
7.2.2 Information Redundancy 194
7.2.2.1 Error Codes for Combinational Logic 194
7.2.2.2 Signature Based Approach 199
7.2.3 Temporal Redundancy 199
7.2.3.1 Various Flavors of RMT 200
7.2.3.2 Error Detection via Detecting Anomalies 206
7.2.3.3 Using shifting operations 207
7.3 Error Recovery 208
7.3.1 Forward Error Recovery 209
7.3.1.1 Triple Modular Redundancy (TMR) 209
7.3.2 Backward Error Recovery 210
7.3.2.1 Checkpointing Techniques for Recovery 211
7.3.3 Other Recovery Schemes 215
7.4 Error Detection and Recovery using Software 216

8 Conclusions 220
8.1 Summary of Research 220
8.1.1 Detecting Particle Strikes for Soft Error Detection 221
8.1.2 Unified Error Detection for Logic & Memory 221
8.1.3 Precisely Locating the Errors 221
8.1.4 Reducing Reliability Cost for Caches and Memory 222
8.1.5 Protecting Entire Processor 223
8.1.6 One Solution for All Computing Segments 223
8.2 Discussions 224
8.2.1 Future Work 224

Bibliography 226

List of Figures

1.1 SRAM bit and SRAM system (e.g., cache) soft error rate for different technology nodes [17]. The soft error rate of a bit is predicted to remain roughly constant. However, the soft error rate of a cache is predicted to increase. 3
1.2 System soft error rate trend for different technologies [29, 33, 34]. The soft error trend has been scaled from the numbers presented for single core in the works of [35] assuming same system wide masking rate as [36]. It also shows the soft error rate trends in dotted lines for three levels of aggressive voltage scaling (V1>V2>V3) for future sub-32nm technologies. 4
1.3 Soft error rate contribution of different components in a processor core [56]. Core frontend includes ITLB, decode queue, RAT, IL1, pre-scheduler, allocate latches etc. Core backend includes DTLB, MOB, DL1, ROB, ALUs, register file, issue queue, AGU etc. Case (a) FIT distribution of a processor assuming caches and TLBs are protected via ECC and therefore, do not contribute to the total FIT rate. Case (b) FIT distribution of a processor with a protection mechanism similar to the redundant multithreading (RMT) [57] and caches, register file, MOB, and queues with data coming from a protected structured are protected. 6
1.4 Scaling of FIT/Core to accommodate more cores per chip while maintaining the FIT/Chip constant 7
1.5 TDP modes in modern multicore processor. TDP1 operates at 0.7 VDD and hence there are 4 active cores. In TDP2 the supply voltage is scaled down to 0.45 VDD to activate 64 cores. The relative FIT in TDP2 is increased by 16× compared to TDP1 due to increased active silicon area. However, due to effects of the supply voltage scaling the relative impact on soft error rate is as high as 30× [77] 8

2.1 Reliability metrics: Mean time to repair (MTTR), Mean time to failure (MTTF) and Mean time between failures (MTBF) 18
2.2 Classification of soft errors: *silent data corruption* (SDC) and *detected unrecoverable error* (DUE) 20
2.3 Realizing reliability pipeline for soft errors: error detection, error containment and error recovery 21

2.4 Alpha particles generate *electron-hole* pairs in silicon by direct ionization. Inelastic collision of neutrons with a silicon atom generate *electron-hole* pairs via indirect ionization by creating a silicon recoil. Elastic collisions of neutron particles are harmless. 24
2.5 Particle strike on a critical node Q on a 6T-SRAM cell 28
2.6 Structure of a DRAM memory cell 29
2.7 Masking effect in combinational logic circuits. 30
2.8 Impact of frequency on soft error rate 34
2.9 DRAM bit soft error rate for different technology nodes [180]. The soft error rate of a DRAM bit is predicted to decrease. The soft error rate of a DRAM memory system has traditionally remained constant over technology generations moreover, it is predicted to be dominated by the soft errors in the DRAM peripheral logic. 36

3.1 Transformation of the energy of particle strike upon its impact on silicon surface into acoustic shock wave 46
3.2 Cantilever beam like structure of acoustic wave detectors [214]. A particle strike is detected by sensing the deflection of cantilever beam. 47
3.3 A comparison of relative slowdown due to false positive recovery for different recovery techniques: Seqoia [226], Swich [227], Carer [228], SPARC64 [229], IBM Z series [59], IBM G5 [58], Encore [230], ReStore [231], ReVive [102], SafetyNet [107], IBM Blue Gene [232], BLCR [233] 49
3.4 TDOA hyperbolas in a system and location of source. Dashed hyperbola is formed using only two detectors S_1 and S_2. Including a third detector S_3 can successfully locate the source via intersecting hyperbolas. 52
3.5 Strike detection and localization via triangulation using TDOA measurements of acoustic wave detectors 53
3.6 Timeline of the events following the particle strike 53
3.7 Strike detection algorithm (firmware) and a hardware control mechanism 54
3.8 Sampling errors in the measurements of the time difference of the arrival at the acoustic wave detectors 55
3.9 Placement of detectors in a mesh formation 64
3.10 Impact of placement of detectors (while solving 4 TDOA equations) on accuracy (area unit is the area of 1 bit SRAM cell) 65
3.11 Impact of placement of detectors (while solving 4 TDOA equations) on location estimation coverage 65
3.12 Impact of *initial guess* on coverage (while solving 4 TDOA equations) on location estimation coverage 66
3.13 Worst-case error area with the selection of different set of detectors (4 to 10) from a given [4×5] mesh 68
3.14 Error area with closest detectors for [4×5] mesh 70
3.15 Comparing accuracy of all algorithms and for the mesh configurations discussed in Table 3.2 72

3.16 Comparing runtime and complexity of all algorithms and for the mesh configurations discussed in Table 3.2 73
3.17 Impact of sampling frequency on error area for configurations of Table 3.2 Iterative Algorithm 4 74
3.18 Impact of sampling frequency on error area for configurations of Table 3.2 for all algorithms 75
3.19 Worst-case detection latency for mesh configurations of Table 3.2 in a processor running at 2 GHz 76
3.20 Adding more detectors to reduce worst-case detection latency in a processor running at 2 GHz 76
3.21 Built-in current sensor (BICS) 80
3.22 Switching current detector 81
3.23 Voltage glitch detector 82
3.24 Metastability detector (BISS) 82

4.1 Mapping of the estimated worst-case error area at the granularity of affected (a) bits (b) bytes and (c) lines. These affected bits, bytes or cache lines contain the actual erroneous bit, byte or cache line. . 92
4.2 Breakdown of the obtained worst-case error area granularity for 1048 particle strikes at random location and instance for different mesh configurations in L1 data cache at the sampling frequency of 4 GHz 96
4.3 Quantification of error area granularity for 5 × 5 mesh for L1 data cache 101
4.4 3*CEP error area mapping to bits to bits of the L1 cache: (a) 1-bit, (b) 2-bits, (c) 3-bits (d) 4-bits and (e) 5-bits 102
4.5 Possibilities of 3*CEP error area granularity patterns : (a) 2-bits, (b) 3-bits, (c) 4-bits and (d) 5-bits 102
4.6 Probability of pin-pointing the erroneous bit using acoustic wave detectors + parity per block for 3*CEP error area granularity patterns of (a) 2-bit, (b) 3-bit, (c) 4-bit and (d,e) 5-bit 103
4.7 Probability of pin-pointing the erroneous bit using acoustic wave detectors + parity per byte for 3*CEP error area granularity patterns of (a,b) 2-bit, (c-f) 3-bit, (g) 4-bit and (h-m) 5-bit 105
4.8 Probability of pin-pointing the erroneous bit using acoustic wave detectors + parity per byte and assuming the bits are physically interleaved with degree of interleaving: 4 107
4.9 Probability of pin-pointing the erroneous bit and correcting it (i.e., DUE improvement) using acoustic wave detectors and combining acoustic wave detectors with parity at byte and block level and assuming physically interleaved parity protected bits in L1 data cache108
4.10 Extending the 3*CEP error area granularity of 1-bit and 5-bits for handling spatial multi-bit upsets using acoustic wave detectors to locate (a) 2 bit MBU and (b) 3 bit MBU 110

4.11 Probability of locating the 2 bit MBU using acoustic wave detectors configuration providing 3*CEP error area granularity of 1 bit and parity per byte . . . 111
4.12 Basic functionality of encoding and decoding of data bits in error codes . . . 114

5.1 Number of detectors vs. detection latency at 2 GHz . . . 128
5.2 Pipeline of a state of the art processor and the latency of stages . . . 129
5.3 Error Containment Architecture . . . 132
5.4 Time-line of the events in cache. *D* indicates the dirty bit and *EDL* stands for error detection latency. Once the cache line has been written the cache line enters in quarantine state. After *ErrorDetectionLatency* cycles the cache line is now in verified state and also error free. . . . 134
5.5 Error containment in cache for evictions caused by read and write operations. *D* indicates the dirty bit. . . . 135
5.6 Checkpointing in the caches due to the evictions caused by read and write operations. *D* indicates the dirty bit and *CH* stands for the checkpoint bit. . . . 137
5.7 A scenario indicating the importance of validating the checkpoint. *CH* indicates the checkpoint bit and *EDL* stands for error detection latency. Notice the *CheckpointValid* counter that indicates the validity of the checkpoint. . . . 138
5.8 Handling error containment in a shared memory accesses for multicore architecture. *EDL* stands for error detection latency. . . . 141
5.9 MOESI protocol: Transitions are shown in the *trigger*↦*action* format. Underlined transition triggers and actions are the same as uniprocessor architecture. The transition triggers in gray boxes are extensions for multicore shared memory architecture. "Wr" stands for write and "Rd" stands for read operation. "Stall"↦*ErrorDetectionLatency* cycles. . . . 141
5.10 Extending the architecture to handle interrupts and I/O traffic. . . . 143
5.11 Checkpoint events in LLC checkpoint boundary . . . 145
5.12 Average dirty lines to be written back from L1 to LLC . . . 149
5.13 Average wait-cycles until LLC is verified . . . 149
5.14 Performance impact of containment and checkpointing LLC cache in single core architecture . . . 150
5.15 Slowdown due to containment and checkpointing LLC cache in the 16-core system for private memory applications . . . 151
5.16 Slowdown due to containment and checkpointing LLC cache in the 16-core system for shared memory applications . . . 151
5.17 Implementation of dual modular redundancy scheme for error detection and recovery. . . . 153
5.18 Lockstep error detection and recovery via retry . . . 155
5.19 Implementation of dynamic implementation verification architecture (DIVA) and the functioning of the checker core . . . 158

6.1 Error detection latency for acoustic wave detectors on embedded core for different mesh configurations 164
6.2 Error containment granularities in embedded processor 165
6.3 Performance overhead of error containment in cache for a checkpoint period of 1 million cycles 167
6.4 Distribution of residency cycles in a state of the art embedded core pipeline 169
6.5 Arrangement of FUBs and placement of acoustic wave detectors on embedded core [313] 172
6.6 Error containment granularities in embedded processor 173
6.7 Reducing AVF by adapting acoustic wave detectors 175
6.8 AVF of issue queue by protecting them with acoustic wave detectors for different detection latency 176

7.1 Triple well technology and the creation of deep n-well which traps the charge generated upon a particle strike. 183
7.2 The suspended body in partially depleted SOI transistor 184
7.3 Reduction of soft errors by introducing capacitance on the critical nodes in an SRAM cell 185
7.4 The C-Element circuit forming the core logic of BISER detection scheme [322] 188
7.5 The control flow checker: A high level program, compiler generated instructions and the corresponding CFG 191
7.6 The hardware assertion and the timestamps 192
7.7 Residue code generation logic for an adder 197
7.8 Functional block diagram of parity prediction circuit in an adder . . 198
7.9 Sphere of replication is shown in shaded part. Both the processor cores are part of the sphere of replication 202
7.10 Functional implementation of RMT scheme on a processor with two cores (P0 and P1). The cross coupled cores with a few dedicated hardware queues can work in unison for error detection. 205
7.11 Using temporal redundancy for error detection via re-execution with shifted operands 207
7.12 Classification of error recovery schemes 208
7.13 Triple modular redundancy 210

List of Tables

2.1 Summary of the sources of soft errors. † indicates the flux at sea level and ⋆ is the flux at 32,000 feet above sea-level. 25
2.2 Parameters that affect the soft errors and impact the overall soft error rate 33
2.3 Impact of important parameters and corresponding impact on soft error rate 33

3.1 Comparing different particle strike detectors. † while protecting memory, ⋆ while protecting combinational logic, ∓ the detection latency is bounded and configurable. 44
3.2 Worst case error area for best configuration of a given mesh for each algorithm. † solves only 2 equations 71
3.3 Comparison of algorithms: Algorithm 1 is deterministic and Algorithms 2, 3 and 4 are non-deterministic; ∓ with careful mesh selections 78

4.1 Summary of the best mesh configurations and the error area granularities for the caches 92
4.2 Summary of the mesh configurations for the caches and corresponding worst case detection latency cycles for a sampling frequency of 2 GHz. Marked configurations are used only for locating errors and extra detectors are added to reduce the detection latencies. 93
4.3 Comparison of protection capabilities of having only error codes versus error codes with acoustic wave detectors. HFaults stands for number of hard faults, SER number of soft errors, D for detection, C for correction, CT for containment 99
4.4 Minimum required degree of physical bit interleaving (DOI) in a cache with bit interleaved parity and acoustic wave detectors 111
4.5 Comparing different mechanisms for protecting caches against soft errors. nD indicates n bits error detection capability, mD–nC indicates m bits error detection and n bits correction capability. † overheads per SRAM cell, †† overhead per chip, ⋆ overhead per 64 bits, ⋆⋆ doesnt include overhead from the interleaving circuit. 119

5.1 Comparison of different error detection schemes († vulnerability holes in LSQ logic (i.e., MOB logic), * cannot detect errors in stores, †† does not detect but prevents error, * only for simple in-order cores, ** cannot detect if fault does not manifest a symptom, $^{\mp}$ latency from actual strike instance) 126
5.2 Required number of detectors for containment in core 130
5.3 Configuration Parameters 146
5.4 Containment cost (i.e., #Stalls and wait cycles for each stall) for containment boundary limited to L1 147

6.1 Configuration Parameters 162
6.2 Required acoustic wave detectors for full error containment coverage. L1 cache is protected separately using an architecture as presented in Chapter 4. 171

7.1 AN codes and the functions for which they are invariant 195
7.2 Residue codes and the functions for which they are invariant. Division is not directly encodable however division holds D - R = Q $\times$ I relation where D is dividend, R is remainder, Q is quotient and I is divisor 196

Publications

The following is a list of all publications subject to peer review that are part of this thesis.

Published papers:

Conferences

- "*Framework for Economical Error Recovery in Embedded Cores*", Gaurang Upasani, Xavier Vera and Antonio González. In the proceedings of 20th International On-Line Testing Symposium (IOLTS) 2014.
- "*Avoiding Core's DUE & SDC via Acoustic Wave Detectors and Tailored Error Containment and Recovery*", Gaurang Upasani, Xavier Vera and Antonio González. In the proceedings of 41st International Symposium on Computer Architectures (ISCA) 2014.
- "*Reducing DUE-FIT of Caches by Exploiting Acoustic Wave Detectors for Error Recovery*", Gaurang Upasani, Xavier Vera and Antonio González. In the proceedings of 19th International On-Line Testing Symposium (IOLTS) 2013.
- "*Setting an Error Detection Infrastructure with Low Cost Acoustic Wave Detectors*", Gaurang Upasani, Xavier Vera and Antonio González. In the proceedings of 39th International Symposium on Computer Architectures (ISCA) 2012.

Journals

- " *A Case for Acoustic Wave Detectors for Soft-Errors*", Gaurang Upasani, Xavier Vera and Antonio González. IEEE Transactions on Computers (ToC). (preprint available)
- "*Particle Strike Detectors for Soft Errors*", Gaurang Upasani, Xavier Vera and Antonio González. IEEE Computer. (under review)

Glossary

ACE Architecturally Correct Execution.

ALU Arithmetic and Logic Unit.

APS Active Pixel Sensor.

AR-SMT Active and Redundant Simultaneous Multi Threading.

AVF Architecture Vulnerability Factor.

BER Backward Error Recovery.

BICS Built- In Current Sensor.

BISS Built- In Single-event upset Sensor.

BIST Built- In Self Test.

CEP Circular Error Probable.

CFG Control Flow Graph.

CMOS Complementary Metal- Oxide Semiconductor.

CMP Chip- Multi-processor.

CRC Cyclic Redundancy Code.

DEC-TED Double Error Correction Triple Error Detection.

DFG Data Flow Graph.

DICE Dual Interlocked CElls.

DIVA Dynamic Implementation Verification Architecture.

DMR Dual Modular Redundacy.

DOI Degree Of Interleaving.

DRAM Dynamic Random-access Memory.

DUE Detected Unrecoverable Error.

DVFS Dynamic Voltage and Frequency Scaling.

ECC Error Correcting Code.

EDL Error Detection Latency.

FER Forward Error Recovery.

FIFO First In First Out.

FIT Failure In Time.

FRAM Ferroelectric Random-access Memory.

GPS Global Positioning System.

HCI Hot Carrier Injection.

IC Integrated Circuit.

IQ Issue Queue.

ISA Instruction Set Architecture.

LET Linear Energy Transfer.

LLC Last Level Cache.

LRU Least Recently Used.

LSQR Least Square Roots.

MBU Multiple Bit Upset.

MCA Machine Check Architecture.

MOB Memory Order Buffer.

MRAM Magnetoresistive Random-access Memory.

MTBF Mean Time Between Failures.

MTTF Mean Time To Failure.

MTTR Mean Time To Repair.

MUX Multiplexer.

NBTI Negative Bias Temperature Instability.

NMOS N-type Metal Oxide Semiconductor.

NOP Null Operation instruction.

NTC Near Threshold Computing.

PBTI Positive Bias Temperature Instability.

PC Program Counter.

PCM Phase Change Memory.

RAT Register Alias Table.

RF Register File.

RMT Redundant Multi Threading.

RNA Register Name Authentication.

ROB Re- Order Buffer.

RTL Register- Transfer Level.

RUU Register Update Unit.

SBU Single Bit Upset.

SDC Silent Data Corruption.

SEC-DED Single Error Correction Double Error Detection.

SER Soft Error Rate.

SES Soft Error Sensitivity.

SET Single Event Transient.

SEU Single Event Upset.

SMT Simultaneous Multi Threading.

SOI Silicon On Insulator.

SRAM Static Random-access Memory.

SRT Simultaneous and Redundant Threading.

SRTR Simultaneously and Redundantly Threaded with Recovery.

SSD Silicon Strip Detector.

STT-RAM Spin-Transfer Torque Random-access Memory.

TAC Timestamp-based assertion checking.

TDDB Time Dependent Dielectric Breakdown.

TDOA Time Difference Of Arrival.

TDP Thermal Design Power.

TLB Translation Lookaside Buffer.

TMR Triple Modular Redundancy.

TTF Time To Failure.

TVF Time Vulnerability Factor.

Physical Constants

Electron Volt	eV	=	$1.60217657 \times 10^{-19}$ joules
Speed of Light	c	=	2.99792458×10^{8} $\mathrm{ms}^{-\mathrm{S}}$
Speed of Sound in Silicon	C_p	=	$10\mathrm{kms}^{-1}$

Chapter 1

Introduction

For several decades, the semiconductor devices have seen tremendous progress in performance and functionality due to the exponential growth in the number of transistors per chip. In 1971, the Intel 4004® processor held 2,300 transistors. In early 2014 Intel released Xeon Ivy Bridge-Ex® with than 4.3 billion transistors [1]. This exponential growth in number of transistors is popularly known as Moore's law [2].

Each succeeding technology generation has introduced new obstacles in fulfilling the on chip transistor count. First, the rate of improvement in microprocessor speed exceeds the rate of improvement in off chip memory (DRAM) speed [3]. This resulted into the *memory wall* problem that drives the innovation in having low latency caches and other higher-level techniques such as prefetching [4, 5] and multithreading [6] that either reduce the memory latency, or keep the processor occupied for the longer latency memory operations.

Later, the power dissipation of the microprocessors started reaching sky high and semiconductor industry hit the *power wall*, where the performance improvements of microprocessor were limited by power constraints [7]. It motivated the research in low power computing techniques such as *dynamic voltage and frequency scaling* (DVFS), *near threshold computing* (NTC) and subthreshold operations. According to Dennard scaling [8], as transistors get smaller their power density stays constant, so that the power used stays in proportion with area (i.e., both voltage and current scale down with length). The breakdown of Dennard scaling and the failure of Moore's law to yield dividends in improved performance [9, 10] prompted a switch among some chip manufacturers to a greater focus on multicore processors [11].

Since the number of cores on chip is growing exponentially fueling the multicore revolution, operating all cores simultaneously requires exponentially more energy per chip. However, whereas the energy requirements grow, chip power delivery and cooling limitations remain largely unchanged across technologies imposing the *power wall* [12]. As a result we will soon be incapable of operating all transistors simultaneously, pushing multicore scaling to an end [13, 14]. This trend is leading us into an era of *dark silicon* where we will be able to build denser devices but we will not be able to power them up.

In this series of challenges, the reliability issues are next in line. Shrinking transistor dimensions and aggressive voltage scaling increase the sensitivity against intrinsic and extrinsic noise sources and a corresponding increase in static and dynamic variations. They lead to higher probability of parametric and wear-out failures, manufacturing defects and particle strike induced soft errors. This has elevated reliability into a prime design constraint for current and future processor design [15, 16]. Among all the failure mechanisms, transient faults from alpha and neutron particle strikes can induce a higher failure rate than the failure rate of all other failure mechanisms combined [17]. As the benefits of fault tolerance solutions come at the cost of area, energy and performance overheads, it may prevent achieving scalable performance leading us to the *soft error wall*.

1.1 Motivation

Charged particles coming from the atmosphere generate electron-hole pairs as they pass through a transistor. Transistor nodes can collect these charges. A particle strike can deposit enough charge to corrupt a data bit stored in the memory (i.e., SRAM), or it can create a glitch in any gate in combinational logic. Such faults in the circuit's operation may cause a failure by corrupting the data leading to a system crash. Since these transient errors occur due to an incorrect charge or discharge of an intermediate capacitive node, they do not cause permanent failure in the hardware and hence are termed *soft errors* in the literature.

The *soft error rate* (SER) is the rate at which a device or system encounters or is predicted to encounter soft errors per unit of time, and is typically expressed as *Failures-In-Time* (FIT). Chip designers have specific FIT targets for different computing segments similar to power or performance budget [18].

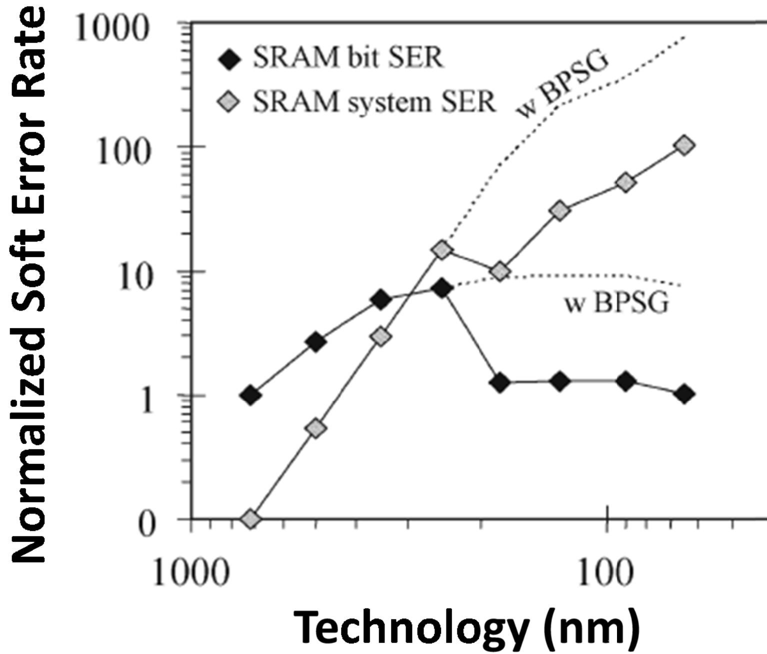

FIGURE 1.1: SRAM bit and SRAM system (e.g., cache) soft error rate for different technology nodes [17]. The soft error rate of a bit is predicted to remain roughly constant. However, the soft error rate of a cache is predicted to increase.

Although soft errors do not permanently damage the device, they are the primary limit on digital circuit reliability [19]. According to the current trends, soft errors are more important than all other causes of computing reliability put together [20]. Typically, the soft error rate can be 250-1000× higher than the hard failure rates [17].

The existence of this problem in space applications was reported in the early 1950s. Later, researchers found three potential radiation mechanisms that can also cause soft errors at ground level. In late 70's alpha particles emitting from the radioactive impurities in the packaging materials were the dominating source of soft errors. High energy neutrons (more than 1 MeV) were the dominating cause of errors in 90's. Currently, low energy neutrons are also responsible for causing soft errors in sub-65nm technology nodes [19, 21, 22]. From then on, soft errors have been consistently reported to be primary cause of failures in many commercial and academic studies [23–28].

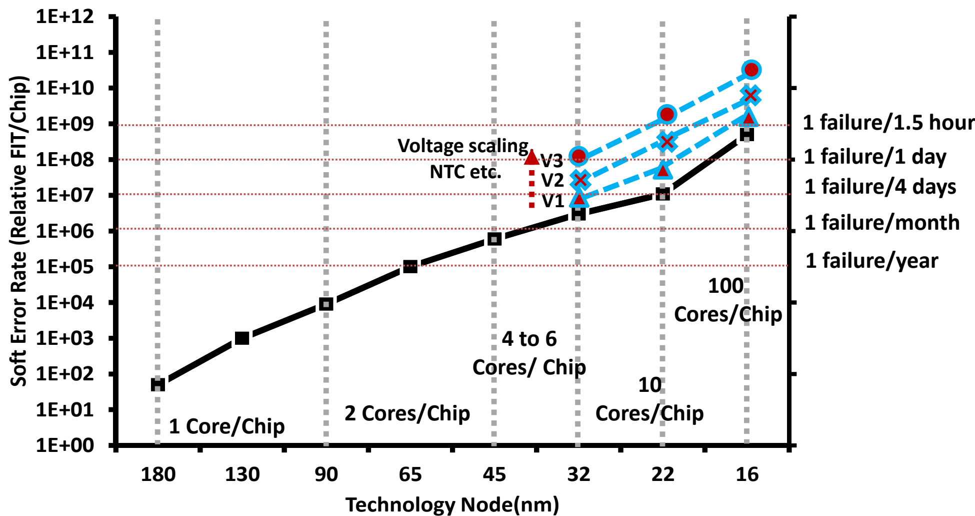

FIGURE 1.2: System soft error rate trend for different technologies [29, 33, 34]. The soft error trend has been scaled from the numbers presented for single core in the works of [35] assuming same system wide masking rate as [36]. It also shows the soft error rate trends in dotted lines for three levels of aggressive voltage scaling (V1>V2>V3) for future sub-32nm technologies.

1.1.1 Soft Error Trends

The Figure 1.1 shows the soft error rate per SRAM bit or latch and the cache (i.e., SRAM system). The soft error rate in an SRAM bit is projected to be constant or decrease slightly per generation [29–32]. This trend is mainly because of contradicting effects of technology scaling. On one hand, with decreasing transistor dimensions the drain area of each transistor (the region sensitive to particle strikes) decreases quadratically and it significantly reduces the charge collection capacity making the SRAM cell less vulnerable. On the other hand, with each technology generation the supply voltages also scales down reducing the critical charge making it easy to upset the SRAM cell. However, a system's error rate will grow in direct proportion to the number of devices we add to a processor in each succeeding generation.

Figure 1.2 shows how the the soft error rate of a system scales with technology scaling and processor design [29, 33, 34, 37, 38]. The soft error rate scaling trend is plotted using the data presented in [33] and [34]. It shows that, the soft error rate of current and future processors is expected to increase exponentially because of exponential growth rate of on-chip transistors, the shrinking feature size and increasing core count [33, 34, 37, 39–41].

A chip with 4 cores is expected to encounter roughly 1 failure every month for a 45 nm technology node. This might not be alarming yet and can be efficiently handled with existing error handling solutions. However, servers with 100 cores and huge memory capacity may encounter 1 failure everyday due to soft errors.

On top of that, process variations will be more pronounced with every new technology generation which may worsen soft error rate [33, 42]. Moreover, for future processors aggressive voltage scaling and NTC will be common for meeting the power/thermal caps escalating the soft error rate. This dramatic increase in the soft error rate requires specific soft error tolerance mechanisms for current and future processors.

Next, we will discuss how the existing solutions to handle soft errors do not scale to cope up with this increase in soft error rate.

1.1.2 Current Solutions and Challenges

Current solutions for protecting processors with caches and large memory arrays against soft errors rely on redundancy techniques. Today's caches and memory components are protected by parity or error codes [43–49] and hardened latches [50–54]. Unfortunately, the FIT rate of the other parts of the microprocessor system have started reaching concerning levels [29, 30, 34, 55].

Figure 1.3 shows the contribution of different elements to the total soft error rate for a modern processor with state-of-the-art technology [56]. Figure 1.3 (a) shows the FIT rate contribution from unprotected parts of the processor. It shows that FIT rate of processor is mainly due to several unprotected components such as IQ, register files (RF), MOB, ROB, RAT and unprotected latches [56].

Figure 1.3 (b) shows the FIT distribution when the caches and TLBs are protected with ECC and the register files, queues and MOB are protected with a redundant multithreading (RMT) approach [57]. Overall, it brings down the FIT of the processor compared to the case of Figure 1.3 (a). Even in this case the majority of the FIT rate comes from unprotected latches and structures such as ROB, IQ, RAT and free–list. These latches and structures are extremely difficult to protect and the cost of protection in terms of area, power and performance overhead is extremely high.

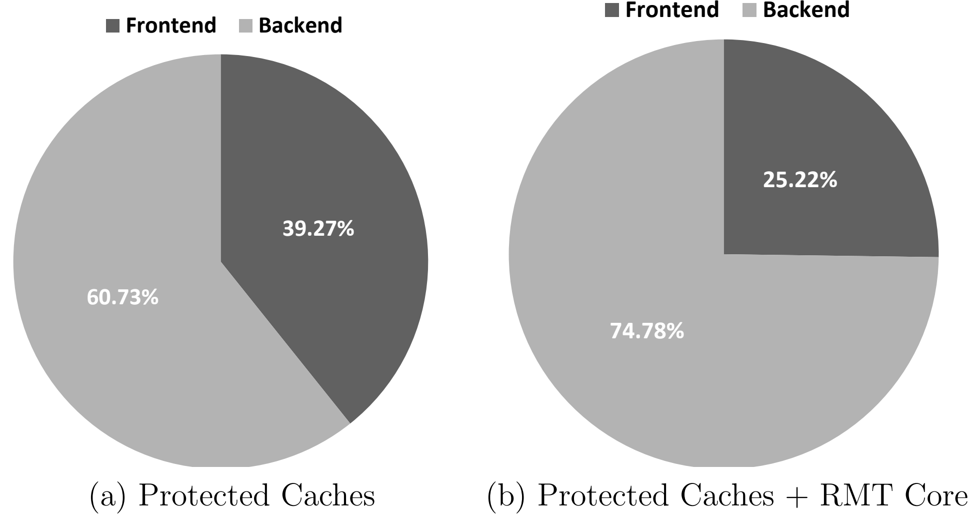

(a) Protected Caches (b) Protected Caches + RMT Core

FIGURE 1.3: Soft error rate contribution of different components in a processor core [56]. Core frontend includes ITLB, decode queue, RAT, IL1, pre-scheduler, allocate latches etc. Core backend includes DTLB, MOB, DL1, ROB, ALUs, register file, issue queue, AGU etc. Case (a) FIT distribution of a processor assuming caches and TLBs are protected via ECC and therefore, do not contribute to the total FIT rate. Case (b) FIT distribution of a processor with a protection mechanism similar to the redundant multithreading (RMT) [57] and caches, register file, MOB, and queues with data coming from a protected structured are protected.

Today's solutions do not scale to cope up with the increasing soft error rate and providing coverage to all the unprotected components on a processor core increases the complexity of soft error solutions. Moreover, the cost of protection is extremely high and the existing solutions have hit the point of diminishing return.

In this thesis, our goal is to propose a soft error mitigation mechanism that is low cost, simple to implement and scalable to handle the increasing soft error rate. Instead of relying on some kind of redundancy, we propose to detect the actual particle strike rather than its consequence. The proposed technique can work for single and multicore architectures, moreover it allows reusing the same design for different computing segments without significant modifications.

1.2 Problem Statement

We saw how the future processors will face greater reliability challenges due to increasing soft errors rates. We also saw how the current solutions to handle soft errors fail to scale and have hit the point of diminishing returns.

In particular, the work of this thesis addresses the following problems:

1.2.1 Soft Error Rate Limits the Core Count

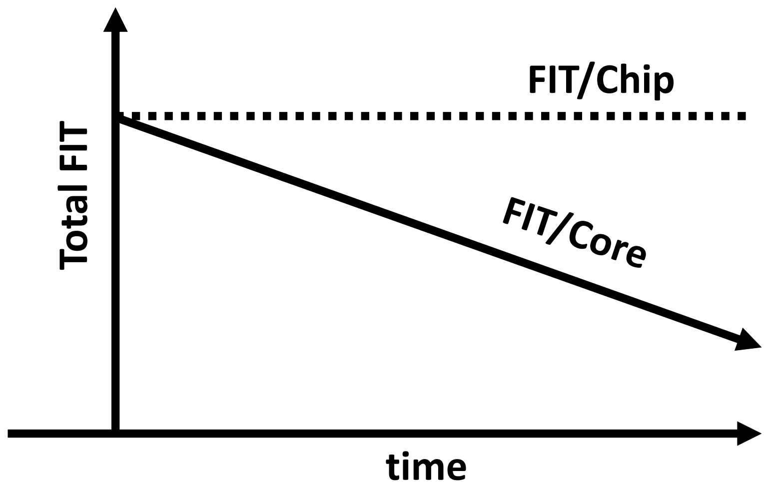

FIGURE 1.4: Scaling of FIT/Core to accommodate more cores per chip while maintaining the FIT/Chip constant

With increased core counts per chip and larger memory arrays, the total FIT per chip (or package) increases. The current soft error handling mechanisms have two exacerbating challenges to meet FIT rate target in the presence of unprecedented transistor densities and higher core count per chip: (i) They have to keep the total FIT of a chip constant and (ii) they have to scale to cope up with the increased soft error rate to accommodate more cores as shown in Figure 1.4. For example, if you want to have 100 cores in a chip, and now you have 4 cores, you need 25× FIT reduction per core to accommodate 100 cores. FIT rate is limiting the number of cores on a chip just like the power/thermal budget.

To reduce the FIT rate and accommodate more cores and larger caches several major vendors have announced aggressive reliability and protection counter measures for current and future processors [54, 58–64].

Time and space redundancy techniques are very effective and provide very good coverage but cause 1.5–2× slowdown [56, 57, 65–76]. The caches and larger memory arrays are equipped with more parity and stronger ECC. While protecting the caches, the extra delay imposed by ECC computation may increase cache hit and miss times. Moreover, smaller caches and memory arrays cannot be protected with

ECC without incurring huge performance penalty. Unprotected latches and flip-flops are replaced with hardened latches. Replacing the latches in critical paths with hardened latches increase the length of the critical path severely impacting performance.

To overcome the performance overhead of the conventional solutions in providing the necessary reliability and keep increasing the core count, in this thesis we propose a novel soft error mitigation technique that uses acoustic wave detectors for detecting particle strikes that may cause soft errors. Upon detection, a hardware or software mechanism would trigger the appropriate recovery action. Our results show that the proposed mechanism protects the whole processor (logic, flip-flop, latches and memory arrays) incurring minimum overheads.

1.2.2 Soft Errors in the age of Dark Silicon

Following the multicore trend, researchers have started designing 100-core and 1000-core chips. These 100-core and 1000-core chips create *dark silicon*. It imposes a limit in terms of the number of active cores per chip leaving some cores underutilized.

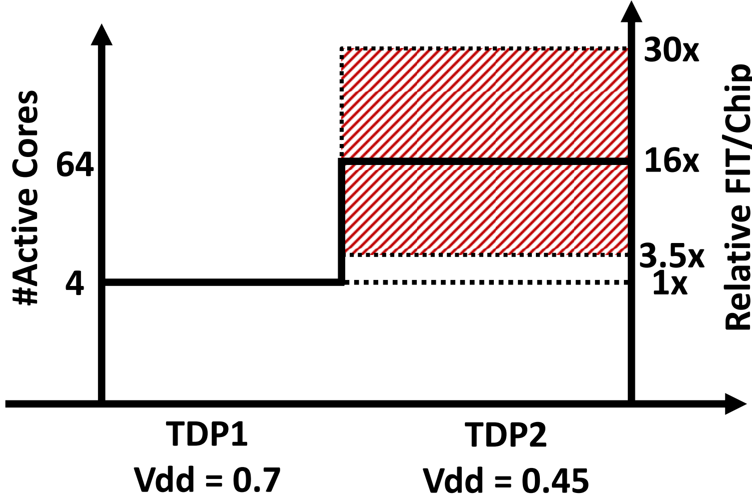

FIGURE 1.5: TDP modes in modern multicore processor. TDP1 operates at 0.7 VDD and hence there are 4 active cores. In TDP2 the supply voltage is scaled down to 0.45 VDD to activate 64 cores. The relative FIT in TDP2 is increased by 16× compared to TDP1 due to increased active silicon area. However, due to effects of the supply voltage scaling the relative impact on soft error rate is as high as 30× [77]

In a conventional multicore processor, there is only one *thermal design power* (TDP) mode. It implies that at peak voltage and frequency all cores are powered on. In contrast, in the age of *dark silicon*, multicore processors have different TDP modes with different operating voltages. Each TDP mode have starkly different and inconsistent impact on soft error rates as well. TDP mode with lower operating voltage, increases number of active cores on the chip as shown in Figure 1.5. This results in higher FIT rate of chip due to two reasons: (i) lower voltages decrease the minimum charge required to cause the soft error and, (ii) due to reduced supply voltages the applications will take longer to execute prolonging the vulnerability window of critical structures. To handle *dark silicon*, powering on 16× more silicon area can increase the soft error rates by 3.5–30× [77].

We propose a solution that is extremely low cost in terms of area, power and performance overhead which is crucial in *dark silicon* era where the chips are already suffering the performance due to the power limitations.

1.2.3 Soft Errors in Large Memories

Cache memory is a fundamental component used to enhance the performance of microprocessors. Current high performance processors employ multilevel on-chip caches. The sizes are in the range of several megabytes and are expected to increase [58, 64, 78]. On-chip caches occupy roughly 50% of chip real estate [79].

The combination of growing cache size, voltage scaling, shrinking SRAM cell dimensions, and increased impact of process variations is causing rapid increase in the soft error rate. Caches benefit from the positive impact of smaller cell sizes. However, this benefit is offset by the negative impact of storing less charge per bit and reduced critical charge to create a soft error; as a result the cache error rate increases linearly with cache size [30, 31, 38, 80].

To protect the caches designers adapt to error detecting codes such as parity codes or ECC such as *Single Error Correction–Double Error Detection* (SEC-DED) [43, 44]. Every read and write operation requires the encoding or decoding of the data bits for error detection or correction. Usually, L1 caches are not protected at all or have only error detection [81]. Large caches (L2 or L3) are usually protected via ECC [82, 83].

Most soft errors are single bit upsets and can be detected by parity codes. To correct single bit errors single error correction can be used. However, larger caches frequently switch to drowsy mode [84] or subthreshold operating modes [85] to save energy. Such optimizations in future processors will be very common and they increase the likelihood of soft errors by 9-10× [86]. Moreover, due to reduced operating voltages, a single neutron strike can upset more than one bit of memory in close proximity, causing *spatial multibit errors*. To handle *spatial multibit errors*, designers usually physically interleave the ECC protected bits [87, 88]. Also, in a cache the error handling policy (e.g., SEC-DED) has to access the erroneous data to correct it. If not accessed, the first single bit errors may not be corrected by it, leading to accumulation of such single bit errors over a long time which are called *temporal multibit errors*. To detect and correct *temporal multibit errors* more complex codes *Double Error Correction–Triple Error Detection* (DEC-TED) [45, 89] or RS codes [90] are required. Alternatively, there have been proposals to use *cache scrubbing* that periodically scans the cache for single bit errors avoiding their accumulation [91, 92].

Error codes combined with *scrubbing* is very widely used in commercial processors. To handle increasing soft error rates complex codes are required. Complex codes need longer time for encoding and decoding data and may not be able to provide *inline* error detection and correction. They may also increase the critical path severely impacting performance [48]. *Scrubbing* techniques may cause large overheads for protecting on-chip caches [93, 94]. Solutions to protect caches in drowsy mode sacrifice the cache capacity [95, 96].

TIn this work, we propose an error detection and correction architecture that reduces the failure rate of caches due to soft errors at minimal overheads. As a result of which larger caches with less complex and economical error protection techniques can also provide higher degree of reliability.

1.2.4 Handling SDC & DUE

Soft errors can be classified as silent data corruption (SDC) or detected unrecoverable error (DUE). Corrupted data may go unnoticed by the user and is harmless. However, corrupted data that ends up as a visible error counts as SDC event. A DUE event occurs when a system detects the soft error but cannot recover from it. An SDC event or a DUE event can cause a system crash. However, unlike an

SDC event, a DUE event prevents data corruption. Once the error is detected the system contains the error by stopping the error propagation beyond the point of detection. The system can then reboot itself or it can resume the normal execution by reverting back to the last known error free state (i.e., checkpoint).

Designers have fixed SDC and DUE FIT rates. Adding error detection can reduce the SDC FIT rate by orders of magnitude. However, in the absence of any recovery mechanism this reduction in SDC FIT transforms into DUE FIT [97]. This interesting effect has been observed in parity protected (write–back) L1 caches and partially protected caches (L2 with parity protected tags). Increasing cache size causes a super linear increase in DUE FIT [98, 99].

DUE events directly impact the server *availability*. Increase in DUE FIT rate causes frequent recovery actions or system reboots and may result into increased unplanned downtime of the server system [100, 101]. To handle the increased DUE FIT rate most of the servers today rely on checkpoint based error recovery. Taking system wide checkpoints for error recovery can be very complex and expensive [36, 66, 102–112]. *Triple modular redundancy* (TMR) can eliminate DUE without halting the system. However, TMR incurs more than 300% area and power overhead [58, 113–115] and it is only affordable in high availability mission critical systems.

This thesis proposes to detect and accurately locate all the particle strikes that may cause soft errors, eliminating SDC. Moreover, proposed solution can significantly reduce DUE FIT of entire core in a multicore processor by implementing an extremely lightweight and scalable checkpoint based recovery mechanism.

1.2.5 Protecting all Computing Segments

Reliability research has focused largely on the high performance server market. High availability systems rely on redundancy to provide fault tolerance. Area, power and performance overheads associated with existing solutions for handling soft errors may be affordable in high performance servers. Unlike high performance servers, area and power are primary constraints in the embedded design space. Embedded processors typically have smaller components, longer clock cycle times and larger logic depths between latches. Due to increased logic depths the relative area occupied by the combinational logic increases [116]. The combinational logic

elements are mostly unprotected making them the largest contributors towards total FIT of the processor. Moreover, in pipelines with larger logic depth the number of target latches per stage increases due to wider fan-out, which increases the probability of a fault to propagate and cause a soft error.

In general, error detection and correction codes are effective but very costly for embedded processors with smaller caches [117–119]. Execution redundancy is not suitable for embedded processors with limited resources. Also, checkpoint based error recovery techniques may be complex. Moreover, the area, power and performance overheads of taking a system wide checkpoint is unacceptable. Other fault tolerant techniques such as radiation hardened latches require 20-30% extra logic [50–54].

In this work, we show that the proposed solution can also effectively protect embedded systems against soft errors minimizing area, power and performance overheads.

1.3 Thesis Scope and Contributions

To tackle the challenges described in Section 1.2, this work focuses on cost effective soft error mitigation in microprocessors. In this work, we primarily target the particle strike induced soft errors since these are the most prevalent soft errors in chips. We aim to protect: (i) the unstructured, inherently complex and irregular processor cores (i.e., combinational logic, latches and other unprotected elements in the pipeline) and (ii) the on-chip caches which occupy large portions of the chip area and are regular in design and behavior.

Many solutions exist to provide error detection and recovery from soft errors in logic and memory components. However, providing robustness minimizing area, power and performance is extremely crucial. The goal of this work is to detect and recover from all soft errors in a processor core minimizing the overheads.

This thesis proposes a soft error mitigation architecture using acoustic wave detectors. Acoustic wave detectors detect particle strikes that may cause soft errors. In this work, we also propose a novel, economical and acoustic wave detector

specific checkpointing technique for error recovery. Proposed architecture is extremely simple, scalable and it can protect different computing segments without significant design changes.

The proposed architecture, besides providing a highly reliable core, is able to recover a significant part of the overheads associated with current reliability techniques by potentially eliminating error codes and radiation hardened latches for soft errors. It also significantly reduces the design complexity compared to other mainstream reliability solutions. The benefits of adapting acoustic wave detectors are numerous and will be detailed throughout this thesis.

Several contributions of this thesis include:

- *Detecting Particle Strikes to Detect Soft Errors:* We propose to use a low-cost dynamic particle strike detection mechanism based on acoustic wave detectors. Instead of relying on error correcting codes or some kind of redundancy, we deploy a set of detectors on silicon for error detection. The benefits of this solution are twofold: (i) it can detect errors on the entire chip, including currently unprotected logic at a very low cost, and (ii) it can decrease the growing costs of protecting large memory arrays.

- *Unified Error Detection for Logic & Memory:* We develop an architecture that detects and locates particle strikes on a processor based on acoustic wave detectors. We first introduce the structure of such detectors, and later propose the architecture to deploy them. Moreover, the proposed mechanism can function stand alone or it can be integrated smoothly with other end-to-end error detection techniques.

- *Locating the Particle Strikes:* We propose a new methodology that uses the acoustic wave detectors to precisely locate particle strikes. To provide successful error correction and recovery, the system must know the precise location of the error. Once the accurate location is found the system can take an available recovery action. Our solution is based on measuring the time difference of arrival across different detectors, generate a set of hyperbolic equations, and solve them. We implement various algorithms for solving the hyperbolic equations and we discuss the different trade-offs in terms of cost versus accuracy.

- *Protecting Caches in a Processor Core:* We apply the architecture based on acoustic wave detectors to detect and correct soft errors in caches. Additionally, we propose a new solution that combines acoustic wave detectors with error correcting codes in such a way that we decrease the total cost of the protection mechanism while providing the same reliability levels.

- *Eliminating SDC & DUE of Core:* We propose an architectural framework to completely eliminate the SDC and DUE related to soft errors in single and multicore processors. We propose a novel recovery solution tailored for acoustic wave detectors. It relies on an extremely light-weight and scalable checkpointing mechanism. We discuss different design parameters and evaluate the cost of checkpointing & recovery. We evaluate the impact of error detection latency on the cost and complexity of the required recovery technique. We present different trade-offs related with complexity of detectors deployment, detection latency and complexity of recovery mechanism. We also show that the proposed architecture can provide cost effective recovery in low cost embedded cores.

1.4 Organization

The rest of the thesis is organized as follows: Chapter 2 discusses in thorough details about the soft errors, their sources and some details about the historical background related to them. We discuss how the soft errors are manifested in logic and memory. We also discuss some important terminologies related to soft errors which are important to understand the rest of the thesis.

Chapter 3 begins with the physics involved behind the soft errors. We show how particle strike detectors can be used to detect soft errors. We introduce the acoustic wave detectors. We discuss several structural aspects of the device and some important properties. Once we have detected the soft error we discuss how we can accurately locate the particle strike and hence the error. Using a basic example we discuss how we can generate the hyperbolic equations based on the relative *time difference of arrival (TDOA)* of the acoustic wave generated by the strike among different detectors. We discuss the implementation of different algorithms to solve hyperbolic equations for location estimation. Finally, we evaluate the

error detection and localization architecture taking an example of the core of a Core™i7 like processor.

In Chapter 4 we show how we can detect and locate errors in caches using acoustic wave detectors. We compare the trade offs in protecting the caches using stand alone acoustic wave detectors and combination of error codes (i.e., parity and ECC) with acoustic wave detectors for error recovery.

Chapter 5 describes the architecture using acoustic wave detectors can be used for protecting an entire core. We discuss the architecture for eliminating SDC- & DUE-FIT in a core. We discuss various aspects of error containment and recovery. We evaluate the architecture on real life workloads and we discuss different design parameters and evaluate cost of checkpointing & recovery.

Chapter 6 explains how we can use the proposed architecture for protecting an embedded core against soft-errors. First, we discuss specific aspects of reliability requirements for an embedded core and tradeoffs involving parameters such as area and performance overhead against cost of recovery.

Chapter 7 reviews some relevant related work in the field of reliability.

Finally, a summary of conclusions and discussion regarding future work is presented in Chapter 8.

Chapter 2

Soft Errors: Background and Overview

In this chapter, we provide a background of soft errors. First, we describe some terminologies and metrics related to reliability in general to which we will adhere to for the remainder of the thesis. Next, we discuss the sources and the physics behind the manifestation of soft error caused by a particle strike, followed by the discussions of the methods to measure the soft error rate. After that we list the parameters that play a role in soft error manifestation and show how the soft errors affect the memory components and logic. Next, we review how the design of future processors will affect the soft error rate. Finally, we will discuss the essentials building blocks for a soft error handling solution.

2.1 Soft Error Terminologies

Precisely modeling soft errors and their impact on electronics, predicting soft error rates and deploying adequate reliability mechanism is challenging and an interesting field of research. The work of this thesis is focused on handling soft errors. Before indulging into the specifics of soft errors, we discuss some metrics and terminologies which are widely used in the field of reliability.

2.1.1 Faults, Errors and Failures

A fault in a computer system is an undesirable event and usually a result of defects, imperfections or interaction of external environment. Typically faults can be classified in three types:

- Permanent or hard fault: As the name suggests permanent faults or hard faults remain in existence for a long period until the faulty part is replaced. *Permanent faults* or *hard faults* can be further categorized as extrinsic or intrinsic faults. Extrinsic faults are caused due to manufacturing defects or due to contamination of the device. Intrinsic faults are caused by wearout of the material over time. Intrinsic faults include faults due to electromigration [120–122], stress voiding, gate oxide wearout [123], hot carrier injection (HCI), negative bias temperature instability (NBTI) [124, 125], positive bias temperature instability (PBTI) [126], errors due to scaled voltages (i.e., low Vccmin errors [127]), high heat flux or thermal cycling across the silicon die [128] and time dependent dielectric breakdown (TDDB) [129].
- Intermittent fault: An intermittent fault is a fault that appears under specific situation (e.g., elevated temperature), and it is usually an early indicator of an impending permanent fault. A partial oxide wearout may cause intermittent faults.
- Transient fault: Transient faults occur only once and are non–repeatable. *Transient faults* in semiconductor devices are caused by noise and erratic voltage fluctuations [130] within the chip or by external factors such as radiation induced soft errors. Soft errors are transient errors which do not permanently damage the processor and do not recur.

Handling both permanent and transient faults are important for reliability. Unlike soft errors, the permanent faults and the transient faults due to noise can be identified during validation and are fixed before the silicon chip is shipped. However, soft errors must be handled in the field.

An error is a manifestation of an underlying fault in a computer system. Just like faults, errors can be permanent, intermittent or transient. A hard fault may cause a hard error, an intermittent fault may cause an intermittent error, and a transient fault may cause a transient error. Particle strike induced bit flips are transient in

nature and do not cause any permanent damage hence they are termed *soft errors*. It is important to note that faults are necessary to cause errors, however, not all faults cause errors.

All those faults that do not cause errors are *masked*. The *masking rate* indicates the percentage of masked faults. Most of the faults get masked or corrected before they can cause an error. For instance, a fault in a branch predictor will not affect the correctness of the end result and hence it will not cause an error. We will discuss about masking effects of combinational logic in a processor in detail in Section 2.6.3.

A failure is a special case of error, in which the error deviates the system from the expected action. It is important to note that not all errors cause failures. For instance, an error in the unmodified L1 cache line will not cause a system failure.

2.1.2 Metrics

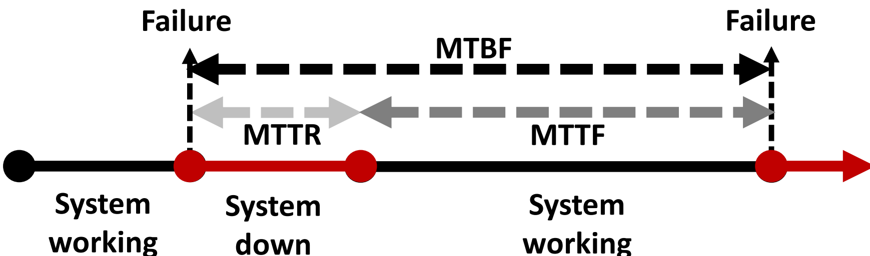

FIGURE 2.1: Reliability metrics: Mean time to repair (MTTR), Mean time to failure (MTTF) and Mean time between failures (MTBF)

Failure rates can be given by *Time to Failure* (TTF). It is the time until the first fault or error occurs. Similarly, *Mean time Between Failures* (MTBF) indicates the mean time that has elapsed between two faults or errors as shown in Figure 2.1. Besides MTBF, *Mean Time to Repair* (MTTR) and *Mean Time to Failure* (MTTF) are also commonly used. MTTR indicates the mean time required to repair an error after it is detected. And MTTF is the time until the system encounters a failure once it is repaired.

Although MTTF is easy to understand, its computation can be complex for larger circuits with millions of components. Hence, to express the failure rate an additive metric *Failure in Time* (FIT) is more convenient. One FIT is equal to one failure

in a billion run-time hours. FIT rate of a system is the summation of individual FIT rates of all the components. For example, if a 6T-SRAM cell with the failure rate of 0.001 FIT/bit is used to design a 1 MB cache, then the total failure rate of the cache is 8389 FIT and the cache has an MTTF of about 4900 days.

$$FIT\ rate = \frac{10^9}{MTTF\ in\ years \times 24\ hours \times 365\ days} \tag{2.1}$$

MTTF and FIT are inversely related to each other as shown in Equation 2.1. MTTF of 1000 years is equivalent to 114 FIT. Chip designers have fixed FIT (or MTTF) target just like power budget.

2.1.3 SDC and DUE

As we discussed in Section 1.2.4 of Chapter 1 errors are classified into two categories: silent data corruption (SDC) and detected unrecoverable errors (DUE).

Correctable errors are errors from which recovery to normal system operation is possible, either by hardware or software. Detected unrecoverable errors are errors that are discovered and reported, but from which recovery is not possible. A failed ECC correction is an example of DUE event. These errors typically cause a program or system to crash. A silent data corruption, also known as an undetected error, alters the data without being detected, thus permanently corrupting program state or user data.

To better understand, we illustrate the possible outcomes once a faulty bit is accessed as shown in Figure 2.2. If the faulty bit is not protected and an error in that bit affects the program outcome then such an undetected error is classified as SDC. Adapting an error detection scheme (e.g., parity codes) can avoid SDC. However, with only error detection capability once the error is detected it is not possible to recover. Such detected but uncorrectable errors are classified as DUE.

Usually, SDC event is more harmful than a DUE event. SDC causes data corruption (or loss) and it goes undetected. Upon a DUE event, once the error is detected it is possible to handle it by rebooting the system. By rebooting system it is possible to avoid any meaningful effect of the error on the system. However, frequent DUE events are responsible for system downtime.

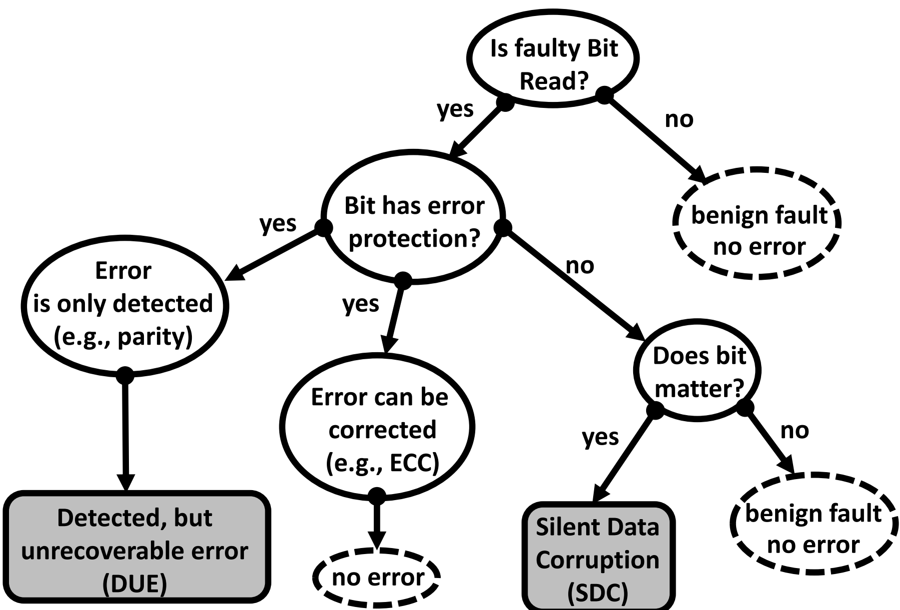

FIGURE 2.2: Classification of soft errors: *silent data corruption* (SDC) and *detected unrecoverable error* (DUE)

Usually, SDC design target is more stringent than DUE since error is undetected and cannot be trace back and identify its origin. Designers may deploy simple error detection schemes (i.e., parity or RMT) to handle SDC [18, 131].

DUE target is relatively relaxed since error will be detected and sometimes contained. Once the error is detected the system should be able to stop the propagation of the error and be able to restore the normal state of operation. For instance, error correction codes are used to provide recovery in memory which can reduce the DUE rate.

The acceptable rate of SDC and DUE events also differ for different market segments. For instance, a database system is expected to maintain data integrity and can tolerate very low SDC. A web application server with extremely low system downtime should rarely have any DUE events. On the other hand, a desktop computer can tolerate relatively higher SDC and DUE events.

2.2 Realizing Reliable Solution

We will now discuss the major components required for an end to end reliability solution. We show the basic components in Figure 2.3.

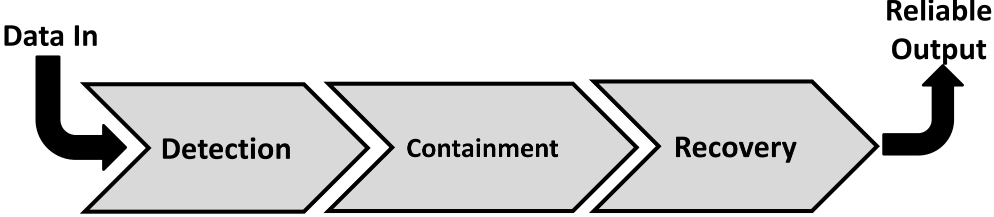

Figure 2.3: Realizing reliability pipeline for soft errors: error detection, error containment and error recovery

Error detection is the first requirement of reliable solutions and it usually involves an error detection mechanism. It may be specific to the structure it is protecting. Error detection is usually done via detection of the symptom (i.e., the error itself). For example, to detect errors in memories one may use parity codes while for error detection in logic a dual modular redundancy can be used. New direction that is growing in interest among researchers is to detect the actual particle strike rather than its consequence [132–135]. Such particle strike detectors detect errors via detection of currents or voltage glitches, shockwave of sound, a flash of light or a small amount of heat and will be discussed in Section 2.4.1.

It is possible that the erroneous data is consumed before the error is detected. To avoid the consumption of the erroneous data and prevent SDC, the detected error must be contained to the affected part. Error containment restricts the spread of the error by isolating it. Error detecting codes contain the data by checking the data every time it is read.

Once the system has detected the error it is desirable to restore the error free state. This is called error recovery. Error recovery is usually done with some kind of checkpointing mechanism. Upon error detection, system can revert back in time to an appropriate checkpoint and restore the correct processor state and resume execution.

We discuss the traditional solutions for error detection, containment and recovery in Chapter 7. Error diagnosis and repair can also be included in the reliability pipeline however, they are specifically used for handling hard errors. This thesis specifically targets the soft error problem and proposes novel error detection, containment and recovery technique which will be discussed in the coming chapters.

Next, we will discuss the sources of soft errors and how they interact with semiconductor devices.

2.3 Soft Error Sources

The sources of soft errors include various extra-terrestrial (i.e., solar flares) and terrestrial (i.e., radioactive decay) phenomena. Terrestrial sources include the particles generated due to decay of radioactive impurities in the material used in packaging of the chip. While in extra-terrestrial phenomena, the primary cosmic rays react with the earth's atmosphere via strong nuclear interactions, producing various particles which can induce soft errors [17].

The main sources are as follows:

- Alpha particles
- High-energy neutrons
- Neutron induced boron fission

2.3.1 Alpha particles

The silicon wafer, the packaging material or the contamination in soldering material are typical sources of alpha particles and they contribute to the ionizing radiation in semiconductors. Basically an alpha particle is composed of two protons and two neutrons.

Primarily, alpha particles come from residual radioactive impurities (e.g., Uranium (U^{238}), Thorium (Th^{232}), and Lead (Pb^{210})) in the packaging material of a chip [17, 136, 137]. Traces have been found in the mold compound and underfill, and most predominantly in solder balls. Packages, which use solder balls for the power supply and I/Os, are particularly vulnerable to soft errors.

In order to reduce the alpha induced soft errors highly refined materials can be employed for packaging materials. Strict design rules can also be adapted to separate the sensitive circuit areas from alpha emitting *hot* zones. It is also possible to shield the chip using thin films coat to prevent the alpha contamination [17]. Alpha emitting materials have an emission rate of 0.0003-0.0017 alphas/cm^2–hr [17, 137].

2.3.2 Neutron particles

The second significant source of soft errors are high-energy neutrons coming from cosmic rays. Cosmic rays react with the Earth's atmosphere and produce complex cascades of secondary particles. Most of the particles are short-lived while protons and electrons are attenuated by Coulombic interactions with the atmosphere and render harmless [17]. Neutrons survive because they carry neutral charge and relatively high flux. Neutrons have the highest charge generation capacity and are the dominant among all other particles in producing soft errors.

The cosmic neutron flux is a function of neutron energy and altitude [117, 138]. Neutron flux decreases with increasing neutron energy and increases with increasing altitude. For example, at flying altitude (32,000 feet above the sea level), the neutron flux increases by 228× compared to sea level neutron flux [139]. Due to varying neutron flux, cosmic neutron-induced soft error rate for the same device will be different in different cities and different altitudes.

Although only 1% of the neutrons created by cosmic rays reach the surface of the Earth, they are still the dominant source of the soft errors in circuits. Both neutron flux and energy determine the soft error rate experienced by circuits. Neutrons with energies of 10 MeV or higher are capable of causing soft errors [17, 20, 32, 137, 140–143]. The exact threshold depends on the properties of the silicon device. At sea-level the flux of neutrons with energies above 10 MeV is approximately 14–20 neutrons/cm^2–hr [37, 137, 138, 144, 145].

Unlike alpha particles, reducing the cosmic neutron flux at the chip level is very difficult and requires mitigation techniques within the chip, such as improving the robustness of the circuit, using error correction techniques or modular redundancy techniques (described in Chapter 7).

2.3.3 Neutron induced boron fission

The interaction of low energy cosmic neutrons with boron nuclei is a third source of ionizing particles in semiconductor devices. Boron is used extensively as a p-type dopant. Its exposure to neutron results into generation of charges in silicon and cause soft errors. Using specific device processing techniques soft errors due to boron fission can be completely eliminated [17, 137].

2.4 Interaction of Particles with Silicon

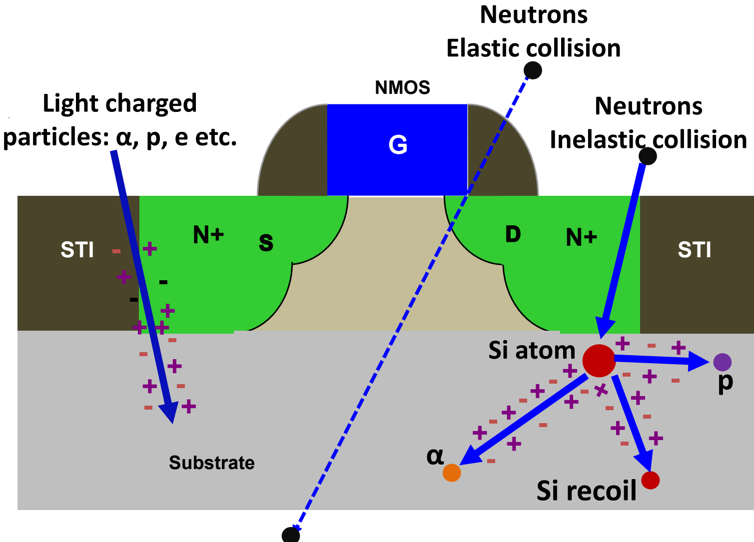

FIGURE 2.4: Alpha particles generate *electron-hole* pairs in silicon by direct ionization. Inelastic collision of neutrons with a silicon atom generate *electron-hole* pairs via indirect ionization by creating a silicon recoil. Elastic collisions of neutron particles are harmless.

For each incoming cosmic ray particle, the collision of the particle with the nucleus in the semiconductor medium can be classified into two categories: *elastic* and *inelastic* scattering (see Figure 2.4) [17].

In most *elastic* events, the cosmic ray particle is deflected slightly from its original trajectory (small-angle scattering) without changing its intrinsic energy state. *Elastic* collisions of alpha or neutron particles are harmless. *Inelastic* collisions are responsible for soft errors. During *inelastic* collisions, large scale of energies are exchanged. In the initial stage, secondary protons, neutrons, and pions are produced, and an excited intermediate nucleus (i.e., recoil) is formed. This nucleus de-excites by the emission of other secondary particles, and it is finally transformed into a stable and lighter residual nucleus.

During the impact of energetic particles on silicon atom large amount of energies are exchanged in a very short duration of time. The amount of energy or charge generated upon the impact depends on the *stopping power* or *linear energy transfer* (LET). The LET is the amount of energy deposited per unit of length travelled in silicon. Typically, the lost energy is converted into charge at the rate of 3.6 eV per *electron-hole* pair in silicon [146, 147].

Particle	**Deposited Charge**	**Flux**
Alpha	16 fC/μm	0.0003-0.0017 alphas/cm^2–hr
Neutron	25-150 fC/μm	14–20 neutrons/cm^2–hr†
		~3000 neutrons/cm^2–hr*

TABLE 2.1: Summary of the sources of soft errors. † indicates the flux at sea level and * is the flux at 32,000 feet above sea-level.

Alpha particles. In an *inelastic* collision involving an alpha particle, electron-hole pairs are generated through direct ionization in silicon as it is shown in Figure 2.4. The total energy deposited from such an event is in the range of several MeV [17, 37, 148]. Roughly, an alpha particle with 10 MeV of energy has a *stopping power* of 100 KeV/μm and can generate approximately 4.5 fC/μm of charge [17, 30].

Neutrons. Unlike alpha particles, when the neutrons are involved in *inelastic* collisions, first silicon recoil (or Li recoil in the case of interaction with boron nuclei) and secondary particles are generated which finally result into generation of *electron-hole* pairs as shown in Figure 2.4. Impact of a higher energy neutron results into higher energy recoils. However, the probability of 1 MeV recoil is 100-3000 times higher than the probability of a 15 MeV recoil [17, 143, 149]. Each neutron can generate about 10× more *electron-hole* pairs compared to an alpha particle [17]. The charge density per distance traveled for silicon recoils (25-150 fC/μm) is significantly higher than that for alpha particles (16 fC/μm) and hence, neutron strikes have higher potential to upset a circuit [30]. Typically, a neutron with 200 MeV energy, generates a recoil that has *stopping power* of 1.25 MeV/μm and maximum penetration range of 3 μm [30]. One such particle strike can deposit total charge of 55.7 fC [150].

Table 2.1 gives a summary of the soft errors induced due to alpha or neutron particle strikes.

2.4.1 Generation of Light, Sound and Heat!

When a high-energy particle collides with a silicon nucleus, it causes an ionization process that creates a large number of electron-hole pairs (shown in Figure 2.4).

In a few picoseconds the released energy may be in the range of several MeVs. The spurious electron-hole pairs subsequently produce unstable quasiparticles (i.e., phonons or photons).

Generation of phonons and photons indicate that a particle strike results into a shockwave of sound, a flash of light or a small amount of heat for a very small period of time. Therefore, it is possible to detect particle strikes by detecting the sound, light or heat.

The unstable quasi-particles gradually result into a cascade of carriers resulting into drift current (i.e., transient funneling current) or diffuse current generated due to diffusion of electron-hole pairs. The generation of electron-hole pairs also result into a voltage glitch. *Therefore, particle strikes may also be detected by detecting currents or voltage glitches.*

In this work, we detect the particle strike that may cause soft errors. We construct an architecture to detect the acoustic shockwave generated by particle strikes upon impact on silicon surface.

2.5 Computing Soft Error Rate

Measuring the soft error rate is very challenging mainly because of extremely low soft error rates. For instance a circuit element with a failure rate of 0.001 FIT will have an MTTF of 10^{12} hours. It is a very long wait to encounter one error. Moreover, several errors must be observed to predict the FIT rate of the component with sufficient statistical confidence. One can measure the soft error rate by exposing the silicon to the radiation in the field and collect real-time data [26, 144, 151–155] or in an environment with accelerated particle flux [128, 137, 138].

Alternatively, to evaluate whether chip's soft error rate meets the desired target or not before fabricating it, microprocessor designers use sophisticated computer models to compute the FIT rate for every component (i.e., SRAM cells, latches, and logic gates) on the chip. Using simulations soft error rate can be modeled at circuit, microarchitecture or architecture level. We have seen how particle strikes generate *electron-hole* pairs. *Linear energy transfer* can explain how many *electron-hole* pairs or charge will be generated upon an alpha particle or a neutron

strike. However, it does not explain whether the strike will cause a soft error or not! In fact, most of the *electron-hole* pairs either recombine or are collected on reverse-biased p–n junctions that are shorted to a power supply rail without disturbing the normal operation of the circuit. For the strike to cause a soft error, it has to generate enough charge and the device has to accumulate enough charge to cause a malfunction.

The minimum accumulated charge that is necessary to cause a circuit malfunction is called the *critical charge* (Q_{crit}) of the circuit. For memory circuits (e.g., SRAM cell) the Q_{crit} is the minimum charge required to flip the value stored in that memory cell. In a logic circuit, Q_{crit} is defined as the minimum amount of induced charge required at a circuit node to cause a voltage pulse to propagate from that node to the output and be of sufficient duration and magnitude to be latched. Since a logic circuit contains many nodes that may encounter a particle strike, and each node may be of unique capacitance and distance from output, Q_{crit} is typically characterized on a per–node basis.

Once the Q_{crit} is determined it can be mapped to the FIT rate. The Q_{crit} of a circuit is not a single valued quantity but is a function of the shape of the transient pulse generated by the particle strike, the position of the circuit on the chip, the supply voltage, and parametric variations. An accurate calculation of the *critical charge* requires a circuit model with detailed process, device, and operating parameters. Q_{crit} is estimated by inserting different current pulses in the circuit model till the circuit malfunctions. Several methods have been proposed to compute Q_{crit} for a given circuit [156–158].

Once we have the Q_{crit} from the circuit simulations, there are several models that relate soft error rate with Q_{crit} [21, 25, 156, 159]. One such model is proposed in [156],

$$Soft\ Error\ Rate = Constant \times Flux \times Area \times e^{-\frac{Q_{crit}}{Q_{coll}}} \tag{2.2}$$

In equation 2.2, constant is a technology dependent constant, Flux is the neutron flux at a specific location, Area is the area of circuit that is sensitive to particle strikes and Q_{coll} is the collected charge. The critical charge is Q_{crit}.

2.6 Soft Error Manifestation in Electronics

The charge deposited upon impact of energetic particles on the silicon devices may cause soft errors and have huge impact on their reliability. The susceptibility to soft errors in on-chip caches (SRAM), main memory (DRAM) and combinational logic differ significantly due to difference in their design and functionality. Moreover, parameters such as operating voltage, sensitive area, node capacitance etc. also impact the possibility of soft errors and over all soft error rate.

2.6.1 Soft Errors in SRAM

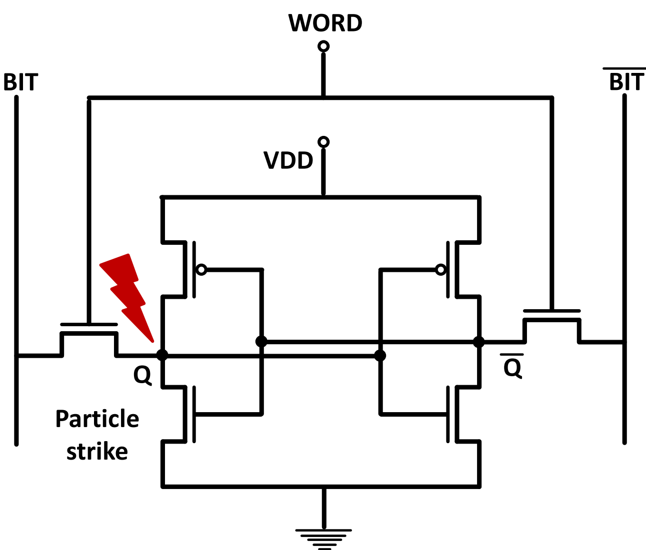

FIGURE 2.5: Particle strike on a critical node Q on a 6T-SRAM cell

An SRAM memory cell is a cross coupled inverter circuit. The cell can retain the data as long as the power is on. An SRAM cell stores the data and its complement between two nodes Q and $\bar{Q}$ as shown in the Figure 2.5. Both these nodes store charges by turning off the driver and load transistors forming reversed bias drain junctions. If a particle strike on a critical node Q generates enough charge (more than Q_{crit}) then it can discharge the node causing the transition. This disturbance may propagate through the decoupled inverter and cause a transient on the $\bar{Q}$. And as $\bar{Q}$ node drives the Q node towards the wrong value a regenerative action causes both the nodes to flip. Due to this regenerative action the SRAM cell is flipped and it now stores a wrong value. Soft errors in SRAM cells are a concern because of the larger area they occupy on the chip caches increase the probability of particle strikes.

2.6.2 Soft Errors in DRAM

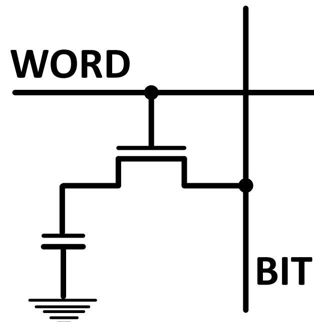

FIGURE 2.6: Structure of a DRAM memory cell

Figure 2.6 shows a DRAM memory cell. DRAM cell consists of a capacitor to store the bit, with a transistor to access the stored data in the capacitor. A particle strike on the capacitor may impart a large amount of charge (more than Q_{crit}) and may alter the stored data causing a bit flip. Initially, the DRAM cells used planar capacitors with large junction area. In a cell with larger cell area it was easier to cause the soft error. However, by adapting to 3D capacitors (e.g., stack, trench etc.) designers could successfully reduce the sensitive volume without decreasing the nodal capacitance making a DRAM cell one of the more robust electronic devices. By adapting to 3D capacitors the soft error rate reduced and it was possible to fit in more memory cells in the same area. The amount of DRAM in computer systems continues to increase every year, and is predicted to increase 50× over 2009 levels by 2024 [160]. In this situation, The contribution of soft errors in total DRAM errors (including hard errors) can be as high as 30% [161].

2.6.3 Soft Errors in Logic

The phenomenon that explains bit inversions remains the same for both memories and logic elements. However, the soft error rate of logic elements and its impact on the system are much harder to quantify because of their non-regular design and their period of vulnerability (when they are active rather than idle) which varies widely depending on the functionality of the design, frequency, and the workload [32, 34, 117, 162, 163].

Sequential Logic: Logic elements include latches and flip-flops that hold system event signals and buffer the data before it goes in or out of the microprocessor.

They provide the interface to other combinational logic (i.e., ALUs) that perform logical operations based on multiple inputs. Flip-flops and latches are fundamentally similar to the DRAM cell and they use cross-coupled inverters to store the data state. However, compared to an DRAM cell, the sequential logic is usually less susceptible to soft errors due to the use of larger transistors (hence larger capacitance and driving strength) in latches and associated logic gates [34].

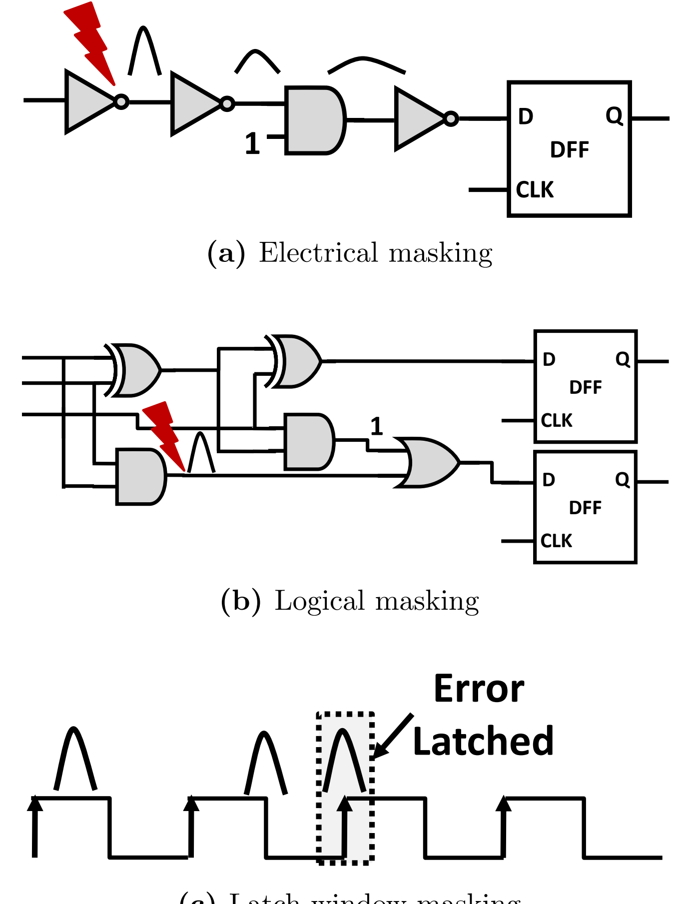

(a) Electrical masking

(b) Logical masking

(c) Latch-window masking

FIGURE 2.7: Masking effect in combinational logic circuits.

Combinational Logic: Unlike caches or memories, a transient pulse (glitch) that is generated in combinational logic can only cause an error at a critical point in the circuit if the following conditions are fulfilled: (i) The glitch has to be strong enough to generate a signal on one of the nodes in the circuit and the signal has to be strong enough to propagate through the combinational logic in the circuit i.e., *electrical masking*, (ii) The path that is traveled by the pulse has to be logically enabled i.e. *logical masking* and (iii) The fault has to be latched i.e. *latch-window masking*. Due to these inherent masking characteristics combinational

logic components are relatively less sensitive towards particle strikes compared to memory. Figure 2.7 shows all the three masking possibilities. Figure 2.7(a) shows the electrical masking where the generated pulse is weak and will not propagate to the latch. Figure 2.7(b) shows that if the one of the inputs of the or gate is set high in that case the patch of the fault is not logically enabled and hence it will not cause an error. The case of latch-window masking is shown in Figure 2.7(c). Although the glitch generated by particle strike is strong enough if it is not latched (in this case the rising clock pulse in edge trigger flip flop), it will not cause soft error.

2.6.4 Evidence of Soft Errors

Soft errors due to cosmic rays have already had an impact on the microelectronics industry. The existence of this problem in space applications was reported in the early 1950s [28]. Due to high solar activity in 2003, 28 satellites were damaged, out of which 2 were unrecoverable [23]. More recently, on October 7th, 2008, an Airbus A330-303 operated by Qantas Airways, en route from Perth to Singapore, suffered a failure. When incorrect data entered the flight control systems, the plane suddenly and severely pitched downwards, injuring 110 passengers and nine crew members [24]. And now the potential havoc caused by this invisible threat is growing as more airborne microchip-based devices are used in drones, aircrafts, spacecrafts and satellites every year.

The threat on the ground is growing too, a number of commercial computer manufacturers have reported that cosmic rays have become a major cause of disruptions at customer sites [25, 26].

In early 2000, Sun Microsystems's Ultra SPARC II workstations were crashing at an alarming rate. The root cause of the problem was traced back to IBM supplied SRAMs that were experiencing upsets due to soft errors. As a result, Sun had to switch memory vendors and also designed error detection and correction mechanisms for their caches [27]. In 2003, due to increased solar activity, the Q cluster located at Los Alamos, recorded highest ever 26.1 errors a week [23]. Soft errors have been blamed for 4096 extra votes being counted by an electronic voting machine in the county of Schaerbeek, Belgium, in 2003 [164, 165], and for repeatedly bringing the $1 billion Cypress Semiconductor Corporation factory to a halt [28].

Modern servers can host hundreds of virtual machines (VMs). While individual VMs may not be mission critical, a system crash that could affect a hundred virtual machines can quickly become a significant outage. On a system without advanced reliability features, CPU and memory errors can cause a system to have a long downtime. This downtime can significantly impact the e-commerce industry. Failure to provide robustness can lead to change in the consumer behavior [100].

The number of chips around us are increasing due to proliferation of semiconductor devices in everyday life, by 2020 it is expected to have 50 billion networked devices [166]. Increase in the number of transistors per user implies increase in the number of soft errors per user for the foreseeable future. We will discuss the existing techniques to prevent soft errors in logic and memory components in Chapter 7.

2.7 Parameters Affecting Soft Error Rate

In this section we will discuss and provide a comprehensive summary of the important parameters responsible for causing a soft error. Ultimately, we will also see how these parameters affect the resulting soft error rate.

Table 2.2 shows the parameters related to the properties of the impacting particles which are the root cause of soft errors. The energetic particle flux depends on altitude and geographical location. Moreover, not all particles cause soft errors, to cause soft error impacting particle must carry enough energy and it has to transfer its energy to generate enough charge to cause a fault, this energy transfer depends on the particle incident angle and its charge production capability. Because of these factors neutrons with less than 10 MeV energy are harmless [17, 137, 140].

Properties of the semiconductor devices or the material also play a role in deciding the occurrence of soft error. The location of particle strike (i.e., strike on the p–n junction, biased region etc.) determines how much charge will be deposited [146, 167, 168]. The doping concentration along with the track length and track angels of the particle also affect the charge collection capacity [169–172].

Each circuit node forms a capacitor and stores a specific amount of charge. Nodal charge determines the Q_{crit} which is exponentially related to the soft error rate (see Equation 2.2). Upon a particle strike a current pulse is generated. The wider

Domain	Parameters
Energetic Particle Properties	• Particle sources and type, Atomic weight, Number of simultaneously produced secondary particles • Particle energy, Particle flux, Incident angle and energy, Charge production capability
Device or Material	• Position of impact, Track lengths, Track angles • Stopping power or LET • Doping Concentration, Charge collection capacity
Circuit	• Nodal Capacitance, Sensitive area, Critical charge (Q_{crit}), Resulting shape of the current pulse • Operating voltage, Frequency, Temperature, Parametric variations • Masking rate (Electrical, Logical and Timing masking)
Microarchitecture	• Operating voltage and frequency, Thermal profile, Parametric variations • Microarchitectural masking rate (e.g., Dead instructions, Unused structures etc.)
Chip	Packaging material, Process technology
Environmental	Altitude, Geographical location

TABLE 2.2: Parameters that affect the soft errors and impact the overall soft error rate

current pulse with higher magnitude are more likely to cause a soft error. Apart from that in circuit or microarchitecture domain the operating voltage, frequency, temperature and parametric variations also affect the soft error rate.

Parameter Trend	Parameter	Soft Error Rate
Increase	Particle flux	Linear increase
	Temperature	Exponential increase
	Frequency	Linear increase
Decrease	Q_{crit}	Exponential increase
	Sensitive Area	Linear decrease
	Voltage	Exponential increase

TABLE 2.3: Impact of important parameters and corresponding impact on soft error rate

Table 2.3 enlists the parameters that have the most significant impact on the soft error rate. According to the equation 2.2, the soft error rate is related to

the particle flux, the sensitive area and the Q_{crit}. However, reducing the supply voltage of the circuit reduces the Q_{crit} and decreasing Q_{crit} exponentially increases the soft error rate. Also, decreasing the area of sensitive region may decrease the soft error rate. However, reduced cell area implies reduced nodal capacitance (i.e., reduced Q_{crit}) and it is usually accompanied with reduced supply voltage which cancels out the positive impact of smaller sensitive area on soft error rate.

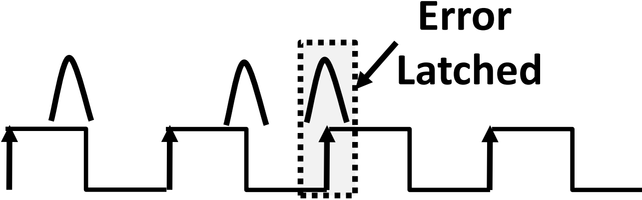

(a) At normal frequency only one fault gets latched others are masked

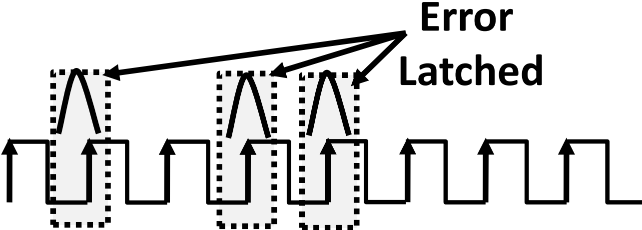

(b) Doubling the frequency can latch all the faults causing errors

Figure 2.8: Impact of frequency on soft error rate

Soft errors in memory and some sequential logic are frequency independent [173] but soft errors in combinational logic are frequency dependant. Increasing frequency increases the probability of latching more faults as shown in Figure 2.8. Increasing the frequency causes all the faults to be latched causing errors as shown in Figure 2.8(b). The soft error rate of combinational logic increases linearly with increasing frequency [174].

Moreover, soft error rates depend on the resulting current pulse widths. Increase in temperature leads to an increase in current pulse widths due to parasitic bipolar charge collection. Wider current pulse deposits more charge [175]. At higher temperature the drain current decreases that in turn reduces the Q_{crit}. This combined effect due to increased temperature may cause more than $3\times$ increase in soft error rate [176].

2.8 Soft Errors and Future Processors

Apart from the parameters of Table 2.2 in Section 2.7, the way future processors are going to be designed have a significant impact on the soft error rate.

2.8.1 Impact of Technology Scaling

We will see how the technology scaling affects the soft error rate in future processors.

2.8.1.1 SRAM

Recall the Figure 1.1 from Chapter 1, which shows the effect of technology scaling on the soft error rate of an SRAM cell and an SRAM system (e.g., cache). The soft error rate of an SRAM cell is almost constant. The SRAM system soft error rate which roughly doubles every technology generation. This increasing trend is because of the increase in the number of transistors following Moore's law [29, 33, 34].

A particle strike may cause single bit upset (SBU) if it affects only one memory cell. Although, SBU is the most common failure scenario for memories, with reduced device dimensions now particles can simultaneously cause multiple bit upsets (MBU) [48, 87, 88]. The phenomenon that explains bit inversions remains the same for both cases [117]. However, the literature indicates that two adjacent bits being upset by a single particle strike is ten times less probable than a single cell upset, and the probability of three bits being upset is one hundred times less likely than a single bit upset [32, 80, 87, 88, 177–179]. Although the probability of MBU is low it is predicted to increasing with technology scaling. MBUs rate have increased by a factor of four when scaling from 90 nm to 65 nm [87, 88].

2.8.1.2 DRAM

Figure 2.9 shows how the soft error rate of a DRAM cell and the logic scale for different technology generations [17, 180]. DRAM cell soft error rate is trending downwards (a reduction of 4 to 5$\times$ per generation). It is mainly because of the

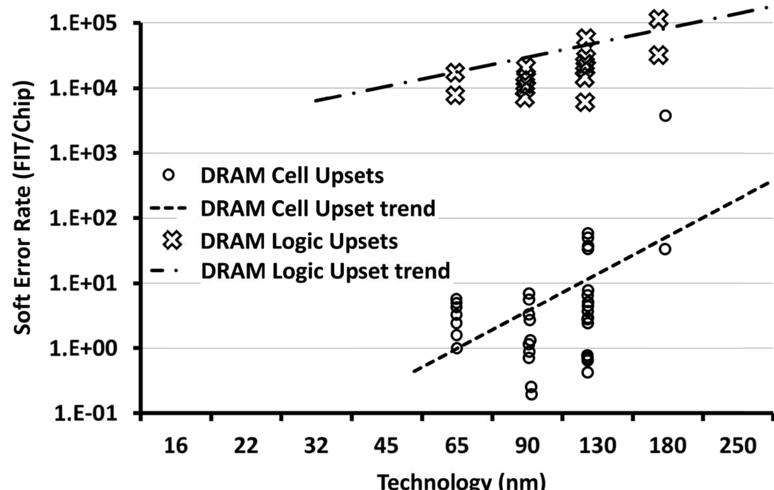

FIGURE 2.9: DRAM bit soft error rate for different technology nodes [180]. The soft error rate of a DRAM bit is predicted to decrease. The soft error rate of a DRAM memory system has traditionally remained constant over technology generations moreover, it is predicted to be dominated by the soft errors in the DRAM peripheral logic.

reduction in charge collection capacity due to reduced cell area which has more dominant effect on the resulting soft error rate compared to the reduction in Q_{crit} due to voltage scaling.

Although the DRAM bit SER has decreased by more than 1,000× over seven generations, the number of memory cells in a DRAM system increased almost as fast as the soft error rate reduction for each memory cell that technology scaling provided. Therefore, the DRAM system SER has remained essentially unchanged [17]. Figure 2.9 also show the trend in the soft error rate of peripheral logic in DRAM. In DRAM memory systems soft error rate of peripheral logic is becoming more significant.

Similar to SRAM memory cells, in the DRAM memories multiple bit upsets are less probable compared to the single bit upsets. However, DRAM memories are becoming denser and with technology scaling the probability of having MBUs is increasing [180–183].

2.8.1.3 Logic Components

With decreasing feature sizes, the relative contribution of logic soft errors increases mainly because of following reasons: (i) Logic gates are typically wider devices but with more rapid technology scaling reduced sizes result into reduced Q_{crit}

of combinational logic compared to SRAM, (ii) with decreasing gate delays the propagation power of transient pulses is increasing and fewer error pulses will attenuate before resulting into an error, (iii) with increasing degree of pipelining in advanced processors, the clock cycle window will reduce significantly without changing the setup and hold time of the latches. This will result in more faults to be latched causing errors and (iv) soft error rate in combinational logic increases linearly with increasing frequency while soft error rates of SRAM, DRAM and latches are frequency independent.

It is also important to notice that most of the mainstream microprocessors are equipped with ECC to reduce soft error rate of caches (SRAM) and the main memory (DRAM). When large portions of the on-chip caches and the memory elements on the chip are protected, logic will quickly become the dominant source of soft errors.

As we already saw in Section 2.8.1.1, the soft error rate per device (e.g., SRAM cell) in a bulk CMOS process is projected to remain constant and this will cause increase in the soft error due to increased number of transistors in multicore processors. To handle the increasing soft error rate designers have considered using different technologies.

2.8.2 Impact of New Technologies

We will see how adapting new technologies for designing future processors and memories affect their soft error rate.

2.8.2.1 Silicon on Insulator (SOI)

A lot of research has been done to explore soft errors in *silicon–on–insulator* (SOI). Unlike bulk CMOS, SOI devices collect less charge from an alpha or neutron particle strike because the silicon layer is much thinner. Experiments on partially–depleted SOI SRAM devices reported 5× reduction in soft error rate [184, 185]. However, this improvement in sequential and combinational logic is unclear. A fully depleted SOI can further reduce the soft error rate by almost eliminating the silicon layer. But manufacturing of fully depleted SOI chips is still a challenge [185].

2.8.2.2 Multigate-FET Devices

As the bulk CMOS is reaching its scaling limits, FinFETs and multigate-FETs (e.g., Tri-Gate FET) devices have been popularized as promising candidates to keep harnessing the benefits of Moore's law. Due to their many superior attributes, especially in the areas of performance, leakage power, intra-die variability, low voltage operation (translates to lower dynamic power), and significantly lower retention voltage for SRAMs, FinFETs are replacing planar CMOS as the device of choice especially in sub–32 nm technologies [186–189].

Upon a particle strike on a planar bulk CMOS device, a lot of generated charge can reach the drain of the device and collect there, causing enough current to upset the storage node. In FinFET devices, the conduction is mainly in the channel and, hence most of the charge dissipates in the substrate and will not collect at the drain. It is worth noticing that for the same technology node, the Q_{crit} of FinFET SRAM and planner CMOS SRAM are same. However, due to reduced charge collection, compared to planned CMOS device, 15× reduction in soft error rate of Tri-gate FinFet devices has been reported using device simulations at terrestrial flux [190].

The soft error rate of FinFET devices depend on their manufacturing process and the measurement technique. Laser and heavy-ion testing of Tri-Gate devices manufactured at IMEC indicated that the sensitive area for charge collection in bulk FinFETs is significantly larger than the actual fin's structure, increasing the probability of single event upsets in the cell [191]. On the contrary, proton beam testing of the 22 nm Tri-Gate SRAM and sequential logic devices observed 1.5–4× reduction in soft error rate compared to 32 nm planner bulk CMOS [192]. Study also shows that in Tri-Gate technology a modest increase in combinational soft error rate relative to sequential soft error rate. Overall, even with Tri-Gate devices unprotected logic will continue to dominate the soft error rate [192].

2.8.2.3 Non-Volatile Memories

Many memory cell technologies are being considered as possible replacements for DRAM mainly because they are nearing their scaling limits. DRAM scaling is especially challenging for sub–30 nm [193, 194].

Phase change memory (PCM), *spin-transfer torque* (STT-RAM), *ferroelectric RAM* (FeRAM or FRAM), *magnetoresistive RAM* (MRAM) etc. promise high density, better scaling, and non-volatility, however, they introduce several new challenges.

DRAM uses a capacitor to store charge and can be upset by an energetic particle strike causing soft error. Resistive memories (PCM, STT-RAM, FRAM and MRAM), which arrange atoms within a cell and then measure the resistive drop through the atomic arrangement, are promising as a potentially more scalable replacement for DRAM.

Because the FRAM cell stores the state as a piezoelectric polarization, an alpha hit is very unlikely to cause the polarization to change cell's state and the MRAM terrestrial soft error rate needs more measurements. PCM cell arrays may not be vulnerable to soft error due to particle strikes but they experience soft errors caused by resistance drift and spontaneous crystallization resulting from gradual atomic motion at high temperatures [195]. A recent study [196] predicted the failure rate of PCM to be 10^9–10^{11} times higher compared to DRAM. Moreover, soft error specific studies for resistive memory technologies do not consider the possibility of soft errors in peripheral circuits which will still use the CMOS transistors [197]. The future solutions for handling soft errors will have to adapt to these new technologies and should be able to protect the peripheral circuits as well [198].

2.9 Calculating SER to Make Architectural Decisions

We discussed how we can compute the soft error rate by computer simulations in Section 2.5. We also quantified the soft error rate in equation 2.2. However, not all the particle strikes can cause soft errors. As we have seen in Section 2.6.3, most of the faults induced by particle strikes are masked. In this situation the equation 2.2, which does not take the masking effects into consideration, gives a very pessimistic estimation of soft error rate. Overly pessimistic estimate of soft error rate may lead to overdesign for reliability and incur huge area, power and performance overheads. For this reason it is important to derate the soft error rate.

To obtain the soft error rate under the masking effects, two main methodologies are used: statistical fault injection and architecture vulnerability factor (AVF) analysis.

2.9.1 Fault Injection:

Fault injection is a way to quantify the reliability of a microarchitecture by injecting faults in each state and examining the outcome. In this brute force approach the number of possible faults to be injected can be astronomical depending on the number of states. Moreover, identifying all the combinations of the possible fault locations and the instances at which the fault can occur in a given set of workload is challenging and complex. Also, to observe the effect a fault has on the final outcome it is necessary to run a complete simulation and observe any abnormal behavior due to the injected fault.

One way to optimize the method is by using a subset of faults to observe the possible outcomes and provide enough statistical confidence in the estimated soft error rate. In sampled fault injection the accuracy is traded off for simulation time [199]. More number of simulations are required if a higher degree of confidence is necessary. Moreover, depending on the design if many corner cases are to be observed then each corner case requires its own set of injected faults for the required confidence.

2.9.2 Architecture Vulnerability Factor (AVF) Analysis:

Architectural vulnerability factor (AVF) is a probability that a user visible error will occur given a bit flip in a storage cell or a glitch in combinational logic. The underlying concept in AVF computation is knowing if a particle strike on a bit matters or not. The fraction of the bit flips that affect the program outcome is captured by AVF. The AVF has a significant impact on the effective soft error rate. The higher the AVF of a structure implies a higher probability of having soft error in that structure.

AVF analysis is performed via architectural simulations. Architectural simulations of a processor is fast and abstract. Moreover, the reliability analysis can be done at design time and hence a detailed RTL or a test chip is not required. By performing

AVF analysis designers can rank the structures based on their vulnerability in a very early stage of design.

The AVF of a processor is related with the FIT rate in the following manner:

$$FIT = FIT_{Raw} \times TVF \times Size_{structure} \times AVF \tag{2.3}$$

The raw soft error rate (FIT_{Raw}) depends on the circuit characteristics and it can be obtained by accelerated soft error rate measurements. *Time vulnerability factor* (TVF) is the fraction of cycle during the circuit is vulnerable. For an example, TVF of an SRAM memory cell is 1, however if a latch is accepting data rather than holding data, a strike on its stored bit may not result into an error, because the erroneous data that was stored will be overwritten by the correct new input data. If the latch is accepting data 50% of the time, the latch is vulnerable only for the 50% of the time it is operational. TVF is dependent on the circuit and frequency. Once we have determined raw FIT rate it has to be derated by TVF. Finally, the effective FIT rate of a circuit is shown in Equation 2.3. It is the product of its raw FIT rate, TVF and AVF.

AVF analysis vastly relies on identifying masked faults and it provides a conservative estimate of processor's reliability. Although it is not accurate, it can help reliability designers. Substantial amount of research has been done in efficiently modeling the AVF of different microarchitectural structures [39, 98, 117, 162, 200–205].

In this work, we implement the AVF model similar to [97]. In Chapters 5 and 6, we use AVF to identify the vulnerable structures for providing protection. Notice in Equation 2.3 that AVF and FIT rate are directly related. If the structure is more vulnerable its AVF increases and it results into increased FIT rate and vise versa. We show how the proposed architecture can significantly reduce the AVF and in turn improves the overall reliability.

Chapter 3

Error Detection using Acoustic Wave Detectors

In this chapter we first study and compare several particle strike detectors. A detailed discussion of the structures, design issues related to several particle strike detectors and their comparison of area, power and performance overhead is given in Section 3.7. We then propose to adopt acoustic wave detectors as a method to detect such particle strikes by detecting the shockwave they generate upon an impact on silicon. We present the structure of the acoustic wave detector and discuss its properties in detail. Next, we will show how to use the acoustic wave detectors in order to precisely locate the particle strike. We will describe different algorithms to precisely locate the particle strikes. Finally, we will present a case study to evaluate how the architecture with acoustic wave detectors performs in detecting and locating particle strikes on a *state of the art* processor core.

3.1 Particle Strike Detectors

Several particle strike detector based techniques have been proposed. These detectors detect particle strikes via detection of voltage or current glitches [132–134, 206] or via detection of the sound [135].

We studied the challenges in adapting the detector based techniques for soft error detection. We compared them based on following parameters,

- Hardware cost, area and power overheads
- Detection latency
- False alarms : False positive is an event when detector triggers indicating an error without any actual error.
- Fault coverage in a processor
- Design cost

Error detection using particle strike detectors involves adding physical redundancy to the protected circuit. Depending on the number of required detectors used to detect particle strikes the overall area overhead varies. Moreover, the detectors are required to be connected to a controller circuit and interconnecting the detectors further increases the area overhead. Due to added hardware the power overhead is also increased.

Detection latency can be defined as the time between a particle strike and when the first detector triggers. Detection latency is important for providing error containment. Efficient error containment restricts the spread of error to a specific region. By containing the error we prevent the error to be visible to the user before its detection and avoid SDC. Error detection with lower detection latency is desirable to avoid SDC. Once the error is detected, a hardware or software mechanism would trigger the appropriate recovery action for correction (e.g., checkpointing).

False alarms include the false positive events for the given detector type. Fault coverage metric indicates the structures a given particle strike detector can cover. In other words some detectors can only detect particle strikes in only SRAM memory cells while some detectors can detect particle strikes in both memory components as well as logic. The detectors that protects memory and logic has higher coverage than the detectors that can protect only memory or only logic. And finally design cost which represents the intrusiveness of the design for including the detectors. It covers the necessary changes required in the process technology, layout, placement and routing etc.

Detector Type		Covered Structure		Detection Latency @2GHz	False Alarms	Fault Coverage	Area Overhead	Power Overhead	Design Cost
		Memory	Logic						
Current Sensing	BICS [132, 206]	✓	✓	~ 3 cycles	Low	High	29%†, 15%* [206]	100%* [206]	Moderate
	Current Mirror [207]	✓	✗	$3-6$ cycles	Moderate	High	$16-20$% [207]	$2-47$% [207]	Moderate
Voltage Sensing	Voltage Monitor [134]	✓	✓	$1-3$ cycles	High	High	20%†, 7%* [134]	20%* [134]	High
Metastability Sensing	BISS [133]	✓	✓	$3-4$ cycles	High	High	45% [133]	High	Moderate
Shockwave Sensing	Acoustic Wave Detectors [135, 208]	✓	✓	$30-100$ cycles$^{\mp}$	Low	100%	<1%	Low	Low
Charge Sensing	Si-PIN Detectors [209–211]	✓	✓	1000s of cycles	Low	High	>100% [209]	>100% [209]	High
	Heavy-ion Detectors [212]	Only DRAM	✗	100s of cycles	Moderate	High	Moderate	Moderate	Low

TABLE 3.1: Comparing different particle strike detectors. † while protecting memory, * while protecting combinational logic, $^{\mp}$ the detection latency is bounded and configurable.

Considering all these parameters mentioned above, an ideal solution would be the one that has minimum area & power overheads and the least detection latency. It would have minimum false negative rates so it can guarantee detection of all strikes. It should cover all the possible sources of particle strikes (i.e., alpha, neutrons, etc.). It can detect particle strikes in both logic and memory components. Finally, the solution should pose no major challenges in the implementation process, placement and routing etc. to minimize design cost. We summarize our study in Table 3.1.

As can be seen in Table 3.1, schemes for particle strike detection via the detection of voltage or current glitches [132–134, 206, 207] provide short detection latency and provide good coverage. However, their area and power penalties are high. They also pose design challenges in terms of selective insertion while providing maximum fault coverage at minimum area penalty.

Charge sensing techniques [209–212] for detecting particle strikes via the detection of deposited charges are very effective but cost more than 100% in area and power overhead.

The overheads in terms of area and power penalty while using acoustic wave detectors are low. Moreover, acoustic wave detectors provide bounded and configurable detection latency. The error is detected within a fixed number of cycles that is known a-priori or can be set by the designer. Acoustic wave detectors act as *unified error detection* mechanism and can detect particle strikes in both logic and memory components. Based on this survey, we conclude that acoustic wave detectors based on cantilever structures are the most attractive solution [135].

Detecting the right particle: At 45 nm technology, any particle strike that will result into a silicon recoil energy less than 10 MeV will not induct enough charge to create an upset in the memory [20, 141, 149]. Therefore, we need to size the cantilever accordingly, in such a way that it only detects particle strikes that result into a silicon recoil energy larger than 10 MeV and therefore avoiding false positive detection [137]. By calibrating the acoustic wave detectors it is possible to detect only those particle strikes that are capable of generating single event transient (SET) in logic or a single event upset (SEU) in memory. The same detectors can be used for memories as well as logic components [20, 32].

3.2 The Microelectromechanical Ears: Acoustic Wave Detectors

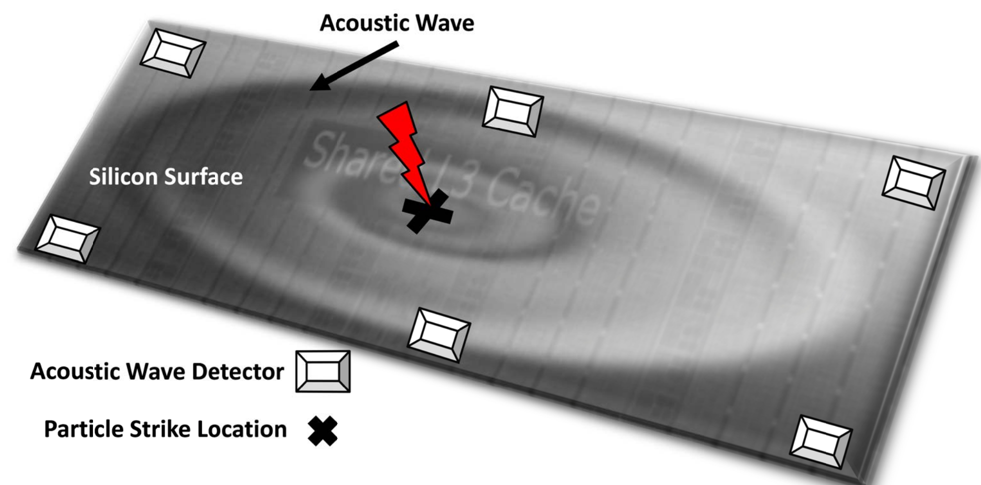

FIGURE 3.1: Transformation of the energy of particle strike upon its impact on silicon surface into acoustic shock wave

Recall from Section 2.3.2 in Chapter 2 that particles with recoil energies of 10 MeV or higher are capable of causing upsets in the circuits. When a cosmic ray collides with a silicon nucleus this energy is released in a very short span of time ($\leq 1ps$). This rapid recombination process results into a cloud of phonons spreading out of the impact site. Hence the cosmic ray is transformed into an intense shock wave as shown in the Figure 3.1. Such a shockwave travels at the speed of 10km/s on the silicon surface [213].

We propose to use cantilever like structures [214, 215] as an acoustic wave detector to detect particle strikes through the sound they generate. To be able to detect the impact of the cosmic particle, the cantilevers must perform two contradictory tasks:

1. For detecting all potent particle strikes that may cause soft errors the cantilever based detector must absorb as much energy as possible resulting due to the collision. This implies a thick pliable structure composed of a high density, high-impedance material, such as gold.

2. For efficient detection at a distance and to avoid thermal noise, the pliable structure must maximally deflect for the given energy deposition. Thus, the levers should be light in weight and highly flexible.

3.2.1 Structure and Properties of Device

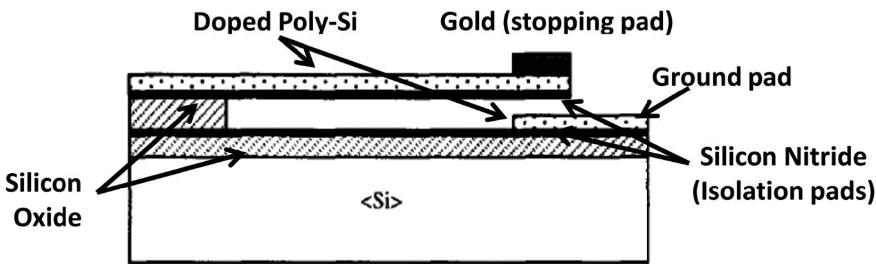

FIGURE 3.2: Cantilever beam like structure of acoustic wave detectors [214]. A particle strike is detected by sensing the deflection of cantilever beam.

Figure 3.2 shows the typical structure of an acoustic wave detector. These devices are rectangular structures of beams and plates on the silicon surface. A doped polysilicon grounding layer forms the lower plate of the sensing capacitor. Silicon oxide serves as the isolating layer between lever and substrate. The fabrication and placement of these detectors on the surface of active silicon can be performed without much complications [215, 216].

The particle strike is detected by detecting the change in the capacitance of the gap between the cantilever and the ground pad of the detector structure as shown in Figure 3.2. A simple capacitance detector can be designed based on a relaxation oscillator [217, 218]. A simple microcontroller can be used for the same purpose. More accurate and faster capacitive detectors circuits can be constructed that are able to detect changes in capacitance on the order of 10 attofarads [219].

The proposed cantilevers occupy an area of one square micron [142], which is roughly the area of one bit (a typical 6T SRAM cell) at 45 nm. The cantilever is designed such that it detects particle strikes that generate silicon recoil with more than 10 MeV energy. The cantilever can detect shockwave of sound at a distance of 5 mm from the source of the sound [142]. This means that our selected cantilever can cover an area of 78.5 square millimeters. This area is equivalent to the die area occupied by the last-level cache in a Core™i7 microarchitecture at 45 nm technology [220].

These micromechanical levers of desired dimensions can be fabricated by microelectronic fabrication techniques [214, 221]. Acoustic wave detectors adopt silicon based fabrication that is similar to IC fabrication technology. This makes it feasible for detectors to be integrated with the rest of the circuitry on the same

chip [222, 223]. Cantilever based devices of varying lengths have been developed and used extensively to study bio-interactions at atomic level [216, 224, 225].

3.2.2 Calibrating the Detector

The length of the cantilever beam is very important in detecting the cosmic particle strike. Too long or very small lever dimensions would not be efficient in detecting the desired particle strikes. Moreover, failing to calibrate the cantilever device may cause false positives.

3.2.2.1 False Positives

Precise calibration of acoustic wave detectors will lead to zero false positives. Failing to properly calibrate the detectors would result into false positives (i.e., detectors' trigger for the particles that do not carry enough charge to create a soft error). Also, the analysis of false positives due to process variations, temperature variations, aging and distance between strikes and cantilevers is beyond the scope of the thesis readers may refer to [214, 221].

Also recall from Chapter 2, that many of the faults induced due to energetic particle strikes will not cause an error because of several masking effects. If a circuit has zero fault masking, all the faults will cause soft errors.

However, in a scenario where 100% faults are masked the solution with acoustic wave detectors will have false positives. The flux of energetic particles at sea level is approximately 14 neutrons/(cm^2-hr), *an improbable scenario of detectors triggering for every harmless particle strike (which also gets masked not causing an error) would imply detecting 1 false positive every 1.3 minutes for a modern general-purpose multi-core processor.*

Increased false positives cause high performance penalty due to frequent error recovery actions. Figure 3.3 shows the performance impact of recovery due to false positive error detection for checkpointing techniques in different granularities. As you can see in the figure saving the checkpoints in the cache has very similar cost as recovering only registers (i.e., microarchitecture checkpoint/recovery) [226–229, 234]. As you include more structures in the checkpoint the cost

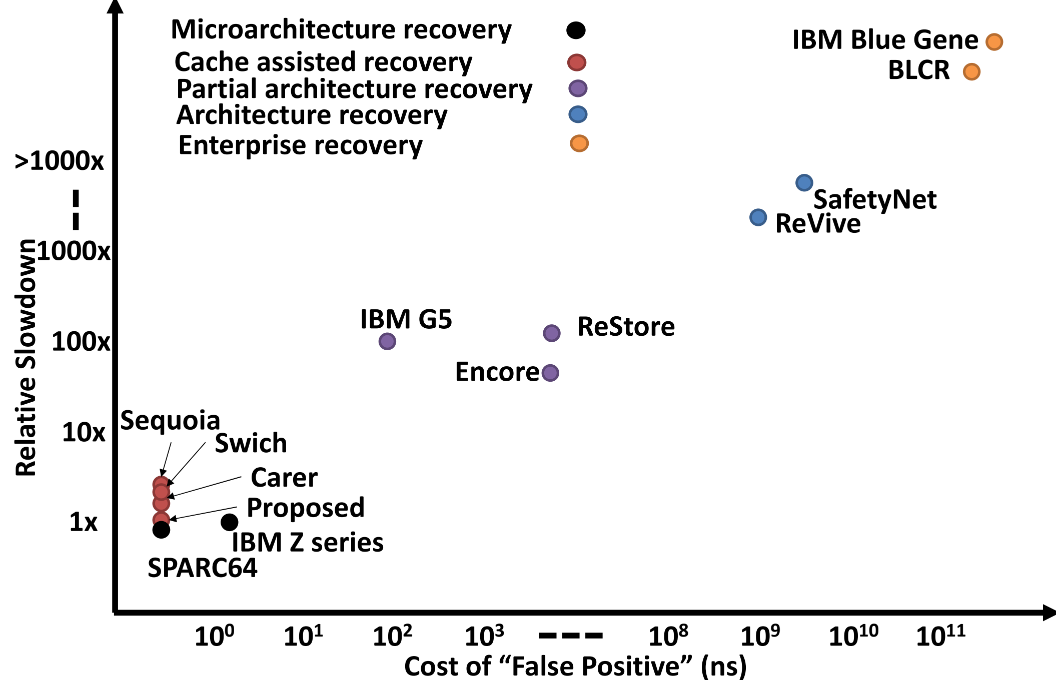

FIGURE 3.3: A comparison of relative slowdown due to false positive recovery for different recovery techniques: Seqoia [226], Swich [227], Carer [228], SPARC64 [229], IBM Z series [59], IBM G5 [58], Encore [230], ReStore [231], ReVive [102], SafetyNet [107], IBM Blue Gene [232], BLCR [233]

of recovery increases as in the case of techniques proposed in [230, 231]. Recovery techniques at architecture level or at system level incur approx 1000× slowdown compared to microarchitecture or cache assisted checkpointing/recovery [102, 107]. The recovery in petascale systems can take significantly long time before a normal operation can resume severely impacting their performance and availability [58, 232, 233, 235].

Now that we are familiar with the structure of the acoustic wave detector we will next discuss how we can use them for error detection.

3.3 Soft Error Detection via Detecting Particle Strikes

In this work, the fundamental idea is to detect the particle strikes via mechanical deflection of acoustic wave detectors. From functionality point of view one such

acoustic wave detector is analogous to one parity bit. The potential of the detectors will be exploited by:

1. Detecting errors in the unprotected logic and memory components and therefore, reduce the SDC FIT rate.

2. Deploying less number of detectors than the required parity/ECC bits in already protected memories and accurately localizing the particle strikes/bit flips in memory arrays.

We discussed that the cantilevers can be used for detecting the *existence* of particle strikes on the silicon surface. The acoustic wave detectors can be placed on or off the chip but on the same silicon surface.

Traditional processor cores have surface are of a few square millimeters. Recall that acoustic wave detectors have a detection range of 5 mm. It means that just one acoustic wave detector is enough for error detection on an entire processor core or a last level cache of Core™i7 microarchitecture.

Acoustic wave detectors detect all soft errors due to alpha and neutron strikes. However, not only the detection of the error but how soon the error is detected is also very important. Recall from Section 3.2, that the sound wave traverses the silicon lattice at 10 km/sec. This means that if only one acoustic wave detector was used, in the worst-case a particle strike occurring at 5 mm away would be detected in 500 ns (or 1000 cycles in a processor running at 2 GHz). By putting more acoustic wave detectors on the surface of silicon, it is possible to reduce the worst case detection latency.

So far, we discussed the use of acoustic wave detectors for detecting the particle strikes on the silicon surface. Now, let's see how to use the acoustic wave detectors in order to precisely locate the particle strike.

Why Locate Particle Strikes? Using the acoustic wave detectors, we can only detect all the particle strikes and hence avoid possible data corruption. However, locating the particle strikes are equally important. Once the error has been detected, a hardware or software mechanism would trigger the appropriate recovery action for error correction. To provide successful error correction or recovery, the system must know the precise location of the error. This can be done by exploiting the localization accuracy of acoustic wave detectors to detect and correct the

errors. Once the accurate location is found the system can take available recovery action. For instance, if the error has occurred in one of the bits in the cache we may correct the error by flipping the bit.

Next, we present an architecture to precisely locate the particle strikes using acoustic wave detectors.

3.4 Location Estimation of a Particle Strike

The estimation location of the particle strike and latency of detection depends on the following parameters:

1. How many acoustic wave detectors are required to be able to locate the particle strike?
2. Where the acoustic wave detectors should be placed?
3. What is the accuracy of the found location?
4. What is the latency in detecting the particle strike?

Unlike GPS, any apriori knowledge of the spatio-temporal information about the impacting particle strike is unavailable. This means that we do not know the actual time span between the particle strikes and when the detectors trigger. The only information we have is the relative *time difference of arrival* (TDOA) [236] of the acoustic wave generated by the strike among different detectors.

TDOA technique estimates the difference in the arrival times of the signal from the particle strike at multiple receivers. A particular value of the time difference estimate defines a hyperbola between the two receivers on which the particle strike may exist, assuming that the source and the receivers are co-planar as shown in Figure 3.4. If we have another receiver in combination with any of the previously used receivers, another hyperbola can be defined and the intersection of the two hyperbolas results in the position location estimate of the particle strike. This method is also sometimes called a hyperbolic position location method [236, 237]. TDOA method offers many advantages. It does not require complex receivers, we use simple acoustic wave detectors as receivers. It does not require any special type

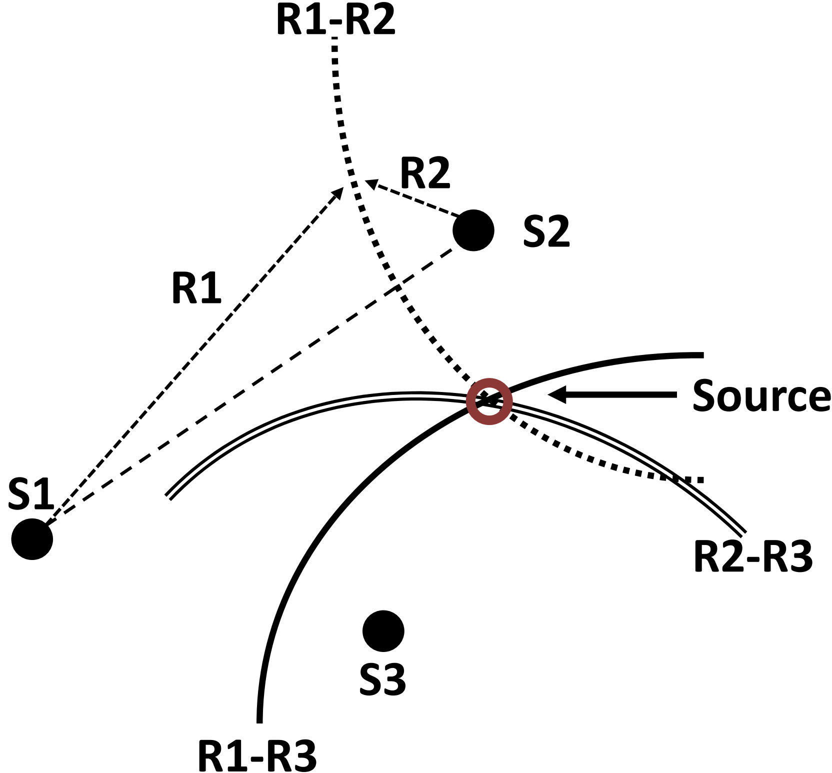

FIGURE 3.4: TDOA hyperbolas in a system and location of source. Dashed hyperbola is formed using only two detectors S_1 and S_2. Including a third detector S_3 can successfully locate the source via intersecting hyperbolas.

of antennas, hence it is cheaper to use it in existing processors. Moreover, multiple TDOA readings can also provide immunity against timing errors and noise as we will see later in this chapter.

Let us assume that a particle strikes at location (X_a, Y_a). Therefore, a system of two equations is required to solve both unknowns. Hence, a minimum of three detectors are needed: with three detectors we obtain two TDOA measurements, which allows us to derive the required equations.

Hyperbolic position location estimation. The estimation of the location is carried out as follows:

- The acoustic wave detectors can be placed on or off the protected area but on the same silicon surface. Notice that the coordinates of the acoustic wave detectors are known.
- Once the strike is detected, we measure the TDOAs of the sound between pairs of detectors through the use of time delay estimation.

- Using the TDOA measurements we construct the system of hyperbolic equations.
- Once the equations are formed, efficient algorithms are applied to obtain a solution to these hyperbolic equations, which represent the estimated position of the particle strike.

3.4.1 Example

To illustrate the particle strike detection and localization problem, a simple case of particle strike localization using 3 acoustic wave detectors is discussed.

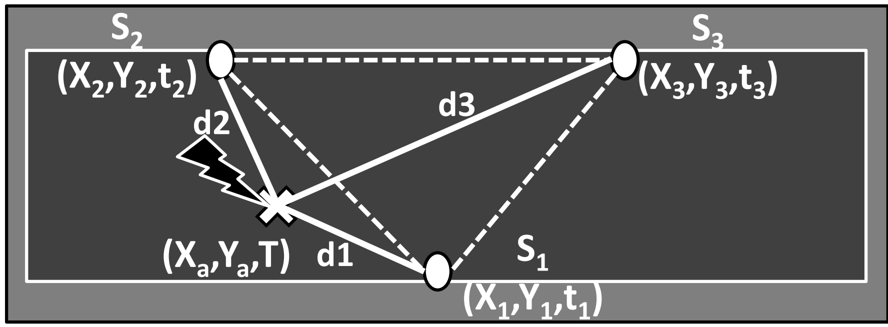

FIGURE 3.5: Strike detection and localization via triangulation using TDOA measurements of acoustic wave detectors

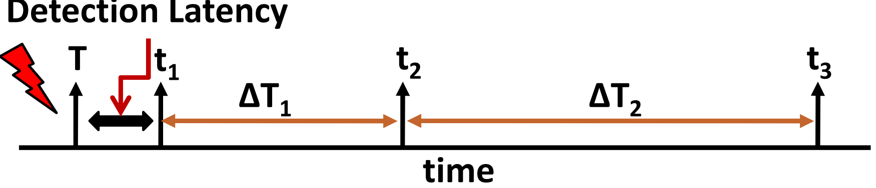

FIGURE 3.6: Timeline of the events following the particle strike

Figure 3.5 displays three acoustic wave detectors (S_1, S_2 and S_3) placed at known coordinates (X_1,Y_1), (X_2,Y_2) and (X_3,Y_3) respectively on the surface of the chip. Let's assume that a particle strike occurs at an unknown time T at unknown location (X_a,Y_a). As shown in Figure 3.5, d_1, d_2 and d_3 are unknown absolute distances from the detectors S_1, S_2 and S_3. Once the strike has occurred, the ripples of phonons will traverse outward in a circular manner and the closest detector from the strike will trigger first. In this case S_1 will trigger at instance t_1.

After that, as the phonons traverse further, other detectors S_2 and S_3 will trigger at instances t_2 and t_3 respectively. A timeline of the events is shown in Figure 3.6.

3.4.2 Obtaining TDOA

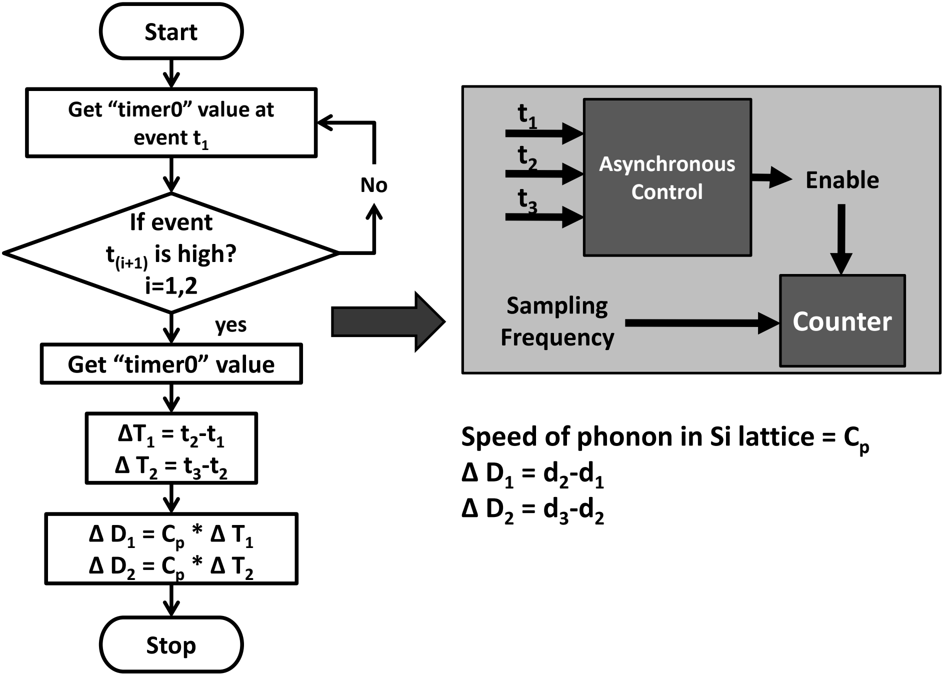

FIGURE 3.7: Strike detection algorithm (firmware) and a hardware control mechanism

Figure 3.7 shows a simple system which can measure the timing differences of the acoustic waves' arrival. The hardware consists of an asynchronous control (e.g., multiple logic OR gates or a multiplexer circuit) which generates an output *Enable* signal.

Enable is high whenever one of the triggered detector raises a flag, and activates the sequential counter that counts the number of clock pulses between two consecutive triggering detectors. The counter runs at the *sampling frequency*, which is a design parameter.

As the speed C_p at which acoustic waves traverse on the silicon surface is known (recall Section 3.2 of this chapter), using the measured timing differences of the arrival of the acoustic waves, we can compute the distance differences ΔD_i.

Errors in measurements. The effect of errors in the measurements of timing differences due to the sampling frequency cannot be ignored. We use the example

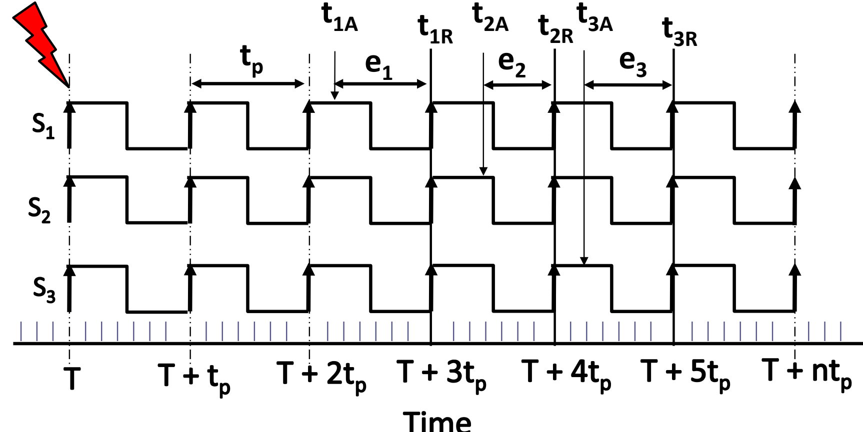

FIGURE 3.8: Sampling errors in the measurements of the time difference of the arrival at the acoustic wave detectors

depicted in Figure 3.8 to illustrate such case: the three detectors S_1, S_2 and S_3 are in synch with each other and are being sampled at the rising edge of the clock with sampling period t_p. The actual arrival times of the acoustic wave generated due to particle strike at detectors S_1, S_2 and S_3 are t_{1A}, t_{2A} and t_{3A} respectively. However, the signal will be read only at the rising edge of the clock pulse (i.e., at the instances t_{1R}, t_{2R} and t_{3R}) by the detectors. This introduces error in the measurements of the time differences.

Assume a particle strike occurring at an unknown instance T, sampling period t_p and the actual arrival time of the acoustic wave generated due to particle strike at detector S_i is t_{iA}. The sampling error e_s at the acoustic wave detector S can be expressed as:

$$e_s = t_p - [(T + t_{iA}) \bmod (t_p)] \tag{3.1}$$

Notice that $e_s \in [0, t_p)$. Hence, the error in the time difference of arrival of the acoustic wave between detectors S_i and S_{i+1} is $e_{s_i} \in (-t_p, t_p)$.

3.4.3 Generating TDOA Equations

In order to generate the equations that describe the localization of the particle strike. We sort detectors based on their proximity to the source of the signal (i.e., the order in which they trigger), S_1 being the closest detector and S_n the furthest one. (X_a, Y_a) denotes the unknown location of strike and (X_i, Y_i) indicates the known location of the ith detector.

A general model for the two dimensional (2-D) location estimation of a source using N detectors is adapted, where the mathematical problem is to estimate the actual location of a strike (X_a, Y_a), utilizing the detector positions and the TDOA readings. First, we define the squared euclidean distance between the source and the ith detector:

$$D_{ia} = \sqrt{(X_i - X_a)^2 + (Y_i - Y_a)^2} \tag{3.2}$$

Next we derive the range difference ΔD_{ia} between detectors S_i and S_{i+1},

$$\begin{aligned} \Delta D_{ia} &= D_{ia} - D_{(i+1)a} \\ &= \sqrt{(X_i - X_a)^2 + (Y_i - Y_a)^2} \\ &\quad - \sqrt{(X_{i+1} - X_a)^2 + (Y_{i+1} - Y_a)^2} \end{aligned} \tag{3.3}$$

Now, we can set up our set of equations based on the TDOA measurements ΔT_{ia} between detectors S_i and S_{i+1},

$$\Delta D_{ia} = C_p * \Delta T_{ia} + e_{s_i}, \; i = 1 \dots N - 1 \tag{3.4}$$

Where, C_p is the speed of the sound wave on the silicon surface. Notice that if $N > 3$, we will have a non-determined system (i.e., more equations than unknowns).

Next, we will see how we can solve these hyperbolic TDOA equations to obtain the estimation of location.

3.4.4 Solving TDOA Equations

Solving a set of hyperbolic equations for accurate location estimation is non-trivial. The simplest way to estimate the location of particle strike, is to generate a deterministic system of TDOA equations. The deterministic algorithms can be used when the number of hyperbolic equations equals the number of unknown coordinates of the source. In this work we implement an algorithm to solve a deterministic system of two hyperbolic equations [238].

A particle strike will be detected by all the detectors within the detection range of 5 mm. Hence, usually we have more than two TDOA measurements. By using the redundant TDOA measurements we can improve the accuracy of the position location estimation. To take advantage of these redundant TDOA measurements, whenever the number of triggered detectors is larger than three we construct a

non-deterministic system of equations (i.e., ≥ 3 hyperbolic TDOA equations). A non-deterministic system of equations is more difficult to solve as a unique solution does not exist. We implement and examine both iterative [237] and non-iterative [239, 240] algorithms to solve non-deterministic system of equations.

The algorithm to solve TDOA equations is stored in firmware (along with the position of all detectors) and is transparently run in any of the cores of the processor. The preferred option is to run the algorithm in a core that is not triggering the error to facilitate the error recovery if necessary, but it could also be done in the same core with some checkpointing. Next, we will discuss the implementation and compare different algorithms for solving TDOA equations.

3.5 Algorithms for TDOA Equations

In this section we implement algorithms to solve deterministic and non-deterministic system of equations and discuss their computational complexity, runtime, their ability to provide exact solutions and the risk of not reaching a valid solution. Later in this chapter, we will discuss in detail how design parameters like number of detector and their location impact all these metrics, and especially, the quality of the location estimate.

3.5.1 Deterministic Method

A high-level description of the algorithm to compute an exact solution when the number of TDOA measurements are equal to the number of unknowns ((X,Y) coordinates) is shown in Algorithm 1.

Algorithm 1 Deterministic location estimation

1: **INPUT:** Locations of 3 detectors $\mapsto (X_i, Y_i), i = 1, 2, 3.$
2: **INPUT:** Range difference between receivers $\mapsto \Delta D_{ia}, i = 1, 2.$
3: **INPUT:** Error in TDOA $e_{s_i} \in (-t_p, t_p).$
4: Generate hyperbolic equations
5: Linearization $\mapsto D_i^2 = (\Delta D_{i,1} + D_1)^2$
6: Quadratic equation in the form of $d{*}x^2{+}e{*}x{+}f{=}0$
7: $X = \frac{-e-\sqrt{e^2-4df}}{2d}$, Y substitute X into line 6.
8: **OUTPUT:** Location (X, Y), CEP.

Lines 1-3 define the inputs for generating the equations: the location of detectors, as well as the statistical distribution of the error in TDOA measurements, which is known at design time. The TDOA measurements are calculated online as explained in Section 3.4.2. First step of the algorithm is generating the equations and linearizing them by squaring (lines 4-5). Notice that in this implementation we use only the first 3 detectors that trigger to build the hyperbolic equations. Then we apply a hyperboloid transformation to obtain a single variable quadratic equation (lines 6-7). Finally, solving the quadratic equation yields the value of one of the coordinates and we can obtain the other by substitution in the line 6.

This solution does not utilize the extra TDOA measurements, available when three or more triggered detectors are available [238].

3.5.2 Non-deterministic Method

Next, we implement iterative and non-iterative algorithms to solve non-deterministic systems of equations.

3.5.2.1 Non-iterative Algorithms

We describe a non-iterative algorithm to solve a non-deterministic system of equations similar to [239]. It provides an unambiguous solution when the number of TDOA measurements are ≥ 3.

A high-level description is shown in Algorithm 2. Lines 1-8 are basically the same as lines 1-6 of Algorithm 1. By introducing an intermediate variable, the nonlinear equations relating TDOA estimates and source position can be transformed into a set of equations which are linear and function of the unknown parameters (i.e., the X and Y co-ordinates) and the intermediate variable. A least square (i.e., LSQR [241]) yields a solution (line 9). By exploiting the known relation between the intermediate variable and the position coordinates, a second weighted LSQR gives the final solution (lines 10-11).

Algorithm 2 is further extended as shown in Algorithm 3. It derives a bias of the source location estimate using Algorithm 2. Two methods, called *BiasSub* and *BiasRed*, are developed to reduce the bias. The *BiasSub* method subtracts the expected bias from the solution of Algorithm 2, where the expected bias is

Algorithm 2 Non-deterministic non-iterative algorithm for hyperbolic location estimation

1: **INPUT:** Number of total detectors $\mapsto N$.
2: **INPUT:** Locations of the detectors $\mapsto (X_i, Y_i), i = 1, 2, ..., N$.
3: **INPUT:** Range difference between receivers $\mapsto \Delta D_{ia}, i = 1, 2, \ldots, N-1$.
4: **INPUT:** Error in TDOA $e_{s_i} \in (-t_p, t_p)$ and error covariance matrix $\mapsto R = [e_{s_i}]$.
5: Identify triggered detectors if $N > 3$
6: Generate hyperbolic equations
7: Linearization $\mapsto D_i^2 = (\Delta D_{i,1} + D_1)^2, i = 1, 2, ..., N$
8: Quadratic equation: $a * \Delta D_1^2 + b * \Delta D_1 + c = 0$
9: $f(X, Y, \Delta D_N) \mapsto LSQR(f(\Delta D_1)), i = 1, 2, ..., N$
10: $\begin{bmatrix} A_3 & B_3 \\ \vdots & \vdots \\ A_N & B_N \end{bmatrix} \begin{bmatrix} X \\ Y \end{bmatrix} = \begin{bmatrix} -D_3 \\ \vdots \\ -D_N \end{bmatrix}$
11: **OUTPUT:** Applying another LSQR yields (X, Y), CEP.

Algorithm 3 Extension of Algorithm 2

1: **INPUT**: Number of total detectors $\mapsto N$.
2: **INPUT**: Locations of the detectors $S_i = [(X_i, Y_i)], i = 1, 2, ..., N$.
3: **INPUT**: Range difference between receivers $\mapsto \Delta D_{ia}, i = 1, 2, \ldots, N-1$.
4: **INPUT**: Error in TDOA $e_{s_i} \in (-t_p, t_p)$ and error covariance matrix $\mapsto Q = [e_{s_i}]$.
5: $R_{d,i} = \Delta D_{i,1} - \Delta D_i, i = 1, 2, ..., N$
6: SLoc using Algorithm 2
7: **BiasSub**:
8: $Bias_t = f(S_i, [0; R_{d,i}] + norm(SLoc - S_{i(:,1)}), Q, SLoc)$
9: $SLoc = SLoc - Bias_t$
10: Return $SLoc$
11: **BiasRed**:
12: Compute $M_1 = f(weights, S_{i(:,1)})$
13: Compute $M_2 = f(weights, M_1)$
14: $SLoc = f(M_1(1 : length(M_2))) * \sqrt{|M_2|} + S_{i(:,1)}$
15: Return $SLoc$
16: **OUTPUT**: $SLoc = (X, Y)$, CEP.

approximated by the theoretical bias using the estimated source location and noisy data measurements (lines 7-10). The *BiasRed* method augments the equation error formulation and imposes a constraint to improve the source location estimate (lines 11-15). The *BiasSub* method requires the exact knowledge of the noise covariance matrix and *BiasRed* only needs the structure of it [240].

3.5.2.2 Iterative Algorithm

A high-level iterative algorithm is shown in Algorithm 4. Iterative Gauss-Newton interpolation uses the Taylor-series expansion method [237].

Algorithm 4 Iterative algorithm

1: **INPUT:** Number of total detectors $\mapsto N$.
2: **INPUT:** Locations of the detectors $\mapsto (X_i, Y_i), i = 1, 2, ..., N$.
3: **INPUT:** Range difference between receivers $\mapsto \Delta D_{ia}, i = 1, 2, \ldots, N-1$.
4: **INPUT:** Error in TDOA $e_{s_i} \in (-t_p, t_p)$ and error covariance matrix $\mapsto R = [e_{s_i}]$.
5: Identify triggered detectors
6: Generate hyperbolic equations
7: Linearization (Tylor series) $\mapsto A\delta \cong Z + E$
8: Gauss-Newton-Interpolation $[(X_v, Y_v), N, (X_i, Y_i), A, \delta, Z]$
9: **while** $(\delta_x \neq 0, \delta_y \neq 0)$ **do**
10: $[\delta_x, \delta_y] \mapsto LSQR((A), (Z))$
11: $X_v \leftarrow X_v + \delta_x, Y_v \leftarrow Y_v + \delta_y$
12: **end while**
13: Compute $Q = [A^T R^{-1} A]^{-1}$, CEP
14: **OUTPUT:** Area of Error Distribution, Radius of the circle(CEP), center (X_v, Y_v)

Lines 1-4 show the required inputs for solving the equations. First step of the algorithm is generating the equations (lines 5-7). Equation 3.3 (and therefore, the set of equations 3.4) is nonlinear in nature. Unlike Algorithms 1, 2 and 3, we opt to linearize these equations through Taylor-series expansion and retain the terms below second order [237].

We also provide an initial guess (X_v, Y_v) as shown in Equation 3.5.

$$(X_v, Y_v) = \sum_{i=1}^{n} \left[\frac{(max(X_i), min(X_i))}{2}, \frac{(max(Y_i), min(Y_i))}{2} \right] \tag{3.5}$$

The system of equations is solved by computing LSQR iteratively (lines 8-12). In order to estimate the solution, we keep iterating until $\delta_x \mapsto 0$ and $\delta_y \mapsto 0$. In each new iteration, the provisional solution is updated through $X_v \leftarrow X_v + \delta_x$ and $Y_v \leftarrow Y_v + \delta_y$, yielding the estimated location (X_v, Y_v) as shown in (line 14) at the end of the iterative process.

3.5.3 Metrics for Evaluating Algorithms

The algorithms described in Section 3.5, have very different behavior in terms of runtime, complexity, accuracy and location estimation coverage. To evaluate them we will first describe the important metrics.

3.5.3.1 Runtime

Runtime of algorithm is the time it takes to obtain the estimated location of strike after the TDOA equations are generated. Once the first detector triggers, we stall the processor and obtain all TDOAs. Once all TDOAs are ready, we can execute any algorithm to generate and solve the equations. It is worth noticing that the more TDOA equation are generated the longer it takes to solve them.

3.5.3.2 Complexity

Algorithm 1 is computationally the least intensive as it is non-iterative and deterministic (i.e., solves just 2 hyperbolic equations to obtain the location). It does not use redundant TDOA measurements.

Algorithms 2, 3 and 4 are more complex as they solve more than two hyperbolic equations to estimate the location. Algorithm 4 is computationally intensive since an LSQR computation is required in each iteration. Simulations show that at least three iterations are required for convergence. It demands computing LSQR at least 3 times. Algorithm 2 and Algorithm 3 also require LSQR computations. However, they are computationally less intensive than the Algorithm 4, mainly because of their non-iterative nature. Note that solving more hyperbolic equations to estimate the location increases the overall complexity.

The runtime memory footprint increases when increasing the number of hyperbolic equations. Since, Algorithms 2, 3 and 4 utilize redundant TDOA measurements, they are more memory consuming than Algorithm 1. Most of the memory goes into storing the data matrices. The LSQR operation itself is less memory intensive [241]. The overall runtime memory footprint of all the algorithms discussed above is not significant.

3.5.3.3 Location Estimation Coverage

Location estimation coverage is the ability to produce a valid estimation of location. Location estimation coverage depends on the placement of detectors. For example, Algorithms 1, 2 and 3 fail to produce an estimation of location when all the TDOA equations are formed consisting detectors having either the same X co-ordinates or Y co-ordinates (i.e., collinear detectors).

Algorithm 4 is an iterative method and requires an initial guess of the location. If the initial guess is not properly provided, convergence may be compromised and that reduces the location estimation coverage. Non-iterative algorithms do not face any convergence problem.

We show a detailed evaluation regarding *location estimation coverage* in Section 3.6.

3.5.3.4 Accuracy

To quantify the accuracy of the estimated location we calculate the error in the obtained position estimate for all the algorithms mentioned above. Apart from the sampling errors in TDOA measurements as explained in Section 3.4.2, linearizing the hyperbolic equations (i.e., by squaring operation as in Algorithm 1, Algorithm 2 and Algorithm 3 or by using Taylor series and eliminating the second order terms as shown in Algorithm 4) can introduce errors in the final location estimation.

Estimation of Error: Because of errors in measurements, we cannot exactly pinpoint the particle strike; instead, we obtain an error distribution area that contains the actual location of the particle strike. We use circular error probability (CEP) to express the area of the error with a given probability. CEP is the measure of the area of the error distribution of the final estimation of the position. Moreover, the location estimation accuracy depends on various design parameters such as, (i) the placement of detectors, (ii) choice of triggered detectors, (iii) number of TDOA equations used for estimating the location and (iv) sampling frequency. Note that these design parameters also affect runtime, complexity, location estimation coverage of the algorithms.

Error Area Granularity: The location of the particle strike is given as estimated (X, Y) coordinates and an estimation of the error area covered by (3*CEP) radius. Using Rayleigh's method for approximating the CEP [242], we guarantee that the actual strike location will always fall within a circle with the center at the obtained estimated location and the radius equal to the 3*CEP. We analyze the 3*CEP error area for all the algorithms discussed above in Section 3.6. The most accurate algorithm has the minimum 3*CEP error area.

For simplicity, we will describe the error area in terms of bits. However, the error area can be easily mapped to relevant functional blocks in the processor pipeline or to specific lines in caches [135].

3.6 Assessing the Algorithms

In this section we assess how the placement of the detectors, and how the number of detectors impact the error in the estimation of location (accuracy), runtime, complexity and coverage for all algorithms discussed in Section 3.5. We demonstrate the utility of the cantilever detectors for detecting and locating particle strikes in the core of a Core™i7-like processor. The core has a rectangular shape with an area of 28 mm^2.

3.6.1 Placement of Detectors

After trying different configurations, we have opted to place the detectors in a mesh as shown in Figure 3.9. Each node in the mesh represents an acoustic wave detector. For a $m \times n$ mesh the area of the core is split into $m - 1$ equal parts along the X-axis and $n - 1$ equal parts along Y-axis.

We have evaluated different mesh configurations. For this experiment, we have opted for a system of 4 hyperbolic equations. Therefore, we need to construct a mesh that guarantees that for all possible particle strikes, at least 5 detectors trigger (recall that only the detectors that are placed within 5 mm of the particle strike will be able to detect the strike). We inject 1048 particle strike at random locations at random instances. We chose the sample set to be 1048 because we wanted to be as accurate as possible in locating the exact erroneous bits while

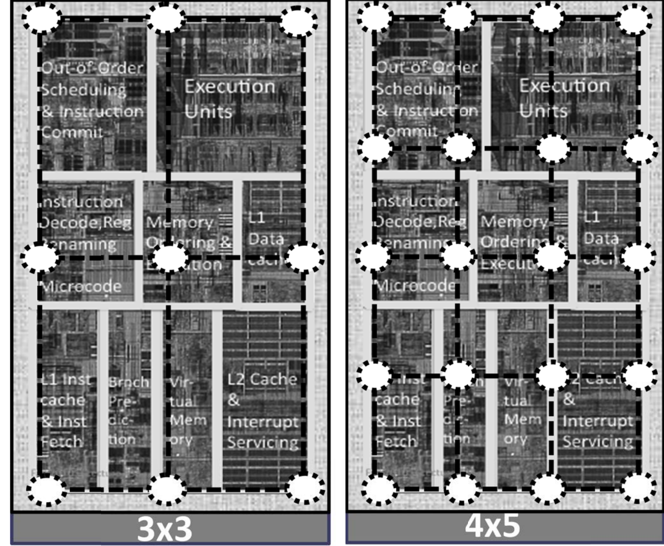

Figure 3.9: Placement of detectors in a mesh formation

using location estimation algorithms with 95% confidence. It is also backed up by confidence interval theory. Our studies show that the minimum configuration is a 3×3 mesh with 9 detectors. In those configurations where more than 5 detectors trigger, we take the first five detectors that trigger and observe the impact of placement of detectors on accuracy and the location estimation coverage. Note that the runtime and computational complexity are independent of the placement of detectors.

3.6.1.1 Accuracy

Figure 3.10 shows how the number and placement of detectors impact the error area (i.e., accuracy). As one can see, for the iterative Algorithm 4, using only 9 detectors yields an error area of 40 bits, which is a 3*CEP radius of 3.5 bits. It is also interesting to note that increasing the number of detectors does not increase the quality of the solution, since the solution is more affected by the location of the detectors. For instance, using 12 detectors (i.e., a 2×6 mesh) the 3*CEP radius increases to 9 bits. However, when we change to a 3×5 mesh, area is significantly reduced to a radius of 3 bits. Algorithm 2 and Algorithm 3 follow a similar pattern. Algorithm 1 does not produce a valid estimation for some mesh configurations. It is worth noticing that for the given analysis the iterative algorithm outperforms all the other algorithms by a factor of about three in terms of area.

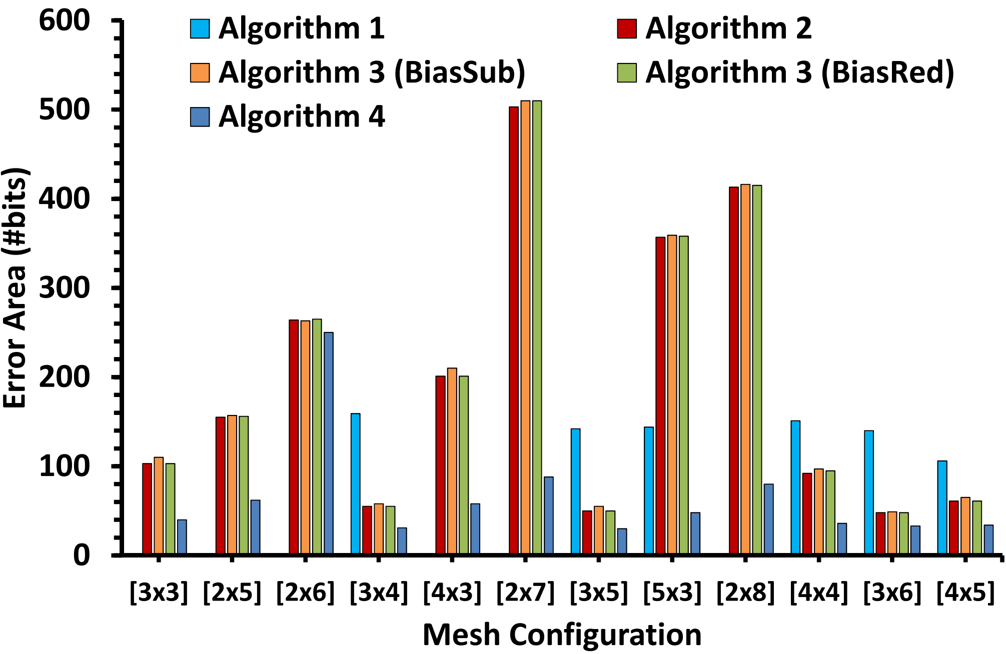

FIGURE 3.10: Impact of placement of detectors (while solving 4 TDOA equations) on accuracy (area unit is the area of 1 bit SRAM cell)

3.6.1.2 Location Estimation Coverage

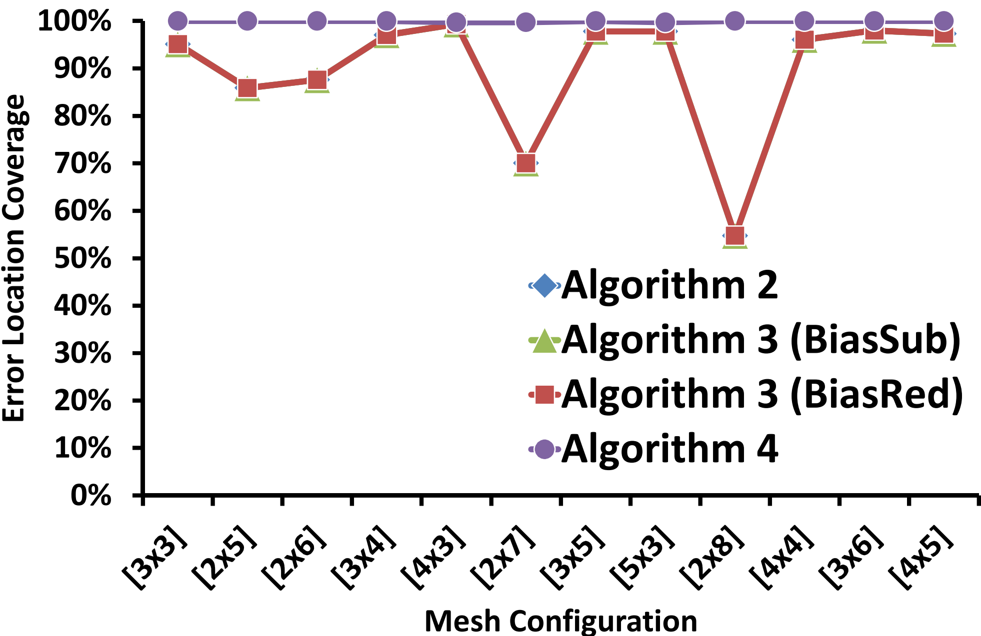

FIGURE 3.11: Impact of placement of detectors (while solving 4 TDOA equations) on location estimation coverage

Figure 3.11 shows how the number (and placement) of detectors impact the estimation coverage explained in Section 3.5.3.3. Note that as the different mesh

configurations alters the placement of detectors but always solves 4 TDOA equations, the runtime and the complexity are not affected.

We can observe the ambiguity problem of Algorithms 2 and 3 in Figure 3.11. This problem is prominent in specific mesh configurations (i.e., 2×5, 2×6 etc.) with more likelihood of having all 5 triggered detectors to be collinear. Ambiguity problem arises mainly because these algorithms linearize the hyperbolic equations by a squaring operation. This ambiguity can be easily solved by using a-priori information regarding the dimensions of the protected area [238–240]. We also show Algorithm 4 to compare the location estimation coverage. Algorithm 4 is not affected by ambiguity problem. However, as discussed in Section 3.5.3.3, Algorithm 4, may have problems regarding the convergence when not provided with a proper initial guess.

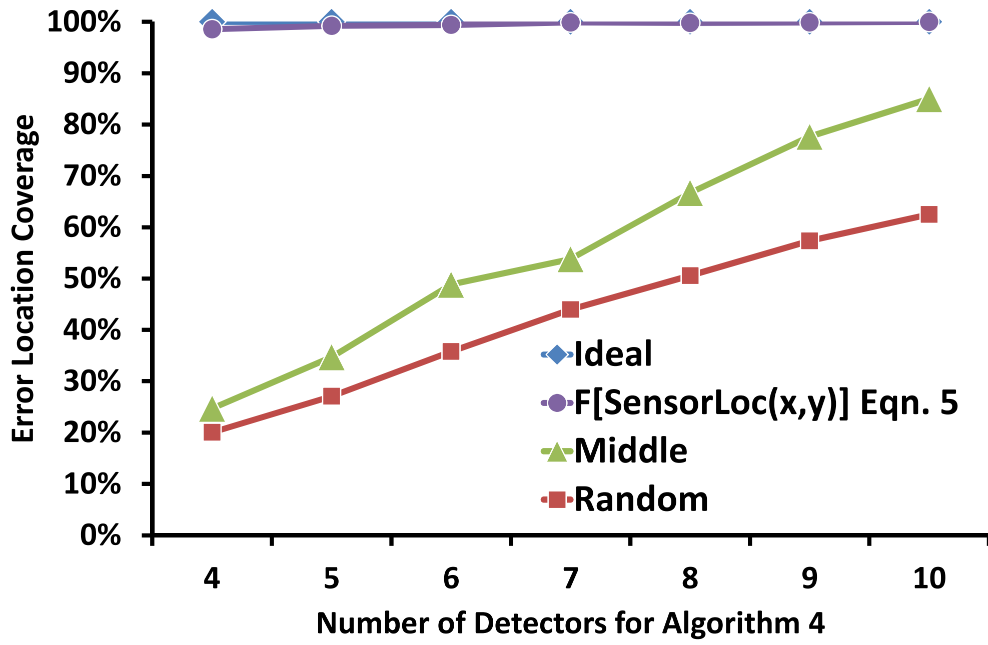

Figure 3.12: Impact of *initial guess* on coverage (while solving 4 TDOA equations) on location estimation coverage

Figure 3.12 shows how the choice of the initial guess affects the convergence and hence the location estimation coverage (for the 1048 analyzed strikes) for Algorithm 4 in a 4×5 mesh. As we can see, when the initial guess is fixed in the middle of the core for all 1048 strikes, even when solving 9 TDOA equations, 16% of times the algorithm is not able to converge. For random guess locations 38% of the times the algorithm does not converge. When the initial guess location is a function of the locations of the selected sensors as shown in Equation 3.5, the

algorithm converges all the times within 3 iterations providing 100% error localization. To compare the effectiveness of the choice of the initial guess we also show the ideal case where initial guess is the actual location of the particle strike. Note that when the algorithm does not converge, the system cannot identify the location of the strike, but the strike is still detected.

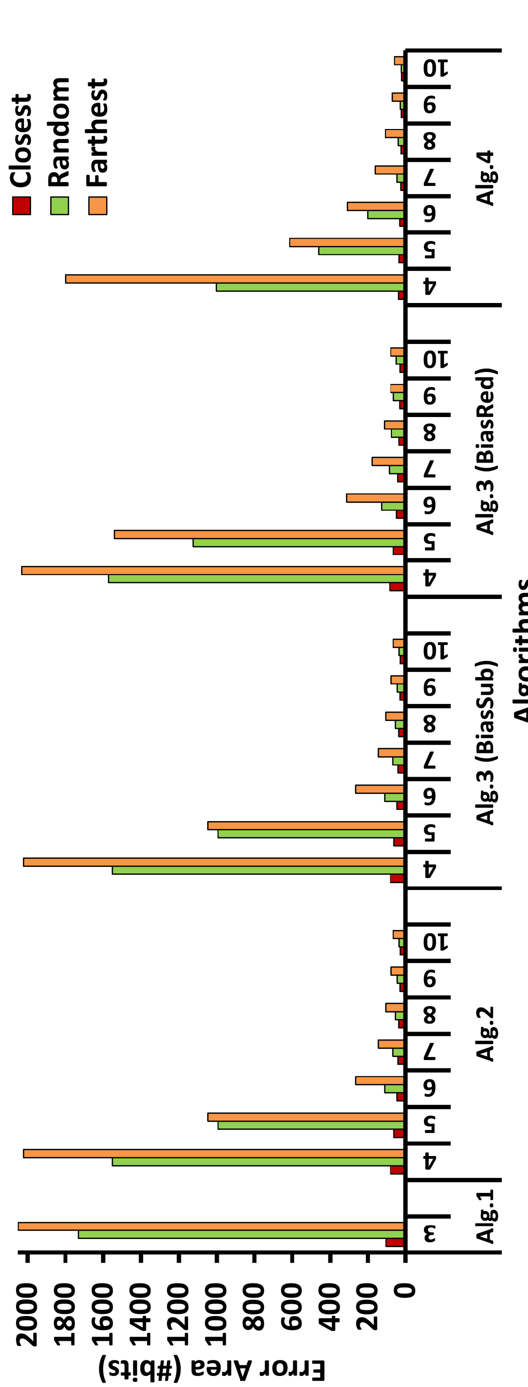

FIGURE 3.13: Worst-case error area with the selection of different set of detectors (4 to 10) from a given [4 × 5] mesh

3.6.2 Choosing Detectors for TDOA Equations

In this section, we assess the impact of the choice of the TDOA equations on the accuracy (i.e. 3*CEP error area) and error estimation coverage. For that purpose, we choose a 4×5 mesh because it guarantees that at least, 10 detectors detect the particle strike. We also assume a 2 GHz sampling frequency. Note that the runtime and computational complexity are unaffected by the choice of the TDOA equations.

3.6.2.1 Accuracy

Figure 3.13 shows the obtained error area for the 4×5 mesh for all algorithms. We show results for three different methods that select the detectors when more detectors than necessary are triggered by: (i) choosing the closest, (ii) the farthest or (iii) choosing randomly. For all the algorithms discussed in Section 3.5, selecting the closest set of detectors is the most accurate option. This is because the nearest detectors are placed at locations where it was possible to generate better TDOA measurements between two detectors. It helps in reducing the error involved in linearizing hyperbolic equations as discussed in Section 3.5.3.4 and yielding more accurate solutions.

3.6.2.2 Location Estimation Coverage

The choice of triggered detectors does not affect the complexity or runtime of the algorithms as same number of equations are solved. However, choosing the closest set of detectors guarantees 100% error coverage for Algorithm 4 and $>$97.7% error coverage for Algorithms 2 and 3 as shown in Figure 3.11.

3.6.3 Effect of Solving More TDOA Equations

Once we select the closest set of detectors, we can observe that solving a higher number of TDOA equations has a very important impact on the accuracy. Moreover, solving more number of TDOA equations can worsen the runtime and increase the computational complexity.

3.6.3.1 Accuracy

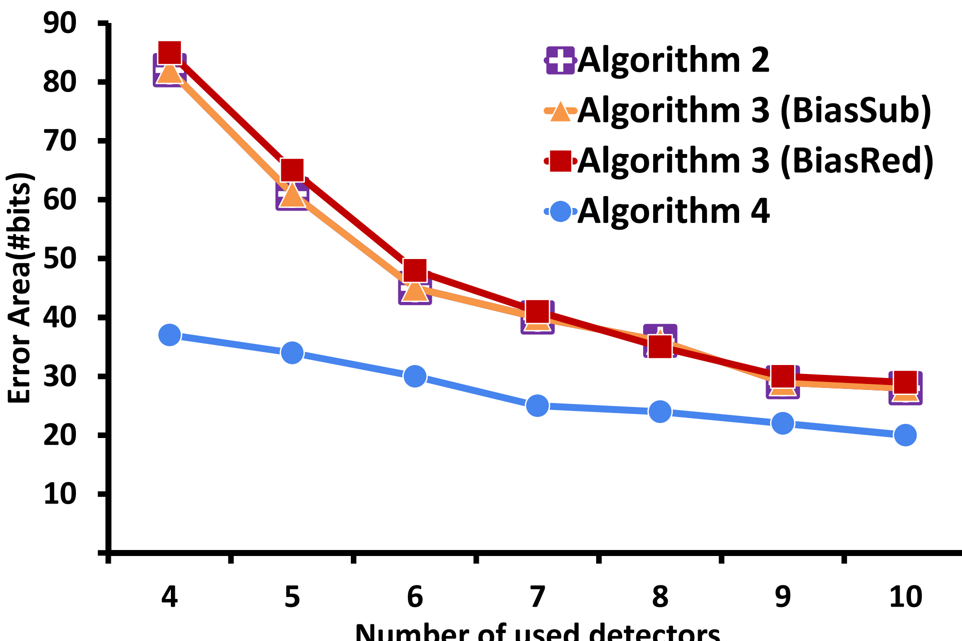

FIGURE 3.14: Error area with closest detectors for [4 × 5] mesh

Figure 3.14 shows that by increasing the selected detectors from 4 to 10, the error area reduces by a factor of 2 for Algorithm 2, Algorithm 3 and Algorithm 4.

Table 3.2 shows the best configurations observed for each algorithm; we consider different mesh configurations and number of equations for Algorithms 2, 3 and 4. Algorithm 1 is deterministic and solves only 2 equations for the given mesh. Second column of the table shows the minimum number of detectors that trigger upon the particle strike. Third column shows the number of detectors used to set up the TDOA equations. Last column shows the worst-case error observed for the 1048 particle strikes for the different algorithms discussed in Section 3.5. It is worth noticing that the improvement in the error area of Algorithm 1 when increasing the number of detectors is mainly due to the improved quality of the 2 equations with a denser mesh (as explained in Section 3.6.1). For all the algorithms the best error area is obtained by setting a 4×5 mesh and using 10 detectors. However, the complexity of setting and solving the equations makes it too expensive as explained in Section 3.5.3.2.

Mesh Configuration [Mesh, #Detectors]	Minimum #Detectors triggered	#Detectors used for TDOA	#TDOA Equations solved	3*CEP Error Area (#bits)				
				Algorithm 1[†]	Algorithm 2	Algorithm 3		Algorithm 4
						BiasSub	BiasRed	
$[3 \times 4, 12]$	4	4	3	159	58	60	57	37
$[3 \times 5, 15]$	9	5	4	142	50	50	51	30
$[3 \times 6, 18]$	10	6	5	140	37	37	40	29
$[3 \times 6, 18]$	10	7	6	140	33	33	35	24
$[3 \times 6, 18]$	10	8	7	140	31	31	33	23
$[4 \times 5, 20]$	12	9	8	106	29	29	30	21
$[4 \times 5, 20]$	12	10	9	106	28	28	29	19

TABLE 3.2: Worst case error area for best configuration of a given mesh for each algorithm. [†] solves only 2 equations

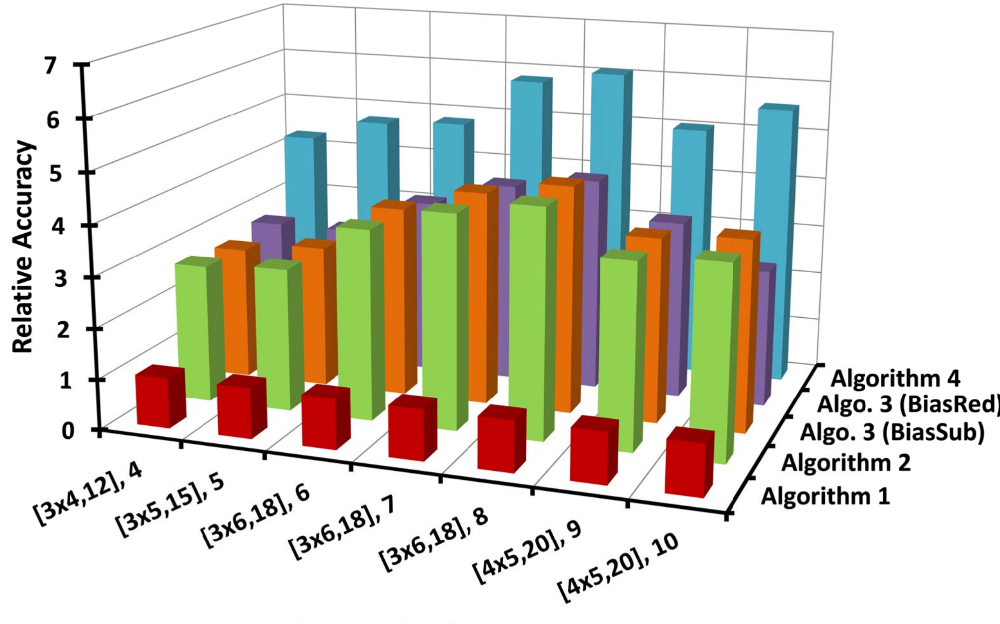

FIGURE 3.15: Comparing accuracy of all algorithms and for the mesh configurations discussed in Table 3.2

The average improvement in the accuracy for the iterative Algorithm 4 is 1.4×, 1.55× and 5.2× compared to Algorithms 2, 3 and 1 respectively as shown in Figure 5.11c.

Figure 3.16 shows how increasing the number of equations (for the configurations of Table 3.2) impacts the runtime and complexity. As per Figure 3.16(a) and Figure 3.16(b), for the same mesh configuration, with increasing number of equations the runtime and complexity of Algorithms 2 and 3 increases linearly relative to the runtime and complexity of Algorithm 1. Algorithms 2 and 3 are non-iterative and the increase in complexity and runtime is mainly because of the increased size of working data set (e.g., more equations). In the case of Algorithm 4, for the same mesh, the runtime and complexity increase exponentially relative to the runtime and complexity of Algorithm 1. This exponential trend is because more number of iterations (and the number of LSQR computations) are required to solve higher number of TDOA equations.

3.6.3.2 Runtime

Generating and solving the TDOA equations has negligible impact on the performance of active tasks and user experience. As per Figure 3.16(a) the iterative

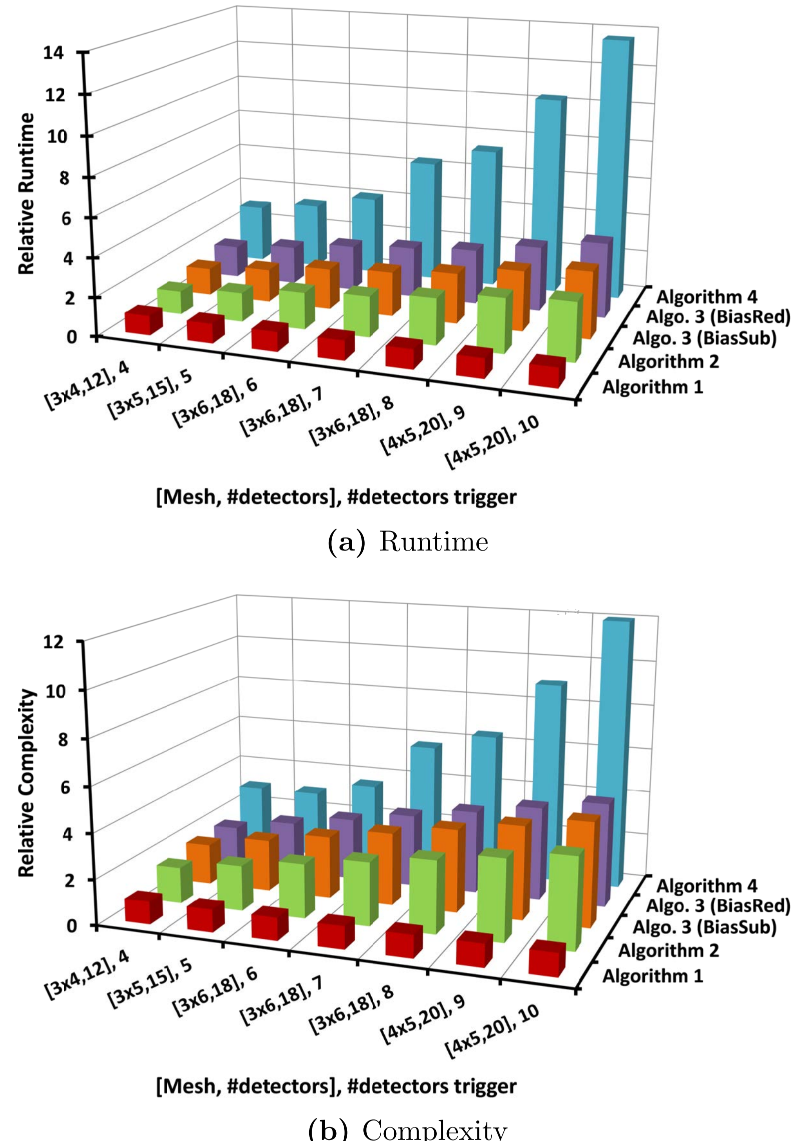

(a) Runtime

(b) Complexity

FIGURE 3.16: Comparing runtime and complexity of all algorithms and for the mesh configurations discussed in Table 3.2

Algorithm 4 takes 3.2×, 2.6× and 6.8× longer runtime to produce location estimation compared to Algorithms 2, 3 and 1 respectively.

In a Core™i7 processor, Algorithm 1 is the fastest and takes 0.011 ms. Algorithm 2 and Algorithm 3 take around 0.02–0.03 ms. Algorithm 4, being an iterative method, has the longest worst-case runtime of 0.07 ms.

3.6.3.3 Complexity

According to Figure 3.16(b) the iterative Algorithm 4 is 2.1×, 1.8× and 6× more complex compared to Algorithms 2, 3 and 1 respectively.

The ideal algorithm for location estimation would be the one that is the least complex, with the least runtime and the most accurate. Choosing the best algorithm is balancing a 3-way trade-off involving complexity, runtime and accuracy. Non-deterministic algorithms are complex but best for accuracy. Deterministic algorithms are least accurate and severely affected by sampling noise and ambiguity problem. For maximum accuracy Algorithm 4 is the best choice. Algorithms 2 and 3 are almost half as accurate as Algorithm 4 but they are faster and less complex. We want to precisely locate the error and hence we opt for Algorithm 4 which provides maximum accuracy.

3.6.4 Effect of Sampling Frequency on Accuracy

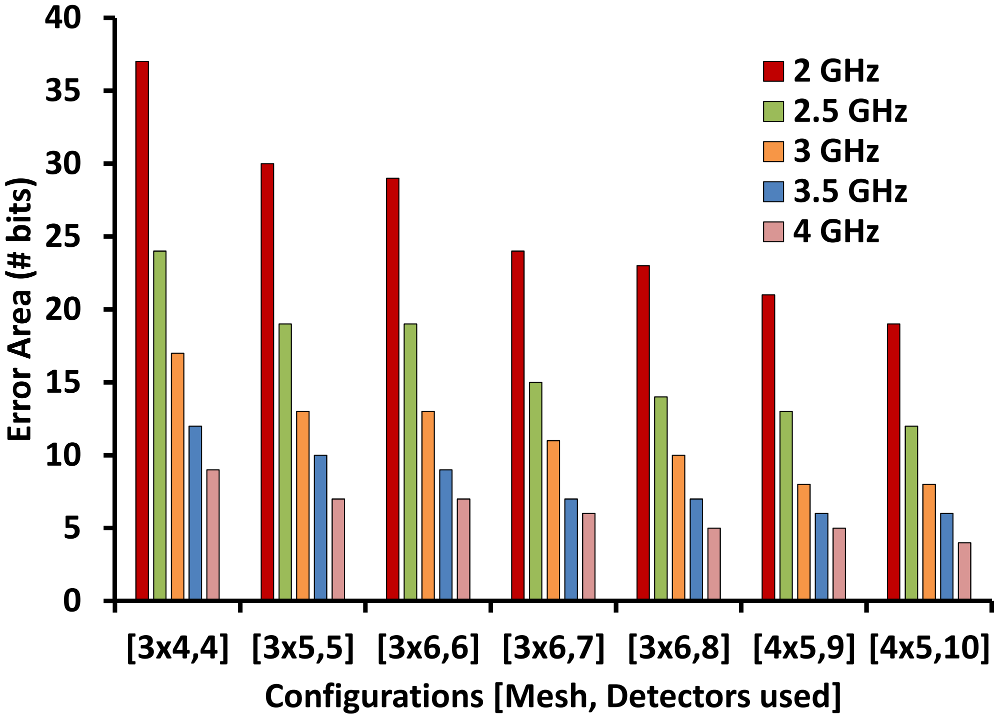

Figure 3.17: Impact of sampling frequency on error area for configurations of Table 3.2 Iterative Algorithm 4

The effect of altering the sampling frequency over the final error area is studied in this section. Figure 3.17 shows the impact of sampling frequency on the worst-case error area for all *best* configurations described in Table 3.2 for the iterative Algorithm 4. The results indicate that doubling the frequency from 2 GHz to 4 GHz reduces the error area by 4×. Our experiments show a similar improvement while doubling the frequency from 2 GHz up to 4 GHz for all the other algorithms discussed in Section 3.5.

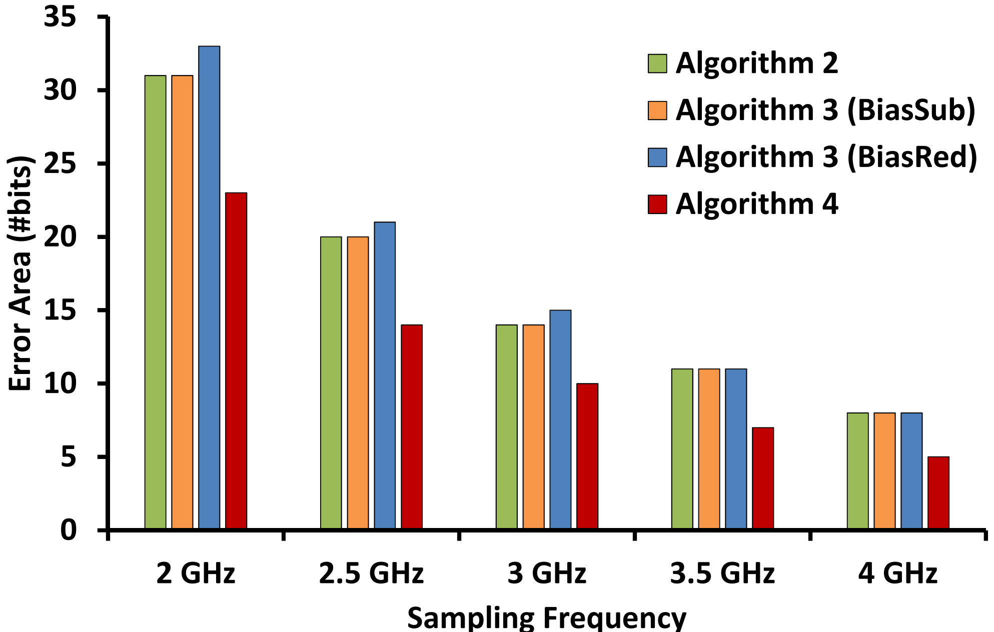

FIGURE 3.18: Impact of sampling frequency on error area for configurations of Table 3.2 for all algorithms

In Figure 3.18, we depict the effect of varying the frequency for the best configuration described in Section 3.6.3 (i.e., a 3×6 mesh employing 8 detectors) for all algorithms. We can see that increasing the sampling frequency reduces the error area; doubling the frequency from 2 GHz to 4 GHz reduces the worst-case error area from 23 bits down to 5 bits (i.e., a radius of 2.7 bits down to 1.3 bits) for iterative Algorithm 4, from 31 bits down to 8 bits for Algorithms 2 and for *BiasSub* method of Algorithm 3. In the case of *BiasRed* method of Algorithm 3 the improvement is from 33 bits down to 8 bits.

Notice that varying the sampling frequency has no impact on the complexity, runtime or location estimation coverage.

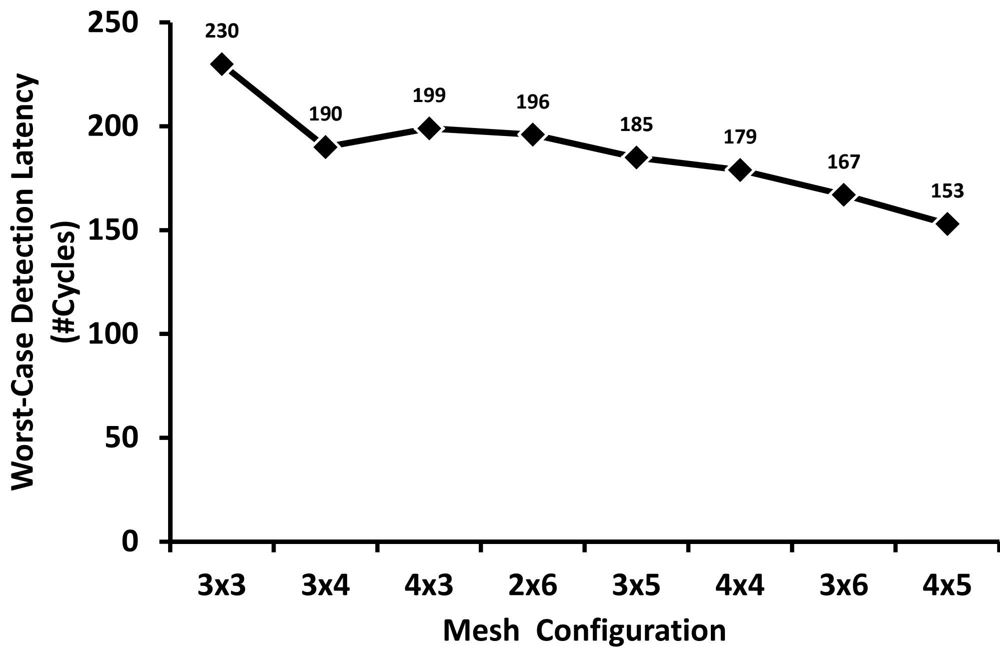

FIGURE 3.19: Worst-case detection latency for mesh configurations of Table 3.2 in a processor running at 2 GHz

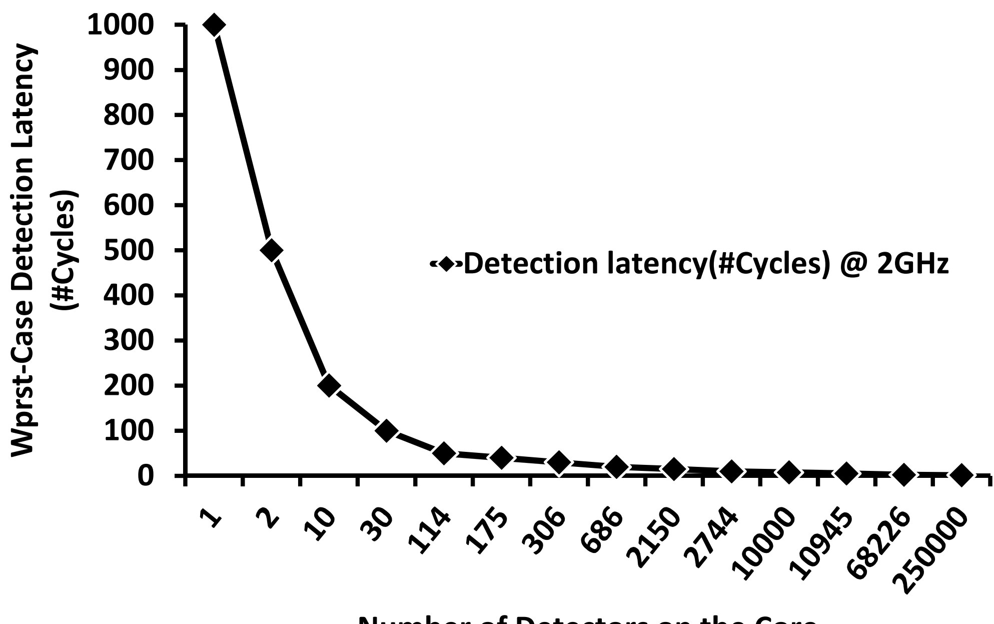

FIGURE 3.20: Adding more detectors to reduce worst-case detection latency in a processor running at 2 GHz

3.6.5 Detection Latency

Figure 3.19 shows the worst-case latency observed for the different mesh configurations of Table 3.2. As one can observe, adding more acoustic wave detectors significantly helps in reducing the detection latency. Figure 3.20 shows that increasing the number of detectors in the mesh reduces the worst-case detection latency exponentially. Small detection latencies allow simple hardware checkpoint and recovery.

We have considered the option of adding, on top of the detectors deployed for precise estimation of location, a set of detectors to minimize the detection latency. According to Figure 3.20, a detection latency of 1 cycle will require $> 68K$ detectors. A mesh consisting of 30-300 detectors can provide detection latency of 30-100 cycles for a processor running at 2 GHz.

3.6.6 Summary of Chosen Configuration

The proposed solution uses of two different meshes. The 3×6 mesh is used to obtain the TDOA. In that case, the hardware mechanism explained in Section 3.4.2 consists of 18 detectors (i.e., roughly 18 bits area), and a 2-level OR tree (7 3-input OR gates and 3 2-input OR gates) to generate the *Enable* signal. Besides, a 10-bit counter is required for the counting TDOA pulses.

We also use a separate mesh to minimize the detection latency. It consists of 30-300 detectors achieving 30-100 cycles of latency at 2 GHz (i.e., an area overhead of 30-300 bits). Depending on the number of detectors in the second mesh we may need an additional controller circuit (i.e., a MUX or a logic-OR tree structure) to generate the detection signal. Note that for latency minimization we do not require a counter since we only want to signal the presence of the strike.

For the given mesh configuration to obtain maximum accuracy in the location estimation we use Algorithm 4.

Algorithms		Runtime	Complexity	Coverage	Accuracy	Limitations
Non-iterative	Algorithm 1	1×	1×	90%	1×	• Cannot benefit from redundant measurements • Less accurate
	Algorithm 2	2.1×	2.8×	100%$^{\mp}$	3.6×	• Fails when detectors are collinear • Ambiguity problem • Requires a-priori knowledge of core dimensions
	Algorithm 3 (*BiasSub*)	2.3×	3.2×	100%$^{\mp}$	3.6×	
	Algorithm 3 (*BiasRed*)	2.65×	3.2×	100%$^{\mp}$	3.3×	
Iterative	Algorithm 4	6.4×	6.1×	100%	5.2×	• Convergence issues • Requires initial guess

TABLE 3.3: Comparison of algorithms: Algorithm 1 is deterministic and Algorithms 2, 3 and 4 are non-deterministic; $^{\mp}$ with careful mesh selections

3.6.7 Summary of Results

Nondetermined system of equations (i.e., when using more than 3 detectors and setting more than 2 equations) reduces the worst-case error area by a huge margin compared to determined system of equations. We have also shown the impact of detectors placement and higher number of equations on the accuracy, runtime and complexity. Using an iterative algorithm (Algorithm 4) is the best option if highest accuracy is desired. It also guarantees convergence independently of the type of the mesh. Algorithms 2 and 3 are almost half as accurate as Algorithm 4 but they are faster and less complex. Error estimation coverage can be an issue if collinear detectors form TDOA equations. Deterministic algorithms are the least accurate and severely affected by sampling noise and ambiguity problem. A comparative summary of all the trade-offs is described in Table 3.3.

We also studied the effect of sampling frequency on accuracy. Increasing sampling frequency reduces the sampling error in the measured TDOA. Raising sampling frequency from 2 GHz to 4 GHz reduces the worst-case error area by 4×. Overall, our results confirm that increasing the sampling frequency is more effective than increasing the number of equations. For instance, a system that uses 3 equations (e.g., 3×4 mesh) sampling at 4 GHz is a better option than a system using 9 equations (e.g., 4×5 mesh) with the sampling frequency of 2 GHz.

Finally, we have also discussed the impact of the number of detectors on the detection latency. We have concluded that the most effective design is the one that uses two independent meshes: a small mesh for precise location of the strike, and a somewhat larger mesh for reducing detection latency. The optimum configuration for maximum accuracy is to use Algorithm 4 on the studied core with a 3×6 mesh and construct a nondetermined system of 7 equations, which gives a worst-case error area of 23 bits (i.e., 23 μm^2). We add another mesh (i.e., 30-300 detectors) for reducing the detection latency, resulting in a latency of 30-100 cycles for a processor running at 2 GHz.

3.7 Related Work

In this section, we review detectors that detect the particle strikes via detection of current glitches, voltage glitches, metastability issues or deposited charge. A

detailed discussion of other existing techniques for error detection is given in Chapter 7. We will compare all the particle strike detectors for the parameters discussed in Section 3.2 against acoustic wave detectors that detect particle strikes by detection of the sound they generate upon impact on silicon surface. A brief summary is also given in the form of Table 3.1.

3.7.1 Current Glitch Detectors

3.7.1.1 Built-In Current Sensors (BICS)

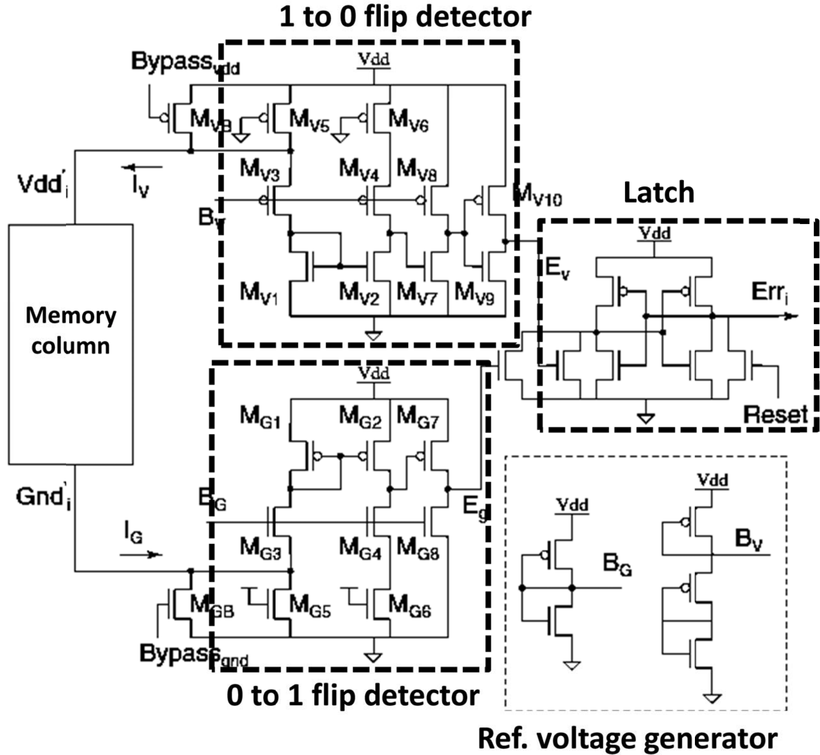

FIGURE 3.21: Built-in current sensor (BICS)

Built-in current sensors (BICSs) detect particle strikes by sensing abnormal current dissipation in the memory cells. BICS is a high-speed current-mode comparator which detects transient current pulses and provides logic level output to set the asynchronous latch. A BICS is composed of two current comparators and an asynchronous latch as shown in Figure 3.21. The fundamental operation of the BICS is based on the current controlled current switches. The two comparators generate logical output pulses which set an asynchronous error latch. They are placed between the memory cells and the power lines as shown in Figure 3.21, where one BICS is used for entire memory column [206].

3.7.1.2 Switching Current Detector

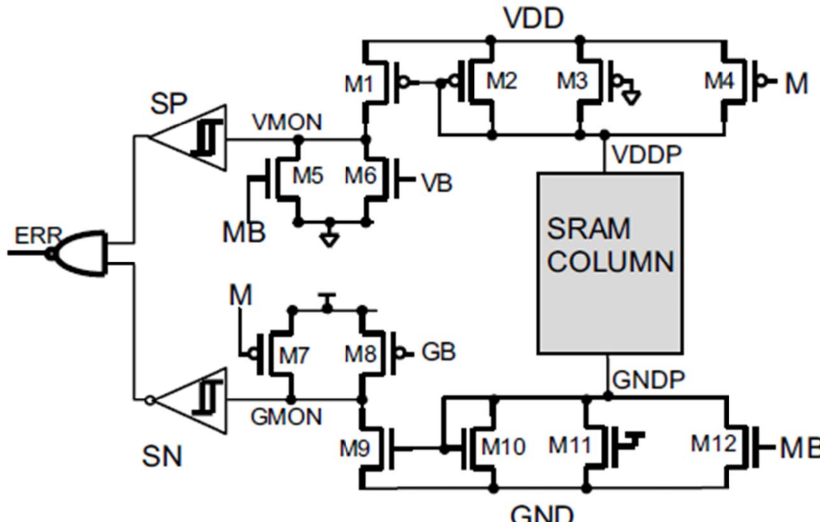

FIGURE 3.22: Switching current detector

This technique detects soft errors in SRAM memories [207]. Any bit flip due to soft error results in a transient switching current. It detects any soft error by monitoring the supply current of SRAM in the standby mode. A current pulse sensing circuit is shown in Figure 3.22. It uses a current mirror circuit to convert a fast current pulse into a transient voltage pulse. Finally, by using a Schmitt trigger it is possible to sense this transient voltage pulse and generate an error signal.

3.7.2 Voltage Glitch Detectors

These detectors monitor the supply rail disturbance caused by a particle strike [134]. A hierarchical soft error detection circuitry which monitors the ground voltage to detect the pulses as a result of particle strike-induced switching is shown in Figure 3.23. The detection circuitry has two levels of voltage comparators (differential amplifier). The first level compares the ground voltages of the functional blocks, while the second comparator amplifies the error signal. In the design, only the ground voltage is monitored to detect error. A single NMOS is connected between the ground bus line and ground terminal of the functional block. The addition of this transistor helps to separate the ground bus from the functional block ground terminal, thus creating a *virtual ground* (GND') at the ground terminal of the functional block.

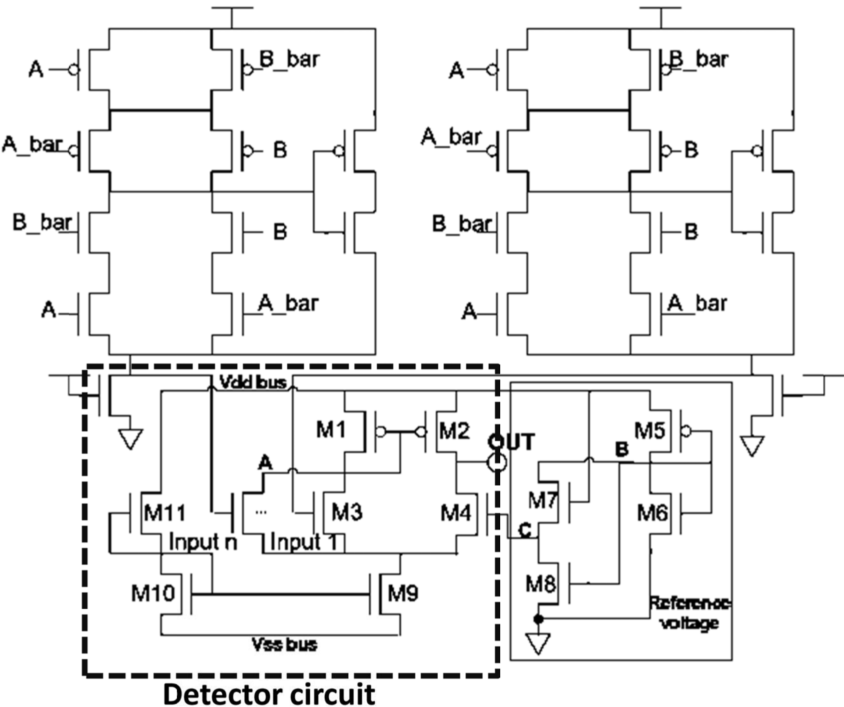

FIGURE 3.23: Voltage glitch detector

3.7.3 Metastability Detectors

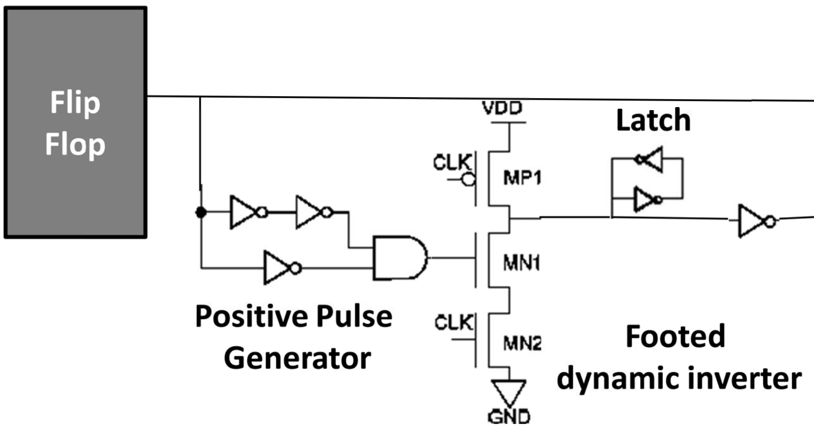

FIGURE 3.24: Metastability detector (BISS)

Unlike BICS, a Built-in single-event upset sensor (BISS), implements a metastability monitor circuit to detect particle strikes. BISS detects the setup and hold time violations in flip-flops that occur due to several reasons (i.e., clock skew, particle strikes etc.) [133]. Designers can insert the BISS to detect SEUs at the output of a flip-flop.

As shown in Figure 3.24, it has three major components: (i) a positive pulse generator, (ii) a footed dynamic inverter and (iii) a keeper latch. The positive

pulse generator transforms SEU-induced positive/negative pulse to positive pulse. The footed dynamic inverter is used to widen the pulse generated by the positive pulse generator, so that it can be easily detected.

3.7.4 Deposited Charge Detectors

3.7.4.1 Thin film silicon detectors

These silicon detectors are constructed as thin planner p-on-n diodes. This planner diode covers the entire target processor to detect any particle strikes. In principle, a silicon detector is a solid state ionization chamber [209, 210]. They detect particle strikes based on the changes in the depletion region of the p-n junction diodes due to ionization.

Most popular ones are listed below:

- Silicon strip detector (SSD) detects collected charge
- Active pixel sensors (APS) detects collected charge
- Scintillator coupled silicon photodiodes: detects flash of light

3.7.4.2 Heavy-ion Sensing

Heavy-ions deposit a huge amount of charge upon impact on the silicon surface. Heavy-ion sensors detect the particle strikes by detecting the deposited charge. The work of [212] proposes to use the DRAM memory cell to collect the charge upon a heavy-ion strike. When the storage node is discharged to a second voltage, a sense amplifier coupled to the storage node generates an output signal indicating that an SEU event has occurred. Also by tweaking the reference voltage to the sense amplifier the DRAM arrays can be tuned to detect heavy-ion particles with different energies.

3.7.5 Comparison of Detectors

In this section, we compare all the particle strike detectors for the parameters described in Section 3.2.

3.7.5.1 Hardware cost/Area overhead

We present the area overhead in terms of extra transistors required to protect one memory column consisting 128 6T-SRAM cells.

As it can be seen in Figure 3.21, one BICS consists of 27-35 transistors [206]. On top of that, it incurs extra area penalty in terms of added transistors that are required to monitor memory columns concurrently to filter the noise due to the read/write operations [206]. The switching current detector circuit of Figure 3.22 uses 12 transistors [207].

The voltage glitch detector circuit of Figure 3.23 consists of two levels of voltage comparators. Every column needs one level-1 comparator. Level-2 comparators take as input all the outputs of level-1 comparators to produce an error signal. For a single column design one such comparator consisting 12 transistors is required [134]. Depending on the size of the protected unit and the switching activity the number of comparators required in the first level increases.

At least one BISS (with 21 transistors) is required to protect one SRAM column [133]. To reduce the area overhead at the cost of error coverage, selective BISS insertion is possible [133]. Area overhead is proportional to the number of BISS inserted at the output of the flip flops.

One acoustic wave detector can detect a particle strike in a circular area of 78.5 mm^2 [135]. This means that one detector (i.e., area overhead of 1 6T-SRAM cell) can detect particle strike anywhere on the area of a last-level cache (LLC) of a state of the art processor.

SSD are the most common structures used as silicon detectors, and have typical dimensions in the range of 25 um-200 um. Pads and (APS) are emerging trends in silicon detectors. A silicon PIN diode is basically used as detector pad or pixel. Typical pad sizes are 200x200 mm^2. Pixels are typically of 50x50 um^2 to 200x200 um^2 [209, 210]. At least one such pixel is required for particle strike detection in the given memory column.

For heavy-ion detectors, a separate column of the 128 DRAM cells is occupied to detect an SEU event. The detector assembly also includes a set of word decoders, a set of sense amplifiers and a bit decoder for multiplexing the set of sense amplifiers. Along with this, a controller to adjust refresh intervals, a pre-charged ballast

capacitor to store charges and a reference voltage generator of the sense amplifier is required to change the sensitivity of the detection [212].

It is important to note that the current/voltage glitch detectors and metastability detectors will have a detection granularity at the column level. To exactly pin-point the location of error they will have to be combined with error detection codes (i.e. parity) [133, 134, 206, 207]. A single parity bit per memory word is used along with one of the detectors for every memory column. The area cost of the parity checker/generator providing parity bit per word is significant.

The area overhead of acoustic wave detectors is very less compared to other particle strike detectors. Moreover, their accuracy can be improved by deploying more detectors to pin-point errors at word/byte level. Even after deploying more acoustic wave detectors they significantly reduce the area overhead compared to ECC [135]. Silicon detectors [209, 210] and heavy-ion detectors are effective but incur $>100\%$ area overhead.

3.7.5.2 Power overhead and detection latency

Particle strike detector that is faster and consumes minimum power is desirable. Worst case power dissipation of one BICS varies from 4.43 to 24.95 uW for 100 nm technology [206]. And, the worst case detection latency ranges from 650 ps-1.1 ns [206]. Inserting the BICS may increase the resistance of the critical path and hence degrades the read-write speed of the memory severely reducing the performance. The leakage power for a The switching current detector is 12.9uw-18.9uW [207]. And the detection latency is in the range of 0.92 ns-1.14 ns. In the low power mode it is even slower and in the range of 2.41 ns-3.0 ns.

The voltage glitch detector [134] consumes less power compared to current glitch detector and per unit power overhead is in the range of 0.8 uW to 5 uW. However, this power savings makes it slower and its detection latency varies from 220 ps-1.4 ns.

In the case of BISS the power overhead is more than 10 uW due to increased number of transistors. To reduce the power overhead, only a selective flip flops are covered using BISS [133]. Detection latency is in a range of 1.5 ns-2 ns.

The acoustic wave detectors are passive and do not consume power. Power overhead of the controller circuit is insignificant [135]. The detection latency for the

particle strike occurring anywhere on the LLC is around 30-100 cycles (1200-161 detectors) and can be further reduced by putting more detectors [135].

Silicon detectors typically operate between 10 Volts and 100 Volts [209, 210]. The power consumption depends on the resistivity of the material used and it normally consumes >10 Watts. The detection latency of a silicon detector alone is around 25 ns. The delay added by the pre-amplifier and other controlling mechanism will further increase the overall detection latency [209, 210].

Heavy-ion detector uses flexible supply voltages and consume a few mW of power. The detection latency is similar to the memory access time.

3.7.5.3 False alarms

BICS, switching current detector and BISS are susceptible to noise. Common sources of noise are power supply lines, higher switching activities and miss-match in the inputs of the dynamic logic gates. Presence of noise increases the chances of false positives. The voltage glitch detector, receives the fluctuations in the voltage due to transient switching noise from the protected block as well as due to the particle strikes. The comparator filters switching noises and amplifies spikes generated by SEU. Tuning the threshold of the comparator is very difficult and if not set properly, the chances of false alarms increase. In the work of [134], while protecting memory, 27% and 7% false positives are reported for $1 \mapsto 0$ flips and for $0 \mapsto 1$ flip respectively.

The acoustic wave detectors are fairly accurate and can be calibrated to detect all particle strikes in the targeted energy spectrum for the given technology. Furthermore, some studies [17, 117, 142] support that the rate of particle strikes (with recoil energy > 10 MeV) is not very high. The false positive rate is practically zero, or in the worst case scenario it is one false positive per 1.3 minutes [135].

The presence of noise in the high voltage supply lines for silicon detectors increases the possibility of false positives [209, 210]. For heavy-ion detectors, imperfect calibration of any of the programmable parameters (i.e., VDD, refresh rate or reference voltage to the sense amplifier) may result into unwanted noise due to read/write operation and trigger false positives [212].

3.7.5.4 Detected particles/Fault types

Alpha and neutron particle strikes induce soft errors are more frequent [17, 117]. Current and voltage glitch detectors, BISS and acoustic wave detectors can detect particle strikes due to alpha and neutron particles. Silicon detectors can detect alpha and neutron strikes and other heavy elements with the energies in the range of 10 to 100 MeV. Heavy-ion detectors are able to detect particle strikes only due to heavy-ions such as proton, alpha or any other ions whose atom has been stripped off its electrons.

3.7.5.5 Intrusiveness of the design

Insertion of particle strike detectors in the design can have significant implications. Insertion of current glitch detectors involve splitting of the power lines of each column into smaller parts. The voltage glitch detectors require generating a virtual ground by partitioning the ground line. These modifications require changes in the physical layouts and routing. Moreover, to reduce huge area overhead, selective insertion is desirable for current/voltage glitch detectors and BISS. Identifying the correct flip-flops for selective insertion of the detector is challenging and can increase complexity.

The fabrication and placement of acoustic wave detectors on the surface of active silicon can be performed without complications [135, 142]. The control circuit is also simple and poses no major challenge to the RTL design or placement and routing [135].

The assembly of the silicon detector is very complex especially to provide reliability in processors. It consists of pre-amplifiers and might need to be pipelined requiring a complex control circuit [209, 210]. Heavy-ion detectors of [212] proposes to use part of the DRAM memory cell and pose no significant design challenge. However, providing adjustable sensitivity to detecting particle strikes can have implications in design cost.

3.7.5.6 Fault coverage vs. Cost

BICS, voltage glitch detectors, BISS, acoustic wave detectors and silicon detectors can detect particle strikes in both memory cells and combinational logic [133–135, 206, 209, 210]. While switching current detector can detect particle strikes only in SRAM memory cells [207]. Heavy-ion detectors can detect particle strikes only in DRAM memories [212].

To understand the cost vs. coverage trade-off lets compute the cost of protection for a level-one data cache of 32 KB with 512 columns and 512 rows. In the simplest arrangement of one BICS per column, it requires 512 BICS. The switching current detector of Figure 3.22 uses only 12 transistors per detector, and hence the area and power overheads will be relatively less compared to BICS. However, as the cache size increases the overhead increases exponentially. To protect a last level cache (8 MB, 16 way, 8K sets, each way with 8192 columns, 512 rows) >1.3 million BICS are required. If voltage glitch detector are used to provide the protection to the last-level cache, the required number of level-1 detectors to protect all caches would be >1.3 million and apart from that it will require 16 level-2 comparators. Also the transistor sizes should be increase to drive larger portions of the circuit.

For combinational logic, even when selective insertion is used (only some latches are protected), protecting a typical 4-bit multiplier with 504 transistors would require 70 BICS. The BICS area overhead for protecting such a multiplier is 29% [206]. For the same multiplier design, the overhead of protecting using hierarchical voltage detectors accounts for 18% of the area of the multiplier [134]. The area overhead of inserting BISS in the design would be 20%-30%.

Because of their large error detection range, acoustic wave detectors and silicon detectors can potentially guard the entire chip against particle strikes [135, 209]. Only 4 acoustic wave detectors are required, to provide detection capability in an entire state of the art chipmulti processor with surface area of $245mm^2$ [135]. However, to accurately locate the strike, 30-40 detectors are required, and to minimize the detection latency the required detectors are in the range of 450-500. This means the total area overhead in protecting entire chip is equivalent to 540 6T SRAM cells. SSD can provide detection coverage to the entire core, chip or system level. If APS are used to detect particle strikes on a chip, they are placed in the form of an array. One such array with 9x9 pixels covers a surface area of

1 cm^2 over the target processor. This area overhead also includes the connectors for the read out channels to deliver the signal to the outside world [209].

If the error rate in DRAM chips due to heavy-ions is a concern, the DRAMs chips can be effectively protected using heavy-ion detectors [212]. Depending upon the size of the DRAM, one or multiple arrays in the same or different DRAMs are dedicated for particle strike detection.

Protecting larger designs using current/voltage glitch or metastability detectors require more detectors. Adding more transistors will increase the power consumption. Applying selective insertion on a full processor core can be extremely challenging. Techniques such as AVF, or fault injection can be used to identify the vulnerable latches and selectively protect them [117]. Moreover, protecting the latches on the critical paths can severely degrade performance. Silicon detectors are very effective and provide excellent coverage but they are not economical. Acoustic wave detectors provide very high levels of reliability at very little area and power overheads.

3.8 Chapter Summary

In this chapter, we saw how acoustic wave detectors are used for soft error detection. They detect particle strikes via detection of the shockwave of sound they generate upon impact on the silicon surface. We first studied several particles trike detectors that detect voltage/current glitches, metastability, sound or deposited charge to detect the soft errors. We compared all the detectors for various parameters such as area, power, performance overheads.

We provided details regarding the structure and important properties of the cantilever based acoustic wave detectors. Due to its detection range it is possible that just one detector can detect a potent particle strike (and hence soft error) any where on the surface of a modern processor core or cache. Error detection using acoustic wave detectors is extremely simple and incurs negligible overheads compared to other detectors.

Once the error is detected, to provide error correction or recovery, the system should be able to accurately locate the error. The architecture based on acoustic wave detectors can be further exploited to precisely locate the particle strikes.

We presented a firmware/hardware approach in which the hardware takes responsibility for TDOA measurements and generating hyperbolic equations while the firmware is responsible for solving the equations using several algorithms.

Lastly, we presented a case study which helps understanding various trade-offs between design parameters (e.g., sampling frequency, location of detectors etc.) and the algorithmic properties (i.e., runtime, accuracy, complexity etc.). We concluded that for the maximum accuracy and coverage Algorithm 4 is the best option.

In the next chapter, we will discusses how we can use the proposed error detection and location scheme for protecting caches.

Chapter 4

Protecting Caches with Acoustic Wave Detectors

In the previous chapter, we understood how we can detect and locate soft errors via locating potent particle strikes. In doing so we observed how to construct the hyperbolic equations based on TDOA measurements. We also identified the best algorithm for accuracy by observing various trade-offs. Now we will proceed to take advantage of this information by demonstrating the utility of the cantilever detectors in detecting and locating particle strikes in the caches of a Core™i7-like processor. Next, we will show how we can leverage the location information in correcting the error using acoustic wave detectors alone. Finally, we will discuss how we can combine the acoustic wave detectors with error detecting and correcting codes and reduce the overall cost of protection.

4.1 Error Detection and Localization in Cache

The underlying architecture for detecting and locating errors in caches is similar to described in previous Chapter 3. The impact of different design parameters on the accuracy of the obtained location in caches is similar to the study of Section 3.4 of Chapter 3.

The location of the particle strike is given as estimated (X, Y) coordinates and the worst-case error area (3*CEP) that contains the actual location of particle strike.

However, this error area can be easily mapped to affected bits, bytes or cache lines that may contain the erroneous byte or cache line.

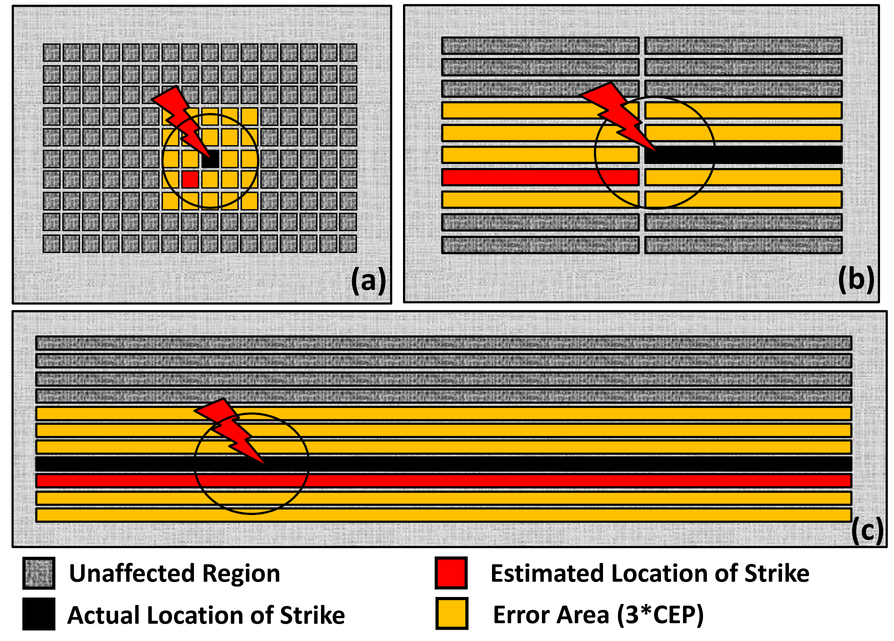

Figure 4.1: Mapping of the estimated worst-case error area at the granularity of affected (a) bits (b) bytes and (c) lines. These affected bits, bytes or cache lines contain the actual erroneous bit, byte or cache line.

We show in Figure 4.1 how the error area maps into bits, bytes and cache lines. From the discussions in Chapter 3, we know that accuracy of the location can be improved either by increasing the sampling frequency or by solving more than 2 TDOA equations.

Cache	Mesh Configuration	#Detectors in Mesh	#Detectors used for TDOA	Frequency	3*CEP Radius (#bits)	Error Area (#bits)
L1	5×5	25	25	4 GHz	1.5	7
L2	3×3	9	9	2 GHz	2.9	26
				4 GHz	1.7	10
LLC	5×3	15	5	2 GHz	3.4	38
				4 GHz	1.8	11

Table 4.1: Summary of the best mesh configurations and the error area granularities for the caches

Table 4.1 summarizes the estimated worst-case 3*CEP error area and the 3*CEP radius for all the caches for the best configurations. The error area of L1 and L2

caches are significantly smaller compared to the area of the LLC. Once the affected bits or cache lines are identified it is possible to isolate the affected cache lines to contain the error and take an appropriate error correcting action. We will discuss about error correction in caches in Section 4.2.

We have learned from Section 3.6.5 of Chapter 3 adding more acoustic wave detectors helps in reducing the error detection latency.

Cache	Mesh Configuration	#Detectors in Mesh	Detection Latency Cycles @ 2 GHz
L1	3×3	9	48
	5×5	25	29
	12×17	204	10
	137×150	20550	1
L2	3×3	9	58
	14×21	294	10
	147×198	29106	1
LLC	5×3	15	483
	23×7	161	100
	200×94	18800	10

Table 4.2: Summary of the mesh configurations for the caches and corresponding worst case detection latency cycles for a sampling frequency of 2 GHz. Marked configurations are used only for locating errors and extra detectors are added to reduce the detection latencies.

Table 4.2 gives a summary of the detection latency for each cache for different mesh configurations. Shaded configurations are the configurations used only for locating errors. We put extra detectors to reduce the detection latency in a separate mesh. Notice that, although the L1 and L2 caches use the same mesh configurations the detection latencies are different due to their different sizes.

4.2 Providing Error Correction in Caches

In this section, we describe how the error detection and localization architecture would interact with the normal operation of a processor and which are the most

important challenges for achieving high levels of error protection and error containment. Later, we will consider the case when the caches are protected only with acoustic wave detectors, and the more reasonable case when they are deployed with protection codes.

4.2.1 Reaction upon a Particle Strike

Once we know the estimate of the localization of the particle strike and the error area, it is time to take the appropriate actions to provide, when possible, fine-grain error correction. The challenges are:

1. We need to provide error containment. For instance, if a read to a cache line or eviction of a dirty cache line happens before the error is detected (i.e., the worst-case 100 cycles detection latency in the case of LLC) the error may propagate through the architectural state and cause SDC.

2. We need to provide recovery capabilities. If we can accurately pin-point the erroneous bit then one possible way to correct it is by flipping it. By recovering from the error it is possible to reduce DUE FIT of cache. Whenever it is not possible to pin-point the erroneous bit and the particle strike has occurred on a dirty cache line it is not possible to recover the error using the detectors alone.

With faster error detection and proper error containment using acoustic wave detectors it is possible to avoid SDC but we also want to provide error correction to reduce the DUE.

4.2.2 Standalone Acoustic Wave Detectors

We discuss the application of acoustic wave detectors for error recovery in caches considering these two scenarios: (i) when the error area granularity is spread over a few cache lines which is more general case and (ii) specific case where we will try to pinpoint the exact erroneous bit.

4.2.2.1 Error Area Granularity: Cache Lines

As discussed in Section 4.1, once the particle strike has been localized the error area would be spanned on several cache-lines. For example, in LLC the worst-case the error area spans over 7 cache lines. This means that we would have 7 potential cache lines where the particle could have hit. Employing 4 GHz sampling frequency for LLC reduces the error area granularity to 4 lines from 7 lines (shown in Table 4.1). Once we have the affected lines, we propose to invalidate the cache lines within the error area provided by the localization algorithm. If any of the cache lines is dirty, no recovery would be possible and we would need to throw a machine check architecture (MCA) exception. Techniques such as early write back may help in providing recovery by minimizing the number of dirty cache lines [243].

4.2.2.2 Error Area Granularity: Exact bit

From the discussions in Chapter 3, we know that accuracy of the location can be improved by either increasing the sampling frequency or by solving more than 2 TDOA equations. We are now interested in finding out for how many strikes out of 1048, it is possible to have the 3*CEP error area at the granularity of one bit. Once the erroneous bit has been located we can correct the erroneous bit is by flipping it.

The area of L1 data cache is 1 mm^2 and the detection range of one detectors is 5 mm. Hence, for L1 data cache, in a mesh with N detectors all N detectors trigger upon a particle strike. Therefore, we can built $N - 1$ TDOA equations. We tried different mesh configurations starting from the most basic overdetermined system (3 TDOA equations) with 4 detectors in 2×2 mesh upto 99 TDOA equations (i.e. 100 detectors in a 10×10 mesh).

Figure 4.2, shows the best choices for the given number of TDOA equations that we solve, out of all the mesh configurations that can be used to construct those many TDOA equations. It summarizes the break-down and the improvement in the precision for the obtained 3*CEP error area. We collect the information regarding how many times out of 1048, we can locate the actual strikes within the area granularity of 1 bit. Figure 4.2 indicates that by increasing number of TDOA equations in solving the localization algorithm we significantly improve percentage

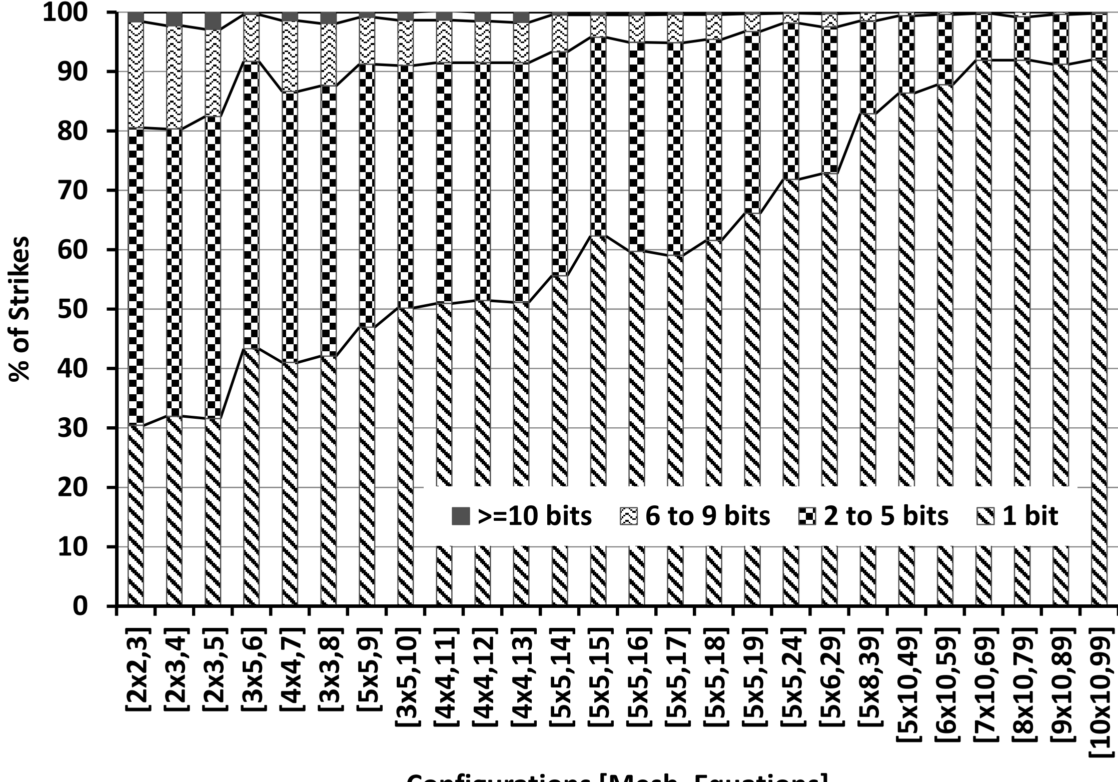

Figure 4.2: Breakdown of the obtained worst-case error area granularity for 1048 particle strikes at random location and instance for different mesh configurations in L1 data cache at the sampling frequency of 4 GHz

of 1 bit error area granularity at sampling frequency of 4 GHz. For example, in the case of solving 10 TDOA equations, out of 1048 strikes 50% of the strikes result in estimated area of $\leq$1 bit. Hence,we improve the DUE by 50%. It is noteworthy that for 50% DUE improvement with 10 equations, we will need a 3×5 mesh with 15 detectors.

As we keep solving more TDOA equations, the improvement curve soon starts to saturate. Using more detectors increases the over all cost and complexity in solving the TDOA equations. Observing the cost of solution in terms of number of detectors against the error area granularity improvement achieved, we conclude that the best trade-off for L1 data cache is obtained by configuring a 5×5 mesh with 25 detectors and solving for 24 TDOA equations with sampling frequency of 4 GHz. This configuration can pin point the exact erroneous bit 71.85% of the times. It also implies that out of 1048 strikes, 71.85% of the times we can correct the erroneous bit by flipping it. And whenever this is not possible, to prevent the corruption of the architectural state, the solution takes advantages of the error

codes already deployed for error detection of hard errors (will be discussed in Section 4.3.2).

Whether it is possible to locate the error at the granularity of several cache lines or a single bit, providing error containment is somewhat more involved using only acoustic wave detectors mainly because of their higher error detection latencies. The error detection latency is summarized in Table 4.2 in Section 4.1. In the case of LLC, detectors would trigger 100 cycles after the particle has hit the LLC. This means that any data (assuming the cache does not have error codes) leaving the LLC may have a bit flip. For cache lines being evicted, this can be easily solved using a victim buffer that delays write to main memory for 100 cycles. On the other hand, data being served to the processor would reach the head of the reorder buffer much earlier than those 100 cycles. A good option to contain the error would be stalling the commit of the load instruction (with its corresponding impact on performance) or enabling checkpointing mechanisms (will be discussed in detail in Chapter 5). Next, we will explore the possibility of combining error codes with acoustic wave detectors.

4.3 Acoustic Wave Detectors with Error Codes

In this section we present the possibility of combining error codes with acoustic wave detectors. Similar to the previous section we will consider two cases: (i) when it is not possible to pinpoint the exact erroneous bit and (ii) the case where we can pinpoint the exact erroneous bit.

4.3.1 Error Area Granularity: Cache Lines

For the case when the obtained error area spans over few cache lines, the baseline implementation is the same as explained in the previous section: once the error is localized, we would go line by line within the error area provided by the localization algorithm and *clear* them. Unlike the previous case, now we have the option of using the error detecting and correcting codes along with the acoustic wave detectors. If the code offers the correction, we would correct the error (the benefits would be similar to those of cache scrubbing [92, 93]). If code only offers detection, we would still need to invalidate the affected cache line.

Combining detectors with error codes offers two other benefits: (i) error codes allow us to contain the error when the cache line is evicted or read before the detectors trigger, and (ii) they allow us to identify if an error is caused by a hard fault or particle strike. If a cache line is read or evicted and the code triggers, we will wait up to the error detection latency cycles (i.e., 100 cycles in the case of LLC). If the error is caused by a particle strike, a detector will trigger. Otherwise, it is a hard fault. In either case, correction will be provided by the code when possible.

Columns *Error Codes+Detectors* in Table 4.3 summarize the error detection, correction and containment capabilities of the combined approach. As one can see, using *Error Codes+Detectors* we can detect all particle strikes, since detectors trigger timely and therefore, latent particle strikes do not accumulate. In general, error containment is achieved when the number of hard faults in the cache line is strictly less than the error code detection capability (1 for double error detection, 2 for triple error detection). Error correction (of dirty lines) is achieved when the number of hard faults in the cache line is strictly less than the error code correction capability (0 for single error correction, 1 for double error correction).

Columns *Error Codes* in Table 4.3 show the error detection, correction and containment of the codes without the acoustic wave detectors. If we compare both approaches (left and right of the table), one can see that the approach of *Error Codes+Detectors* is able to detect *all* temporal particle strikes that cause bit upsets (i.e., with recoil energy $\geq 10MeV$), whereas in the case of only *Error Codes* the detection is limited by their detection capability. Moreover, *Error Codes+Detectors* provides better error containment. Interestingly, in a scenario where there is presence of 1 hard fault, SEC-DED codes with detectors provide the same detection level as DEC-TED, at a much cheaper cost in area and latency (see light shadowed cells).

Usually, designers use error detection and correction codes to provide detection as well as correction (i.e., SEC-DED). L2 and L3 caches are often protected by error detection and correction codes (i.e., SEC-DED) [64, 244–246]. SEC-DED codes are less attractive for L1 caches because they take a long time to decode [46, 119, 247–249] and may add some extra cycles to executing the *load* instruction in high-speed microprocessors.

Code	HFaults	Error Codes SER	C	D	CT	Error Codes+Detectors SER	C	D	CT
Parity	0	Odd	✗	✓	✓	Odd	✗	✓	✓
		Even	✗	✗	✗	Even	✗	✓	✗
	1	Odd	✗	✗	✗	Odd	✗	✓	✗
		Even	✗	✓	✓	Even	✗	✓	✓
SECDED	0	1	✓	✓	✓	1	✓	✓	✓
		2	✗	✓	✓	2	✗	✓	✓
		≥ 3	✗	✗	✗	≥ 3	✗	✓	✓
	1	1	✗	✓	✓	1	✗	✓	✓
		2	✗	✗	✗	2	✗	✓	✓
		≥ 3	✗	✗	✗	≥ 3	✗	✓	✓
DECTED	0	$1 \ldots 2$	✓	✓	✓	$1 \ldots 2$	✓	✓	✓
		3	✗	✓	✓	3	✗	✓	✓
		≥ 4	✗	✗	✗	≥ 4	✗	✓	✓
	1	1	✓	✓	✓	1	✓	✓	✓
		2	✗	✓	✓	2	✗	✓	✓
		≥ 3	✗	✗	✗	≥ 3	✗	✓	✓
	2	1	✗	✓	✓	1	✗	✓	✓
		2	✗	✗	✗	2	✗	✓	✓
		≥ 3	✗	✗	✗	≥ 3	✗	✓	✓

Table 4.3: Comparison of protection capabilities of having only error codes versus error codes with acoustic wave detectors. HFaults stands for number of hard faults, SER number of soft errors, D for detection, C for correction, CT for containment

L1 caches are usually protected only with parity codes. Parity codes can be implemented at byte level [250] at word level [251] or at cache block level [64]. Due to incapability of correcting errors using parity, parity protected write-back cache is the largest contributor towards the total DUE-FIT of the processor due to soft errors. This forces designers to provide error correction in L1 cache. However, to have correction capability, each byte should be protected with ECC. Implementing ECC for every byte is complex and expensive. Hence, instead of providing ECC for each byte in a cache block, to reduce the cost of protection designers opt to protect cache block with ECC. But caches closer to the core have a lot of partial write operations. Having ECC at cache block level will result into an increase in read-modifies-writes operations. This incurs huge performance and energy penalty.

Without any error correction mechanism handling DUE-FIT of L1 cache is a big challenge. Moreover, processors can experience a superlinear increase in DUE-FIT when the size of the write-back cache is doubled [93]. By combining acoustic wave detectors with parity codes it is possible to handle the DUE problem in L1 cache.

4.3.2 Error Area Granularity: Exact bit

To provide error correction, the system should be able to accurately locate the error. To reduce the DUE-FIT, the architecture should be able to recover from all the errors that are detected. This can be done by exploiting the localization accuracy of acoustic wave detectors to detect and correct the errors. As discussed in Section 4.2 using only 25 detectors it is possible to pinpoint and correct the error in L1 cache for 71.85% of the times. By correcting the erroneous bit we can improve the DUE-FIT rate of L1 cache by 71.85%.

If an L1 data cache is protected with only acoustic wave detectors in 5×5 mesh, 71.85% of the times we can exactly locate the upset bit, we call this $P_{1bit_{AWD}}$. A further quantification of error area obtained by 5×5 mesh is shown in Figure 4.3. It reveals that for 14.59%, 7.53%, 2.88% and 1.33% of the times we can locate the error at the granularity of 2 bits, 3 bits, 4 bits and 5 bits respectively. We call them $P_{2bit_{AWD}}$, $P_{3bit_{AWD}}$, $P_{4bit_{AWD}}$ and $P_{5bit_{AWD}}$ respectively.

$$DUE_{(AWD)} = P_{1bit_{AWD}} = 71.85\% \tag{4.1}$$

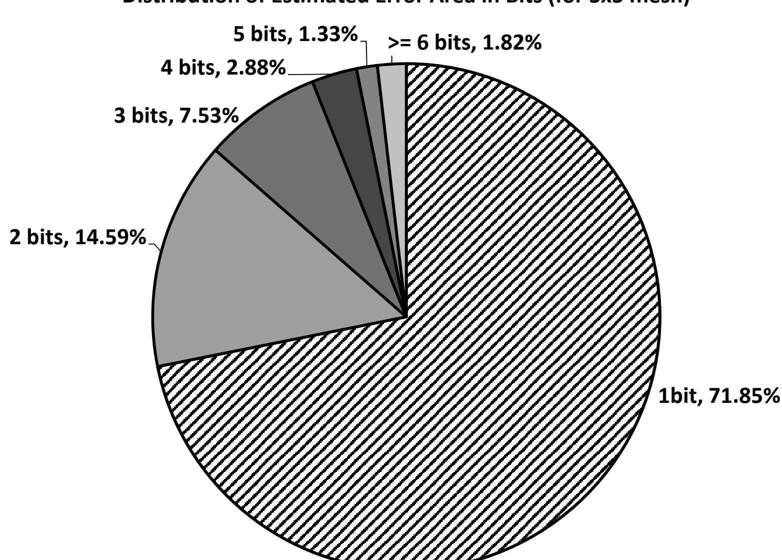

FIGURE 4.3: Quantification of error area granularity for 5×5 mesh for L1 data cache

By using only acoustic wave detectors in L1 data cache we can improve the DUE by 71.85% as shown in Equation 4.1.

Interestingly, we noted that the granularities of error area (i.e. circular area with CEP radius) obtained by acoustic wave detectors are mapped to bits in specific patterns as shown in Figure 4.4. The circle in the Figures 4.4(a-e) show the estimated error area obtained by localization algorithm. The bits that are overlapped or intersected by this circle are also shown in Figure 4.4. For single bit upsets, one of the bits covered by this circular area is erroneous. Using this mapping, we show all the possible error area patterns (not to be confused with multi-bit upset patterns) for bit granularities of 2 to 5 bits in Figure 4.5.

Because of this characteristic, *we can further improve the DUE if we can exactly isolate the erroneous bit out of the error area granularities of 2-5 bits by combining acoustic wave detectors with error codes.* To detect hard errors already parity codes can be deployed for each block or for every byte in a block. Now we will see how we can take advantage of combining acoustic wave detectors with parity codes.

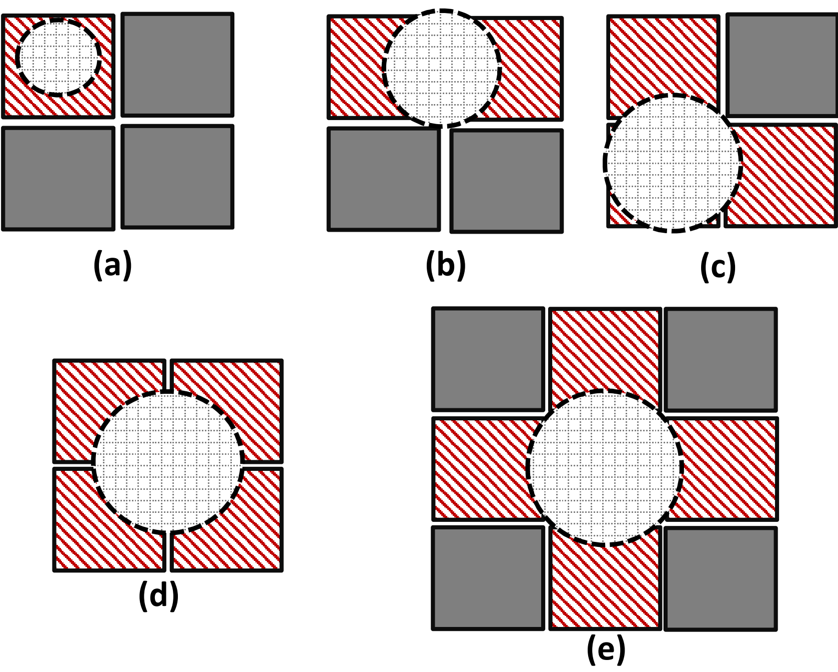

FIGURE 4.4: 3*CEP error area mapping to bits to bits of the L1 cache: (a) 1-bit, (b) 2-bits, (c) 3-bits (d) 4-bits and (e) 5-bits

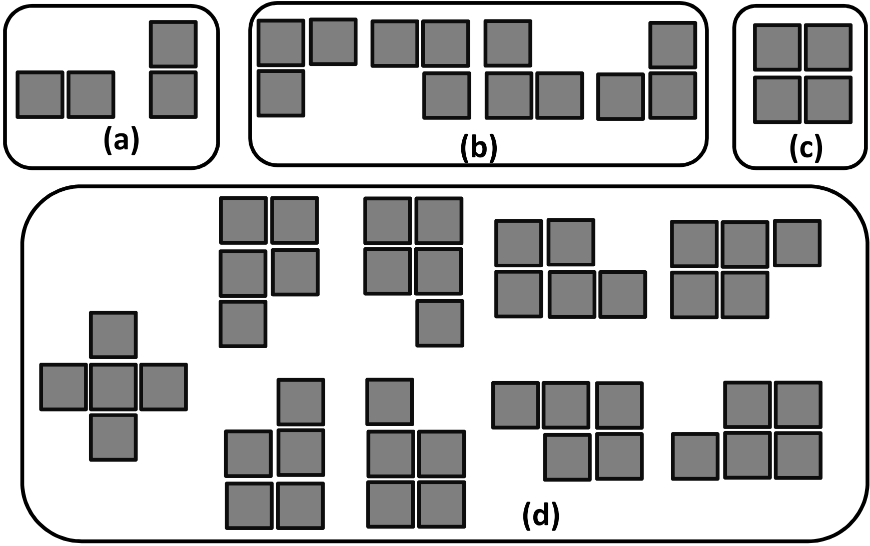

FIGURE 4.5: Possibilities of 3*CEP error area granularity patterns : (a) 2-bits, (b) 3-bits, (c) 4-bits and (d) 5-bits

4.3.2.1 Acoustic Wave Detectors + Parity per Block

Let's assume that each cache block is protected by parity bits. Figures 4.6(a-e) show the error area granularity from 2-5 bits obtained by acoustic wave detectors.

In the case of **2-bit patterns**, we assume that 2-bit patterns shown in Figure 4.5(a) are equiprobable (i.e. probability of having each of them is 50%). If both the bits are located in the same cache block as shown in case 1 of Figure 4.6(a), we will not be able to locate the exact bit. However, if the 2 bits are located as shown in case 2 of Figure 4.6(a) we will be able to locate the exact bit that was upset. This means that out of 2 cases involving 2-bit error area granularity we can always detect the patterns, that are similar to case 2. Parity per block can improve the 2-bit contribution towards DUE by further 50% $\times$ $P_{2bit_{AWD}}$.

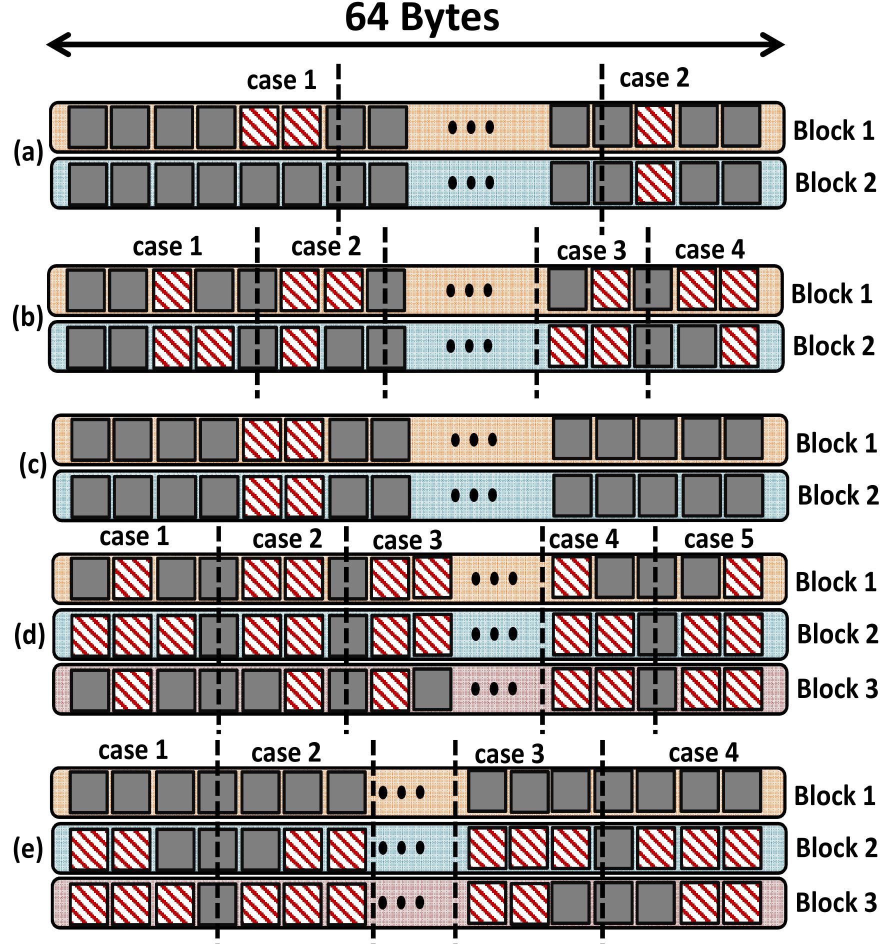

FIGURE 4.6: Probability of pin-pointing the erroneous bit using acoustic wave detectors + parity per block for 3*CEP error area granularity patterns of (a) 2-bit, (b) 3-bit, (c) 4-bit and (d,e) 5-bit

Likewise, in the case of **3-bit patterns** all the 3 bits are located in two different blocks as shown in all the cases of Figure 4.6(b). We will be able to locate the error only when the erroneous bit is the only bit lying in a different cache block out of the 3 bits of error area.

Again we consider all the 4 cases shown in Figure 4.5(b) are equiprobable(i.e. probability of having each case is 25%). Furthermore, we can detect the exact location of the error only when the error is in specific 1 bit out of 3 bits in each case. This means that we can improve DUE for each case of Figure 4.6(b) by $(1/3) \times 25\%$. This yields an overall improvement for the 3-bit contribution towards DUE by $34\% \times P_{3bit_{AWD}}$.

In the case of **4-bit pattern** as shown in Figure 4.6(c) it is not possible to locate the exact erroneous bit.

Figures 4.6(d) and (e) show the **5-bit patterns**. Here also we consider that all the patterns shown in Figure 4.5(d) are equiprobable. Hence, each can occur with a probability of 11.12%.

Similar calculation in the case of 5-bit pattern, shows that for the case 1 of Figure 4.6(d) when the strike is either in the bit that is in block 1 or block 3, it is possible to locate the exact error. This means we can correct the error if it is only in either of the two bits out of the 5 possible bits. The probability of locating exact error in case 1 of Figure 4.6(d) like patterns is $(2/5) \times 11.12\%$.

And as shown in other cases of Figure 4.6(d), it is possible to locate the exact error only when the erroneous bit is in a different block and it is the only bit of the 5 bits. This means we can correct the error if it is in only one specific bit out of the 5 possible bits. The probability of locating exact error bit in case 2, 3, 4 and 5 of Figure 4.6(d) is $(1/5) \times 11.12\%$ each. As they are all equiprobable the improvement is $(4/5) \times 11.12\%$.

Also in the occurrence of patterns shown in all the cases of Figure 4.6(e) it is not possible to locate the exact bit that was upset. As each block contains two or more bits that can be erroneous.

Putting it all together, for 5-bit pattern, parity per block on top of acoustic wave detectors can increase the DUE improvement by $(2/5) \times 11.12\% + (4/5) \times 11.12\%$ giving overall DUE improvement of $14\% \times P_{5bit_{AWD}}$.

$$
\begin{aligned}
DUE_{(AWD+Parity_{block})} = & P_{1bit_{AWD}} + 50\% \times P_{2bit_{AWD}} + \\
& 34\% \times P_{3bit_{AWD}} + \\
& 14\% \times P_{5bit_{AWD}} \\
= & 81.89\%
\end{aligned} \tag{4.2}
$$

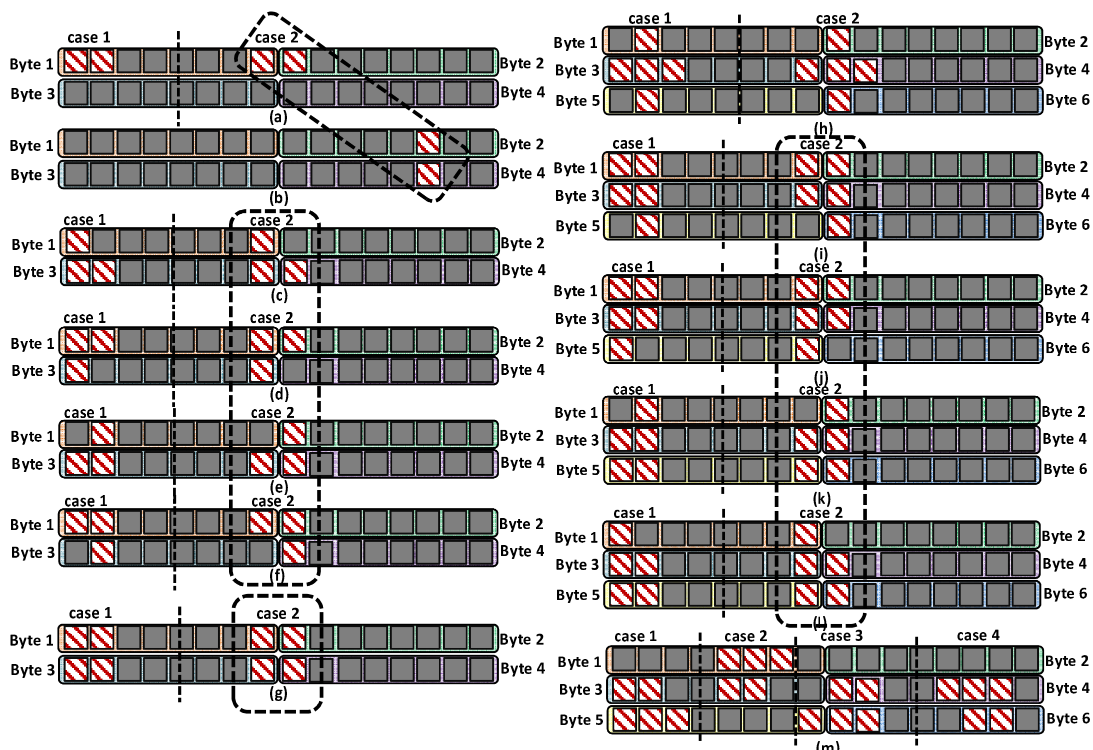

FIGURE 4.7: Probability of pin-pointing the erroneous bit using acoustic wave detectors + parity per byte for 3*CEP error area granularity patterns of (a,b) 2-bit, (c-f) 3-bit, (g) 4-bit and (h-m) 5-bit

Hence, deploying *parity per block + acoustic wave detectors* in L1 data cache will improve the DUE by 81.89% as calculated in Equation 4.2.

4.3.2.2 Acoustic Wave Detectors + Parity per Byte

Now, we will see the case when each byte in a cache block is protected by parity bits along with acoustic wave detectors. A cache block in L1 data cache of a Core™i7-like processor has 64 Bytes. Figures 4.7(a-m) show all the possible cases for locating the erroneous bit for 2-bit, 3-bit, 4-bit patterns and 5-bit patterns.

As it is obvious that if all the estimated error bits are in the same byte, we will not be able to locate the exact bit with upset. But if the bits are in different bytes it is possible to locate the exact erroneous bit.

All **2-bit patterns** are shown in Figures 4.7(a) and (b). For the patterns as in the case 1 of Figure 4.7(a), as both the error area bits are in the same byte we cannot locate the upset bit. But for the patterns similar to case 2 of Figure 4.7(a)

or patterns similar to Figure 4.7(b) both the bits are into two different bytes and as we have parity at byte level, we can exactly pin-point the upset bit out of the two bit error area.

For a 64 byte block the probability of having 2-bit pairs, in which both bits are in different bytes as shown in case 2 of Figure 4.7(a) is 12.3% (i.e. 63 pairs out of 511 total possible combinations). Which also yields probability of having patterns like case 1 of Figure 4.7(a) to 87.7%. We know that the 2-bit patterns shown in Figure 4.5(a) are equiprobable (i.e., each of them have probability of 50%). This concludes that the probabilities of having patterns like case 1 and case 2 of Figure 4.7(a) are 43.85% and 6.15% respectively and the probability of having patterns similar to Figure 4.7(b) is 50%. This implies that 56.15% of the times we can exactly pin-point the upset bit for 2-bit error area granularity. Hence, parity per byte helps improving the 2-bit DUE rate by 56.15% $\times$ $P_{2bit_{AWD}}$.

Figures 4.7(c-f) show the **3-bit patterns**. For each 3-bit pattern there are two possibilities, either these 3 bits are spread over 2 different bytes (i.e., case 1 of Figure 4.7(c)) or all the 3 bits are in 3 different bytes (i.e., case 2 of Figure 4.7(c)). Probability of having patterns similar to case 1 and case 2 of Figure 4.7(c) is 87.7% and 12.3% respectively. Moreover, all the 4 possibilities of 3-bit granularities, shown in Figure 4.5(b) are equiprobable each with the probability of 25%.

For patterns similar to case 1 of Figure 4.7(c) we will be able to locate the exact upset bit if the upset is in the one bit that is in a different byte from the other two. This means that we can improve DUE for case 1 of Figure 4.7(c) by (1/3) $\times$ (87.7%) $\times$ 25%. However, We can exactly pin-point the erroneous bit in the patterns similar to case 2 of Figure 4.7(c) and this can improve DUE by (12.3%) $\times$ 25%. Summing it up for all 4 possibilities shown in Figures 4.7(c-f) we conclude, parity per byte helps improving the 3-bit DUE rate by 41.5% $\times$ $P_{3bit_{AWD}}$.

For **4-bit pattern**, as can be seen in Figure 4.7(g) there are two possibilities. If the pattern bits are spread as shown in the case 2 over 4 different bytes in 2 rows it is possible to correct the upset. Or if they are spread as shown in the case 1 it is not possible to find the upset bit with the help of parity per byte. Parity per byte helps improving the 4-bit DUE rate by 12.3% $\times$ $P_{4bit_{AWD}}$.

Similar observation for **5-bit patterns** of Figures 4.7(h-m) reveal that for 5-bit patterns shown in Figure 4.7(h) we can locate the upset for case 1 only in only 2 bits out of 5 and the probability of having 3 bits in the same byte in a 64 byte

block is 75.3% (i.e., 384 out of 510 total combination of triplets in a block). This results into the probability to locate the upset for case 1 as $(2/5) \times (75.3\%)$ and for case 2 as we can locate 3 bits out of 5, the probability is $(3/5) \times (24.7\%)$. Again all the 9 possibilities of 5-bit granularities as shown in Figure 4.5(d) are equiprobable each with the probability of 11.12%. This yields the joint probability for 5-bit patterns shown in case 1 and case 2 of Figure 4.7(h) as $((2/5) \times (75.3\%) + (3/5) \times (24.7\%)) \times 11.12\%$.

Similarly, we can correct all the upsets in all case 2 like patterns of Figures 4.7(i-l), but we can correct only 1 upset out of 5 possible locations in all possibilities similar to case 1 like patterns in Figures 4.7(i-l). This results into a probability of $(4 \times (12.3\%) + (4/5) \times (87.7\%)) \times 11.12\%$. Also for Figure 4.7(m) the probability of locating the upset is $((4/5) \times (24.7\%)) \times 11.12\%$. Parity per byte improves the 5-bit DUE rate by $20.5\% \times P_{5bit_{AWD}}$.

$$\begin{aligned} DUE_{(AWD+Parity_{byte})} =& P_{1bit_{AWD}} + 56.15\% \times P_{2bit_{AWD}} + \\ & 41.5\% \times P_{3bit_{AWD}} + \\ & 12.3\% \times P_{4bit_{AWD}} + \\ & 20.5\% \times P_{5bit_{AWD}} \\ =& 83.8\% \end{aligned} \tag{4.3}$$

Summing up, *Parity per byte + acoustic wave detectors* for L1 data cache will result into 83.8% improvement in DUE as shown in Equation 4.3.

4.3.2.3 Acoustic Wave Detectors with Physical Interleaving

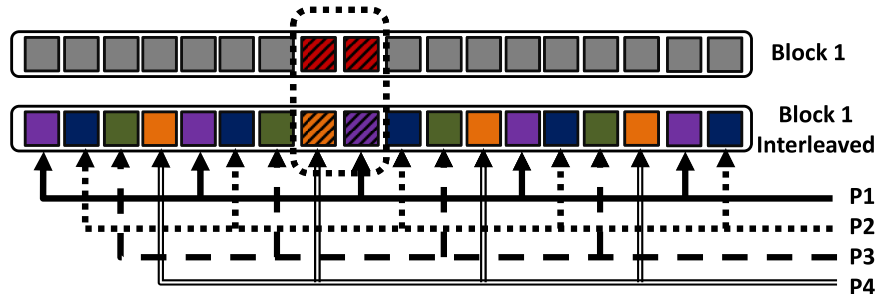

FIGURE 4.8: Probability of pin-pointing the erroneous bit using acoustic wave detectors + parity per byte and assuming the bits are physically interleaved with degree of interleaving: 4

Now, consider the L1 cache bits are parity protected and physically interleaved. Usually the degree of interleaving (DOI) of parity protected bits of L1 data cache is in the range of 4 to 16 [87, 248]. Let's assume, every byte of an L1 data cache protected with bit interleaved parity and the DOI is 4 along with acoustic wave detectors as shown in Figure 4.8. This combination will make sure that all the bits in all the patterns of Figure 4.5 are associated with a different parity code. This implies that with DOI of 4 it is possible to exactly locate the upset bit in 2-5 bit error area patterns of Figure 4.5.

Combining physical bit interleaving with DOI = 4 and acoustic wave detector will improve the DUE to 98.18%.

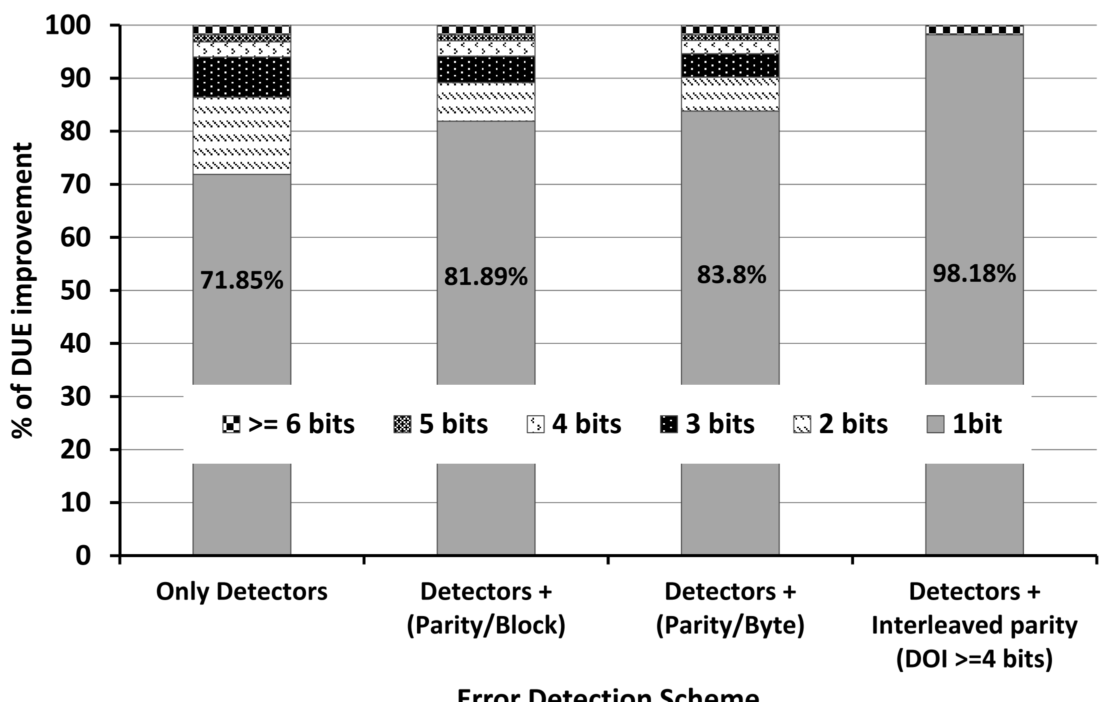

FIGURE 4.9: Probability of pin-pointing the erroneous bit and correcting it (i.e., DUE improvement) using acoustic wave detectors and combining acoustic wave detectors with parity at byte and block level and assuming physically interleaved parity protected bits in L1 data cache

Figure 4.9 sums up the improvement in the DUE achieved by using only acoustic wave detectors, and combining acoustic wave detectors with parity per block and parity per byte scheme. It also shows the improvement in DUE by combining interleaving of parity protected bits with acoustic wave detectors.

4.4 Handling Multi-bit Upsets in Caches

A single neutron strike can upset more than one bits of memory in close proximity, causing *spatial multibit errors*. Bit interleaving [87, 248] can be used to demote the spatial multi-bit fault to several single-bit faults, then simple coding techniques can correct the several single bit faults separately [252–254]. Temporal multi-bit fault is the cumulative effect of several single-bit faults in a period of time. For temporal multi-bit errors, cache scrubbing [91, 92] techniques are more effective.

As explained in Section 4.3, in a system that employs error codes without scrubbing, particle strikes may linger and increase the chance of a multiple bit error if locations go a long time without being read. The approach of *Error Codes+Detectors* presented in Table 4.3 of Section 4.3 can detect all temporal particle strikes and do not let them accumulate eliminating temporal multi-bit errors.

Our scheme takes the spatial multi-bit upsets into account in a very easy manner. We assume that a set of templates for the shape of the multi-bit upsets caused by a particle strike are available. Then, we only need to map on top of the perimeter of the 3*CEP circle the MBU templates of [87], and therefore, extend the area of affected bits. In the case of L2 and LLC as we studied in Section 4.3 usually a stronger ECC code (i.e., SEC-DED or DEC-TED) is present and can take care of multi-bit upsets. We will see how acoustic wave detectors with parity codes can handle spatial multi-bit upsets with an example of L1 cache.

We consider the spatial multi-bit upset patterns studied in [87]. Figure 4.10(a) shows the 2-bit upset patterns and Figure 4.10(b) shows 3-bit upset patterns. As we have already seen in Section 4.3.2, according to Figure 4.3 for the case of single bit upsets the acoustic wave detector can locate the bit at the granularity of 1 bit (best case) or 5 bits (worst case).

Now in the case of 2-bit MBUs, as shown in Figure 4.10(a) to be able to cover all 2-bit upsets the single bit error area mask will be transformed into an area mask of 9 bits. Similarly, the 5-bit error mask will now be transformed into an area of 21 bits. The same scenario for 3-bit MBUs, as shown in Figure 4.10(b) will require the area masks of 25 bits and 45 bits for the error area accuracy of 1 bit and 5 bits respectively.

This implies that using only acoustic wave detectors to point out the exact locations of upsets in 2 and 3 bit MBUs is not possible. Also the combination of

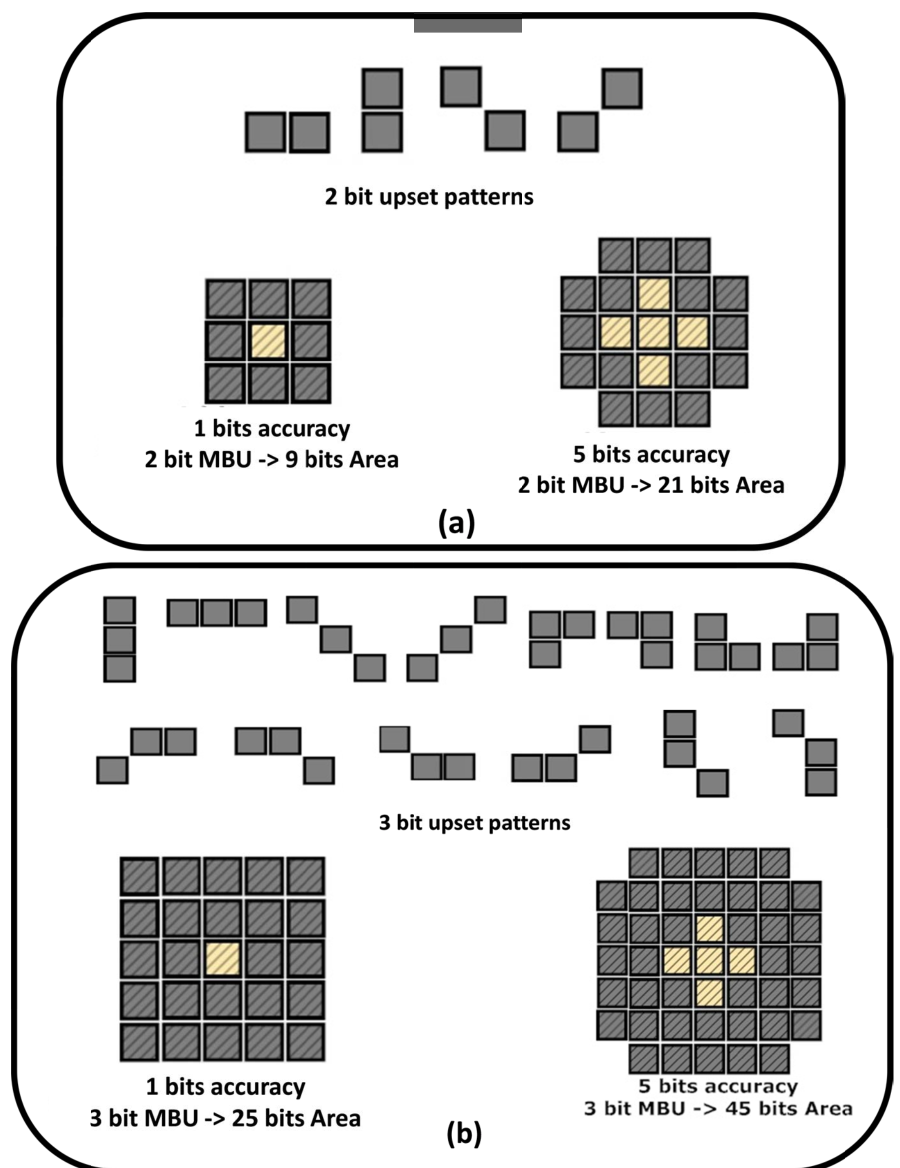

FIGURE 4.10: Extending the 3*CEP error area granularity of 1-bit and 5-bits for handling spatial multi-bit upsets using acoustic wave detectors to locate (a) 2 bit MBU and (b) 3 bit MBU

acoustic wave detectors + parity per block cannot locate the exact locations of the upset bits.

Figure 4.11 shows the scenario for the combination of *acoustic wave detectors + parity per byte.* Undertaking similar exercise as done in the case of single bit upsets earns, a DUE improvement for 2-bit MBUs by of $(3/8) \times 24.7\%$ when the error area granularity of acoustic wave detector is 1 bit. It is worth mentioning here that *acoustic wave detectors + parity per byte* cannot detect any 2-bit MBU when the

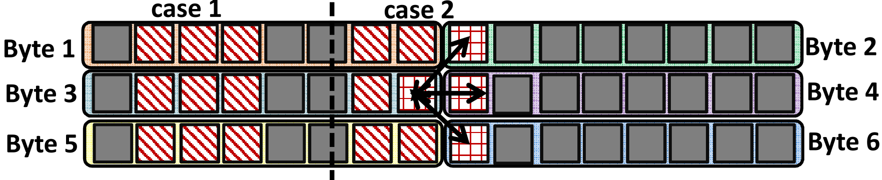

FIGURE 4.11: Probability of locating the 2 bit MBU using acoustic wave detectors configuration providing 3*CEP error area granularity of 1 bit and parity per byte

MBU type	Area gran. bits (#bits)	MBU area mask(#bits)	Min. required DOI
2 bits	1	9	4
	5	21	6
3 bits	1	25	6
	5	45	8

TABLE 4.4: Minimum required degree of physical bit interleaving (DOI) in a cache with bit interleaved parity and acoustic wave detectors

error area granularity of acoustic wave detector is 5-bits. Also, this combination is ineffective against 3-bit MBUs.

Acoustic wave detectors + bit interleaving is very effective in improving DUE by locating both bits in 2-bit MBU and all 3 bits in 3-bit MBU. This can achieve 98.18% DUE improvement for 2-bit and 3-bit MBUs. However, in adapting *Acoustic wave detectors + bit interleaving*, the minimum required degree of interleaving to be able to locate all bits in the given MBU pattern of Figure 4.10 increases with the increase in the number of bits required to be located. Increasing degree of interleaving increases the cost and the complexity of the solution.

Table 4.4 summarizes the minimum required degree of interleaving for adapting *acoustic wave detectors + bit interleaving*. In the L1 data cache, to be able to correct 98.18% 2-bit and 3-bit MBUs the optimum solution is to have acoustic wave detector with bit interleaved parity with DOI = 8.

4.5 Cost of Protection

The proposed solution will make use of two independent meshes: a small mesh for precise location of the strike (summarized in Table 4.1), and a somewhat larger mesh for detection latency given in Table 4.2.

In LLC the 5×3 mesh will be used to obtain the TDOA. In that case, the hardware mechanism will consist of 15 detectors (i.e., roughly 15 bits area), and a 2-level OR tree to generate the *Enable* signal. The tree will use 6 3-input OR gates and 2 2-input OR gates. To count the worst-case TDOA clock pulses a 10-bit counter is necessary. We will also use a 23×7 mesh to minimize the detection latency. One one hand, it requires 161 detectors (i.e., roughly 161 bits area). On the other hand, we will need a 4-level OR tree to generate the detection signal. Such tree is composed of 66 3-input OR gates and 28 2-input OR gates. Notice that in the second mesh we do not require a counter since we only want to signal the presence of the strike.

In the case of L1 cache, the area overhead includes 25 detectors (area of 25 memory bits) and a control circuit (consists of a counter and a few logic gates). Because of smaller dimensions of L1 data cache and denser mesh, the detection latency is 14.5 ns for 5×5 mesh with 25 detectors. The latency in solving 24 equations is small compared to the error detection latency. Moreover, once the error is detected we stall the processor so the delay in locating error is harmless. The detectors are passive and do not consume power and the control circuit is trivial and adds minimal power overhead.

Overhead in combined approach, such as parity per block, parity per byte and bit interleaving adds to the overall cost of protecting the caches.

4.6 Related Work

A variety of mitigation techniques have been reported to handle the SDC- and DUE-FIT related to soft errors in caches. In this section we review the basic works on soft error protection for memory arrays and peripheral logic. Many of these methods were first proposed for main memory systems. However, due to cache size increases, these methods have now been adapted to caches.

The reliability techniques can be classified into three broader categories: (i) particle strike detection for soft error detection, (ii) soft error detection and (iii) soft error mitigation.

4.6.1 Particle Strike Detection for Soft Errors

Several particle strike detector based techniques have been studied in Section 3.7.1 of Chapter 3. These techniques can also be used to detect soft errors in the caches. These particle strike detectors detect voltage or current glitches [132–134, 206] or sound [135] generated upon a particle strike. A detailed comparison is provided in the previous chapter in Section 3.7 and a summary of comparison of particle strike detectors is given in Table 3.1.

4.6.2 Soft Error Detection

Error detection techniques work by alerting the system when the system is exposed to erroneous data. For instance, in caches data usually spend a long time before being read by the processor. In a cache with error detection mechanism the data is checked for errors on every read and if found corrupted it is marked invalid. Many error detection techniques are also accompanied by error correction or recovery methods. Once the error is detected usually an error correction mechanism is invoked to correct the data.

4.6.2.1 Error Codes

The most popular method of dealing with soft errors in caches is to use error codes for error detection and correction. Error codes such as parity are often employed to detect the error and ECC is employed for simultaneously detecting and correcting errors in caches.

Figure 4.12 shows the basic process of implementing error codes. Error codes have to encode the data bits for every store operation in the cache and decode data bits upon every load operation. Every encode operation generates code word using the check bits. Upon every access to the protected data a decoding operation is performed and, the code word is re-computed and compared with the original code

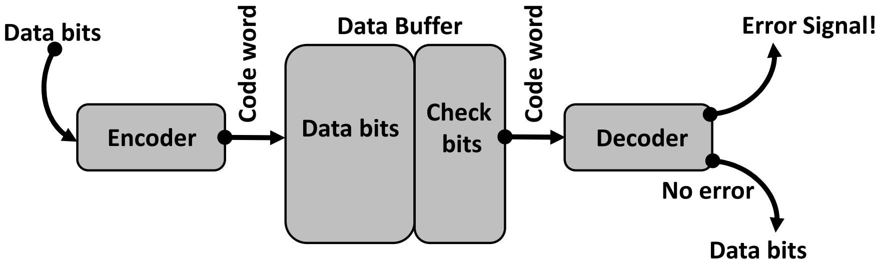

FIGURE 4.12: Basic functionality of encoding and decoding of data bits in error codes

word to protect against errors in original data. The check bits require separate storage which incurs area overhead; moreover, if the encoding and decoding of the data bits is on the critical path it may increase the cache read/write time.

Parity:
Parity is the most common technique for error detection. Parity is a simple form of information redundancy where one extra bit added for every protected group of data bits. Parity bit can be encoded based on the number of 1s in the protected bits. If there are odd number of 1s in the data bits the parity bit is set to zero and is termed as odd parity. In even parity, the parity bit is set to one if the number of 1s in the protected data bits is even. Due to this encoding, parity code cannot detect even number of errors in the protected data bits as two errors will generate the same parity bit as in the case of error free data bits.

In caches parity is computed whenever the protected cache line is modified. Upon a read to the cache line parity bit is re-computed. A parity bit match indicate the error free data. If the parity bits do not match an error is detected and the cache line can be mark invalid.

Parity can be implemented at byte level [250] at word level [251] or at cache block level [64]. Parity at byte can allow the architecture to avoid computing the parity for entire word or block for read/write operations on a byte in a cache block. Usually, L1 caches are protected with parity codes [81, 255–257] combined with error mitigation technique.

ECC:
Error correcting codes (ECC) encodes more information redundancy for providing error detection as well as correction. Similar to parity codes ECC generates a code word for every protected data word. This code word is computed upon every write

and re-computed and compared upon every read to the cache. ECC encoding is based on the concept of Hamming distance [43]. Hamming distance between two same length data words is defined as the number of bits by the two data words differ. For instance, the Hamming distance between data words 0011 and 0001 is one since they differ only in position two. In order to protect a data word against a one bit error, Hamming-distance-based ECC assigns code words such that any two data words having a Hamming distance of less than two will never share the same code word. By providing code words with Hamming distances greater than the minimum required for protection, ECC can also provide for error correction. To correct an n bit error requires a code word of size ($2\times n + 2$). In addition to correcting n bit errors, this will also detect (n+1) bit errors.

Single error correction double error detection (SEC-DED) can correct one bit error as well as detect double bit errors. By adding more code bits a DEC-TED can correct double bit errors and detect triple bit errors. Most common ECC codes used in today's processors to protect caches are SEC-DED [43, 44] and DEC-TED [89]. L2 and L3 caches are protected by SEC-DED or DEC-TED [64, 244–246, 258]. Error codes are effective way of handling single-bit as well as multi-bit errors (as explained in Table 4.3 of Section 4.3 and Section 4.4).

4.6.3 Soft Error Mitigation

Unlike error detection techniques, error mitigation techniques can avoid the soft errors altogether by employing some process or device hardening schemes. At architecture level soft error mitigation techniques may employ means to overwrite the erroneous data and hence architecturally masking the error before it is consumed.

At process level several techniques can be used to reduce the charge collection capacity of the sensitive nodes in an SRAM memory cell [259]. Using multiple well structures have been proposed to show improved robustness by limiting charge collection [260]. Another effective process technique for reducing the charge collections is to use the SOI substrates. Other process techniques include wafer thinning, mechanisms to dope implants under the most sensitive nodes etc. Process level techniques are effective and significantly reduce the soft error rate of the memories. However these techniques require modifications in the standard CMOS fabrication process and therefore are less attractive.

Another way of protecting the caches at circuit level is by making the memory cell physically robust. One way of implementing robust SRAM cell is by increasing the Q_{crit} of the SRAM cells used in caches. Radiation hardening is another circuit level approach for handling soft error rates in caches. We talk about soft error mitigation techniques at process and device level in Chapter 7.

4.6.3.1 Physical Interleaving

Physical interleaving is a technique to arrange physically adjacent bits into different logical code words. Bit interleaving [87] can be used to demote the spatial multi-bit fault to several single-bit faults, then simple encoding techniques can correct the several single-bit faults separately [252–254]. Error codes accompanying with bit interleaving can detect and correct several spatial multi-bit errors. An example of physically interleaved parity code is shown in Figure 4.8. If two adjacent bits are affected by a single particle strike and as the adjacent bits are physically interleaved the affected two bits will be detected as two single bit errors. Degree of interleaving (DOI) is defined as the number of adjacent bit errors the interleaving scheme can detect. Figure 4.8 shows a scheme with DOI=4. As the degree of interleaving increases the capacity of error codes to detect or correct spatial multi-bit errors increases. However, with increased degree of interleaving the depth of XOR logic tree for computing the parity increases and will require longer encoding and decoding time which may impact the overall performance.

4.6.3.2 Cache Scrubbing

Temporal multi-bit faults are the cumulative effect of several single-bit faults in a period of time. When the probability of having temporal multi-bit error is high cache scrubbing [92, 93] technique is often combined with ECC. Temporal multi-bit errors can be seen more frequently in large memories (e.g., LLC) where the data stays without being accessed for a very long time. Because the data is not accessed the error due to first particle strike goes undetected and upon a second particle strike it is transformed into double bit error and the SEC-DED will not be able to correct it. Cache scrubbing avoids the accumulation of errors by periodically accessing all the cache blocks and hence invoking the error codes for possible single bit error detection and correction. Typical scrubbers step through cache lines at fixed times, guaranteeing that all words will be scrubbed at least once during some

larger interval. Usually, the scrubbing frequency is set such that each cache line will be scrubbed on average more often than a bit flip occurs. Determining the cache scrubbing period can be challenging and also as every cache block is accessed periodically to check for errors the overall power consumption increases.

4.6.3.3 Cache Flush

As a part of error mitigation in cache flushing techniques a hardware of software controller mechanism is employed to periodically flush the entire contents of the cache [203, 226, 261]. By removing all the data from the cache the erroneous data is also removed improving the overall reliability. However, frequent cache flushing techniques can incur huge performance overhead due to increased cache miss rate.

4.6.3.4 Early Writeback

Usually, a cache line remains in the cache until it is replaced by another cache line according to an appropriate replacement policy (i.e., least recently used (LRU)). The *early writeback* scheme is motivated by the observation that the dirty cache lines that have not been accessed recently are unlikely to be read again. Several proposals have been made in the direction to replace the dirty cache lines in the cache after a fixed time period, earlier than they would be replaced by the usual LRU policy [243, 262, 263]. Early writeback schemes enhance reliability of writeback cache by reducing the exposure of dirty cache lines to the soft errors.

4.6.4 Comparison of Techniques

In this section, we summarize the area, power and performance overheads associated with techniques discussed above for protecting caches. Table 4.5 gives compares the process, circuit and architecture level solutions for their area, power and performance overheads. Process level techniques can be effective in terms of the reduction in the soft error rate they can achieve. However these techniques require modifications in the standard CMOS fabrication process and hence difficult to adapt in existing technology.

Circuit level solutions either employ larger transistors or include redundant transistors in the SRAM cell. For instance, the DICE cell employs 2× more transistors

than a normal SRAM cell it can incur 1.5-2× higher area overhead [264, 265]. Because of the large number of transistors per cell, these designs consume more area (and consequently more power) than six transistor cells. Employing larger cells or increasing the node capacitance can impact performance in other ways (usually degrades the read/write time of cache). Including redundant transistors may also increase the overall energy consumption.

	Mechanism	Detection Latency	False Alarms	Chip SER Reduction	Area Overhead	Power Overhead	Performance Overhead	Design Cost
Process Level	Multi-well [260], SOI [184, 185]	–	✗	5× [184]	Low	Low	Low	High
Circuit level	(V-I) sensing [132–134]	3-6 cycles	✓	Moderate	20-45% [206]	upto 100% [206]	1-10% [206]	Moderate
	Decoupling capacitor [28, 266, 267]	-	✗	25-32% [268]	Moderate	3%†† [268]	High	High
	Hardened cell [54, 264, 265, 269]	0-2 cycles	✗	10× [265]	1.5-2× † [264]	40-50%† [265]	6-8% [270]	Moderate
Architecture level	Parity	0 cycles	✗	1D	1.5%⋆	Low	Low	Low
	SEC-DED	0 cycles	✗	2D-1C	13%⋆	Moderate	Moderate	Low
	DEC-TED	0 cycles	✗	3D-2C	23%⋆	High	High	Moderate
	Interleaving (DOI=8) + Parity	0 cycles	✗	8D	1.5%⋆⋆	High	High	Moderate
	Scrubbing + SEC-DED	1000s of cycles	✗	42% [203]	13%⋆	High	High	Moderate
	Cache Flush	1000s of cycles	✗	10-25× [261]	Low	High	10% [261]	Low
	Early Writeback	1000s of cycles	✗	High	5% [263]	High	<1% [243]	Low

TABLE 4.5: Comparing different mechanisms for protecting caches against soft errors. nD indicates n bits error detection capability, mD–nC indicates m bits error detection and n bits correction capability. † overheads per SRAM cell, †† overhead per chip, ⋆ overhead per 64 bits, ⋆⋆ doesnt include overhead from the interleaving circuit.

At architecture level, while employing error detection and correction codes, the generated check bits adds to the original data bits and they are required to be stored causing area overhead; however, the relative overhead diminishes as the width of protected data word increases.

Generation and checking of parity and ECC occurs during data reads and writes and adds energy overhead. ECC encoding is done using complex bit-wise XOR logic gates across portions of a cache block and generating check bits which are stored along with the original data in the cache. Employing ECC for protecting caches can cause area and power overheads [270, 271]. Due to encoding and decoding delay of code words the ECC may add extra cycles to the cache access time incurring significant performance penalty [119, 243].

Moreover, as the complexity of code increases the overheads increase exponentially. Compared to parity the SEC-DED and DEC-TED can increase the energy overhead by 25% and 50% respectively [254]. In addition, reading and computing the ECC bits for error checking can be a performance bottleneck parity and ECC are best applied to data that is not manipulated often. Caches closer to the core have a lot of partial store operations (i.e., store instructions operating on a few bytes in a cache block). Having ECC at cache block level will result in computations of check bits for the entire cache block, incurring huge performance and energy penalty. The extra area and energy overhead to implement multi-bit error detection and correction grows quickly as the code strength is increased. Employing complex codes may also require pipelined encoding and decoding schemes which may increase the length of the critical path. Thus, parity and ECC protection of data is difficult to efficiently integrate into modern processor cores that are performance, power, and complexity constrained.

Cache scrubbing techniques can avoid the ECC latency by periodically scanning the cache, checking the data integrity. Scrubbing period may vary from 80 ns to 1000 s of ns [91–93]. Because scrubbing avoids the inline error correction of traditional ECC; it has lower error coverage than checking ECC on every read [92]. Physical bit interleaving can handle spatial multi-bit errors at the cost of additional power due to the unnecessary read access of the undesired words in the row as all cells in a row share common word-line [64, 87, 179, 244]. Additional area and performance penalty incurs due to the long word-line and column MUX circuits. The overheads grow significantly as the interleaving factor increases depending on the memory design [248, 254, 272].

The benefits of the early writeback cache against the incurred performance penalty largely depends on the behavior of the workload. If in a given workload there is only a portion of the cache that is dirty the benefits achieved will be small.

Plenty of research has been done in inventing schemes to reduce the overheads associated with error codes [46, 47, 248, 254, 273–276]. We highlight the major features for reducing the overheads related to error codes for protecting caches:

1. Existing error codes mostly protect a cache block (64 bytes) in caches. However, by protecting more bits the protection coverage can be increased at minute increase in area, power and performance overheads. Method proposed in [249, 273] protects multiple cache block or entire cache and significantly reduce the area overhead.

2. Another way of reducing the overheads is by decoupling the correction capability of ECC from the critical path. As we have seen in Table 4.5 the cost of error detection is significantly smaller than the cost of error correction. Decoupling the error detection and correction mechanisms can be beneficial especially where the soft error rate is low. One way of implementing it is to detect error on every read operation and invoke error correction only when needed [87, 248, 249, 253, 275]. Using such two-tired schemes it is possible to off load the error correction codes to DRAM to further reduce the area overhead [248].

3. Decouple the multi bit correction capability and single bit correction capability of ECC. A variable length ECC proposed in [258] that protects the common case of large number (about 96%) of cache lines with zero or one failures using a simple and fast ECC and the smaller portion of cache lines with multi-bit failures use a strong multi-bit ECC that requires some additional area and latency.

4. An alternative approach includes the mechanisms that protect only dirty cache lines in the cache. The idea is based on the observation that most of the time a majority of cache contains clean data and as this data is unmodified, another copy of correct data already exists in the lower levels of caches. Any error in the clean data can be recovered by restoring the clean data from the lower level of cache. Therefore, clean data does not require complex and expensive error correction mechanism. Work of [277] protects

the dirty cache lines in L2 and LLC via SEC-DED and the clean lines with parity code. In [86] authors proposed to protect dirty cache blocks using ECC and once the dirty cache block turns clean the correction capacity of ECC is disabled by gating some bits and converting ECC into parity code. Another variant [274] proposed to use a small cache for saving check bits for ECC or replicated cache lines. Techniques protecting the dirty cache lines in a cache can be further benefited by employing policies such as *eager write-back* to reduce the number of dirty cache lines in the cache [243, 262, 263].

5. Similar to the idea of protecting only dirty cache lines, cache replication technique [278] proposes to protect only subset of cache lines using ECC. The cache lines are selected based upon the access frequency. The mechanism proposes to store the replicas of frequently accessed cache lines in place of cache lines that are no longer required. It reduces the ECC overheads by not protecting the selected cache lines by employing redundancy in terms of replication. Not all cache lines are replicated leading to a potentially higher uncorrectable error rate than with the baseline uniform ECC. The work has been further extended that utilizes replicating dirty cache lines or parts of dirty cache lines for providing error protection [279].

4.7 Chapter Summary

In this chapter, we saw how acoustic wave detectors are used for soft error detection and localization in the caches. We first studied the implications of error detection and localization architecture on the design parameters, detection latency and error area granularity. Based on the obtained error area granularity, we explored the possibility of correcting errors. We observed that acoustic wave detectors can correct the error whenever the exact location of the error is identified. Our experiments concluded that using only 25 acoustic wave detectors it is possible to correct 71.85% errors in L1 cache.

We then explored the possibility of combining acoustic wave detectors with error codes. We discussed the architectural modifications for integrating error codes with acoustic wave detectors. We then studied the DUE problem in caches closer the the core (i.e., L1 cache). Because of the higher cost of error correction L1 caches only have error detection capability. We showed how by accommodating

acoustic wave detectors with bit interleaved parity codes, we can correct 98% of single bit errors in the L1 cache.

Lastly, we presented a mechanism to handle the multi-bit errors in caches. We observed how SEC-DED codes with acoustic wave detectors provide the same detection level as standalone DEC-TED, at significantly low overheads. We also studied how adapting acoustic wave detectors and parity protected physically interleaved bits can provide protection against 2-bit and 3-bit MBUs at very low cost.

In the next chapter, we will discusses how we can use the proposed error detection and location scheme for protecting entire processor core.

Chapter 5

Protecting Entire Core with Acoustic Wave Detectors

In the previous chapter, we understood how we can protect caches against soft errors using acoustic wave detectors. In Chapter 3 we developed an architecture that detects and locates the errors in processor core. Now we will proceed to take advantage of error detection architecture based on acoustic wave detectors in providing efficient error containment and recovery in the core of a Core™i7-like processor. By providing error containment and recovery the proposed architecture can potentially eliminate the SDC and DUE of a processor core. The architecture uses acoustic wave detectors for dynamic particle strike detection. Moreover, the architecture does not allow errors to escape to user (i.e., updating main memory or i/o devices) before detection, eliminating SDC. Eliminating DUE of core is more involved and our proposal relies on a novel and cantilever-specific checkpointing for recovery. Next, we will show how the proposed architecture scales to protect multi-core systems. Finally, we will evaluate the performance impact of the proposed architecture using real life workloads.

5.1 "SDC & DUE 0" Architecture

The main objective of the proposed architecture is to achieve 0 SDC- and DUE-FIT per core. SDC occurs when errors escape and become visible to the user. And DUE occurs in the absence of an error recovery mechanism. Error correction is handled by either moving the system to a state that does not contain the error

(e.g., using checkpointing) or by an on-the-fly error correction method, which is possible only when the error is detected before the erroneous data is consumed. Next, we will see how error detection latency plays an important role in deciding the overall cost of SDC and DUE.

5.1.1 Effect of Detection Latency on SDC & DUE

Acoustic wave detectors detect all soft errors due to alpha and neutron strikes. However, not only detection of error but how soon the error is detected is also very important. Detection latency defines the degree of error containment. Depending on the detection latency, errors can be contained at various granularities in a processor (i.e., within pipeline or caches etc.). Efficient error containment is essential for avoiding SDC (e.g., error is visible to user before its detection) and it also has an impact on the recovery process.

Detection Mechanism		Post Consumption Detection Latency	Containment Cost	Size of Checkpoint	Protects	Detection Coverage	Area Overhead	Performance Overhead
Redundant execution	Lockstep [58, 115], DMR [280], DCC [281]	Cycle-by-cycle detection	Low	Small	Core	100%	100% [58, 115, 280], 1% [281]	>1.5-2×
	RMT [72], CRT [57], AR-SMT [68]	Hundreds of cycles & unbounded	High	Large	Core	<100%†	Low	>2×
Instruction duplication	EDDI [282], SWIFT [283], CRAFT [284]	Low & unbounded	Low	Small	Core & Main memory [282]	<100%* [283]	Low	>150% [282]
Symptom checks	Error Codes [117], Hardened latches†† [54, 264, 265, 269]	0 cycles & bounded	Low	–	Main memory [117], Logic [54]	100% [117]	12.5% [117], ∼55% [54]	Low
	BIST [285], Bulletproof [286]	Periodic & bounded	High	Large	Core	Only hard errors 90% [286]	5%-6%	5%-25%*
	SWAT [287], Shoestring [35], Restore [36], Perturbation [288]	Millions of cycles & unbounded	High	Large	Core	<100%** [35]	Low	5-16%
Monitoring invariants	DIVA [67], Argus [289]	Low & bounded	Low	Small	Core Backend [67], Core [289]	100% [67], ∼100% [289]	6% [67], 17% [289]	5-15%
Sensor based	Acoustic detectors [135]	100 cycles$^{\mp}$ (configurable) & bounded	Low	–	Cache	100% detection	<1%	Low
	(V-I) detectors [132–134]	3-6 cycles & bounded	Low	–	Main memory & Logic	Moderate	20-45% [206]	1-10% [206]
Proposed Architecture		30-100 cycles$^{\mp}$ (configurable) & bounded	Low	Small	Core	100% detection & recovery	<1%	0.6%

TABLE 5.1: Comparison of different error detection schemes († vulnerability holes in LSQ logic (i.e., MOB logic), * cannot detect errors in stores, †† does not detect but prevents error, * only for simple in-order cores, ** cannot detect if fault does not manifest a symptom, $^{\mp}$ latency from actual strike instance)

Table 5.1 reviews the detection latencies for different error detection techniques once the error is consumed. Bounded latency means the error is detected within a fixed number of cycles, that is known a-priori or can be set by the designer (e.g., periodic BIST). Longer detection latency enforces the error containment to be done at higher degree of abstraction in a processors, and results in more complex hardware and/or software checkpointing/recovery mechanisms. Excessively long detection latencies may not be even recoverable. Long detection latencies can also prevent the fault diagnosis due to weak correlation between the fault and its symptoms or due to the limited on-chip tracing storage (i.e., log sizes).

Error detection mechanisms with lower detection latency provide the best tradeoff. Therefore, to achieve SDC-& DUE 0 core at minimum cost we next explore error containment and recovery for minimum latency (i.e., containment before error updates architectural state).

5.1.2 Achieving SDC-& DUE 0 per Core

In order to achieve 0 SDC, we can equip a processor core with acoustic wave detectors so it detects all particle strikes that may cause an error. To have DUE 0 per core, the architecture must be able to recover from all the errors and restore correct processor state; this includes architectural register file, RAT, PC etc.

Previous work [135] proposed using acoustic wave detectors in combination with error correction codes to detect and locate errors in memories. In this section, we extend it and assess its detection latency and capabilities to address challenges in achieving SDC-& DUE 0 for an entire core.

Achieving SDC 0 per core: The first option that we explored is protecting the core for the minimum error detection latency. It requires that the error is captured before the wrong value is committed.

Given the dimensions of current core designs, a single detector would suffice to detect all errors. Recall from Section 3.2, using just 1 detector implies the worst-case detection latency of 1000 cycles at 2 GHz, which may give time for erroneous instructions to commit before being detected.

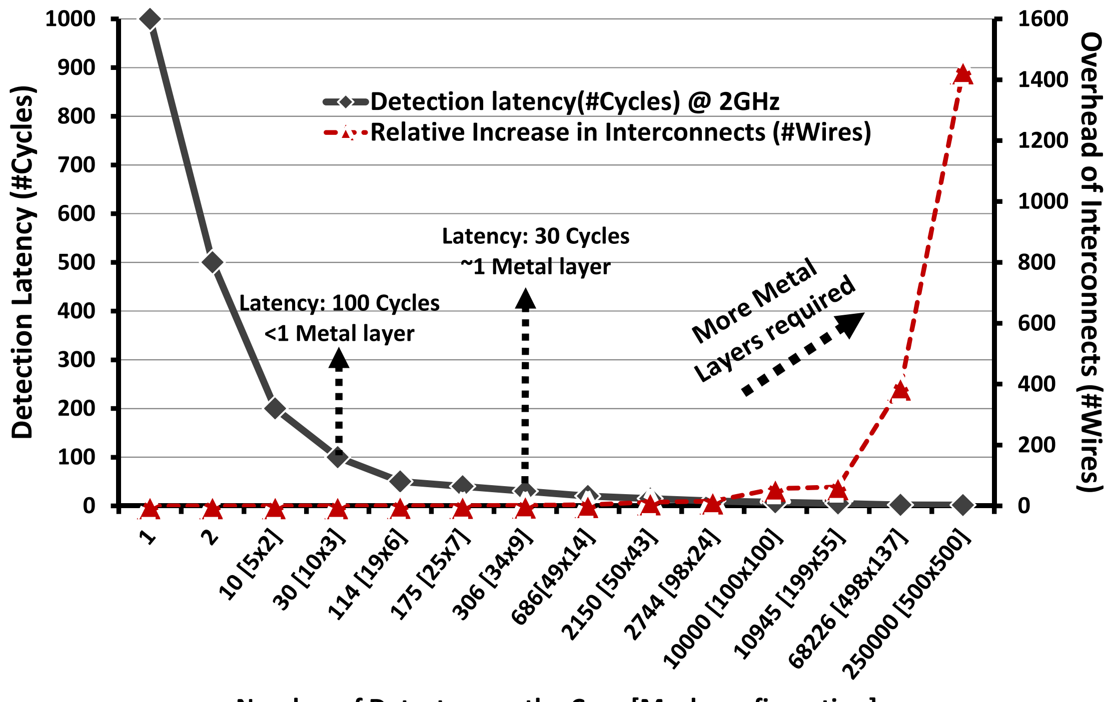

Figure 5.1: Number of detectors vs. detection latency at 2 GHz

Obviously, in order to reduce the detection latency, we can deploy more detectors, for instance in a mesh formation. Figure 5.1 shows the detection latency and complexity for various mesh configurations. Complexity in terms of increased number of wires is calculated. It is clear that the detection latency varies exponentially with number of detectors. Also complexity increases with number of detectors.

According to Figure 5.1, we will need >68,000 detectors to guarantee that no instruction will be committed before it is checked for errors (error detection latency of 1 cycle).

Achieving DUE 0 per core: With 68K detectors we contain the errors before they are committed. If the strike happened in speculative state, a nuke and retry will suffice to recover. However, if the strike is in the architectural state, recovery is somewhat more involved. One option is using error correcting codes; nevertheless, majority of the structures that hold the architectural state (i.e., architectural register file) do not have error correcting codes. Therefore, we opt to periodically take checkpoints (that include shadow copies of the architectural state).

In a nutshell, for SDC- & DUE 0 core we will need 68K detectors. This implies

an area overhead equivalent to having 68K bits of SRAM (∼7KB cache). Moreover, as shown in Figure 5.1 the interconnects to the micro-controller from 68K detectors increases the complexity and require >5 metal layers and pose significant challenges in place and route [290, 291].

Next, we will explore an optimized architecture that reduces the number of detectors without compromising the reliability coverage.

5.1.3 Divide and Conquer for SDC and DUE 0

We made the observation that errors in different stages of pipeline take different time until they propagate outside the containment area (i.e., before they commit). We know from previous section that providing detectors to all the functional blocks for the same detection latency is expensive in terms of area overhead and it is complex. To reduce the number of detectors for containment before erroneous

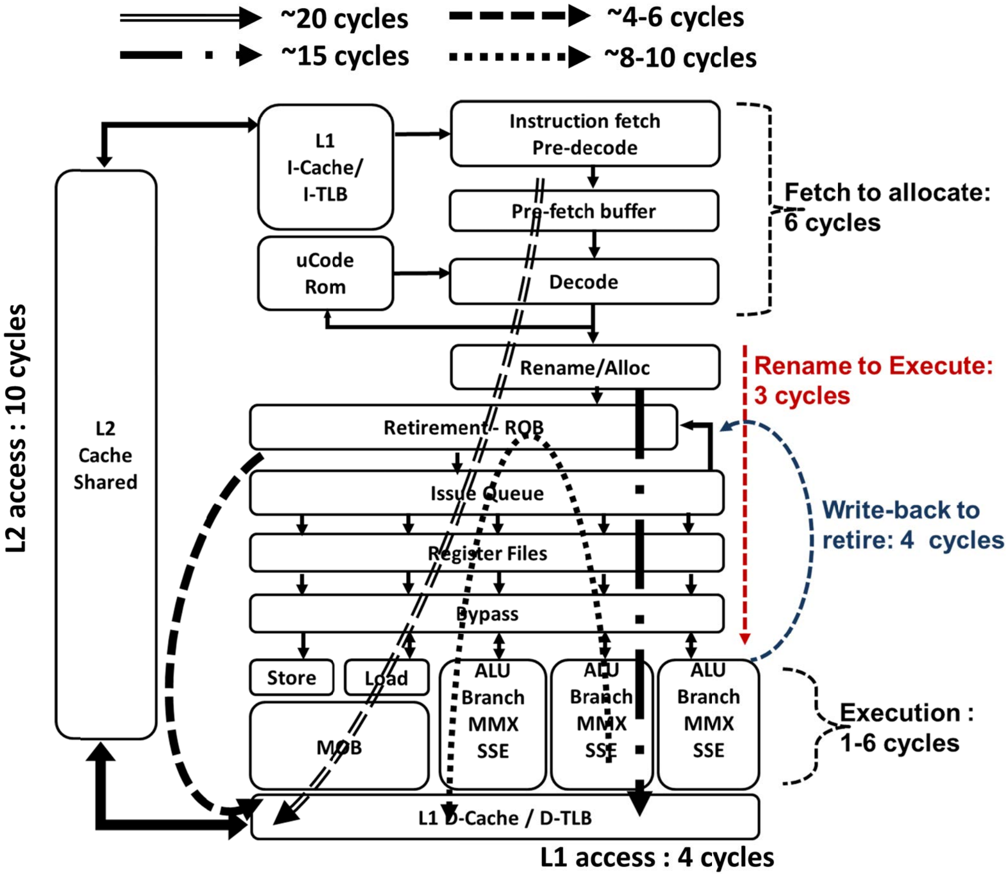

Figure 5.2: Pipeline of a state of the art processor and the latency of stages

instruction is committed, we study pipeline structures and analyze the time each

instruction spends in traversing through the pipeline. We collect the latency requirements for all structures to provide coverage to all instructions. This gives us an insight of the required detection latency for each structure in the core.

Figure 5.2 shows the pipeline of our base core running at 2 GHz. It shows the latency for different stages of the pipeline up to commit. We identified four different paths with different latency: (i) fetch/decode until commit takes 20 cycles, (ii) rename/scheduler to commit takes 15 cycles, (iii) execute to commit takes 8-10 cycles, and (iv) write-back/retire to commit is 4-6 cycles.

For example of fetch stage, once fetched, all instructions will take minimum 20 cycles (considering best case) to reach the commit stage. Providing single cycle detection latency for structures in fetch stage (i.e., prefetch, branch-predictor etc.) would be unnecessary.

Pipeline stage	**#Detectors**
Fetch + Decode (including I-Cache, D-Cache, TLBs)	1787
Rename + Schedule	170
Execute	461
Writeback + Commit	139
Total	**2561**

Table 5.2: Required number of detectors for containment in core

From this initial observation, we identified that some data-flow paths are more critical (i.e., writeback to commit) and will need stricter detection latency requirements for error containment. So, instead of protecting all the functional units in pipeline for a common detection latency we propose to put detectors for individual functional units. By protecting each functional units for respective *allowable* detection latencies we can reduce the number of detectors and still achieve 0 SDC. And for 0 DUE we keep low cost shadow copies of architecture state as described in Section 5.1.2.

Now we contain errors before they commit and as shown in Table 5.2, it requires 2.5K detectors for functional blocks in pipeline for their *allowable* detection latency requirements.

Overheads. 2.5K detectors cause an area overhead equivalent to 2.5K bit SRAM. Complexity for accommodating 2500 (low latency) interconnects occupy ∼4 metal

layers causing an unacceptable area overhead as shown in Figure 5.1. Moreover, control circuit for handling 2500 logic inputs is complex and requires a 2500×1 MUX (∼22K extra CMOS cells).

5.1.4 Containment in Core: Recap

We realized that achieving DUE 0 by recovering within the core demands 68K detectors. To reduce the area overhead, we explore a modification that protects each pipeline stage based on its *allowable* detection latencies. By relaxing error detection latency requirement, the required number of detectors for efficient error containment goes down to 2.5K. However, the resulting design is complex and the area overhead of 2.5K interconnects is still unacceptable.

Hence, we propose to extend the error containment area beyond the commit stage to the cache hierarchy.

5.1.5 Proposed Architecture

There are several advantages of containing and recovering from errors within cache hierarchy [228, 234, 292], such as (i) cache assisted containment and recovery techniques are not intrusive on the architecture and require little modifications, (ii) they accommodate larger checkpoint periods reducing the need of frequent checkpointing and (iii) the cost of recovery in terms of the amount of work to be undone is little.

Including caches in the error containment boundary implies that we can further relax the detection latency requirement which in turn reduces the required detectors. According to Figure 5.1 relaxing detection latency constraint by 10× (i.e., from 10 cycles to 100 cycles) reduces the number of required detectors by 90× and this reflects in 100× decrease in complexity and interconnects overhead. We believe that a good trade-off between detection latency, area overhead and complexity lies within 30-300 detectors, which means 30-100 cycles latency at 2 GHz.

Our proposed architecture to provide DUE 0 cores consists of the following steps:

Error detection. We use acoustic wave detectors to detect particle strikes in the core. We opt for a simple configuration with a number of detectors in the range of

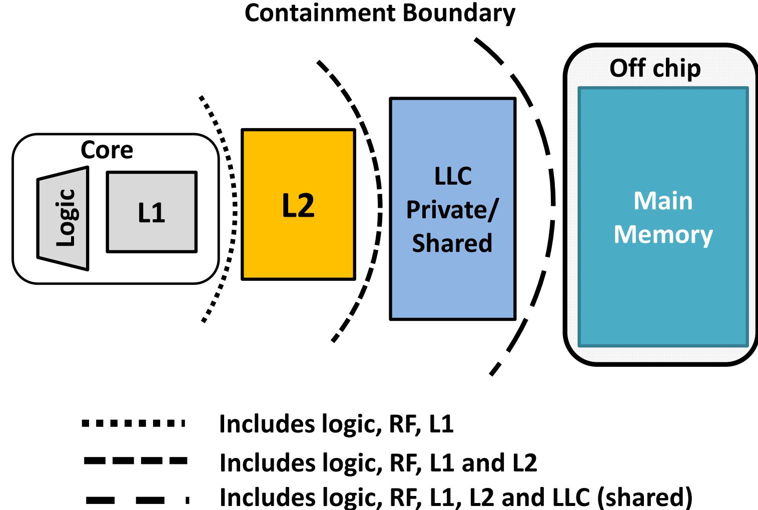

FIGURE 5.3: Error Containment Architecture

30-300, which provides a detection latency in the range of 30-100 cycles running at 2 GHz.

Data error containment. We choose our containment area to be the cache hierarchy. Figure 5.3 shows the different error containment boundaries for an architecture with a single core and three levels of cache. Notice that the boundary of the containment area can be configured to be at any cache level. We assume that the caches themselves are protected by some mechanism. A datum will be correct once it has spent more time than the worst-case error detection latency in the cache (this way, we guarantee that the datum was produced correctly). In order to guarantee containment, we do not allow any data to go out of containment region before making sure that data is error free.

Data checkpointing. Containment boundary helps deciding the checkpoint boundary. By definition, containment boundary lies within the checkpoint boundary. If not, then there is a possibility of corrupting the checkpoints. Every *conceptual* checkpoint will consist of the architectural state (e.g., RF, PC, etc) and the memory data. Process of checkpointing would include saving register values and flushing cache block values within the checkpoint boundaries that have been modified since the last checkpoint.

Data recovery. Upon an error, data recovery consists of invalidating all temporal data within the checkpoint boundary, and resume execution from the latest checkpoint. Notice that this checkpoint will consume the data from outside the

checkpoint area (and therefore, the containment area), that is guaranteed to be correct.

Next, we will discuss implementation aspects of proposed architecture.

5.2 Implementation of Proposed Architecture: Unicore Processor

Without loss of generality, we will use as a running example of a system comprising a single core and two levels of cache, with LLC as the boundary of the containment and checkpoint area. For instance, a system with three levels of cache, and L3 as the boundary would be implemented exactly the same way, with L3 acting as our described LLC, and L1 & L2 collectively acting as our L1 cache. For the rest of the text, we assume that worst-case detection latency for the acoustic wave detectors is $ErrorDetectionLatency$.

5.2.1 Error Containment Mechanism

The purpose of the containment mechanism is to make sure that only error free data goes beyond the containment area. In our implementation, where we use acoustic wave detectors as error detection mechanism, only data that has spent more than *ErrorDetectionLatency* (EDL) cycles within the containment boundary has been produced in the right way.

We propose to add one counter for entire cache within the containment area. The counter monitors the modified data in the cache and keeps track of the correctness by counting *ErrorDetectionLatency* cycles.

Initially, the counter is set to force unknown state (i.e. counter = "X") as there is no modified data in the cache. We reset the counter (i.e., counter = "0") once any cache line in the given cache is modified following a *write* operation. Until counter finishes counting *ErrorDetectionLatency* cycles, the cache is in quarantine as we are not sure if it contains erroneous data or correct data. Once counter reaches *ErrorDetectionLatency* cycles the cache is said to be verified. A verified cache means that the updated data is error free as no error has been detected.

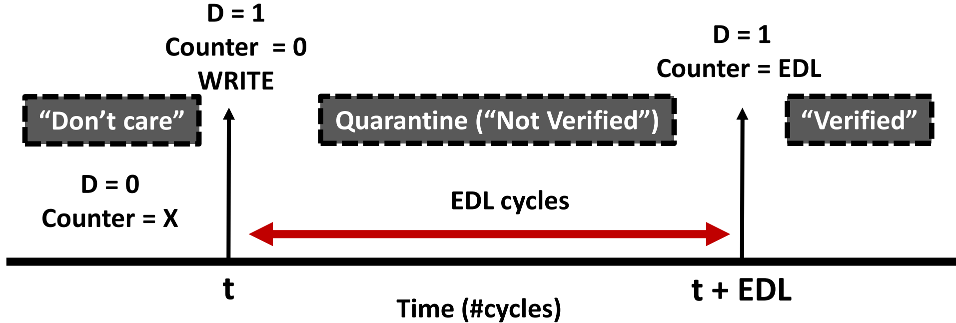

FIGURE 5.4: Time-line of the events in cache. *D* indicates the dirty bit and *EDL* stands for error detection latency. Once the cache line has been written the cache line enters in quarantine state. After *ErrorDetectionLatency* cycles the cache line is now in verified state and also error free.

Remember, counter is reset (i.e., counter = "0") upon every *write* operation from the core. *Read* operations do not affect the state of counter.

Example. Figure 5.4 shows the basic events for a cache line in the cache. Before the *write* operation the line is clean (i.e., *dirty bit*, D = "0") and counter = "X". Following a *write* operation at time *t*, D = "1" and counter is reset (i.e., counter = "0"). After *ErrorDetectionLatency* cycles entire cache is verified. Now, we will discuss how the normal cache operation is carried out in proposed architecture. For that purpose we will be using Figure 5.5, which shows different events that may happen to cache lines within the cache of containment area.

5.2.1.1 Dealing with Verified Cache.

Figure 5.5(ii) shows the case of evictions of dirty cache lines in a verified cache, we allow them to make forward progress and leave the containment boundary. Later, they can be part of the new checkpoint.

5.2.1.2 Dealing with Not-Verified Cache.

Not-verified cache is in quarantine. *Read* operations from the core do not alter the state of counter, since potentially erroneous data will not leave the containment area.

Evictions from L1 cache. Figure 5.5(i) shows the actions to be taken upon an eviction of a dirty cache line when the L1 cache is not verified. First, we will evict

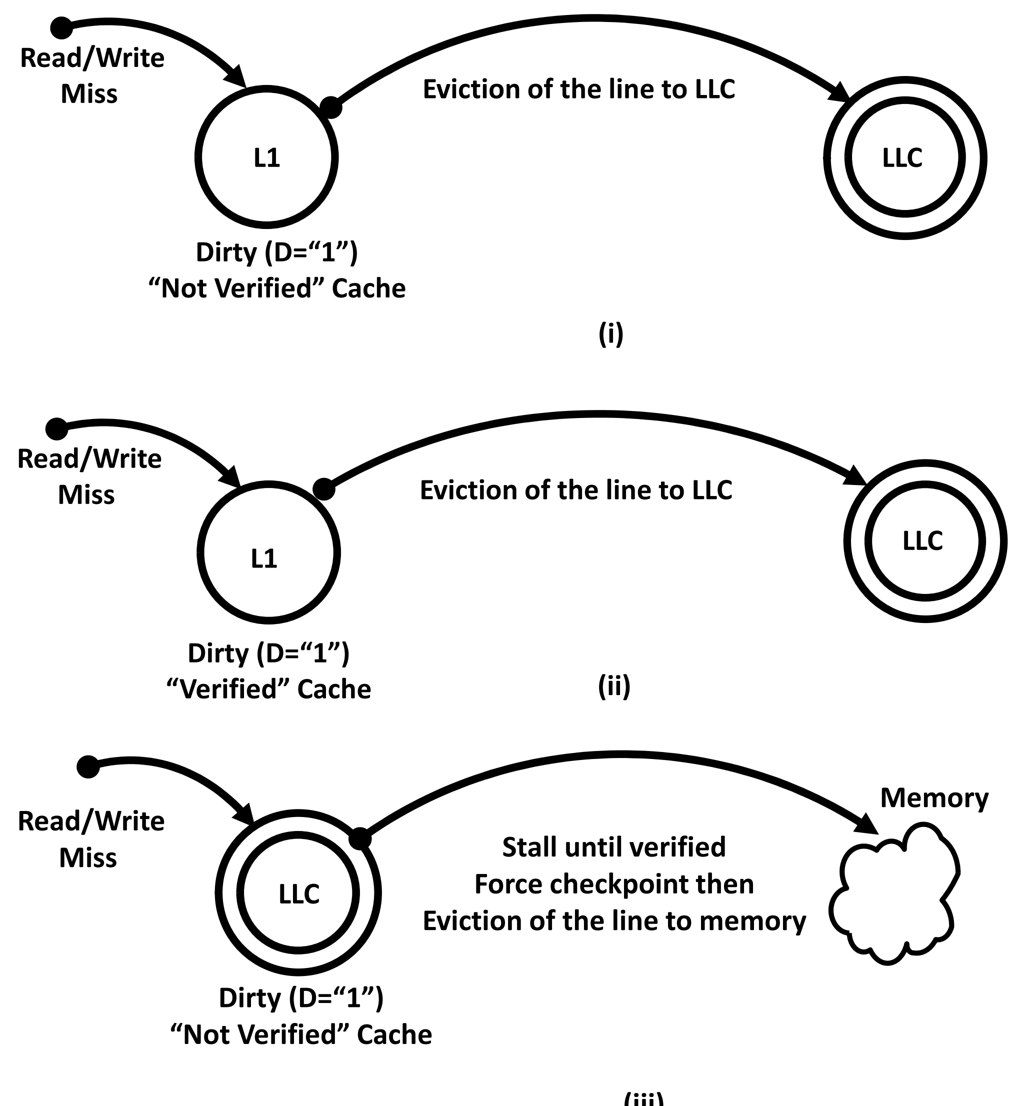

FIGURE 5.5: Error containment in cache for evictions caused by read and write operations. D indicates the dirty bit.

the cache line to LLC. The counter could be inherited or pessimistically reset at LLC. Alternatively, we could stall until the L1 cache is verified before evicting modified cache line to LLC.

Evictions from LLC. Evictions of dirty cache lines from LLC (i.e., containment boundary) when LLC is not verified are not allowed as is the case of Figure 5.5(iii). In such event we will stall until LLC is verified.

In Section 3.6 we analyze all the cases discussed above for their impact on performance and observe tradeoff between error containment area and cost of containment using real life workloads.

5.2.2 Creating Checkpoints

The checkpointing process should include:

- Copying the architectural state.
- Saving the program counter.
- Wait for all caches to be verified.
- Writeback all dirty data in lower (verified) caches to main memory.

For checkpointing architectural state we suggest to use shadow structures as proposed in [293]. The copy of program counter is stored in a special register. All these structures are assumed to have error recovery capabilities (e.g., ECC).

We anticipate that writing all dirty data present in all caches to memory may be expensive. Similar to previous works [228, 292], we adopt an *incremental checkpointing* where only dirty lines from the caches closest to the core (L1 in our running example) are written back to the cache in the boundary of the checkpoint area (LLC in our running example). Dirty lines in the LLC are now part of the checkpoint. In this configuration, the *data part* of the checkpoint will be split between the LLC and main memory.

In order to implement such optimization, we add a *checkpoint bit (CH)* in every cache line of the cache in checkpoint boundary (i.e., every cache line of LLC). Initially the *checkpoint bit* is set to "0", which means that the line is not part of the checkpoint.

Periodicity. In this proposal we take periodic incremental checkpoints. The frequency of checkpoints and its implications are further discussed in Section 5.5. Next, we discuss how we handle events to cache lines of cache in the checkpoint boundary (LLC in our running example).

Figure 5.6(i) shows the the case of a dirty cache line in LLC that is part of checkpoint. In that case we allow any eviction since the cache lines are already part of the checkpoint and do not affect the recovery of the correct architectural state. Moreover, write hits to a cache line that is part of the checkpoint will result into an eviction as the cache line cannot be modified without having a safe copy in main memory. Therefore, we evict the cache line to memory, reset the *checkpoint*

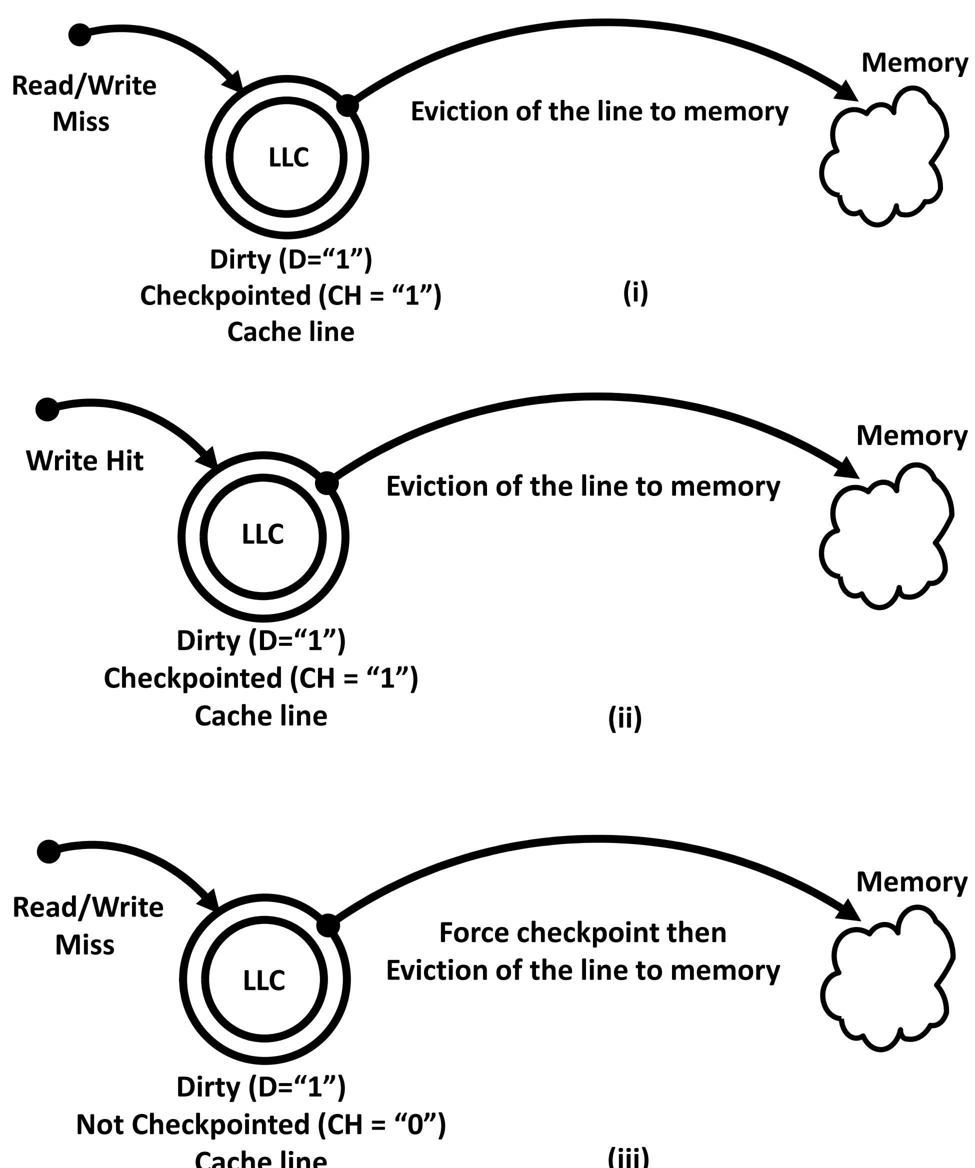

FIGURE 5.6: Checkpointing in the caches due to the evictions caused by read and write operations. *D* indicates the dirty bit and *CH* stands for the checkpoint bit.

bit and then serve the write as shown in Figure 5.6(ii). Finally, in the case of Figure 5.6(iii) an eviction of dirty line that is not part of a checkpoint in LLC will force a checkpoint before being evicted to memory.

Waiting for verified data. It is important to note that in order to take a checkpoint, we need to stall until the caches (L1 and LLC) are verified. Once they are verified, we can start writing back all cache lines to checkpoint boundary to take checkpoint.

5.2.2.1 Validating the Checkpoint.

Checkpointing process is not free from suffering particle strikes. Therefore, we need to pay careful attention to guarantee that the checkpoint is valid.

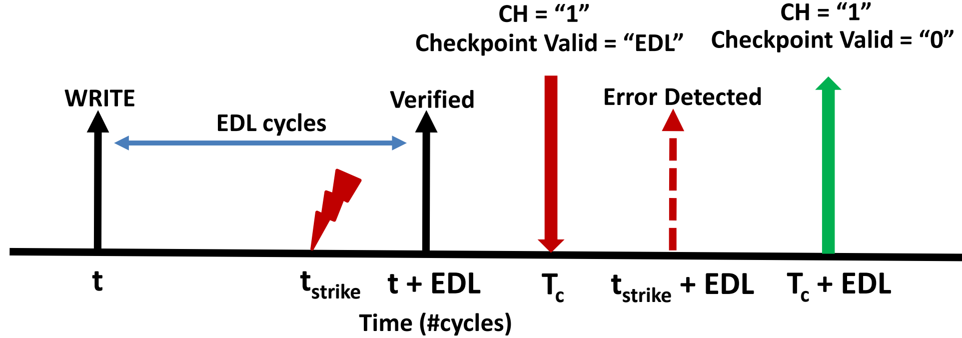

FIGURE 5.7: A scenario indicating the importance of validating the checkpoint. *CH* indicates the checkpoint bit and *EDL* stands for error detection latency. Notice the *CheckpointValid* counter that indicates the validity of the checkpoint.

Consider a scenario as shown in Figure 5.7. It shows a cache line in LLC. The cache line is part of checkpoint at instance T_c. Assume a situation where the cache line is hit by a particle at instance t_{strike}, where $t_{strike} \in [t, t + ErrorDetectionLatency]$. In this case if $T_c < (t_{strike} + ErrorDetectionLatency)$ the strike will be detected after taking checkpoint, resulting in incorrect checkpoint.

To avoid creation of corrupted checkpoints, we also add one global counter *CheckpointValid* to LLC (i.e., cache in the checkpoint boundary). As soon as the checkpoint process is finished the *checkpoint bit* is set, at the same time the counter *CheckpointValid* is set to *ErrorDetectionLatency*, and we let it decrement. After *ErrorDetectionLatency* cycles, When *CheckpointValid* reaches 0, it asserts *valid* signal indicating a valid checkpoint as no error was detected.

CheckpointValid counter guarantees the correctness of the checkpoint in the LLC. However, in order to be able to recover we must keep two copies of the state (one for the *yet-to-be-valid* checkpoint, and the other of previous *valid* checkpoint) of RAT, RF and PC. If an error was detected before the *CheckpointValid* reaches 0, we would just rollback to last *valid* checkpoint, ignoring the *checkpoint bit* of all cache lines in LLC.

5.2.3 Recovering from Error

Upon a particle strike, one of the detectors would trigger detecting the error. Recovering from an error requires a few steps:

1. Once we know the checkpoint is valid ($CheckpointValid$ = "0") the recovery may begin. If not, we have to discard current checkpoint as explained earlier, and apply the recovery algorithm.
2. Restore architectural state from shadow copy.
3. Invalidate all the dirty lines and set the counter of L1 cache to force unknown state (i.e. counter = "X").
4. Invalidate all the dirty lines of LLC that are not part of the checkpoint.
5. Set the counter of LLC to force unknown state (i.e. counter = "X").

5.2.4 Intrusiveness of Design

The proposed architecture is extremely simple. It achieves SDC- & DUE 0 core using just one counter for caches within the containment area (i.e., L1 and LLC). It also requires one *checkpoint bit* for every cache lines in the cache that is the checkpoint boundary (i.e., LLC). To validate the checkpoint we have one global counter $CheckpointValid$ for LLC.

Regarding the checkpoint itself, we maintain 2 of the most recent copies of RAT, RF and PC, encoded using ECC. Having a shadow register file for checkpointing register files and keeping the log of RAT incurs little area and power overhead [293]. Besides their impact on performance is minimal as retrieving and saving the data can be done simultaneously and in 1 cycle.

Also during the recovery process, invalidation of cache lines and clearing the checkpoint bits and counters can be done in one cycle as proposed in [294].

5.3 Implementation of Proposed Architecture: Multicore Processor

In this section, we discuss the scalability of the proposed architecture in multicore systems and describe the interaction with the processor during normal operation. We also define the most important challenges for achieving high levels of error protection and error containment.

5.3.1 Shared Memory Architecture

In a shared memory architecture, the LLC is physically distributed in multiple banks but logically unified among all cores. As data are shared among different cores, the allocated blocks and all cache accesses are controlled via a coherency protocol. For our baseline core, we have chosen a MOESI protocol [7].

5.3.1.1 MOESI Protocol for Error Containment.

The MOESI protocol allows several copies of cache lines across multiple processors to be different from the copy in shared LLC. Owned *(O)* cache lines are responsible to share data among the requesting processors. Owned state also writes back the data in the case of replacement. All other cache line copies remains in Shared *(S)* state. Moreover, cache lines in Modified *(M)* and Owned *(O)* states hold dirty data.

The most important issue in a shared memory architecture is that a dirty block can be directly read by another processor without writing back to the shared memory.

Let us show the potential issue through an example. We consider 2 cores with shared memory. Figure 5.8 shows a scenario in which “core 0” has taken a checkpoint at time T_c. At instance t_1 “core 0” writes in cache. At time t_2 “core 1” requests a read from the cache in “core 0” following a cache miss in local cache. Now, if there is an error at time t_{strike} in “core 0”, detectors from “core 0” trigger after $ErrorDetectionLatency$ cycles at time t_3. Now, as soon as “core 0” recovers using the local checkpoint taken at time T_c, “core 1” will have invalid data. To

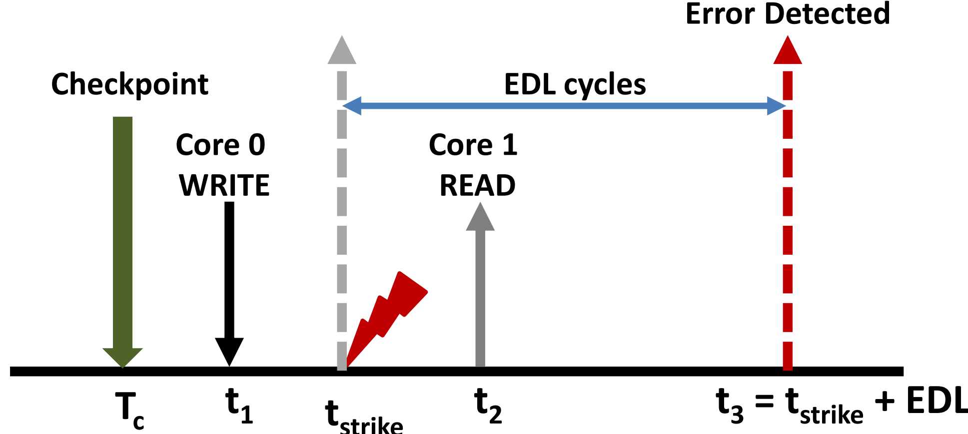

FIGURE 5.8: Handling error containment in a shared memory accesses for multi-core architecture. *EDL* stands for error detection latency.

avoid such cases we propose to stall all the read requests coming from other cores and once the cache is verified, it can service read requests from other cores.

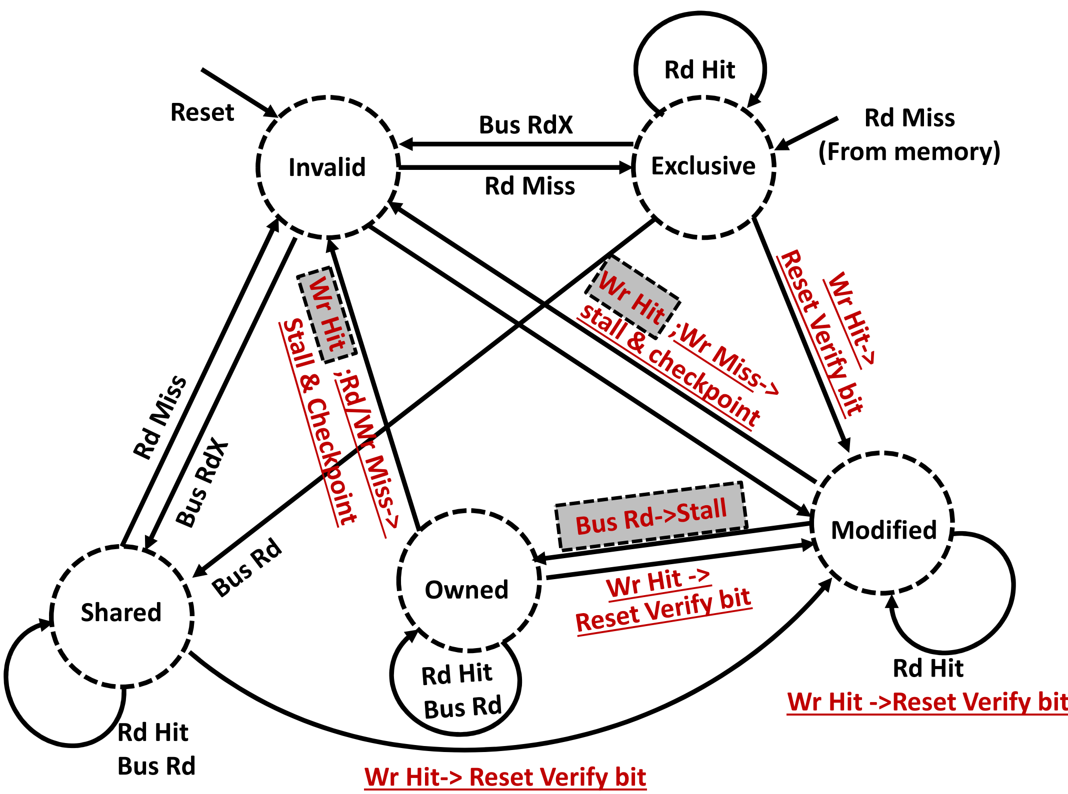

FIGURE 5.9: MOESI protocol: Transitions are shown in the *trigger*↦*action* format. Underlined transition triggers and actions are the same as uniprocessor architecture. The transition triggers in gray boxes are extensions for multicore shared memory architecture. "Wr" stands for write and "Rd" stands for read operation. "Stall"↦*ErrorDetectionLatency* cycles.

5.3.1.2 MOESI Protocol for Checkpointing.

We adopt an incremental checkpointing, similar to the case of uniprocessor architecture explained in Section 5.2.

Compared to uniprocessor system, shared memory introduces a new situation that needs to be handled to properly create checkpoints: when one processor invalidates dirty data from another processor that is not part of the checkpoint. If it turns out that the requestor processor suffers an error, and triggers a recovery, it has to trigger another recovery in the owner processor in such a way that invalidated data can be recovered. In order to deal with this case, we employ previously proposed solutions that keep track of the sharing history [295, 296]. We summarize the adapted MOESI protocol in Figure 5.9.

5.3.1.3 Recovering from Error.

If a core triggers an error, data recovery takes place in the same way as described for uniprocessor. The only caveat is that we will have to check the sharing history in order to initiate the recovery process in other processors cores [295].

5.4 Managing System Calls, Interrupts and Exceptions

In this section we will discuss how we can handle I/O requests and exceptions.

5.4.1 Handling Interrupts.

Interrupts are asynchronous events coming from the core and external devices (i.e., disk controller). Interrupts are crucial, as the requestor is outside the error containment area.

Similar to [297], we allow only error free stores to propagate to memory. We propose to buffer the requests in local memory, protected with ECC for $ErrorDetectionLatency$ cycles. This assures the correctness of each outgoing store and all its preceding instructions. The size of the buffer should be large enough to hold the I/O requests

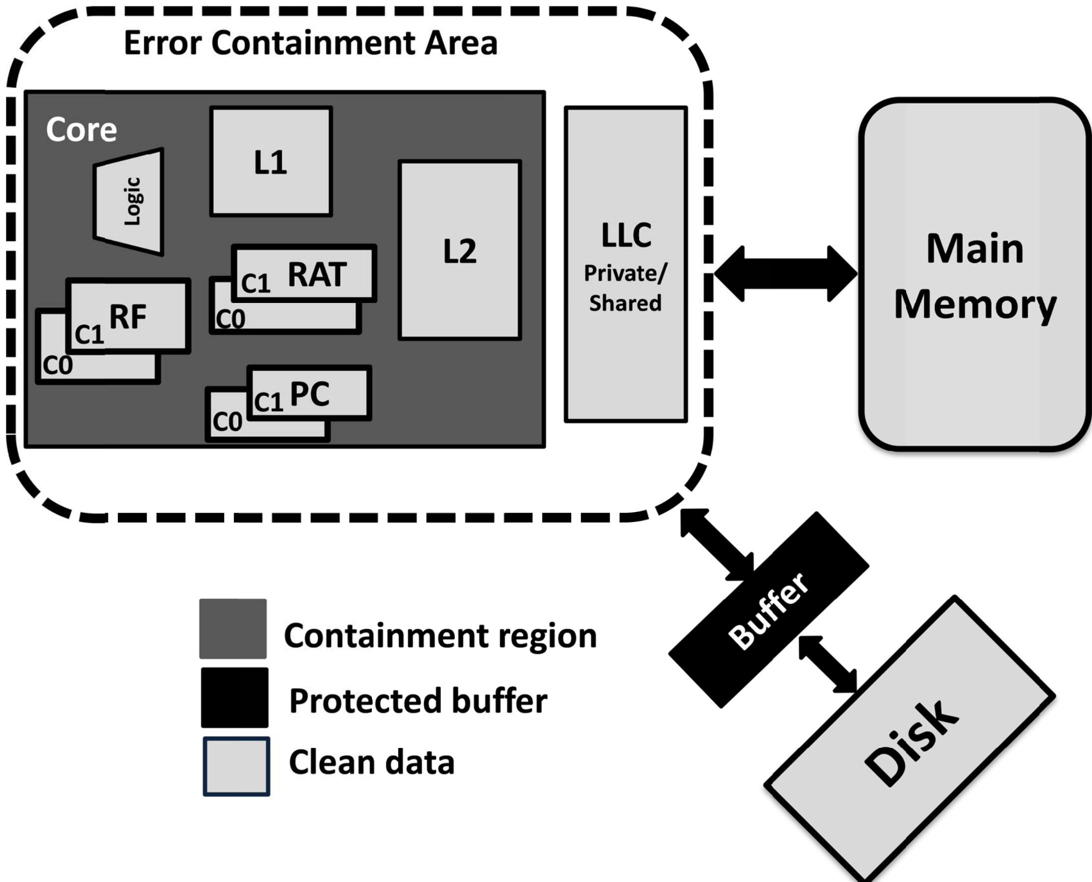

FIGURE 5.10: Extending the architecture to handle interrupts and I/O traffic.

for *ErrorDetectionLatency* cycles. Also, in order to facilitate successful recovery, as we allow all the error free stores to commit to memory after the last checkpoint, we must keep the load values issued so far in the buffer. Upon recovery we replay the loads so all the committed stores are correctly reproduced.

We propose to have one buffer for each I/O device to facilitate successful recovery, with an expected interrupt response time penalty of 30 to 1000 ns, which is acceptable for typical asynchronous interrupts.

5.4.2 Dealing with Exceptions.

Exceptions are synchronous events such as a "div 0" instruction or a page fault on instruction fetch. When the exception occurs, the corresponding entry of ROB is marked. Since in modern processors exceptions are rare events [7], we propose to delay the exception service by *ErrorDetectionLatency* cycles until all potential

errors have been detected. In case of no error detection, we assume the exception to be genuine and invoke the respective handler and handle it precisely.

5.4.3 Context switching and Multi-programming.

In order to handle context-switching, we allow the preempted thread to swap out and we propose to stall for *ErrorDetectionLatency* to make sure the preempted thread is error-free. After the context switch we take a checkpoint of the incoming thread. This is to make sure that in an event of error due to particle strike the thread can recover its state from the instance after the context switch.

5.5 Performance Evaluation of "SDC- & DUE 0" Architecture

In this section, we analyze how error detection latency impacts the choice of error containment boundary. Next, we study the trade-off between checkpoint period and the checkpoint boundary. Finally, we evaluate the performance impact of the selected configuration for uniprocessor and multicore system with data sharing and non-sharing applications.

5.5.1 Experimental Setup

To evaluate the proposed architecture, we use a full-system execution-driven simulator extended with OPAL and GEMS tool-set [298]. We modified the memory hierarchy model to adapt it to the proposed architecture. Table 5.3 enlists the important configuration parameters.

We simulate two different configurations as follows:

5.5.1.1 Single core system.

All caches are private to the processor. All the LLC misses will be served by the main memory. We evaluate the performance of single core system using SPEC CPU2006 benchmark set with the reference input set.

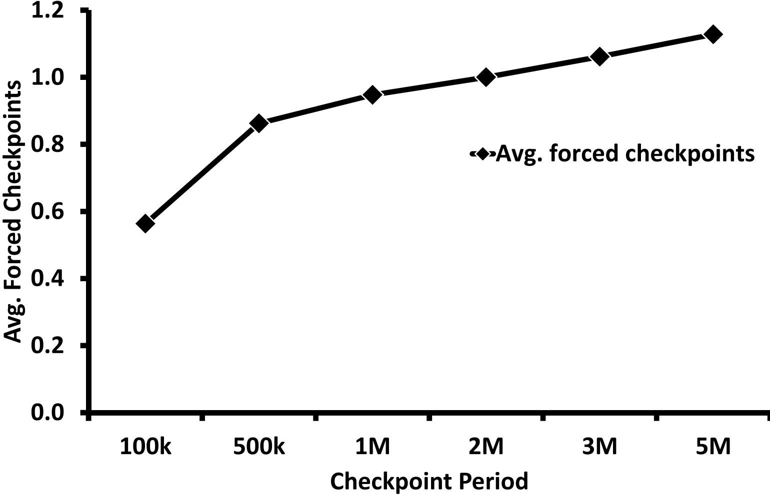

(a) Forced checkpoints

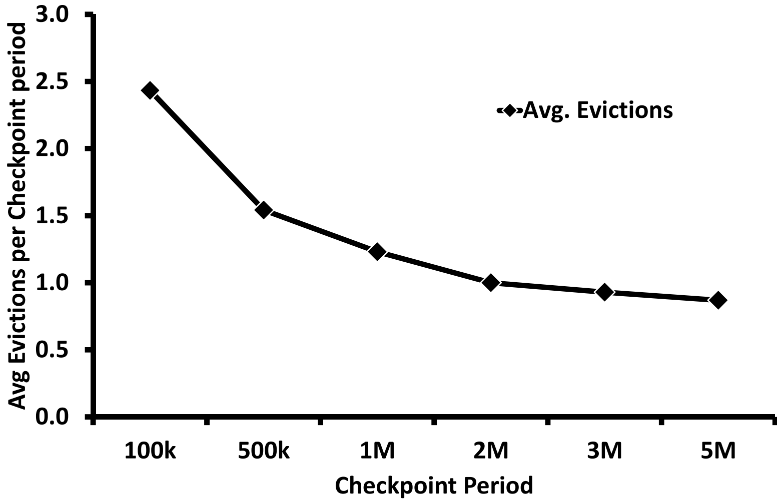

(b) Eviction due to write hits

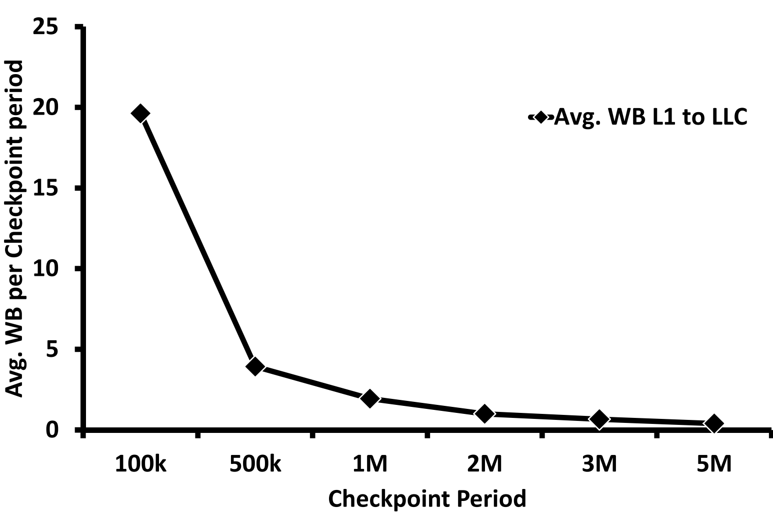

(c) Writeback from L1 to LLC

FIGURE 5.11: Checkpoint events in LLC checkpoint boundary

Parameter	Value
Number of Processors	1-16
Instr Window / ROB	16/48 entries
Frequency	2GHz
L1 I/D Cache per Core	16 KB, 4-way, 64B
LLC Cache per bank	256 KB, 4-way, 64B (distributed 1-16 banks)
L1 access Latency	2 cycles
LLC access Latency	6 cycles

Table 5.3: Configuration Parameters

5.5.1.2 Multicore system.

Multi-core system consists of 16 cores. We present analysis of multicore systems with following categories of applications, where each trace runs for 20 million cycles.

- **Data non-sharing applications:** To obtain various trade-off details for data non-sharing applications we replicate the same application for all 16 cores (i.e., all 16 cores running the same application independently). We evaluate performance of this configuration using SPEC CPU2006 benchmark set with reference input set.
- **Shared Memory Applications:** For this 16 core system we use SPEC OMP2001 benchmark set with appropriate input set to observe various trade-offs.

5.5.2 Error Detection Latency vs Containment Area

We first analyze the trade-off between the error detection latency and the size of the error containment area. As we mentioned in Section 5.2.1, non-verified data is not allowed to leave the error containment and we need to stall until data is guaranteed to be correct, which degrades performance. We evaluate the range of detection latency 30 to 100 cycles as proposed in Section 5.1.5.

Table 5.4 shows result for having one counter for entire L1 cache. It shows total number of evictions that create stalls when L1 is not verified. With detection

Detection latency	**Total #Stalls**	**Avg. Wait cycles**
10 cycles	6111	3.45
30 cycles	15729	25.99
100 cycles	38049	40.67
1000 cycles	55164	108.2

TABLE 5.4: Containment cost (i.e., #Stalls and wait cycles for each stall) for containment boundary limited to L1

latency of 100 cycles the total stalls (i.e., over a period of 20 million cycles) are more than 35K, which implies that having one stall every 1K cycles. It also shows the average number of cycles that we need to stall for the non-verified L1 cache to be verified. Overall, we observe that for *ErrorDetectionLatency* of 100 cycles, we experience a 7% slowdown only due to containment in L1. Even for 30 cycles, slowdown is 2%.

For the sake of comparison, we also experimented with more expensive solutions: (i) having one counter for each line, and (ii) one counter per set. Compared to having a counter per line, we observe an increase in total stalls by 5% for one counter per set, and 21% to one counter for the whole cache. Unfortunately, the slowdown due to containment is still high when having a counter per line, with 5.4% slowdown with 100 cycles of *ErrorDetectionLatency*, and 1.6% for 30 cycles.

When moving containment boundary to LLC, we observed only a handful of stalls. Therefore, we conclude that the best option is to have LLC as containment boundary, with error detection latency of 100 cycles (which requires 30 detectors) and slowdown of 0.01%.

5.5.3 Checkpoint Length vs Checkpoint Area

Now, we observe the tradeoff between the checkpoint length and the cost of the checkpointing. LLC is the checkpoint boundary. In our adopted architecture as described in Section 5.2.2, we have identified the major factors that affect the performance as follows:

1. Wait cycles to guarantee that caches in containment boundary are verified.

2. The write-back of dirty cache lines to the checkpoint boundary upon checkpoint creation.

3. Forced checkpoint events due to evictions of dirty lines that are not part of checkpoint.

4. Evictions to memory due to write hits on dirty and checkpointed lines.

Notice that factors 3-4 are runtime factors, and will largely depend on the footprint of the application (and therefore, the size of the selected checkpoint boundary and the checkpoint period). On the other hand, factors 1-2 are the overhead that is paid at checkpoint creation.

Figure 5.11(a) shows the number of forced checkpoints, per checkpoint length, for different checkpoint periods. As one can see, the number of extra checkpoints is negligible, and therefore we can opt for long checkpoints in the order of millions of cycles. Figure 5.11(b) shows the number of extra evictions to main memory caused by write hits on checkpointed lines. Numbers are relative to the length of the checkpoint period. Regarding the cost of creating a checkpoint, we show in Figure 5.11(c) the extra write-backs we have to perform when taking a checkpoint. As shown in the figure, increasing the checkpoint period from 100K cycles to 2 million cycles brings down the write-back traffic by more than 10×, and after that benefits flatten. Therefore, we opt for 2 million cycles checkpoint length.

We detail the results for a checkpoint period of 2 million cycles for our workloads in Figure 5.12. The results indicate that, for every 2 million cycles we will have to write-back 97 dirty cache lines from verified L1 cache to LLC.

Finally, we assess how much time we need to wait until we can create the checkpoint. Figure 5.13 shows the average wait cycles for the LLC to be verified before taking a checkpoint for a checkpoint period of 2 million cycles. For detection latency of 100 cycles, every 2 million cycles we will have to wait 50 cycles to take a checkpoint in LLC.

Next, we will see how the performance is impacted in the proposed architecture.

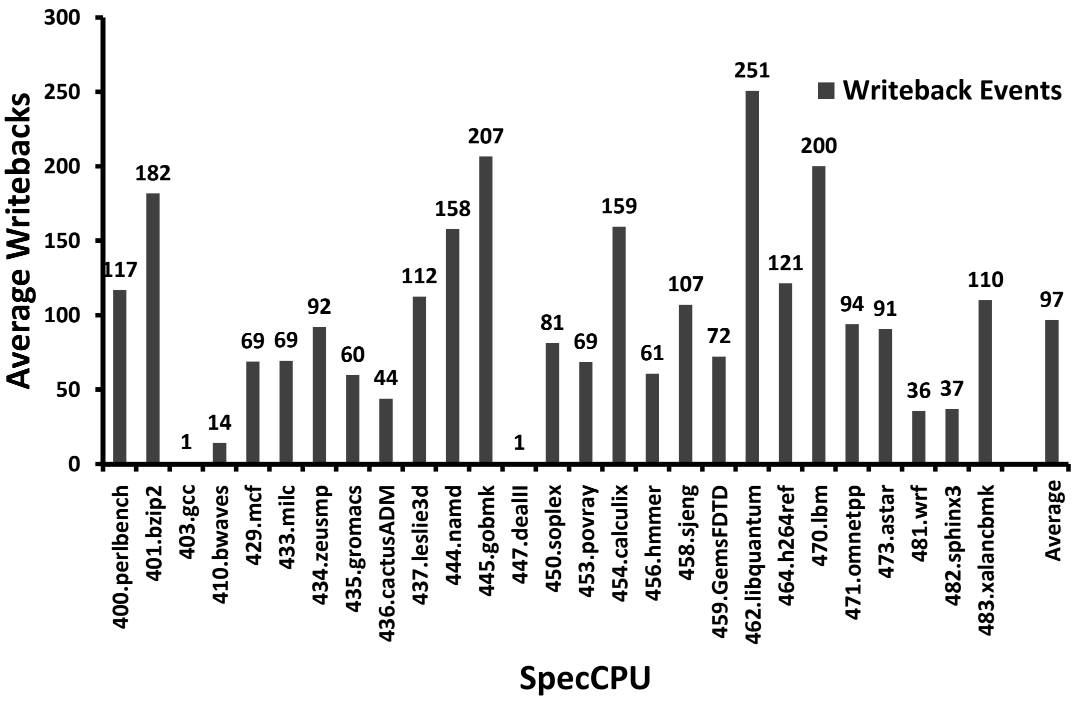

Figure 5.12: Average dirty lines to be written back from L1 to LLC

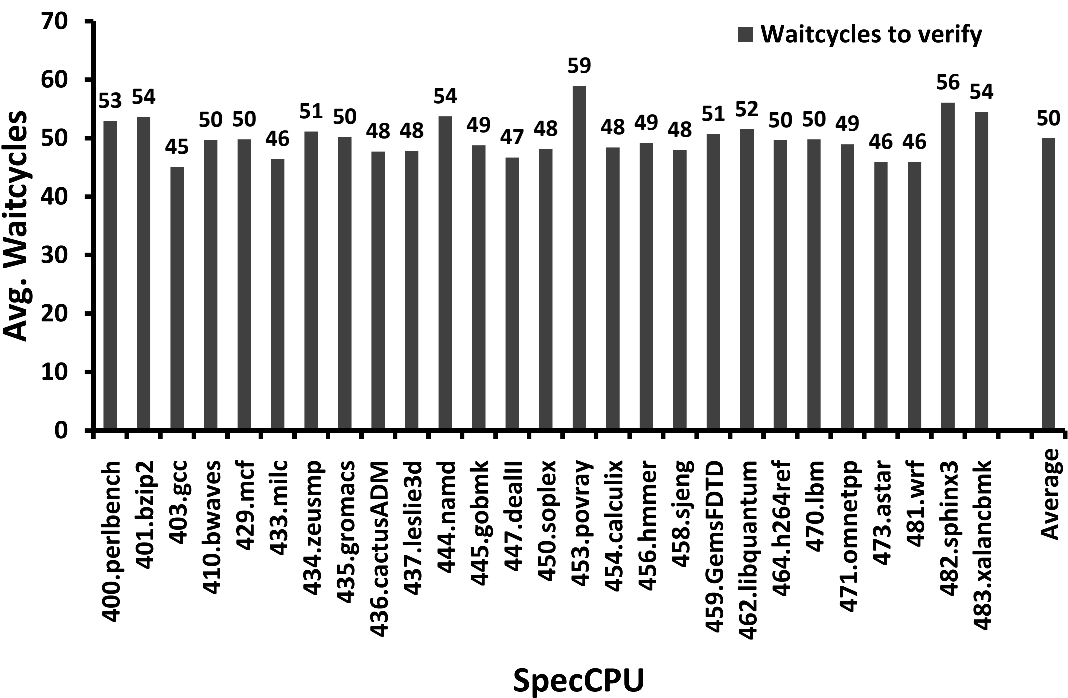

Figure 5.13: Average wait-cycles until LLC is verified

5.5.4 Uniprocessor Performance

Figure 5.14 evaluates the proposed single core architecture in terms of performance vs. cost of containment and recovery. The experimentation shows that the average performance slowdown is 0.1% and the worst case performance degradation is 0.42%. We notice that the average performance degradation due to containment is almost 0, since there are no eviction of dirty lines from non-verified LLC. The performance degradation comes from writing back dirty data from L1 to LLC during periodic and forced checkpoints.

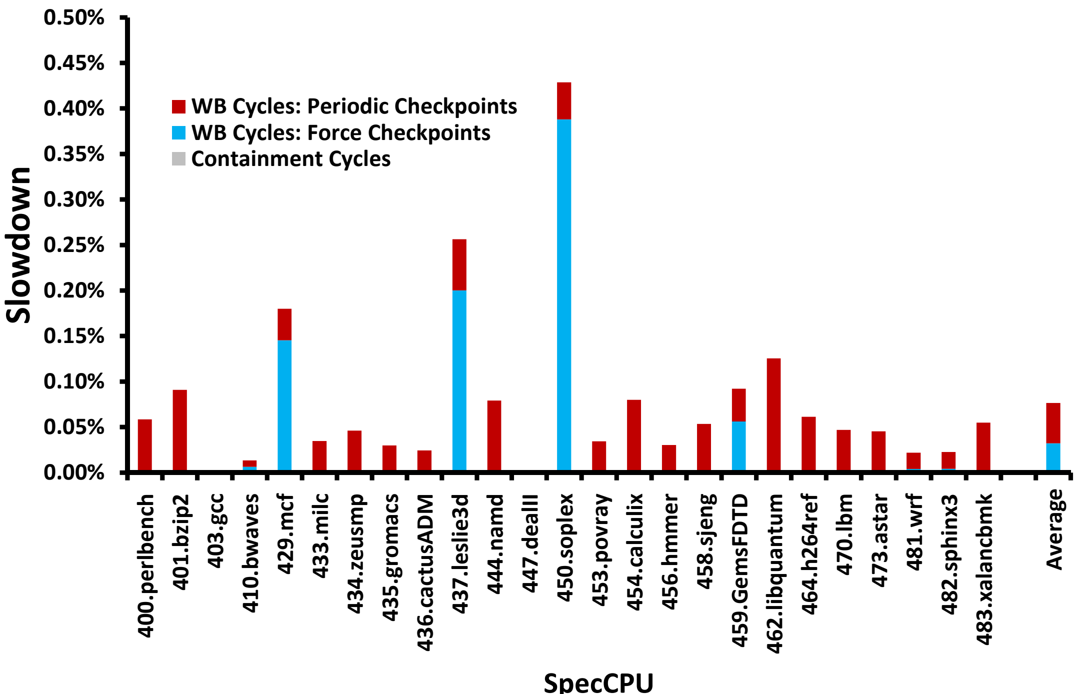

Figure 5.14: Performance impact of containment and checkpointing LLC cache in single core architecture

5.5.5 Performance of Multicore for Data Non-Sharing Applications

We observe similar results for 16 core system for data non-sharing workloads in Figure 5.15. Notice, that we depict the results for the slowest core of the 16 running cores. The average total degradation in performance is 0.1% and the worst case degradation is 0.45%.

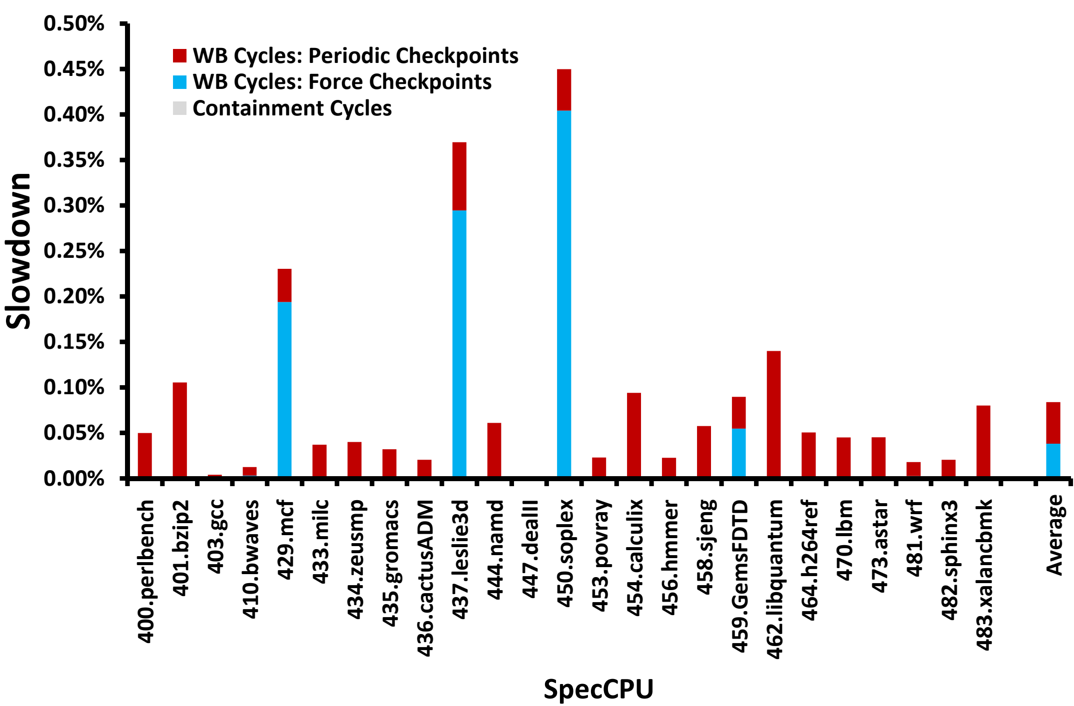

FIGURE 5.15: Slowdown due to containment and checkpointing LLC cache in the 16-core system for private memory applications

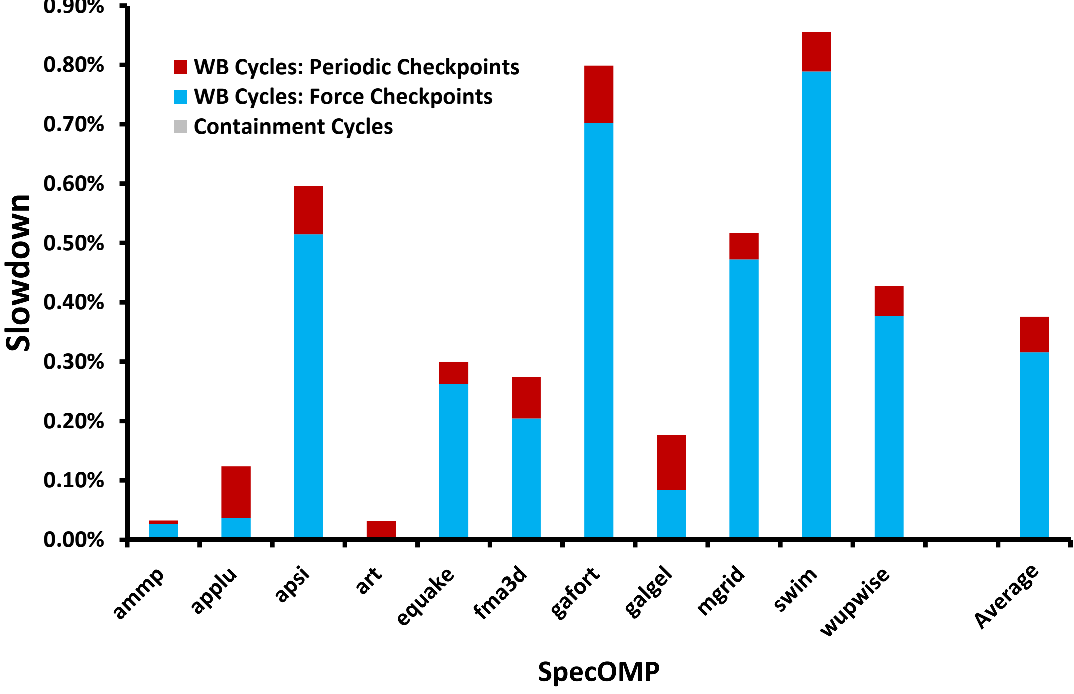

FIGURE 5.16: Slowdown due to containment and checkpointing LLC cache in the 16-core system for shared memory applications

5.5.6 Multicore Shared Memory Performance

Figure 5.16 shows the impact on performance for 16 cores shared memory architecture. Again, we collect data for the slowest core to reach the 20 million executed cycles. As one can see, the average slowdown is 0.4%. Again even in the case of shared memory we do not have any dirty evictions from LLC before LLC is verified. Hence, the slowdown due to containment is zero. In shared memory architecture we have more cache lines evicting after the LLC is verified. This results into increased forced checkpoints. Forced checkpoints attribute to about 0.3% average slowdown.

5.6 Related Work

In this section, we will describe some techniques used for protecting the entire core. We will discuss techniques for detecting and recovering from errors. Usually, an error detection scheme (i.e., DMR) is combined with error recovery scheme (i.e., Checkpointing) for providing recovery. Several popular error detection mechanisms have been compared and summarized in Table 5.1.

5.6.1 Error Detection and Recovery in Core

Unlike error codes, the execution redundancy techniques resort to fault detection via comparing outputs from redundant stream of instructions. Execution redundancy is a widely used technique to detect errors in entire core, either using the multithreading capabilities [57, 68] or hardware redundancy [58, 115]. Execution redundancy techniques can provide higher error coverage across the processor chip compared to other error detection techniques (i.e., error codes). However, execution redundancy can cost a lot in terms of area, power and performance overheads compared to error codes as detailed in Table 5.1.

5.6.1.1 Dual Modular Redundancy with Recovery

Modular redundancy can be applied to provide error detection for entire modules of both data storage and combinational logic. DMR is the simplest form of modular redundancy with a comparator as shown in Figure 5.17(a). DMR provides

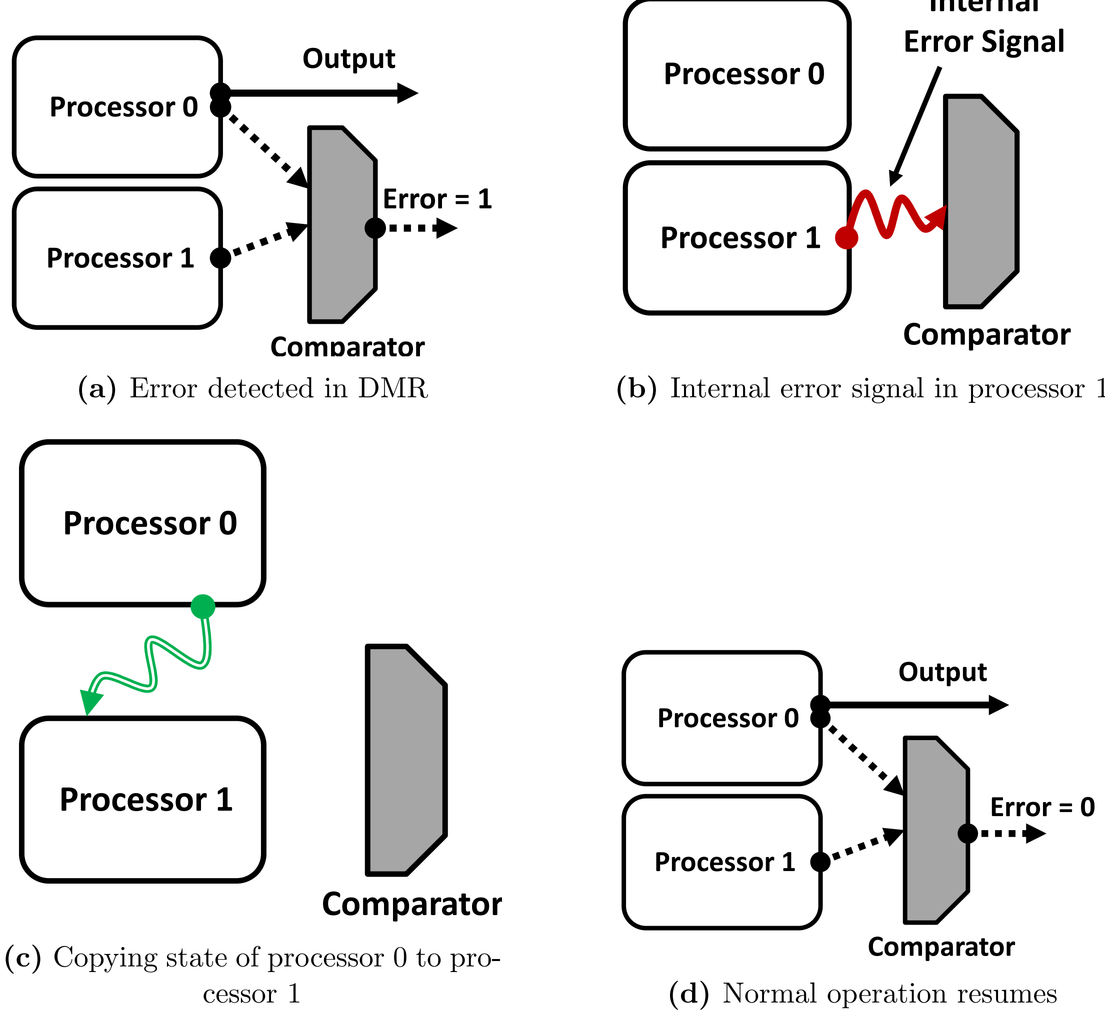

(a) Error detected in DMR

(b) Internal error signal in processor 1

(c) Copying state of processor 0 to processor 1

(d) Normal operation resumes

FIGURE 5.17: Implementation of dual modular redundancy scheme for error detection and recovery.

excellent error detection because it detects all errors except for errors due to design bugs, errors in the comparator, and unlikely combinations of simultaneous errors that just so happen to cause both modules to produce the same incorrect outputs.

For error detection DMR can be implemented at various granularities. For instance, in a coarse grain implementation it is possible to replicate an entire processor or replicate a cores within a multicore processor as shown in Figure 5.17. At a finer grain, it is possible to replicate individual functional unit or a cache line. Finer granularity can provide finer diagnosis, but it also increases the relative overhead of the comparator. In modular redundancy the redundant modules do not have to be identical to the original hardware.

Once the output mismatch is detected as shown in Figure 5.17(a). The system triggers an error and stalls until the error is located and an internal error signal is generated which is shown in Figure 5.17(b). For instance, in processor 0 and processor 1 the caches are parity protected and any bit flip will be detected via parity which is responsible to generate the internal error signal. Without this information it is not possible to identify location of the error. Once the erroneous processor is identified the clean processor state from processor 0 is copied to processor 1 (Figure 5.17(c)). Once both the processor states are identical normal operation can resume. Such a system's recovery depends on its ability to generate the internal error signal and the internal error detection mechanisms. Alternatively, a DMR system can also recover using checkpoints. Checkpointing mechanisms will be discussed in Chapter 7.

A system with DMR uses more than two times as much hardware (one redundant module and a voter) compared to an unprotected system. Adding redundant hardware also increases corresponding energy consumption. These overheads are unavoidable while designing systems in which the reliability requirements are extremely high. However, these overheads are not acceptable for commodity processors where extracting maximum performance in a given power envelope is a primary concern.

5.6.1.2 Lockstepping with Recovery

Lockstepping detects the error by executing the same instructions in redundant threads and comparing them. Figure 5.18 shows one such implementation of lockstepped architecture where thread–0 and thread–1 both execute same instructions.

In lockstepping, both the redundant copies are cycle synchronized. A hardware comparator compares the state of redundant computations every cycle as shown in Figure 5.18. As a result, any error in one of the copies will produce different output and will be detected in the same cycle. Lockstepped architectures are very popular and provide great degree of coverage because of which they are part of several commercial architectures [54, 113, 299, 300]. A lockstepped architecture can reduce the SDC of system. However, for reducing the DUE it still requires a separate error recovery mechanism. As the lockstepped architectures have detection latency of 1 cycle, usually the recovery can be done via maintaining copies of

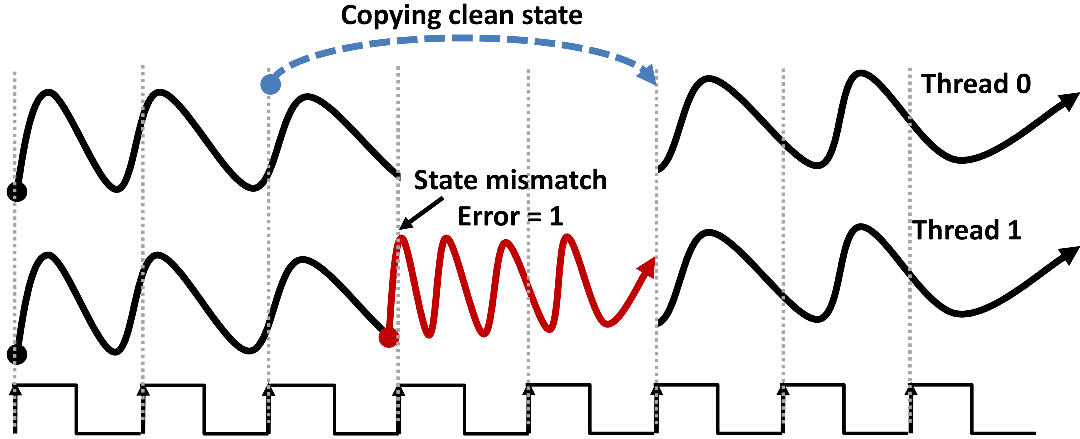

FIGURE 5.18: Lockstep error detection and recovery via retry

architecture states (i.e., shadow copies of register file etc. per thread). As the instructions commit the speculative state is written to a temporary state from where subsequent instructions can read and execute. Once the threads are checked for errors (after one cycle) the temporary state can be copied to architecture state. Upon an error the architecture state is loaded back to both the redundant threads and execution can restart from the instruction after the last correctly retired instruction.

Lockstepping can be implemented purely in hardware which makes it easy to implement. It can detect almost all soft errors and permanent errors as long as the two redundant copies are fed the exact same inputs. The errors it cannot detect are the ones which affect both the redundant threads in exactly the same way.

Lockstepping has significant disadvantages. Due to redundantly executing threads it incurs huge area and power overheads. Moreover because of redundantly executing threads the performance impact is more than 1.5–2×. Cycle synchronization in shared memory architectures can pose additional challenges. Validating lockstepped architectures are also considerably challenging. Lockstepping requires both the redundant copies to execute deterministically to produce the same output. This can be a problem in the floating point computations where modern processors assume random values due to the circuit properties. This will not cause incorrect execution, however, it can cause a lockstep failure. Lockstepping on its own can only provide error detection and hence additional mechanisms are essential for providing error recovery.

5.6.1.3 Redundant Multithreading (RMT) with Recovery

Redundant Multithreading (RMT) is an error detection mechanism, that like lock-stepping, runs redundant copies of the same instruction set and compares the output to detect the error [113, 301, 302]. Unlike lock-stepping in RMT solution compares the outputs of only committed instructions. Because of this the internal states of redundant threads can be significantly different in RMT. By relaxing the constraint of cycle by cycle comparison RMT is more flexible compared to lockstepping. For the same reason RMT is also known as loose lockstepping. RMT can be implemented on any mutlithreaded architecture (i.e., *Simultaneous Multithreading* (SMT) [68]) or a multicore architecture [281].

An SMT core with N thread contexts can simultaneously execute N threads of the given application [303, 304]. The fundamental idea is to use the unutilized threads for error detection by executing redundant threads, whenever an SMT core has fewer than N useful threads to run. RMT, depending on its implementation, may require little additional hardware beyond a comparator to determine whether the redundant threads are behaving identically. Implementing RMT on an SMT core impacts on performance mainly because of the extra contention for core resources due to the redundant threads [69]. The reason for using multiple cores, rather than a single SMT core, is to avoid having the threads compete for resources on the SMT core.

A large amount of work has been done in implementing redundant multithreading for both SMT cores and multicore processors. Usually, RMT is also accompanied by a recovery mechanism for providing error recovery. Most of the research is in the direction of enhancing the RMT to provide recovery and reduce the associated power and performance overheads [56–58, 65, 68–72, 75, 111, 115, 280, 281, 305, 305–307].

Now, we will discuss one such RMT implementation *simultaneous and redundant threaded processor* (SRT) that protects the core in which the error is detected before the instruction commits as proposed in [65]. The SRT architecture utilizes an underlying SMT core [6]. In the SRT implementation one of the two redundant threads is designed to run ahead of the other thread. The outputs of the leading and trailing threads are compared to detect the error. Here, we will discuss the SRT implementation that compares the outputs before the register value is committed to the architecture state. The register value comparison from the leading

and the trailing threads can be done in the register update unit (RUU) as the instruction retires. However, this implementation will have significant performance overhead due to limited RUU entries. Alternatively a buffer can be employed to hold the values of retiring instruction of the leading thread. Once the same instruction of the trailing thread retires the values can be compared with the values stored in the buffer and if there is a match then only the architecture state is updated. To avoid complex issues such as forwarding values to the subsequent instructions in the same thread it is possible to employ separate register file per thread [308]. These separate register files will hold the unverified register values. Once the register values are compared and are verified to be error free they can be written back to another register file that is protected (i.e., via ECC) and holds the architectural state. Having separate register file to hold verified and protected copy of architecture state also facilitates simpler recovery as upon a mismatch in the outputs of leading and trailing thread the processor can revert back to the clean architecture state.

The replication of the register values for leading and trailing thread is trivial in SRT implementation. However, replicating the cached data is more involved and require special hardware modifications [65].

In the proposed SRT technique, the trailing thread can benefit from the a-priori information of the leading thread's cache and branch prediction behavior to reduce the performance impact. However, due to the comparisons of outputs the average performance degradation is 32% compared to the SMT processor running a single thread. The leading cause of this performance overhead is the comparison of store instructions. Increasing the size of store queue can improve the performance by 5%. Another disadvantage of the proposed SRT technique is in a multicore processor with SMT cores, enabling the SRT mechanism will reduce the throughput by 100% since half of the threads are occupied with redundant threads.

Several implementations of Core and Chip level RMT have been proposed. These techniques try to achieve locakstepping architecture's error coverage and reduce the power, performance and area overheads of SRT technique. Notice that RMT techniques have unbounded and large detection latencies (refer to Table 5.1). To handle large detection latency some RMT proposals include checkpointing the caches and main memory for successful error recovery. The cost of taking system wide checkpoint is very high and we will discuss in detail various implementation in along with other RMT enhancements in Chapter 7.

5.6.1.4 Error Detection and Recovery using Checker Core

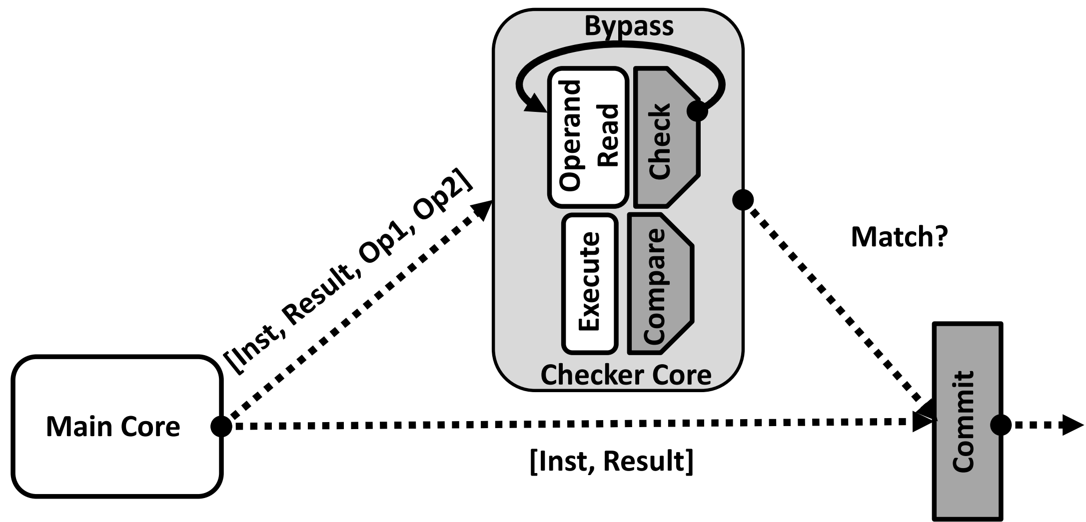

FIGURE 5.19: Implementation of dynamic implementation verification architecture (DIVA) and the functioning of the checker core

Similar to RMT where the outputs of leading and trailing threads are compared to detect errors. *Dynamic implementation verification architecture* (DIVA) [67] uses a simple in-order core that is paired with an out-of-order core as a checker as shown in Figure 5.19. As processor designs grow in complexity, they become increasingly difficult to fully verify and debug. DIVA proposes to implement a relatively simple and fully verified backend processor to perform dynamic (while the processor is in use) verification of a processor. While the main purpose of DIVA is to ease the challenge of verification and debugging complex processor cores, DIVA also serves to detect soft error events. Assuming that a fault affects only the complex processor core or the backend checker, DIVA will detect the fault and can be configured to attempt recovery.

As can be seen in Figure 5.19, DIVA ensures the error free state by making sure that for each instruction the operation has executed correctly and also the operand values of the given instruction flows correctly through register, memory or bypass logic. DIVA implements simpler checker core to perform the verification. The checker core recomputes all the operations based on the source operands and compares it with the value that the main processor has generated. If the values match it verifies the error free operation. However, in the event of an error it triggers an error flag. To verify that the instructions executed in the main processor

received the correct operands the checker core also reads the operands from its own register file (or bypass network) and it verifies the correctness of the operands.

DIVA can detect permanent, transient as well as design errors in the main core. The main disadvantage of DIVA is that it assumes the checker is always correct and upon a mismatch in the result it commits the output of the checker core. This can lead to reliability issues in the cases of executing uncached load/store operations which cannot be executed twice. Due to added hardware DIVA causes an average slowdown by 3–15%.

5.7 Chapter Summary

This proposed architecture potentially eliminates particle strike induced SDC & DUE-FIT in a processor core. The architecture uses acoustic wave detectors to detect errors. It is extremely light-weight and uses 30 detectors (i.e., area is 30 SRAM memory cells) for error detection, and provides a worst-case detection latency of 100 cycles. The area overhead of 30 interconnects is also minimum. Controller circuit to signal error detection is extremely simple and requires 6 3-input and 2 2-input logic-OR gates.

Next, we proposed an error containment mechanism within the cache hierarchy to manage the detection latency. We implement the containment boundary at the LLC. By containing all the errors we eliminate SDC. The containment architecture consists of L1 and LLC with one counter each, to count 100 cycles. Additionally, we will need one counter for LLC to check the checkpoint validity. All 3 counters are 7-bit, non-repeating word counters.

Finally, we eliminate DUE-FIT by enabling a low cost checkpointing mechanism. Checkpointing requires a physical *Checkpoint bit* for every cache line in LLC. We propose to use 2 million cycles as checkpoint length, which guarantees a good trade-off between checkpoint overhead and recovery time. For recovery of architecture state it requires 2 shadow copies of the architectural state (register files, RAT and PC). We also make use of a trivial control circuit for clearing *Checkpoint bit* and counters in one cycle.

Proposed architecture eliminates particle strike induced SDC & DUE-FIT, for systems ranging from one core to 16-core with shared memory with the worst-case performance overhead is 0.8% for shared memory systems.

Chapter 6

Protecting Embedded Core with Acoustic Wave Detectors

In the previous chapter, we understood how we can protect an entire processor core against soft errors using acoustic wave detectors in a unicore and multicore processor chip. Now we in this chapter we will take advantage of error detection architecture based on acoustic wave detectors in providing efficient error containment and recovery in the core of an embedded processor. We target embedded processors which are used to provide moderate performance. The architecture proposed in Chapter 3 can detect and locate the errors. The architecture uses acoustic wave detectors for dynamic particle strike detection. To provide error containment and recovery in the embedded core first we will utilize the architecture proposed in Chapter 5. However, our experiments conclude that in an embedded core architecture proposed in Chapter 5 is not economical. Therefore in this chapter we will show the modification required in the architecture to provide economical error containment and recover in embedded domain. Finally, we will evaluate the performance impact of the proposed architecture using embedded applications.

6.1 Experimental Setup

First, we describe the evaluation method and experimental set-up of the proposed architecture. We evaluate the performance impact of the selected configuration for single core embedded system.

Parameter	**Value**
Number of Cores	1
Issue Queue (Int/FP)	15 entries
ROB	8 entries
Frequency	333 MHz
Issue Width	2
Commit Width	2
Load Queue	8 entries
Store Queue	8 entries
L1 Inst./Data Cache	16 KB, 2-way, 32B
Memory Bus Latency	100 cycles

Table 6.1: Configuration Parameters

Table 6.1 enlists the important configuration parameters and their respective values. Notice that the embedded core is extremely simple and has just L1 cache. Such architectures have been used in many applications including smartphones [309]. To evaluate the proposed architecture for embedded core we use SimpleScalar [310]. A new version of SimpleScalar has been adapted to the ARM instruction set and is used to evaluate the performance of architectures of current and next generation of embedded processor. It is a cycle accurate microarchitecture simulator that is modified to necessitate the changes required to simulate a state of the art embedded processor [309]. Using this experimental set up we evaluate the error containment architecture presented in this chapter.

In this work we evaluate the performance of proposed architecture on real-life workload for embedded systems using the Mibench benchmark set [311]. It consists of six categories including: Automotive and Industrial Control, Network, Security, Consumer Devices, Office Automation, and Telecommunications. These categories offer different program characteristics that enable us to examine the architecture more effectively.

The small data set represents a light-weight, useful embedded application of the benchmark, while the large data set provides a more stressful, real-world application. We run each trace for complete execution with the reference large input set.

6.2 Handling SDC & DUE in Embedded Core

As we have seen in Section 1.2.5 of Chapter 1, unlike high performance servers, embedded processors typically have smaller components, longer clock cycle times and larger logic depths between latches. Since the design constraints for the embedded systems differ from those in the high-performance domain, it implies that the robustness techniques also differ dramatically.

Now we will explain how we can contain the soft-errors in embedded cores using acoustic wave detectors. First, we briefly discuss the placement of acoustic wave detectors and corresponding detection latency for the studied embedded core. Later, we detail various error containment granularities and tradeoffs involving error containment boundary and its impact on cost of recovery for embedded core.

6.2.1 Acoustic Wave Detectors and Error Detection Latency

As proposed in Chapter 3 we use acoustic wave detectors to detect errors on the core of an embedded processor. Recall from Chapter 2, the speed of acoustic waves on silicon surface is 10 km/s and the detection range of acoustic wave detectors is 5 mm. Given the dimensions of current embedded core designs, the surface area of an embedded core is about $4 - 6mm^2$ including caches [309]. A single detector would be sufficient to detect all errors occurring anywhere on the entire core area.

However, with just 1 detector the worst-case detection latency (i.e., latency to detect a strike that is 3.5 mm away from the detector) is 350 ns (117 cycles at 333 MHz). By deploying more detectors we can reduce the detection latency. We propose to deploy detectors in a mesh formation as discussed previously in Chapter 3, Chapter 4 and Chapter 5.

Figure 6.1 shows the error detection latency for various mesh configurations covering an entire core area. It shows that with 18 detectors we can detect an error on the entire core (including cache, register files etc.) within 10 cycles. To decrease the detection latency by 10×, the required number of detectors in the mesh formation increases by 140×. As we can see in from the figure, 2.5K detectors are required to obtain single cycle detection latency.

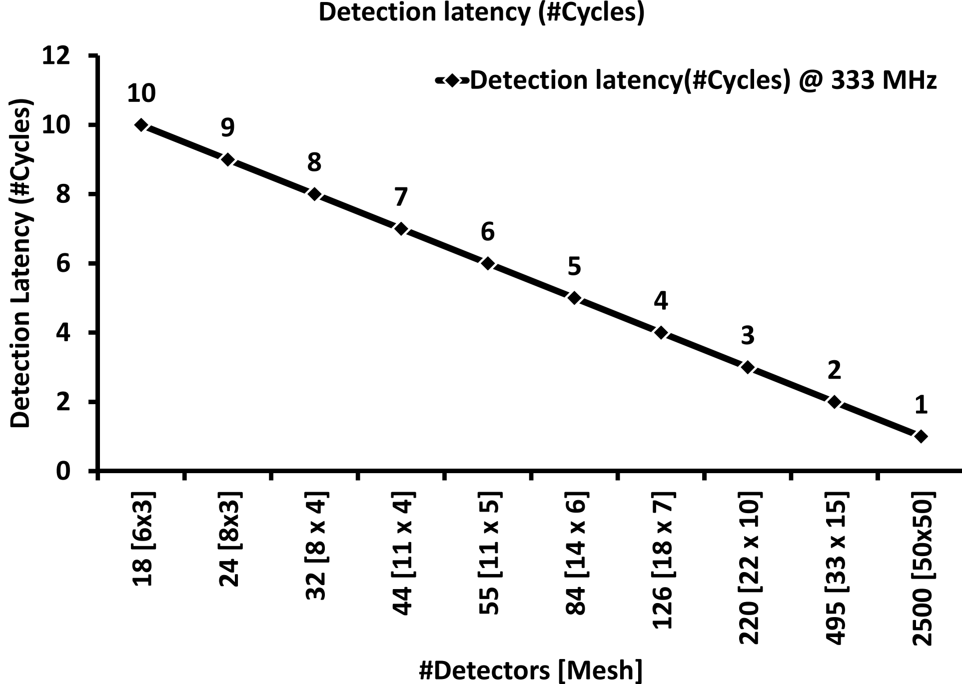

Figure 6.1: Error detection latency for acoustic wave detectors on embedded core for different mesh configurations

Since, we want to eliminate SDC and DUE of the embedded core we must provide error containment and recovery. As discussed in detail in the Chapter 5, the detection latency of acoustic wave detectors is important in deciding error containment boundary. Smaller detection latencies are desirable. Next, we will analyze different error detection latency for different error containment granularities and its impact on cost of containment.

6.2.2 Error Containment Granularity

The main objective of the proposed architecture is to provide error containment for economical recovery in an embedded core. This means that we need to detect all errors, and once an error is detected, we must contain it in order to avoid the penetration of error into a state that is free from errors. Choosing the correct error containment boundary is very important. It impacts the complexity and cost of containment and recovery.

Different granularities of error containment in an embedded processor is shown in Figure 6.2. If error is contained within the core, it implies that we guarantee

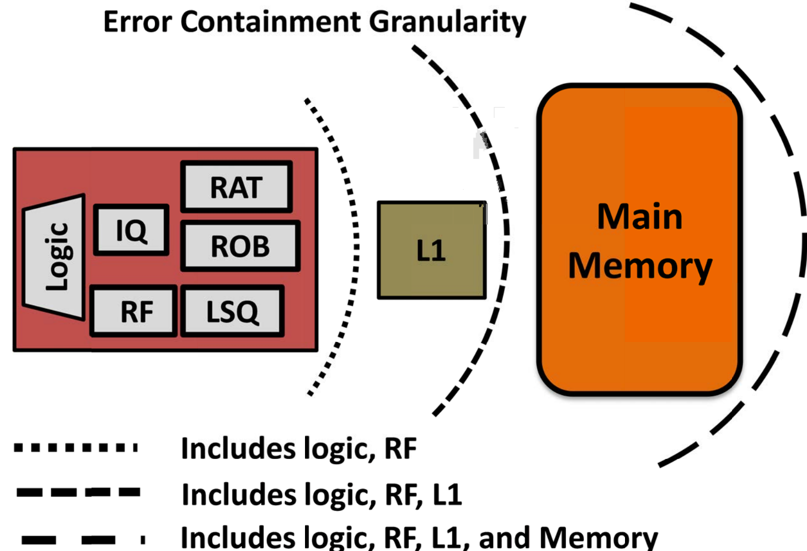

FIGURE 6.2: Error containment granularities in embedded processor

that every instruction that is being committed is error free. At this granularity, a simple nuke & restart mechanism [312] can act as checkpointing and recovery.

Another option, similar to the proposal of previous chapter, is to contain the error in cache hierarchy (i.e., the L1 cache). Containing errors in L1 cache implies that we allow the erroneous data from core to go to the L1 cache but not beyond that. In other words, the dirty data in the L1 cache can be erroneous. Containing errors in L1 cache means that nuke & restart will not be enough to recover from errors, and a more expensive checkpoint that includes the modified data in L1 cache will be necessary.

The selection of the error containment boundary is deciding factor to determine size and frequency of costly checkpointing for recovery. The closer we are to the core, the fewer components are required to be included in checkpoint.

6.2.2.1 Error Containment Granularity: Core

The first option that we have is to contain the error within the core. The core holds the speculative architectural state until the instruction is committed. The error containment in core requires that every instruction is checked for error at every cycle before it commits to the architectural state. Summarizing from Chapter 5, the advantages of containing error in core are: (i) Error is confined to such a small

boundary that avoids system-wide recovery, (ii) A simple nuke & restart can be used for recovery that will have little or no performance impact.

Error containment within core is lucrative especially for embedded cores due to above mentioned advantages. The only caveat is it demands an error detection latency of <1 cycle. Latency of 1 cycle will not be enough since in 1 cycle instruction is committed and if the error is in the commit stage it will end up outside the containment boundary. So to contain the error in the commit itself we have to have detection latency of <1 cycle. To eliminate SDC one option is to stall the instructions by 1 cycle but that will have huge performance penalty. Alternatively, hardened latches can be used to protect the "commit" stage (i.e., ROB, RF etc.).

According to Figure 6.1, it will need more than 2.5K detectors to achieve error detection latency of <1 cycle for entire embedded core. This causes an area overhead equivalent to a 2.5Kbit cache without counting for the overhead of interconnects and controller circuit. This area overhead is unreasonable especially for an embedded core where silicon estate is scarce.

6.2.2.2 Error Containment Granularity: Cache

Having minimum error detection latency is best-case scenario for having cost effective and trivial error containment. Figure 6.1 shows that for error detection latency of 1 cycle for the entire embedded processor we will need 2.5K detectors. This area overhead is unacceptable. However, for detection latency of 10 cycles we will need just 18 detectors in the mesh covering embedded processor. This reduces the area overhead by a huge margin. But now we have to contain the error for 10 cycles. One option is to stall the commit for 10 cycles until we make sure that there is no error. But this will have huge performance impact. So we go for the other option and allow the error to commit and go outside the core into L1 cache.

Now, we include the core and the L1 cache in the error containment boundary as shown in Figure 6.2. By extending error containment boundary to L1 cache we can afford to have longer detection latency and minimize number of required detectors. The advantages are similar to the ones discussed in Chapter 5.

In our implementation we assume that the L1 cache itself has an error detection and recovery mechanism via ECC or a technique based on acoustic wave detectors as discussed in Chapter 4 to detect & correct the errors occurring on the L1 cache.

The error containment in L1 cache can be implemented in similar manner as discussed in Chapter 5. To contain the error in L1 cache, we have to include one counter that counts 10 detection latency cycles. This is to make sure that any data in the cache is error free before it goes out of the cache. We need one counter for entire cache. This counter is reset on every write operation to the cache to keep track of all modified data. With the help of single counter, we can identify error free cache lines which are modified. We can also know "dirty and unverified" cache lines, lines which are modified and in the process of being verified. Evictions of the dirty unverified cache lines causes a stall impacting performance due to error containment.

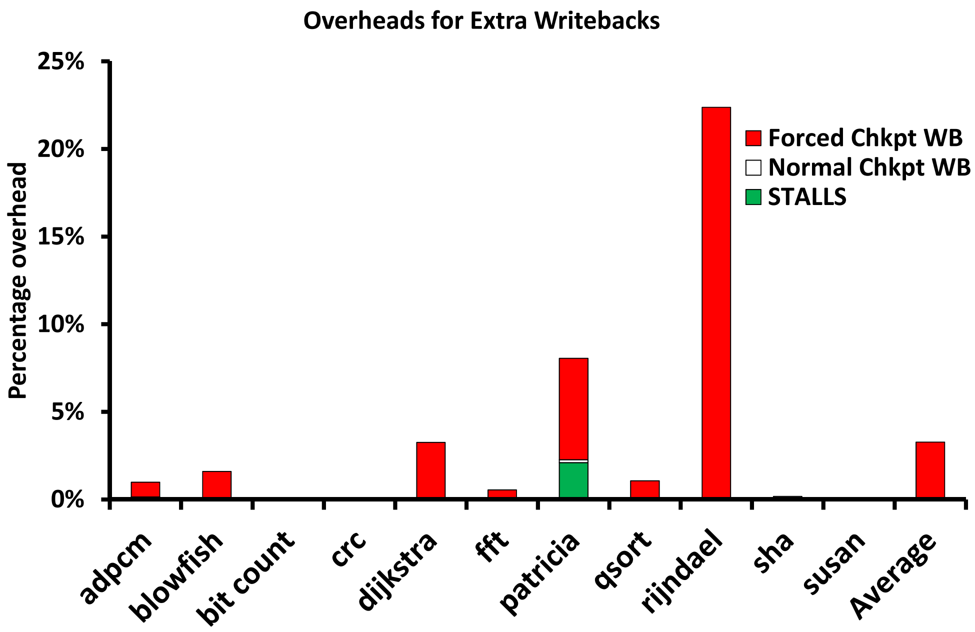

Figure 6.3: Performance overhead of error containment in cache for a checkpoint period of 1 million cycles

Now that we can contain the errors, we want to provide error recovery eliminate the DUE. To provide error recovery we will need a checkpointing mechanism that includes L1 cache. We implemented a simple checkpointing mechanism similar to the one described in previous chapter.

We evaluate the architecture to analyze the cost of recovery for containing errors in L1 cache. Our analysis shows that a checkpoint period of 1 million cycles is enough to balance the cost of containment, checkpointing and performance. Figure 6.3 shows the impact on performance due to the write-back of updated cache lines to memory for both periodic checkpoints and forced checkpoints (eviction of dirty

lines that are not part of checkpoint from L1 cache causes a forced checkpoint). It also shows the cost due to stalls to make sure evicting dirty lines are free from error. Our results show that stalls have little impact on the average performance. The worst case slowdown (in the case of *patricia*) due to stalls is 1.4%. The average slowdown due to checkpointing is 3.8% and worst case is 22.3% due to high memory footprint of *rijndael*. The performance overhead of error containment in L1 cache is not affordable.

6.2.3 Putting everything together

Overall, we saw that error containment in the core will benefit from cheap recovery (i.e., nuke & restart) but requires detection latency to be less than one cycle and that is expensive in terms of the number of required detectors. On the other hand error containment in L1 cache, relaxes the required number of detectors but it requires little modification in microarchitecture. However, it will require an expensive checkpointing mechanism for recovery and results in an average performance penalty of 3.8% and for worst case 22.3% which is unaffordable. Extending error containment boundary to main memory invites non-trivial challenges associated with checkpointing entire main memory.

This demands the necessity of a more refined error containment in the core that reduces the overall cost of containment and recovery.

6.3 Selective Error Containment

Now, we will see how acoustic wave detectors can help in providing selective error containment within core, reducing the overall area, power and performance overheads.

6.3.1 Protecting Individual Data Paths & Latency Guard Bands

As we have seen from the Section 6.2.2.2, to reduce the impact of error containment on performance, we want to contain the error in the core. At the same time,

according to Section 6.2.2.1, to contain the error within core we have to pay the area overhead of 2.5K detectors. We want to reduce the number of required detectors and still be able to contain the error within the core without compromising reliability.

Similar to what we have seen in Section 5.1.3 of Chapter 5, we limit our analysis to the pipeline structures and collect the latency requirement of each structure for providing error containment coverage to all instructions. We analyze the time each instruction spends in traversing through the pipeline. This gives us an insight of minimum required detection latency constraint for every structure in the core. Later, we further try to relax the detection latency requirement and observe the tradeoff of required number of detectors vs. error containment coverage.

6.3.1.1 Traversal of Instructions in Pipeline

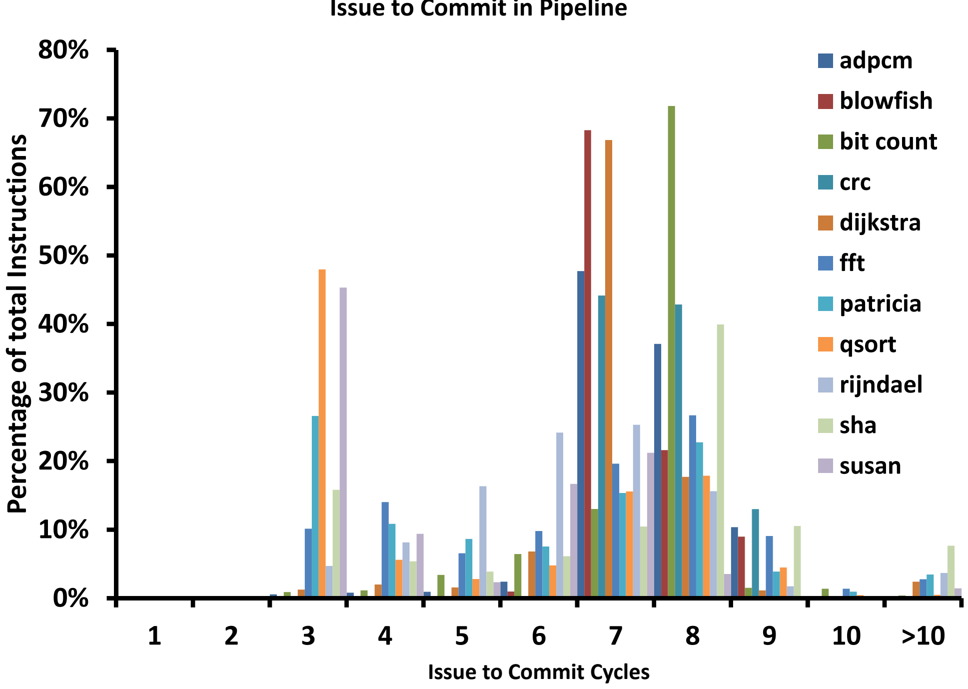

FIGURE 6.4: Distribution of residency cycles in a state of the art embedded core pipeline

A typical out-of-order embedded core has 9-stage pipeline. We identified four different paths with different best case latencies: (i) Once the instruction has been fetched from instruction cache until commit takes 9-10 cycles, (ii) decode to

commit 7-8 cycles (ii) rename/issue to commit takes 3-5 cycles, (iii) execute to commit takes 2-3 cycles, and (iv) writeback to commit is 1-2 cycles [309].

Consider an example of fetch stage: from our observation we noticed that all instructions that are fetched will take minimum 9 cycles (considering best case) to reach the commit stage. Providing single cycle detection latency for structures in fetch stage (i.e., prefetch, branch-predictor etc.) would be unnecessary. The same holds true for structures in decode stage.

From this initial observation, we identified that paths from issue to commit, execute to commit and writeback to commit are critical and will need stricter detection latency requirement for error containment. To have a better understanding of the error detection latency constraints of issue, execution unit and writeback we have to know how much time each instruction spends to reach commit from issue, execution units and writeback.

Figure 6.4 shows the distribution of number of cycles it takes for each instruction since they are issued until commit (including the wait cycles in ROB). Histogram of Figure 6.4 shows that 100% of instructions are committed in $\geq$3 cycles. Similar experiments indicate that from write-back stage 100% of instructions reach commit in $\geq$1 cycle and 100% of instructions reach commit in $\geq$2 cycle from execution units. Once in ROB, instructions wait until it is their turn to commit.

6.3.1.2 Cost of Error Containment

Now we know that to provide error containment coverage for 100% instructions before they commit, the issue queue requires error detection latency of 3 cycles, for ALUs detection latency should be 2 cycles and structures of writeback stage (i.e., register file, ROB) must have error detection latency of 1 cycle.

However, error containment in the ROB is little more involved. It is also responsible for instruction commit. If the detection latency of error in commit (i.e., ROB) is 1 cycle, implies that an error in the commit itself cannot be contained within core (i.e., before the commit is over). So to have full error containment coverage (i.e., including errors in commit), detection latency for ROB must be less than 1 cycle.

Table 6.2 summarizes the required number of detectors to provide selective error containment before the instruction is committed. It shows the number of detectors

Structure	**Detection Latency (#Cycles)**	**#Detectors**
Fetch	9	3
Decode	7	4
Issue queue	3	4
ALU (3 in total)	2	4
ROB and Commit	0.15	2
Load Queue	1	1
Store Queue	1	1
Total		**19**

Table 6.2: Required acoustic wave detectors for full error containment coverage. L1 cache is protected separately using an architecture as presented in Chapter 4.

required for given detection latency constraints. It shows that to provide selective error containment we will need 19 detectors for 100% error containment coverage.

It is worth mentioning that with 2 detectors ROB achieves error detection latency of 0.15 cycle. This implies that a glitch generated by a particle strike in commit needs to propagate within 0.15 cycles to cause SDC, this increases the possibility of masking the error before it will be committed. Alternatively, hardened latches can be used to protect ROB [117].

Figure 6.5 shows the structural map of an embedded core and also the placement of acoustic wave detectors. Majority of the area is occupied by caches, TLBs and register files. To contain the error in these structures, we propose to use ECC, or adapt a low cost acoustic wave detector based solution similar to the one that is described in Chapter 4.

Overheads. The area overhead for selective error containment for full coverage is equivalent to 19 6T-SRAM bit cells at 45 nm. The controller circuit is also very cheap and will require (roughly 10 logic-OR gates). As the number of detectors are less the intrusiveness of solution on placement and routing is minimum. Acoustic wave detectors are passive and hence they do not consume power, so the power overhead comes only from control circuit and interconnects, which is negligible. Protecting caches alone for 1 cycle detection latency costs 1680 detectors. Using the architecture for protecting caches as presented in Chapter 4, it is possible to reduce detection latency to 10 cycles for L1 cache with just 15 detectors.

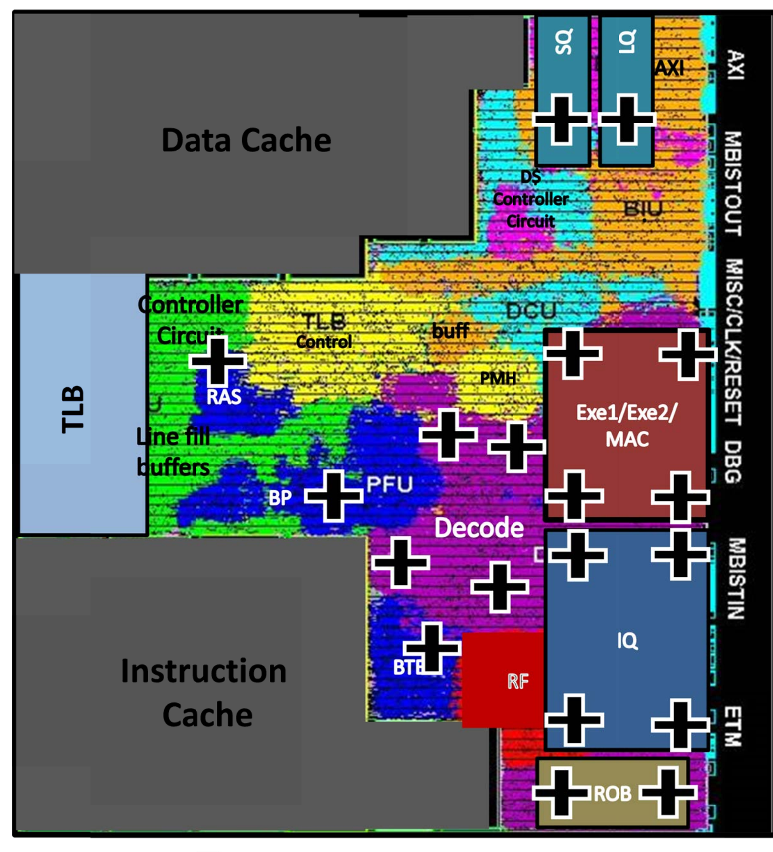

FIGURE 6.5: Arrangement of FUBs and placement of acoustic wave detectors on embedded core [313]

6.4 Error Containment Coverage vs. Vulnerability

Now, we want to see if we can further relax the detection latency constraint to reduce the required number of detectors for reducing area overhead even further compared to what we saw in previous section. Reducing the number of detectors may result into some instruction escaping the error containment boundary reducing the error containment coverage. To observe the tradeoff of relaxing detection latency requirement and its impact on reliability, we perform an estimation of structure's AVF. The concept of AVF is discussed in great detail in Section 2.9 of Chapter 2.

6.4.1 ACE Analysis

To estimate a structure's AVF we track the state bits required for architecturally correct execution (ACE) for all committed instructions. Let's understand the concept of ACE bit via one example in a program that runs for 10 billion cycles in a processor. Out of these 10 billion cycles a particular bit in the processor core is required to be correct just for 1 billion of cycles. The state of the bit during the rest of the 9 billion cycle does not affect the correctness of the program. In this case, the AVF of the bit is 10%. This concludes that the bit is ACE for 1 billion cycles and un-ACE for 9 billion cycles.

Similar to the notion of an ACE bit at architecture level instructions can be ACE or un-ACE. In ACE instructions all the bits are ACE bits. However, in un-ACE instructions only some of the bits are ACE. It is possible to compute the ACE and un-ACE bits for an instruction through out its journey in a processor pipeline. If the error is in one of the ACE bits, it will cause the silent data corruption if it is not contained. ACE analysis of the entire execution is difficult and hence conservatively we assume every bit is ACE unless we can prove it to be un-ACE. Once we classify ACE and un-ACE bits for a structure, AVF of a structure is simply the fraction of time that it holds ACE bits. AVF analysis gives us better insight into a structure's vulnerability because depending upon the application, a structure holds ACE bits at some times and un-ACE bits at other times.

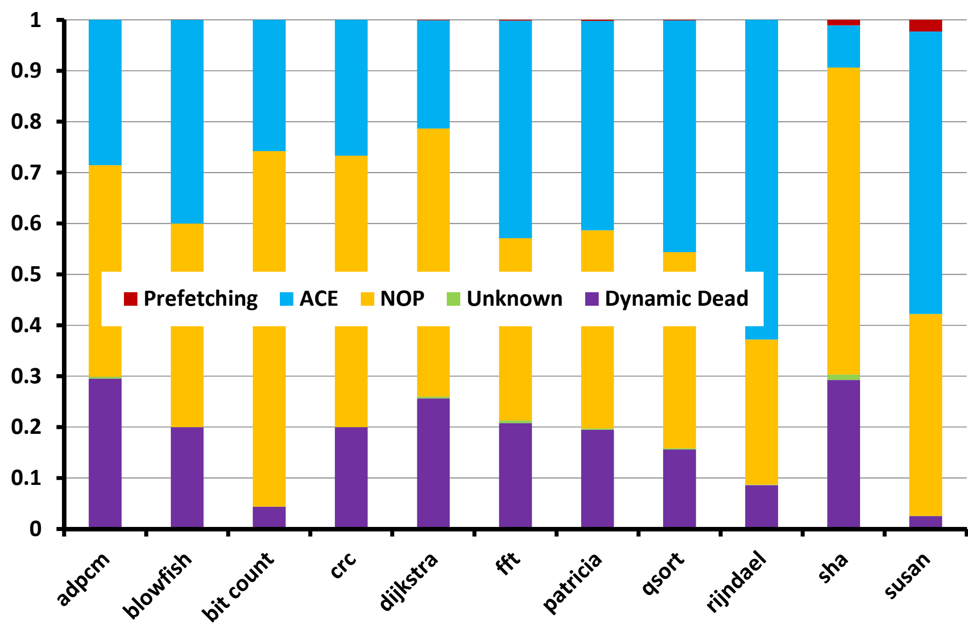

FIGURE 6.6: Error containment granularities in embedded processor

Using cycle accurate simulation, we track average ACE bits through structures holding both microarchitecture and architecture states and we collect the residency cycles of ACE bits and structure usage cycles. We identify sources of un-ACE instructions (i.e., NOP instructions, Performance enhancing instructions etc.) similar to [117]. Figure 6.6 shows the distribution of instructions in the analyzed benchmark suit.

As suggested in [97], we classify the instructions into 5 clusters. The *Unknown* category includes the instructions whose destination registers's lifetimes can not be determined within the instruction analysis window. Dynamically dead instructions include instructions whose computation results are simply not utilized by any other instructions. NOP instructions and perfecting instructions are easily identified.

Once we have obtained the information of ACE and un-ACE bits it is possible to compute the AVF of a given hardware structure. As discussed in Section 2.9 of Chapter 2 the AVF of a storage cell is the fraction of time (i.e., ACE cycles) an upset in that cell can cause a user visible error. AVF of a hardware structure (i.e., issue queue) is the average of the AVF of all storage bits in the structure.

$$AVF_{structure} = \frac{\sum_{i=0}^{N} ACE\ cycles_i}{Total\ cycles \times Size\ of\ the\ structure\ (N\ bits)} \tag{6.1}$$

The AVF of a hardware structure can be given as shown in Equation 6.1. $ACE\ cycles_i$ denotes the ACE state of ith bit and the *Total cycles* are the cycles over which the state of the ith bit is observed. N represents the total number of storage cells in the observed structure.

The equation can be further simplified to,

$$AVF_{structure} = \frac{Average\ number\ of\ ACE\ bits\ in\ a\ structure\ in\ a\ cycle}{Size\ of\ the\ structure\ (i.e.,\ total\ number\ of\ bits)} \tag{6.2}$$

Now, that we are familiar with how to obtain AVF of a structure, next we will analyze the AVF undertaking an example structure. Moreover, we will also explore the possibility to reduce the AVF of a structure in an architecture protected via acoustic wave detectors.

6.4.2 Reducing AVF using Acoustic Wave Detectors

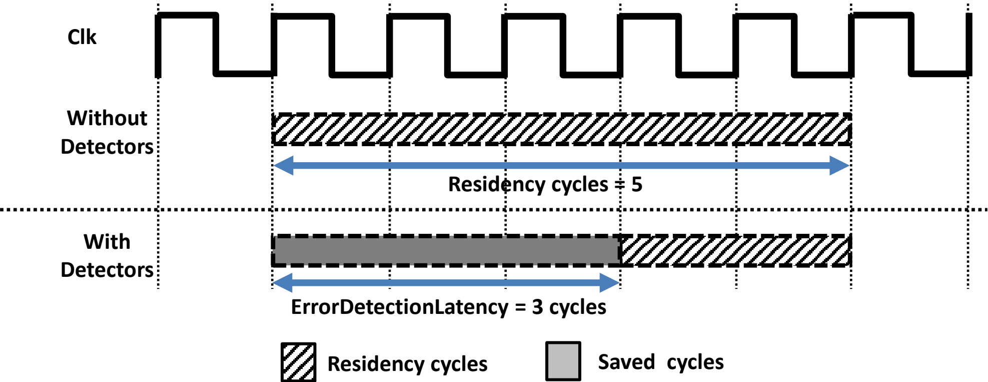

Figure 6.7: Reducing AVF by adapting acoustic wave detectors

Figure 6.7 shows how the vulnerability of a structure protected by acoustic wave detectors can be reduced. Consider an example as shown in Figure 6.7(a) where the residency time of ACE bits of an instruction in a structure is 5 cycles. So the ACE bits are vulnerable for all the 5 cycles they spend in the structure, and all 5 cycles contributes towards AVF.

Now, imagine the structure is protected with acoustic wave detectors as in the case of Figure 6.7(b). The error detection latency is 3 cycles. Instruction still stays for 5 cycles in the structure but now the ACE bits are vulnerable only for 2 cycles as we will detect the error within 3 cycles. Only 2 cycles will contribute towards AVF. This implies that *if the detection latency of the acoustic wave detectors protecting a structure is less than the residency cycles of ACE bits in that structure then the AVF of given structure can be reduced substantially.*

We leverage this observation to evaluate vulnerability factor of issue queue protected with detectors. We collect the ACE bits and the amount of time they spend in issue queue for different detection latency cycles. And we show how the architecture with different detection latency cycles impacts the AVF of issue queue.

Figure 6.8 shows the AVF of issue queue (relative to the AVF of unprotected IQ = 100%) for containing errors using acoustic wave detectors for different error detection latency. Figure 6.8 shows that for error detection latency of 6 cycles, the average AVF of IQ is 45%. And if provided with enough detectors to achieve detection latency of 4 cycles the AVF of IQ goes down to 2.2%.

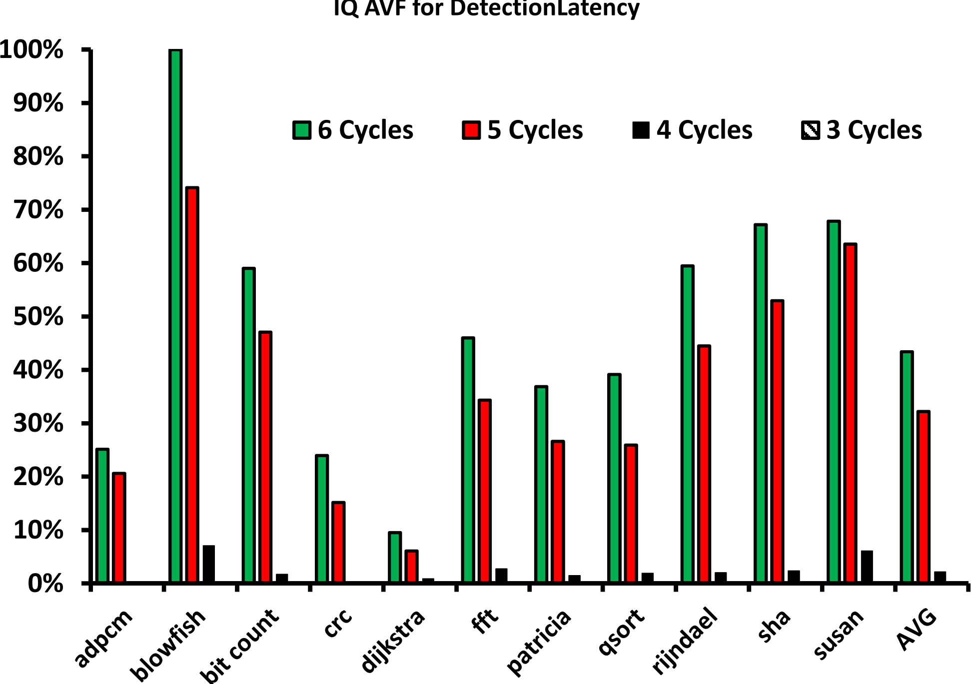

FIGURE 6.8: AVF of issue queue by protecting them with acoustic wave detectors for different detection latency

Summarizing, containing the error with acoustic wave detectors for error detection latency of 3 cycles will provide 100% error containment coverage and in this case the AVF of IQ is 0. Now, if we provide error containment for just 4 cycles to IQ, the AVF is 2.2%. This means that the error detection latency of 4 cycles reduces the error containment coverage of IQ reducing the reliability of IQ by 2.2.%. Similarly, providing error containment for 5 cycles reduces the error containment coverage of IQ to reduce its reliability by 31%. It is worth mentioning that this reduction in reliability is computed considering that there is zero error masking. In reality, error masking can mask many errors that we are allowing to escape and hence, it may not have any impact on the overall correctness of the architectural state and reliability.

6.5 Related Work

Several fault tolerant methods exists that detects and recovers from soft errors. Thus, the techniques discussed in Section 5.6 of Chapter 5 and Chapter 7 can be used with any design including embedded processors. However, other techniques

exist that are specific to embedded processors. These techniques depend on the architecture and functionality of microprocessors. The most well known of those techniques are briefly explained in this section.

6.5.1 Soft Error Sensitivity Analysis

In this section we will see the proposals that characterize the soft errors and soft error rate specifically embedded processors. The presented work suggests that soft errors in embedded processors are important and require specific techniques to handle them.

The work of [314] conducted fault injection on an RTL model of the PicoJava-II microprocessor to characterize the soft error sensitivity of logic blocks within the embedded processor. Similar to the AVF, they derive a soft error sensitivity (SES) metric. And SES represents the probability that a soft error within a given logic block will cause the processor to enter an incorrect architectural state. Similar to the AVF, the SES information is used in devising an integrity checking scheme for the picoJava-II, and evaluate how well the existing robustness techniques of current microprocessors reflect the soft error behavior.

The main outtakes of their analysis are as follow: (i) Most of the faults are masked and do not cause soft errors. Similar to AVF, few structures with a very high SES are more vulnerable to soft errors. The SES of a structure is a function of its architectural properties; logical situation, its behavior in collaboration with other structures; and the operating frequency, (ii) Variations in the tested workloads do not significantly vary the SES of a structure, (iii) Based on the SES analysis primer concern of soft errors are the memory components and should be protected. Soft errors in control logic generally have a shorter lifetime than those in the memory arrays and can be easily masked, and (iv) The sensitivities of many structures in the pipeline are easily predictable from processor architecture and organization.

A similar soft error sensitivity analysis is presented in [315]. It performs the soft error injection in both sequential state elements and combinational logic on a DLX microprocessor model. It collects the soft error sensitivity data to assess (i) the soft error sensitivity of control and speculation logic compared to that of other functional blocks, (ii) how vulnerable the combinational circuits are compared to flip-flops, and (iii) how many errors get masked while propagating from one

functional unit to the other. Their analysis indicates that sensitivity of control and speculation blocks in an embedded core to soft errors is comparable to the soft error sensitivity of ALUs. Moreover they conclude that the combinational logic, though less sensitive than flip-flops, could potentially lead to increased soft error rate in future technologies.

6.5.2 Soft Error Protection

Now, we will see some hardware, software and hardware/software hybrid techniques for handling soft errors in embedded domain.

6.5.2.1 Hardware Only Approach

The proposal of [118] focused on circuits for detecting delay faults caused by electrical noise, particle strikes and inadequate voltage levels. The fundamental idea relies on strategic placement of transient fault detectors. The work exploits the circuit-level characteristics of embedded microprocessors in order to efficiently place the detectors on the given chip. For mitigating soft errors, two complementary techniques are proposed. The first technique, uses a register value cache. It is an architectural solution that provides twice the fault coverage compared to ECC when applied to the register file and costs less to implement in terms of both area and power. The register value cache maintains duplicate copies of only the most recently used register data in order to provide high fault coverage. Unlike traditional mechanisms, such as ECC, the register value cache can handle faults in both the combinational logic and the memory buffers. By storing redundant values it can yield more than double fault coverage compared to ECC. The coverage provided by the register value cache may be increased by adding more redundant entries to the cache.

The second technique uses time delayed shadow latches for fault detection. In this technique all high fan-in nodes in the processor pipeline are covered with shadow latches. These shadow latches stores the redundant data and compares it to detect the transient errors. Moreover, once error is detected it is possible to use these detectors to flush speculative state and correct transient errors occurring in microarchitectural state. The process of determining the most effective location for these pulse detectors and inserting them into the design can be challenging.

The two proposed fault tolerance techniques can be used in conjunction and they collectively provide approximately 84% fault coverage while incurring less than 5.5% area overhead and about 14% power overhead.

6.5.2.2 Software Only Approach

A software only approach for detecting soft errors in embedded processors was proposed in [316]. It is based on two well known areas of prior research in the field of soft error detection: symptom-based fault detection and software-based instruction duplication (will be discussed in Chapter 7).

This work uses use edge profiling, memory profiling and value profiling in the context of code duplication for protection against soft errors. With profiling information we can exploit the common case behavior of a program to duplicate only those critical instructions. Different types of profiling information enables us to ignore unnecessary duplication of instructions that are unlikely to cause program output corruption in the presence of a transient fault.

1. Edge profiling is based on the intuition that frequently executed instructions should not be duplicated to protect an infrequently executed instruction. The probability of a soft error affecting an infrequently executed instruction is relatively low and so to protect such a instruction, unnecessary duplication of frequently executed instructions should not be performed.
2. Memory profiling is used to obtain information about load/store dependency, aliasing between loads and stores and information about silent stores (i.e., stores that update the same value to a memory location that is already present at that location).
3. Value profiling is used to observe the values generated by an instruction during the execution. If an instruction generates the same value almost 100% of the time, it is possible to use that value and compare it to the value generated by the same instruction at runtime for error detection. If the value generated at runtime differs from the one that the instruction generates very frequently an error is detected and appropriate recovery action is triggered.

The solution also uses of symptom-based detection, which relies on anomalous microarchitectural behavior to detect soft errors. And it can achieve 92% fault

coverage. However, this technique requires redundant instruction to be added for fault detection and causes upto 20% instruction overhead. These extra instructions may cause average 51% performance overhead.

6.5.2.3 Hybrid Approach

A hardware/software approach for detecting and recovering from errors is proposed in [317]. The fundamental idea of this approach is to re-engineer the instruction set. The proposal decomposes the application into multiple instructions for a specific processor. These instructions typically are composed of micro-ops. Several micro-ops are added to the native instruction set of the embedded processor to enable checkpointing. The checkpoint based error recovery mechanism is implemented using three custom instructions. These custom instructions can recover from (i) the changes in the general purpose registers, (ii) the data memory values which were modified and (iii) the changes in the architecture special registers (PC, status registers etc.).

At run-time, instructions execute the native functionalities (e.g., adding two operands of the ADD instruction) as well as the additional functionality which is to generate checkpoint data of destination register for the given instruction. The checkpointing storage varies for each executing application. Results show that the hardware/-software approach degrades performance by 1.45% under fault free conditions. In the event of an error the recovery takes 62 clock cycles (worst case). Due to added storage for checkpointing and recovery it incurs area overhead of 45% on average and 79% in the worst case. Due to the added functionality to each instruction the power overhead of this approach is upto 75%. The main disadvantage of this approach is that the the processor's architecture needs to be modified to support the additional custom instructions.

6.6 Chapter Summary

In this chapter we presented an architecture that uses acoustic wave detectors to detect and contains the error with minimal hardware overhead incurring zero performance cost. We have shown how the choice of error containment granularity can affect the cost of recovery and performance for embedded core. Containing error in

the cache can cause 22% performance overhead in the studied embedded core. For error containment in the core, we show that providing selective error containment can reduce the required number of detectors by 130×. The solution proposed in Chapter 5 may be useful for some complex embedded multicore processors.

Next, we explained how we can obtain AVF of a structure using performance simulator. We presented the sources of un-ACE and ACE instructions for embedded core while simulating real world embedded applications. Moreover, we also explored the possibility to reduce the AVF of a structure in an architecture protected via acoustic wave detectors. We also showed that by trading off the error containment coverage by as little as 2.2% the required detectors can be further reduced to 17.

Chapter 7

Related Work

Along with power, performance and temperature, reliability is now considered as a key design parameter. Typically, silicon chip vendors have market specific SDC and DUE FIT budgets that they require their chips to meet [18, 318]. Keeping the consumer needs in mind chip vendors decide a certain FIT budget. FIT budget is typically kept constant across years. In other words, designers are motivated to incorporate various techniques to satisfy the FIT budget, by making the system more robust. This section will describe such techniques at device and circuit level, this section will also discuss techniques to improve reliability by adding redundancy at circuit, micro-architecture and system level.

7.1 Soft Error Protection Schemes

Soft error protection schemes can protect the device against soft errors by making the device inherently robust by deploying various device and circuit enhancement techniques.

7.1.1 Device Enhancements

The most famous and effective device enhancement schemes to reduce the avoid soft errors are triple well and SOI technology. We have already introduced these techniques in Section 4.6.3 of Chapter 4.

7.1.1.1 Triple-well technology

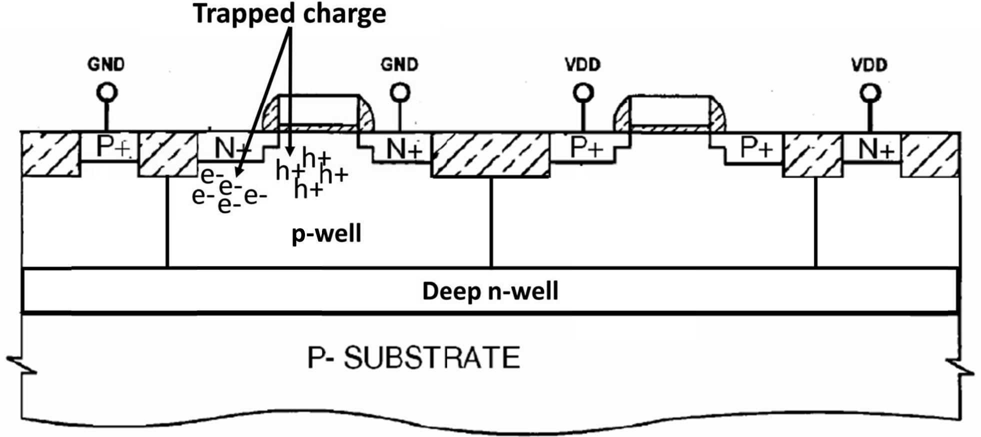

FIGURE 7.1: Triple well technology and the creation of deep n-well which traps the charge generated upon a particle strike.

At process level several techniques can be used to reduce the charge collection capacity of the sensitive nodes in an SRAM memory cell [259]. Using multiple well structures have been proposed to show improved robustness by limiting charge collection [260]. Triple-well technology is used in deep submicron CMOS technology to improve the device performance. As shown in Figure 7.1, a triple-well device completely isolates the NMOS in a p-type substrate reducing the substrate noise and resulting into better performance of the NMOS. This helps reducing the device soft errors because the deep n-well makes it difficult for the electrons generated by the particle strike to penetrate and collected by the drain of the NMOS.

7.1.1.2 Silicon-on-insulator

SOI primarily introduced due to its benefits in improving the performance in deep submicron technologies. As shown in Figure 7.2, SOI technology introduces a buried oxide layer between the source (or drain) and the substrate. This eliminates the junction capacitance of traditional CMOS technology improving the switching speed.

Apart from improving the performance, SOI also reduces the sensitive volume, which ends up reducing the charge collection capacity and hence improving the soft error rate. SOI techniques can reduce a reduction of soft errors by as much as 5× [184, 185]. No detailed data is available to give any insights of SOI in

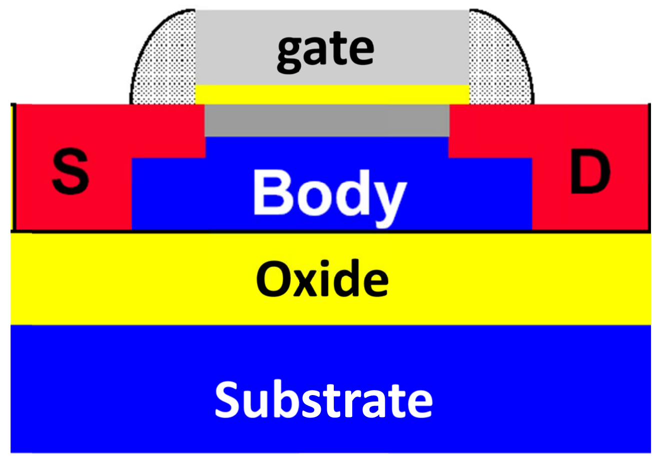

FIGURE 7.2: The suspended body in partially depleted SOI transistor

reducing soft errors in latches and combinational logic. Literature shows that a fully depleted SOI has the lowest sensitive region and can be the most effective in reducing the soft error rate. Nevertheless, manufacturing fully depleted SOI devices in large volumes still remains a major challenge. Physical solutions are hard to implement and may end up alleviating the cost of handling soft errors.

7.1.1.3 Process techniques

Other process techniques include wafer thinning, mechanisms to dope implants under the most sensitive nodes etc. Process level techniques are effective and significantly reduce the soft error rate of the memories. However these techniques require modifications in the standard CMOS fabrication process and therefore are less attractive.

7.1.2 Circuit Enhancements

The most common and obvious techniques to reduce the vulnerability against the soft errors at circuit level is to increase the nodal capacitance of the cell and to use the radiation hardened cells. We have discussed the use of circuit level techniques for protecting caches in Section **??** in Chapter 4.

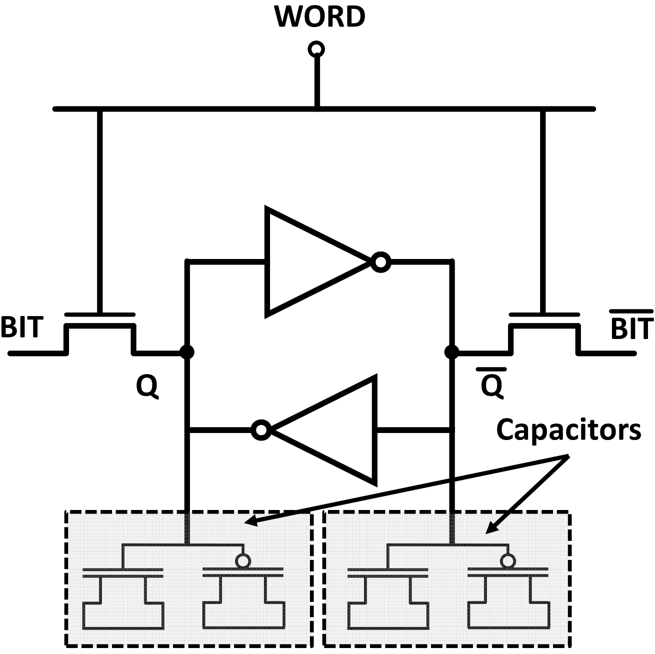

FIGURE 7.3: Reduction of soft errors by introducing capacitance on the critical nodes in an SRAM cell

7.1.2.1 Increasing nodal capacitance in the circuit

Another way of protecting the caches at circuit level is by making the memory cell physically robust. One way of implementing robust SRAM cell is by increasing the Q_{crit} of the SRAM cells used in caches. Such SRAM cells are designed via incorporating extra resistors or capacitors in the feed back path of the decoupled inverter circuit of the SRAM cell [266]. One such implementation is shown in Figure 7.3. Adding the capacitor to the critical node can also significantly increase the Q_{crit} making the cell more robust. Such techniques can reduce the soft error rate of latches upto 3× but due to higher capacitance, this results into a slower latch and also 3% increase in chip-level power according to the studies [319] and [320].

However, addition of the resistor or a capacitor may increase the cell area by 13-15%, moreover RC response delay increases due to increased capacitance making the cell slower and it may increased access time by 6-8% [270]. Increasing Q_{crit} by adding extra RC elements can also increase the power [28, 267, 321].

7.1.2.2 Radiation hardened cells

Radiation hardening is another circuit level approach for handling soft error rates. In radiation hardening the SRAM cell is made stronger by increasing its overall size or by adding more transistors. Increasing the size of an SRAM cell may make it slower impacting performance. By adding more transistors to the original SRAM cell to make it more robust the underlying idea is to maintain a redundant copy of the data which can provide the correct data upon a particle strike and also recover from the error [264, 269]. Such DICE can reduce the soft error rate upto 10× [265]. Another set of circuit level solutions include, a high speed scan logic circuit in which the transient fault is detected by quickly by comparing the outputs of the redundant SRAM cells [85, 322, 323]. However, such high speed scan logic adds extra hardware increasing the area overhead. Moreover, the scan logic must be maintained at the same speed as the protected cache all the time increasing the power overhead [117]. However, it is worth noticing that this robustness comes at the cost of 1.7× to 2× increased area and almost doubled energy penalty.

All the circuit level soft error protection techniques are attractive at first because they guarantee higher levels of robustness but on the other hand this robustness comes at huge penalties in terms of area and energy. Also they increase the complexity of post silicon validation.

7.2 Soft Error Detection Schemes

Detecting faults is the most crucial problem for any fault tolerance system. A system cannot recover from a problem of which it is not aware of. Fault detection provides the minimum measure of safety and efficient fault detection helps to reduce the SDC to almost zero. Error detection can be implemented in three ways: (i) physical or spatial redundancy, (ii) information redundancy and (iii) temporal redundancy. In this section we will see each one of them in greater detail with examples.

7.2.1 Spatial Redundancy

Spatial redundancy is very common and simplest techniques to detect transient and permanent errors. Basically these techniques add extra hardware (redundant hardware) to detect the errors. Spatial redundancy can be implemented via executing the same task on two different components as is the case of the most basic implementation of the DMR technique. A DMR system comprises of a comparator as explained in Section 5.6 of Chapter 5.

Modular redundancy is a widely used technique in the industry as it can detect and recover from both transient and permanent faults in microprocessors by using non homogeneous replicas which provides design diversity. It is possible to implement physical redundancy at various granularities. Replicating the entire system or a core within multi-core processors are also possible and replicating parts of the core has also been explored depending upon the required level of robustness and amount of overheads. The IBM G3 [58] employs lockstepped pipeline implementation and to reduce the performance penalty, instruction fetch and execution units were replicated and the error checking was performed at the end of the pipeline. This however, led to area penalty of 35%.

These techniques provide excellent error detection for all kinds of failures provided that the redundant copies are non-homogeneous but they have huge impact in area, power and delay, as the output of each replicated component has to be compared.

7.2.1.1 Detectors for Error Detection

Implementing physical redundancy for error detection also includes adding detectors. The detectors that detect the particle strikes via detection of current glitches, voltage glitches, metastability issues or deposited charge are discussed in great detail in Section 3.7 in Chapter 3.

Several other detector based techniques have been proposed. One such famous circuit level technique is Razor [85, 323]. It mainly deals with the voltage drop induced errors (caused by transient and intermittent errors) in combinatorial logic. The fundamental idea behind this mechanism is to use double-sampling of values at certain pipeline stages, to guarantee robustness but at the cost of huge area overheads. Razor works via pairing each flip-flop within the data path with a

shadow latch that is controlled by a delayed clock. After the data propagates through the shadow latch, the output of both of the blocks is compared. If the combinational logic meets the setup time of the flip-flop, the correct data is latched in both the data path flip-flop and the shadow latch and no error signal is set. Upon a mismatch between the outputs of the flip-flop and shadow latch an error signal is triggered and hence an error is detected. Razor uses extra circuitry to determine if the flip-flop is metastable. If so, it is treated as an error and appropriately corrected. An important property of Razor flip-flops is that the shadow latch is designed to pick up the correct result upon the delayed clock. Using Razor it is possible to correct the value via stalling the result from the latch by one cycle.

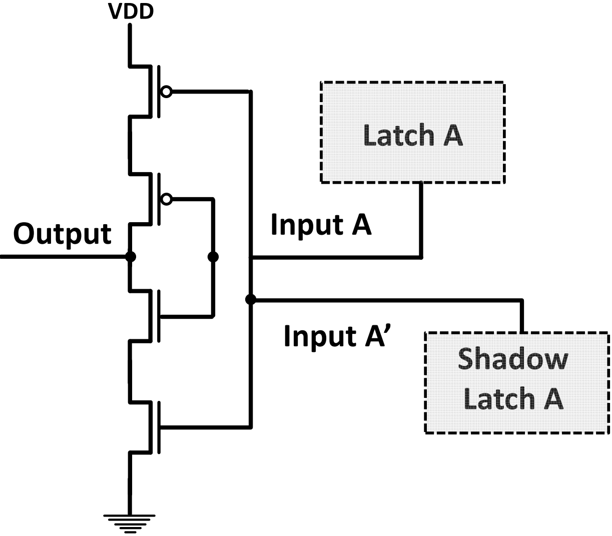

FIGURE 7.4: The C-Element circuit forming the core logic of BISER detection scheme [322]

Another circuit level technique is proposed in [322]. It relies on a at-speed scan logic based on a C-Element circuit as shown in Figure 7.4. It can be used to detect the error by comparing the stored values in the storage elements. It acts as an inverter when both inputs A and A' are same. However, it does not let any input to propagate when the inputs are different.

7.2.1.2 Error Detection via Monitoring Invariants

Rather than replicate a piece of hardware, another approach to error detection is dynamic verification. Added hardware checks whether certain invariants are being satisfied at runtime. These invariants are true for all error-free executions and

thus dynamically verifying them detects errors. The key to dynamic verification is identifying the invariants to check. As the invariants become more end-to-end, checking them provides better error detection. Ideally, if we identify a set of invariants that completely defines correct behavior, then dynamically verifying them provides comprehensive error detection. That is, no error can occur that will not lead to a violation of at least one invariant, and thus, checking these invariants enables the detection of all possible errors. We present work in dynamic verification in an order that is based on a logical progression of invariants checked rather than in chronological order of publication.

DIVA as discussed in Section 5.6 of Chapter 5 uses heterogeneous physical redundancy. It detects errors in a complex, speculative, superscalar core by checking it with a core that is architecturally identical but microarchitecturally far simpler and smaller.

DIVA [67] uses a simple in-order core as a checker for an out-of-order core. As processor designs grow in complexity, they become increasingly difficult to fully verify and debug. DIVA proposes to implement a relatively simple and fully verified back-end processor to perform dynamic (while the processor is in use) verification of a processor. While the main purpose of DIVA is to ease the challenge of verification and debugging complex processor cores, DIVA also serves to detect soft error events. Assuming that a fault affects only the complex processor core or the backend checker, DIVA will detect the fault and can be configured to attempt recovery.

Argus framework consists of checkers for each control flow, data flow, computation, and interacting with memory [289]. It achieves near-complete error detection, including errors due to design bugs, because its checkers are not the same as the hardware being checked. However, it cannot detect errors that occur during interrupts and I/O. Moreover, checkers use DFG signatures (will be discussed in Section refDFG). Signatures represent a large amount of data by hashing it to a fixed length quantity. Because of the lossy nature of hashing, there is some probability of aliasing, that is, an incorrect history happens to hash to the same value as the correct history. It cannot detect the errors whenever the checker is using lossy signatures.

Similar to DIVA implementation, a watchdog processor can be employed to observe the invariants and detect an error. A watchdog processor is a simple co-processor

that watches the behavior of the main processor and detects violations of invariants [324].

7.2.1.3 Error Detection via Dynamic Control/Data Flow Checks

Detecting errors in control logic is generally more difficult than detecting errors in data flow. Data errors can be easily detected via parity codes. Checking errors in control flow involves monitoring errors in control logic as well as control flow.

Efficient control checking is based on the observation that for a given instruction a subset of the control signals are always the same as proposed in [325]. Special hardware is added that compute a fixed-length signature of these control signals, and the these signature that is generated runtime is compared with a signature that is stored a-priori for that instruction. If the comparison results into a mismatch of signatures an error is detected.

In another approach as proposed in [326] specific microarchitectural checkers are added to check a set of control invariants. These added hardware also compute signatures for control signals. However, instead of computing signatures for every instruction, microarchitectural checkers generate a signature over a cluster of instructions. Instead of comparing signatures for every instruction, now the runtime comparison is done between the runtime signature with the signature that is generated when the last time that cluster of instructions was encountered. A mismatch indicates an error.

In high-level control flow checker a program's expected control flow graph (CFG) can be generated and compared to detect errors. A control flow checker [324, 327–331] compares the statically known CFG generated by the compiler and embedded in the program to the CFG that the core follows at runtime. If they differ, an error has been detected. In an example as shown in Figure 7.5, the CFG represents the sequence of instructions executed by the core. Now the control flow of instruction can be stored a-priori and any deviation from the desired flow can be due to an error. The most challenging aspect of the control flow checker is the complexity of the compiler. Due to conditional branches, indirect jumps, and returns it impossible for the compiler to know the entire CFG of a program in advance.

Similar to control flow checking, checkers that can check for error by comparing the data flow graph (DFG) of a program have also been explored. A data flow

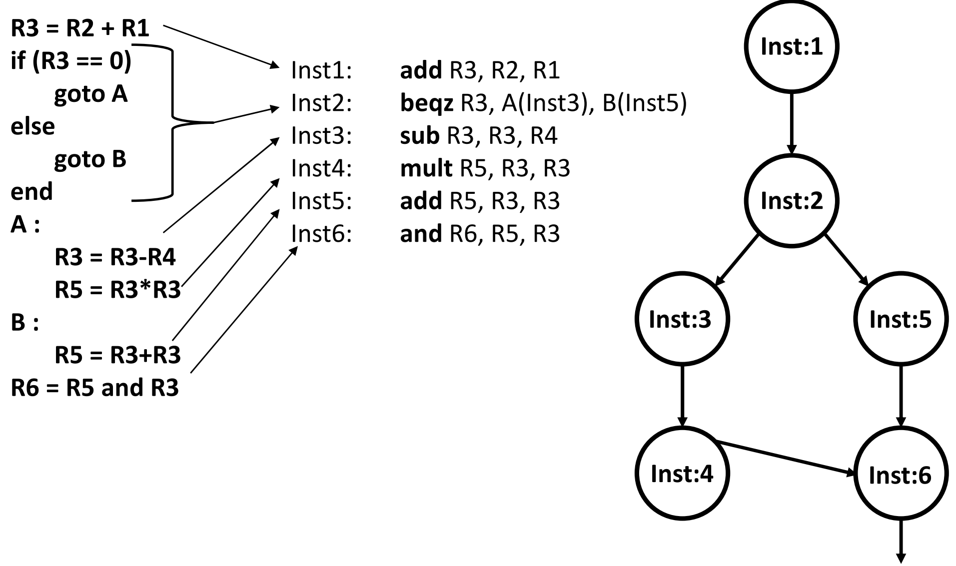

FIGURE 7.5: The control flow checker: A high level program, compiler generated instructions and the corresponding CFG

checker [332] generates a cluster of instructions called basic block. A DFG of each basic block in the program is stored. At runtime the comparison between the DFG of currently executing basic block and the statically generated DFG of the same basic block is used to indicate an error.

A data flow checker can detect any error that manifests itself as a deviation in data flow and can thus detect errors in many core components, including the reorder buffer, reservation stations, register file, and operand bypass network. A data flow checker must also check for the generated values and not only the flow. Data flow checking faces similar challenges as control flow checking. Additionally data flow checkers face a non trivial challenge which is the size of the generated DFG. To handle the unbounded size of the DFG it is possible to generate a fixed-length hash entry for each DFG.

7.2.1.4 Error Detection via Hardware Assertion

Similar to invariant monitors hardware assertions are used to detect errors [333]. We will discuss assertions that require architecture specific knowledge. Hardware assertions are specific to each hardware structure and cannot be generalized. For example, one such hardware assertion can be used to monitor the coherence engine in the caches. Assuming a MOESI cache coherence protocol is implemented. The

finite state machine should have five states for each cache block namely: *Modified*, *Owned*, *Exclusive*, *Shared* and *Invalid*. A specific implementation of the protocol requires the cache block to follow the transition in specific order *Invalid* $\mapsto$ *Exclusive* $\mapsto$ *Modified*. Now if a block undergoes *Invalid* $\mapsto$ *Modified* transition skipping the *Exclusive* state a hardware assertion can trigger an error.

		Timestamps
InstA:	**mul** R2, R1, R1	0x01
InstB:	**add** R1, R2, R3	0x02
InstC:	**add** R3, R1, R4	0x03

Figure 7.6: The hardware assertion and the timestamps

The work of [333] proposed two such assertion techniques: (i) Timestamp-based assertion checking (TAC) and (ii) Register name authentication (RNA). TAC implementation specifically targets the instruction issue logic. To detect errors it timestamps the instructions as they are issued to the execution units. For instance, as shown in Figure 7.6 each instruction waiting in the issue buffer has been assigned a timestamp. Notice that the instruction A updates the *R2* with a multiplication. It has a timestamp associated with it. The the instruction B utilizes the *R2*. The latency of the instruction A is L. The assertion holds if Timestamp(B) $\geq$ Timestamp(A) + L. In the event that condition doesn't hold (i.e., multiplication operation of instruction A takes longer than one cycle) an error signal is asserted.

In an another approach towards hardware assertions the work of [334] implements a separate checker engine which takes care of asserting error signals upon failure to meet the assertion condition for number of hardware structures.

7.2.1.5 Error Detection via Symptom Checks

Detecting errors by symptom checks include error detection via detecting anomalous behavior of generated data. Symptom checks can be implemented via using some sort of information redundancy (i.e., error detecting codes). Using spatial redundancy for symptom checks relies on checker core or watchdog core which can trigger an error signal.

The idea of symptom checks is based on the observation that the value of generated data remains constant for a given window of execution time. Any deviation from this constant value within the execution window may be used to indicate the presence of an error. The expected range of values within the execution time window can be obtained either by statically profiling the program's behavior or by dynamically profiling it at runtime [335]. However, if the value of datum goes beyond the known profiled range of values it may result into false positive.

The work of [288] proposes hardware fault screener that employs several anomaly detectors that check data value ranges (i.e., history based approach), data bit invariants (i.e., generating bit-masks for each static instruction), and whether a data value matches with the one of a set of recent values (i.e., bloom filter based approach). A fault screener operates by examining program state for internal inconsistencies with past behavior. Consider an example of a static instruction that generates a result value between 0 and 16 the first thousand times it is executed, then generates a value of 50. Since the new value of 50 does not fall within the profiled range of values for that static instruction, the new value is an example of a perturbation. Other works in the same direction that detects the anomalous.

7.2.1.6 Error Detection via Selective Protection

Another scheme to detect the errors is by providing selective protection. One way of implementing it is by duplicating a subset of values in the shadow latches and comparing them with the generated values. For instance, a core's register file holds a significant amount of architectural state that must be kept error-free. A simplest approach for protecting the registers would be to protect them using error codes. However, associating error codes can cause huge area, power and performance overhead at this granularity.

Alternatively, proposals have been made to selectively protect the most vulnerable registers by copying their values in the shadow register files [336]. The register file that includes a primary storage portion configured to store a first value, and a secondary storage portion that is coupled to the primary storage portion. The secondary storage portion is configured to act as a shadow register buffer and holds replicas of live register values. The mechanism also includes an error detection scheme that is coupled to the primary register file and the secondary storage

portion (i.e., shadow register file) and is configured to indicate a difference between the first value and the second value, caused by a soft error. Every read to the register file is also done twice on both the original register file and the shadow register file. Then the two values are compared. If they are unequal, an error has been detected.

Similarly, the work [337, 338] realized that protecting all registers is unnecessary. Intuitively, not all registers hold live values, and protecting dead values is unnecessary. They proposed maintaining error codes only for those registers predicted to be most vulnerable to soft errors.

7.2.2 Information Redundancy

The fundamental idea behind information redundancy for error detection is to add some extra bits to a set of data bits to detect an error. Error coding techniques incur two kinds of area overheads : (i) number of added redundant bits and (ii) logic to encode and decode. However, the penalty due to added logic is negligible compared to the area penalty due to added redundant bits.

The most common technique for detecting errors in the cache and memory components is to use parity codes and are discussed in detail in Section 4.6.2.1 in Chapter 4. Now we will see the error detection codes for protecting execution units in a processor core.

7.2.2.1 Error Codes for Combinational Logic

The most effective method of dealing with soft errors in memory components (i.e., caches, main memory, register file etc.) is to use codes like parity, or ECC [117]. Unlike memory components the data in functional units in the processor pipeline is less vulnerable to soft errors mainly due to masking properties discussed in Section 2.6.3 of Chapter 2. Another important factor that affects the overall vulnerability of the functional unit is the period of time the instruction stays in the functional unit. For instance, instruction queue holds the issue until they can be issued and hence the period of time instructions spend in issue queue is much higher compared to the execution units. Vulnerable functional units can be

protected with error codes such as arithmetic codes (i.e., AN codes and residue codes) and parity prediction codes [76].

Arithmetic error codes are those codes that are preserved under a set of arithmetic operations. This property allows us to detect errors which may occur during the execution of an arithmetic operation in the defined set. Such concurrent error detection can always be attained by duplicating the arithmetic unit, but duplication is often too costly to be practical.

We expect arithmetic codes to be able to detect all single-bit faults. Note, however, that a single-bit error in an operand or an intermediate result may well cause a multiple-bit error in the final result. For example, when adding two binary numbers, if stage i of the adder is faulty, all the remaining *(n i)* higher order digits may become erroneous.

AN codes:

The simplest arithmetic codes are the AN codes, formed by multiplying the data word N by a constant A. The encoded data word N_c is given as: $N_c = A \times n$ where $A > 1$. Only multiples of A are valid code words and every operation processing AN-encoded data has to preserve this property. Code checking is done by computing the modulus with A. For a valid code word it is zero: $N_c \bmod A = 0$. The data value N is retrieved by an integer division $N = N_c/A$.

Function	**Residue Relation**
Addition	$N_{1c} + N_{2c} = A(N_1) + A(N_2) = A(N_1 + N_2)$
Subtraction	$N_{1c} - N_{2c} = A(N_1) - A(N_2) = A(N_1 - N_2)$
Multiplication	$N_{1c} \times N_{2c} = (A(N_1) \times A(N_2))/A = A(N_1 \times N_2)$
Division	$\lfloor N_{1c} / N_{2c} \rfloor = \lfloor (A \times A(N_1))/A(N_2) \rfloor = A\lfloor \frac{N_1}{N_2} \rfloor$

TABLE 7.1: AN codes and the functions for which they are invariant

The arithmetic operations valid for AN codes are given in Table 7.1. For example, two bit strings N_1 and N_2 then the AN code would hold $A(N_1 \Theta N_2) = A(N_1) \Theta A(N_2)$, where Θ can be addition, subtraction, multiplication or division. The choice of A determines the number of extra bits require to encode N. For example, if $A = 3$, we multiply each operand by 3 (obtained as $2N + N$ which can be obtained by a left shift operation on N followed by an addition). It is possible to check the result of an add or subtract operation to see whether it is an integer

multiple of 3. Let's understand the functionality of AN code by an example, the number $0110_2 = 6_10$ is represented in the AN code with A = 3 by $010010_2 = 18_10$. A fault in bit position 3 may result in the erroneous number $011010_2 = 26_10$. This error is easily detectable, since 26 is not a multiple of 3.

Using AN codes all error magnitudes that are multiples of A are undetectable. Therefore, we should not select a value of A that is a power of the radix 2 (the base of the number system). An odd value of A will detect every single digit fault, because such an error has a magnitude of 2_i. Setting A = 3 yields the least expensive AN code that still enables the detection of all single errors.

Residue codes:

Residue code are also arithmetic codes. Unlike AN codes, residue codes can be used to protect large range of function units including multipliers, dividers and shifters [339–341].

Function	Residue Relation
Addition	$(N_1 + N_2)$ mod M = $((N_1$ mod M) + $(N_2$ mod M)) mod M
Subtraction	$(N_1 - N_2)$ mod M = $((N_1$ mod M) - $(N_2$ mod M)) mod M
Multiplication	$(N_1 \times N_2)$ mod M = $((N_1$ mod M) $\times$ $(N_2$ mod M)) mod M
Division	((D mod M) - (R mod M)) mod M = ((Q mod M) $\times$ (I mod M)) mod M
logical `and`	$(N_1$ && $N_2)$ mod M = $((N_1$ mod M) $\times$ $(N_2$ mod M)) mod M
logical `or`	$(N_1 \|\| N_2)$ mod M = $((N_1$ mod M) + $(N_2$ mod M) - $((N_1$ mod M) $\times$ $(N_2$ mod M))) mod M
logical `not`	$(!N_1)$ mod M = (1 - $(N_1$ mod M)) mod M

Table 7.2: Residue codes and the functions for which they are invariant. Division is not directly encodable however division holds D - R = Q $\times$ I relation where D is dividend, R is remainder, Q is quotient and I is divisor

Residue codes use modulo operation as the bases. For instance, two bit strings N_1 and N_2 then the residue code would hold $(N_1 \Theta N_2)$ mod M = $((N_1$ mod M) Θ $(N_2$ mod M)) mod M, where Θ can be addition, subtraction, multiplication, division or shift operation. The invariant functions and the relationship they hold is given in Table 7.2.

Figure 7.7 shows the functional block diagram of the logic to generate the residue code to detect error in an adder. In the error detection block shown in this figure, the residue modulo-M of the $N_1 + N_2$ input is calculated and compared to the result of the mod M adder. A mismatch indicates an error. Taking an example, assume in the figure $N_1 = 5$, $N_2 = 14$ and M = 3. Now the $(N_1 \Theta N_2)$ mod M yields (19 mod 3) which is 1. And (((5 mod 3) + (14 mod 3)) mod 3) also yields 1. Similar computation can be done on subtraction, multiplication and division.

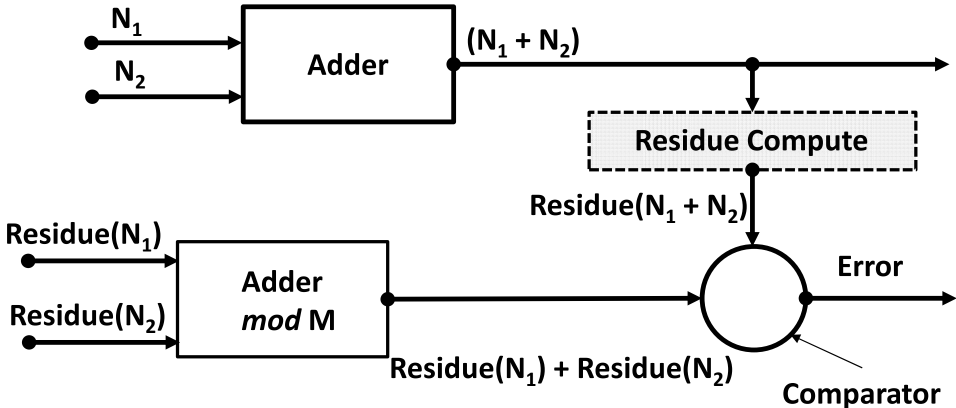

FIGURE 7.7: Residue code generation logic for an adder

Shifting operation is also very similar to multiplication with 2 or division with 2 and can be performed in similar manner as multiplication or division.

A residue code with M as a check modulus has the same undetectable error magnitudes as the corresponding AN code. For example, if M = 3, only errors that modify the result by some multiple of 3 will go undetected, and consequently, single-bit errors are always detectable. In addition, the checking algorithms for the AN code and the residue code are the same: in both we have to compute the residue of the result modulo-M. Even the extra bits needs to be added in word length is also same for AN codes and residue codes. The most important difference is known as the property of *separability*. A code is separable if functional part and redundancy of a code word are processed separately and the functional value can directly be read from the code word. In other words, it has separate fields for the data and the code bits (e.g., Parity, ECC etc.). A non-separable code has the data and code bits integrated together and extracting the data from the encoded word requires some processing. In the case of residue codes the arithmetic unit for the generating the residue is completely separate from the main unit operating on data, whereas only a single unit (of a higher complexity) exists in the case of the AN code.

Parity prediction:

Parity prediction circuits similar to arithmetic codes computes the parity of the results of an operation. It computes the parity from the source operands and then computes the parity on the result itself. By comparing these two parity codes it

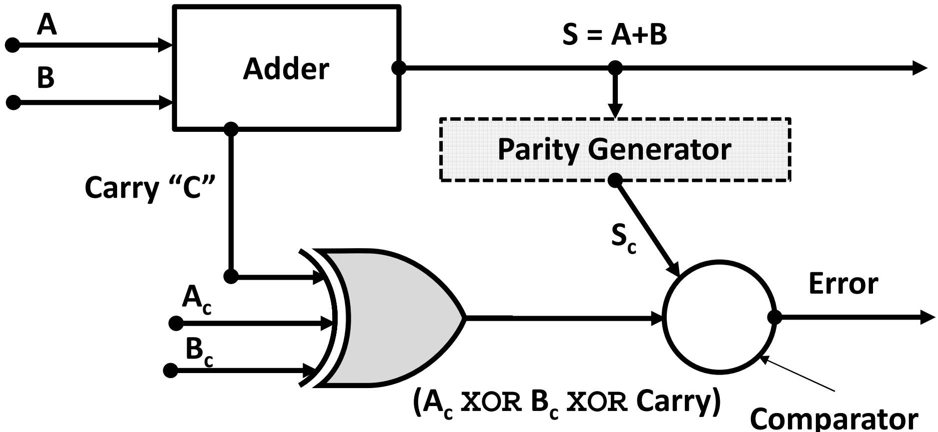

FIGURE 7.8: Functional block diagram of parity prediction circuit in an adder

can detect an error upon a mismatch. Parity prediction circuits have been used in commercial processors [229].

A functional block diagram of parity prediction is given in Figure 7.8. In the figure a parity prediction is implemented for the addition: S = A + B. A, B and S are bit strings. In the figure A_c, B_c and S_c are the parity coded bits for A, B and S respectively. S_c can be obtained by $\overset{n-1}{\underset{i=0}{\mathtt{XOR}}}\, S_i$. S_c can also be computed by A_c XOR B_c XOR Carry. Where Ccarry = $\overset{n-1}{\underset{i=0}{\mathtt{XOR}}}\, C_i$. Comparing S_c by two independent ways it is possible to compare them for a mismatch and detect an error. For example, assume $A = 01010_2 = 10_10$, $B = 01001_2 = 9_10$ then $S = A + B = 10011_2 = 19_10$. Obtaining the parity on A, B and S yields $A_c = 0$, $B_c = 0$ and $S_c = 1$. Now the summation of A + B also gives the carry $C = 01000_2$. Computing S_c from A_c XOR B_c XOR C yields 1.

Parity prediction circuits have been successfully implemented for adders [342–344] and multipliers [345, 346]. It is worth mentioning here that the circuit must ensure an error is not triggered due to an error or particle strike in the comparator. Moreover, if the error is in the carry itself which feeds to both the modules that are computing S_c. If the same error propagates to both the data that computes S_c the error will not be detected.

Arithmetic codes and parity prediction circuits both are effective in protecting functional blocks. Parity prediction circuits incur less in terms of area overhead for smaller adders and multipliers. Arithmetic codes are better option while protecting larger functional units. Both these techniques incur little performance degradation

as they strive for near-instantaneous error detection putting detection to be on the critical path.

7.2.2.2 Signature Based Approach

Another mechanism was proposed in [347], where a Π bit is used to identify possible errors in each instruction and only for the instructions that are needed for architecturally correct execution signals an error before they leave the pipeline. Also, they propose to stall the fetch (and therefore reduce the AVF) on long latency stalls.

Signatures have been used to protect the control flow [324]. A signature is calculated at compile time and inserted in the code. Later, a new signature is generated at runtime and compared to the one generated at compile time. This approach implies a non negligible design cost, due to the required modifications to the ISA, as well as power consumption increase and impact on performance, because of the required signature calculation during runtime.

The work of [348] proposes an end-to-end protection scheme based on signatures which is a token associated to a chunk of information. The concept of end-to-end protection is based on identifying a path either for data or instructions where there is a source from which data or instructions originate, and a consumption site where they are finally consumed. The end-to-end scheme involves generating a protection code at the source, sending the data or instructions with the protection code along the path, and checking for errors only at the end of the path, where data or instructions are consumed. Any error found at the consumption site can be caused by any logic gates, storage elements, or buses along the path. Other works have focused on using signature based mechanisms to protect the microprocessor pipeline against errors caused by defects and degradation [349].

7.2.3 Temporal Redundancy

There are several ways to incorporate temporal redundancy for error detection. The most common idea is to be able to detect faults from redundant streams of instructions within a single core or multiple cores. Once executed the outcome of the instructions on redundant threads are compared to detect possible faults.

Redundant execution techniques are widely accepted by the industries in the forms of lockstepping and redundant multithreading as discussed in detail in Section 5.6 of Chapter 5. The Stratus ftServer [299], HP Himalaya [350] and IBM-Z [300] series are all lockstepped in which the redundant streams are run on two separate but identical cores and they must have exact the same state at each cycle, which is very costly and incur huge performance penalty. More recent server architectures such as Marathon Endurance and HP's NonStop Advanced Architecture implement RMT [350].

These techniques can provide greater fault coverage across a processor chip compares to error coding techniques. It is important to note that these methods cannot detect hard faults and design bugs. The main reason for this is, as both threads use the same hardware it is impossible to find permanent errors, and due to homogeneous nature of the chip design errors can not be found due to lack of design diversity among the cores. Moreover, due to redundant execution these class of techniques cause huge power and performance overheads (almost 2×). The area overhead can be as much as 100% since the multithreading capability is used for error detection. A lot of modifications to the classical RMT technique has been attempted to reduce the performance penalty, by using only the idle resources for error checking [73, 74] and by replicating instructions only when the processor has available resources [71].

7.2.3.1 Various Flavors of RMT

Implementing RMT on an SMT core was first proposed in the work of AR-SMT [68]. The redundant threads are called active (A) and redundant (R) thread. The A-thread runs ahead of the R-thread and saves the results of each committed instruction in a FIFO. The R-thread compares the result of each instruction it completes with the corresponding result of A-thread in the FIFO. Whenever the results of instructions match they are committed. The R-thread commits instructions that have been successfully compared. By checking for error before commit they establish an error free recovery state. Since RMT can only detect error, this error free recovery state can be later used for recovery upon an error.

If the instructions have to be compared before commit huge performance overhead may occur due to the limited size of the FIFO. When the FIFO is full the A-thread must stall and it cannot complete more instructions. When the FIFO is

empty the lagging R-thread has no value to compare its result with. R-thread cannot commit more instructions. The slowdown can be even worse if RMT is implemented on multiple cores (instead of an SMT processor) due to longer latency in communicating the results between threads. To avoid the performance overhead AR-SMT allows the A-thread to commit instructions before the comparison [111].

To consistently detect errors due to hard faults AR-SMT suggests to bound the A-thread and R-thread to use specific and different resources in the pipeline. For instance in a core with multiple ALUs, the two threads can be enforced such that they always use different ALUs.

Three main causes of the performance overheads have been identified while employing RMT schemes for error detection. We go through them one by one and briefly discuss the enhancements in each category.

Choice of Sphere of replication:

It was observed that the majority of the performance overhead comes from where and when to the redundant threads are compared. The work [65] concludes that by carefully managing core resources and by more efficiently comparing the behaviors of the two threads it is possible to reduce the performance impact of traditional RMT core. The authors introduced the notion of *sphere of replication*. *Sphere of replication* includes the logical domain that is protected by the RMT scheme. It also implies that any error within the *sphere of replication* will be detected by RMT. *Sphere of replication* clearly defines the components that must be protected by RMT scheme. It provides necessary freedom for deciding what needs to be replicated. For example, should the thread be replicated before or after each instruction is fetched? Moreover, *sphere of replication* clearly sets a boundary and decides when comparisons need to be performed. For example, the threads can be compared at every store or at every I/O event.

Figure 7.9 shows the concept of *sphere of replication*. It shows that the *sphere of replication* includes both the processor cores and one of them is redundant. The *sphere of replication* does not include the main memory, storage disks and any I/O devices. Moreover, specific hardware takes care of replicating all the inputs coming from the components out of the *sphere of replication*. Similarly, all the outputs from the main and the redundant cores leaving the *sphere of replication* are compared via hardware comparator.

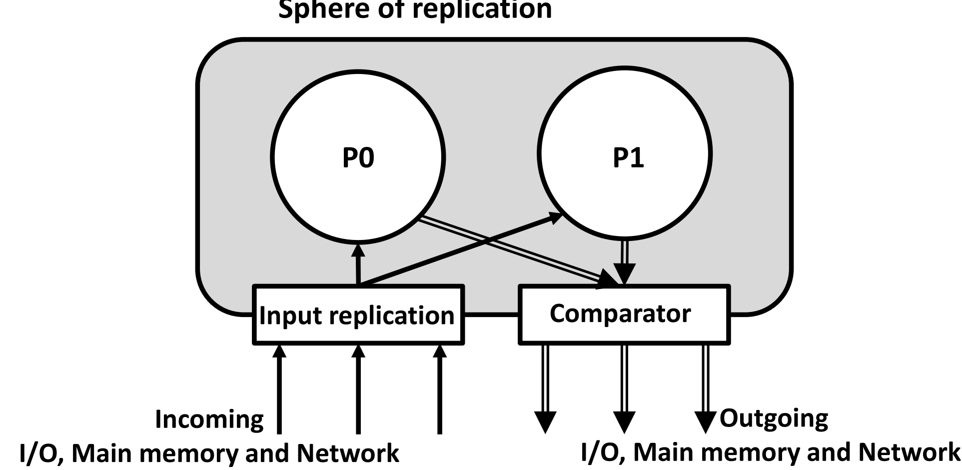

Figure 7.9: Sphere of replication is shown in shaded part. Both the processor cores are part of the sphere of replication

Sphere of replication can also be defined within a core. For example, if the thread is replicated after each instruction is fetched, then the sphere of replication does not include the fetch logic and the scheme cannot detect errors in fetch. Similarly, if the redundant threads share a data cache and only the R-thread performs stores, after comparing its stores to those that the A-thread wishes to perform, then the data cache is outside the sphere of replication.

The work of [305] analyzed the tradeoffs between different *sphere of replication*. Specifically their study was focused on the impact of the point of comparison on the size of the data to be compared. Moreover, they also study the impact of *sphere of replication* on the detection latency. Including more components into the *sphere of replication* drastically increases the number of instructions to be compared and verified for errors. The authors proposed an optimized the storage *fingerprint*. *Fingerprint* is a cryptographic hash value (generated using a linear block code such as CRC-16) computed on the sequence of updates to a processor's architectural state during program execution. A simple *fingerprint* comparison between the mirrored processors effectively verifies the correspondence of all executed instructions covered by the fingerprint. The threads' *fingerprint* are compared at the end of every checkpointing interval. Compared to a traditional RMT scheme that compares the threads on a per-instruction basis *Fingerprint* has longer error detection latency. Since *fingerprints* are generated using lossy hash function over the thread execution history there is a possibility of aliasing causing false positive error detection.

Partial/Selective Thread Replication:

Alternative research explores the possibility to replicate only selective instructions or a subset of instructions from the active thread.

Slipstream core [115] provides some degree of the error detection of classical redundant multithreading. However, it provides a performance that is greater than a single thread operating alone on the core. The contribution is based on the intuition that the partially redundant A-thread can run ahead of the original R-thread. By doing so the lagging thread can benefit from various performance enhancing decisions already made by the leading thread. For instance, the lagging thread can utilize the branch predictor decisions and prefetcher decisions to speed up the execution of the trailing thread. A compiler takes care of partially replicating instructions in leading thread by using heuristics that effectively guess which instructions are most helpful for generating predictions for the trailing thread. Retaining more instructions in the leading thread enables it to predict more instructions and provides better error detection because more instructions are executed redundantly. However, due to more redundancy the leading thread takes longer to execute and may not run ahead enough to help the trailing thread in improving performance.

An extension to this work has been proposed in [307]. It assumes a mixture of partial duplication and confident predictions in the context of slipstream processors to approximate full coverage. A similar approach [70] adapts the register renaming to issue instructions from a single thread redundantly in the dynamic execution path. As a result, the effective dispatch bandwidth, entries in the ROB, and size of the register file are reduced by the factor of 2 which is the total amount of redundancy.

Proposal of [75] suggests to partially replicate the leading thread. Further, it views RMT scheme as a leading thread generating outputs stores that emanate from the processor, and a redundant thread verifying the integrity of these outputs. The redundant thread can be further envisioned as intertwined dependency chains of instructions that ultimately lead up to these stores. They suggest to choose a partial set of instructions for redundant execution from these chains. For instance, for each store instruction, if either the address or the store value predictor produces a misprediction, the mechanism considers that an indication of a possible error that

should be checked. In this situation, the proposal replicates the backward slice of instructions that led to this store instruction.

Furthermore the work of [71] proposed to keep the leading thread unchanged. And observe the impact of selectively replicating the trailing thread and its impact on performance and error detection coverage. They observed that the amount of redundancy can be tuned at runtime and that there are often times when redundancy can be achieved at minimal performance loss. For example, when the leading thread misses in the L2 cache, the core would otherwise be partially or mostly idle without trailing thread instructions to keep it busy. They further claim that instead of replicating each instruction in the leading thread, they can store the value produced by an instruction and, when that instruction is executed again, compare it to the stored value.

The work of [56] proposes *Selective replication*. Their *selective* replication scheme is guided by the vulnerability of the instructions to protect the back-end. They opt for an inexpensive way of estimating the AVF that allows re-execution as soon as possible. To selectively reissue and re-execute those instructions that are above the selected vulnerability threshold in order to achieve maximum coverage by replicating a minimum number of instructions. Instructions that are placed in the IQ are also inserted into the Selective Queue (SQ). They use the time that an instruction spends in the IQ as an indicator of the AVF. Whenever there is an empty port for execution, an instruction in the SQ (whose counterpart in the IQ has already been issued) is issued and executed. Once instructions finish their execution, they keep the result in the widened ROB. When the replica execution finishes, it compares its result against the one stored for validation purposes.

A dependence based checking scheme was proposed in [66] and extended in [111]. They selectively try to reduce the number of instructions required to be compared for detecting errors. The proposal is based on the intuition that as instruction execute, the fault propagates through instructions via control or data flow creating a chain. The proposed scheme builds short chains of instructions which are required to be checked for errors.

Redundant Threads in Multicore System:

There have been attempts to implement the RMT on a chip multiprocessor. The basic idea of implementing RMT in a CMP is to generate logically redundant threads similar to SRT scheme [65]. The difference however comes from the fact

that the leading and the trailing threads execute on different cores. The redundant threads can run on different cores within a multicore processor or on different cores that are on different chips. The reason for using multiple cores, rather than a single SMT core, is to avoid having the threads compete for resources on the SMT core.

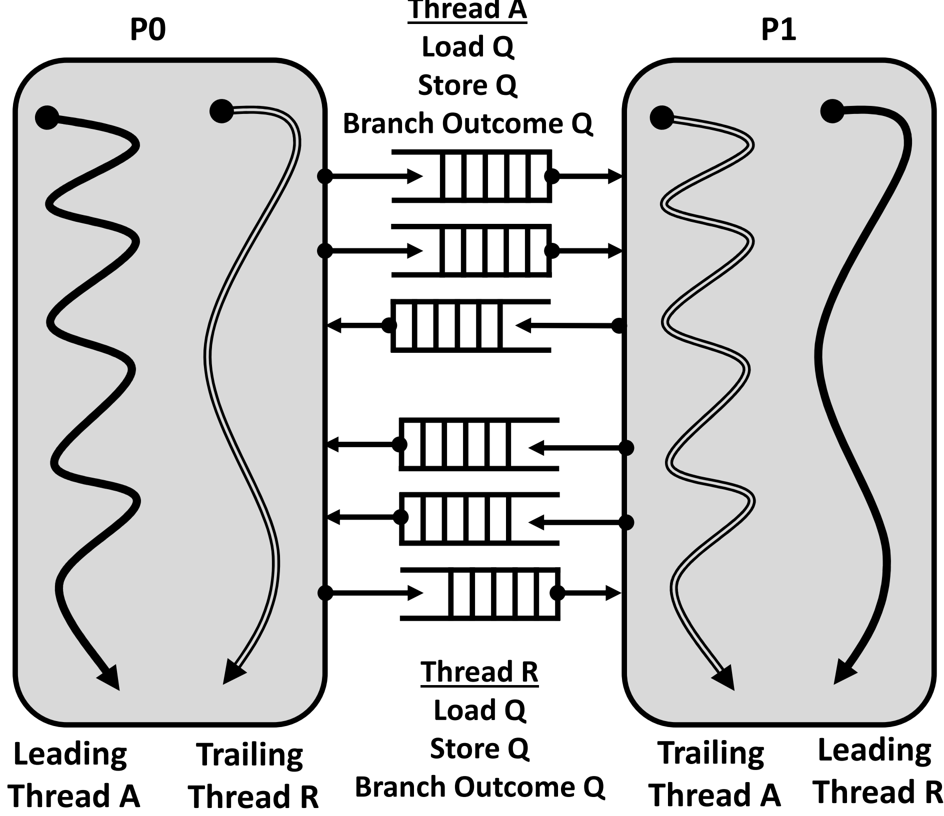

FIGURE 7.10: Functional implementation of RMT scheme on a processor with two cores (P0 and P1). The cross coupled cores with a few dedicated hardware queues can work in unison for error detection.

The proposal [57] performed a detailed simulation study of redundant multithreading. We show this implementation in Figure 7.10. Trailing thread's load value queue and branch outcomes now receive inputs from the leading threads executing on another core [301]. The same holds true for store instructions. It may also possible that the cores executing the two threads are very far from each other increasing the latency to forward data back and forth. However, the advantage is that the queues implemented to store the values of load, stores and branch outcomes decouple the execution of the redundant threads and now they are not on the critical path. This design point differs from lockstepped redundant cores in that the redundant threads are not restricted to operating in lockstep. They

show that this design point outperforms lockstepped redundant cores, by avoiding certain performance penalties inherent in lockstepping.

The DCC technique proposed in [281] uses redundant threads on multiple cores, but it removes the need for dedicated hardware queues for the leading thread to communicate its results to the trailing thread. DCC uses the existing interconnection network to carry this traffic.

While implementing RMT on multicore the biggest challenge is in handling the interaction between the threads and the memory system. The threads perform loads and stores, and these loads and stores must be the same for the threads in normal conditions. If the threads share the same address space then a load instruction in the leading thread may return a different value than the same load instruction in the trailing thread. For instance, if both threads load from address X. If the leading thread loads X before the trailing thread loads X it may possible that the leading thread also try to modify the content following a store to address X causing an invalidation. In this event the trailing thread may read a different value from X. A solution was proposed in [351], which is to let the trailing thread perform reads and detect those violations when the trailing thread's load reads different value from that of the leading thread and recover to a checkpoint from which forward progress is guaranteed.

7.2.3.2 Error Detection via Detecting Anomalies

Error detection via data and control value anomalies have been discussed in Section 7.2.1.3. Restore [36] architecture detects transient errors by detecting a higher level microarchitectural anomalies.

Errors are detected through temporal redundancy on demand. The symptom detectors trigger in situations that are likely to occur in the presence of an error. These behaviors include exceptions, page faults, and branch mispredictions that occur despite the branch confidence predictor having high confidence in the predictions. Their intuition is that these anomalous behavior are possible in an error-free execution but they are rare enough to be suspicious. If ReStore observes any of these behaviors, it recovers to a pre-error checkpoint and replays execution. If the anomalous behavior does not recur during replay, then it was most likely due to a

transient error. If it does recur, then it was either a legal but rare behavior or it is due to a permanent fault.

7.2.3.3 Using shifting operations

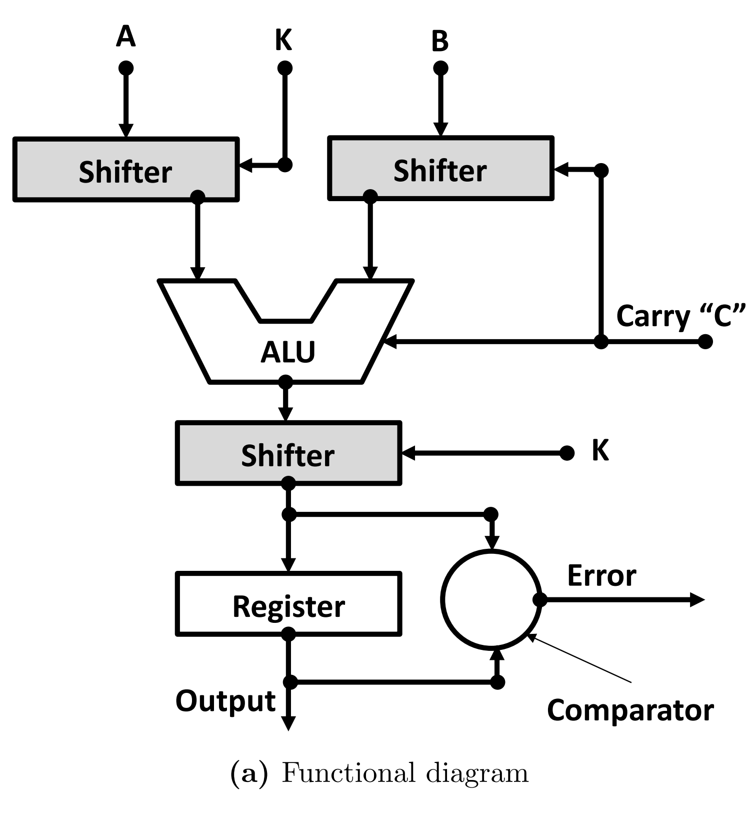

(a) Functional diagram

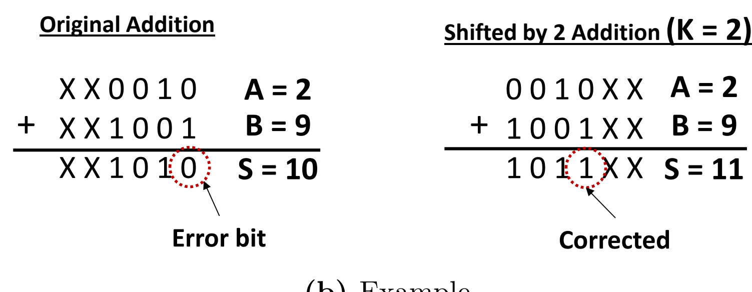

(b) Example

FIGURE 7.11: Using temporal redundancy for error detection via re-execution with shifted operands

Another approach to functional unit error detection is a variant of temporal redundancy that can detect errors due to permanent faults. A permanently faulty functional unit that is protected with pure temporal redundancy computes the same incorrect answer every time it operates on the same operands; the redundant computations are equal and thus the errors are undetected. Re-execution

with shifted operands (RESO) [352] overcomes this limitation by shifting the input operands before the redundant computation. RESO can detect errors in both the arithmetic and logic operations. RESO uses the principle of time redundancy in detecting the errors and achieves its error detection capability through the use of the already existing replicated hardware in the form of identical bit slices.

The example in Figure 7.11(a) illustrates how RESO detects an error due to a permanent fault in an adder. During the first step, three shifters don't shift the data, therefore the input and output of shifter is same. During the second step, the first two left-shifter shift input data by K bits and the right-shifter shifts input data by K bits. Note that a RESO scheme that shifts by K bits requires an adder that is K-bits wider than normal. Figure 7.11(b) shows the error detection by an example of addition. By comparing the 0th bit of the output of the original addition with the second output bit of the shifted-left-by-K (K=2) addition, RESO detects an error in the ALU.

7.3 Error Recovery

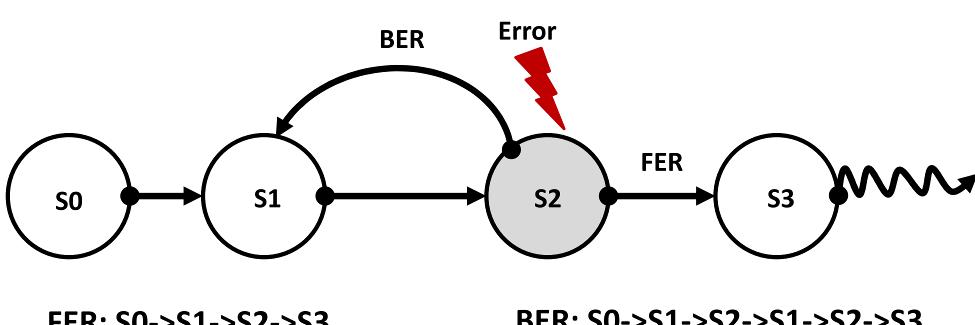

FIGURE 7.12: Classification of error recovery schemes

Error recovery schemes are classified based on the state where the system is taken when the error recovery mechanism is triggered. As shown in the Figure 7.12, the system has two options upon encountering the error in state `S2`: (i) it can go to state `S3` or (ii) fall back to state `S1`. In this section we will discuss two fundamental methods to handle the error recovery: (i) Forward error recovery and (ii) Backward error recovery.

7.3.1 Forward Error Recovery

Forward error recovery (FER) techniques can correct the errors on the fly. In other words the system is allowed to make forward progress under the event of an error. According to Figure 7.12 in FER the system goes to state `S3` from `S2`. FER systems are required to maintain redundancy that allows the system to reconstruct the most recent error free state. FER can be implemented by incorporating physical, temporal or information redundancy in the system. Error correcting codes can also provide forward error correction by incorporating information redundancy as explained in the Section 4.6.2.1 in Chapter 4. The most common example of forward error recovery technique is to employ modular redundancy (i.e., a TMR). Implementing FER via modular redundancy in full computing systems (i.e., replicating all the memory, registers, ALUs etc.) can be very hardware intensive and can cause huge power overhead.

7.3.1.1 Triple Modular Redundancy (TMR)

We have seen the use of DMR system for error detection in Section 5.6.1.1 in Chapter 5. It detects the error by comparing the outcomes of two replicas. Adding one more replica of the modules gives the TMR, that is *triple modular redundancy* system [353] as shown in Figure 7.13. The TMR system consists of three identical replicas of the execution system and the state and a comparator. The fault detection can be similar to the lockstepping (i.e., cycle by cycle comparison) or similar to the RMT techniques (i.e., comparing before the output goes out of the sphere of replication). So long as a majority (2 or 3) of the modules produce correct results, the system will be functional. Usually, after detecting and identifying the erroneous module the TMR system isolates the faulty module and keeps running in a degraded DMR system. To bring back the faulty module the DMR system copies the new system state from the error free modules to the faulty module and resumes the execution. The advantage of TMR is that it can provide error correction. It can also help to isolate the erroneous module and assist in system diagnosis. TMR can significantly improve the system downtime and can eliminate DUE without requiring to roll-back.

The first use of TMR in a computer was the Czechoslovak computer SAPO, in the 1950s [354]. Today triple redundancy systems are used in several commercial

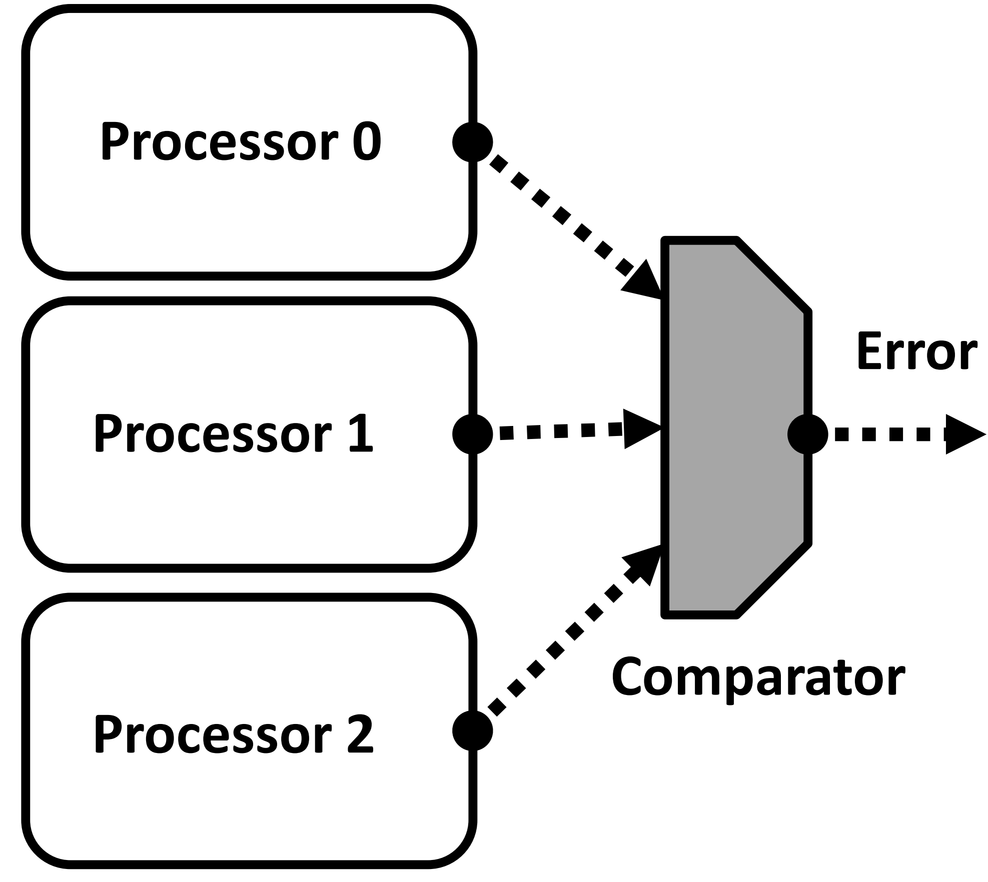

FIGURE 7.13: Triple modular redundancy

processors (i.e., HP NonStop architecture [113]) and "Pair & spare" systems [114]. Many variations of the traditional TMR have been proposed and implemented. The Boeing 777 [355] uses heterogeneous *triple-triple* modular redundancy [76].

7.3.2 Backward Error Recovery

Unlike forward error recovery schemes, backward error recovery (BER) restores the system to the last known error free state and resumes the execution from that state. As shown in Figure 7.12 the system state is traced back to `S1` once the error has been detected in `S2`. To be able to trace back the system to `S1` the exact system state must be saved in a checkpoint. Moreover, the backward error recovery mechanisms should also make sure that any output which the system cannot recover from is error free before exiting the recovery boundary. Thus, errors must be contained within the sphere of recoverability so that the error

does not propagate to a component that cannot be recovered. If an error escapes the sphere of recoverability, then the error is unrecoverable and the system fails. For instance a backward error recovery scheme that does not save the I/O state cannot recover from any erroneous outputs that has propagated and modified the I/O state. Similarly, a backward error recovery mechanism should make sure that once the system reverts back to the checkpoint all the inputs including the ones that have arrived from outside of the recovery boundary are replayed.

Basically a checkpoint can comprise any or all of the following: (i) architecture register files, (ii) caches and memory and (iii) I/O state of the processor. What comprises the checkpoint directly depends on the fault detection mechanism and the detection latency. There are several options for choosing the sphere of recoverability [356] and the options are discussed at length in Chapter 5. If checkpointing is implemented just on the core, then errors cannot be allowed to propagate to the caches or memory or beyond. If checkpointing includes the memory hierarchy, then errors can be allowed to propagate into the memory system but not to I/O devices. A backward error recovery scheme recover the system to a precise, consistent and error free state from which it can resume execution. For a processor to resume execution, it requires all of the architectural state, including the program counter, architectural registers, status registers, and the memory state.

Checkpoints can be taken at regular periodic intervals or in response to certain events. Taking checkpoints more frequently is likely to increase the performance penalty of checkpointing, but it reduces the amount of error-free work that must be replayed after a recovery. Logging, like checkpointing, is useful in contexts other than architectural BER. Many programs, such as word processors and spreadsheets, log changes to data structures so that they can provide recovery. Because checkpointing and logging have different costs for different types of state, many BER systems use a hybrid of both [107].

7.3.2.1 Checkpointing Techniques for Recovery

Now, we will discuss the most relevant checkpoint based hardware error recovery techniques in which the system maintains snapshots of the architectural state of the system to which it can revert back to in the event of an error.

1. **Error recovery before register commit:** Backward error recovery within core has been adapted in many commercial cores as a mainstream solution for error recovery [58, 62, 229]. Checkpoint/recovery hardware is used for recovering from the effects of misprediction instead of being used for error recovery. The proposal modifies the speculative recovery mechanism to meet two important criteria: (i) guaranteeing creation of error free checkpoints and (ii) by performing the error detection before the instruction is committed [66, 357]. These recovery technique can be used only when the error detection happens before the register values are committed to the architecture register file. For recovery the processor just have to flush the speculative register values as the architecture register files holds the most recent and error free state.

   Now, we will discuss one such implementation *simultaneously and redundantly threaded processor with recovery* (SRTR) which was proposed in [66]. SRTR is an enhancement of redundant multithreading on an SMT core which provides in core error recovery. To avoid stalling leading instructions at commit while waiting for their trailing counterparts, SRTR exploits the time between the completion and commit of leading instructions. SRTR compares the leading and trailing values as soon as the trailing instruction completes, typically before the leading instruction reaches the commit point. SRTR relies on the register value queue (RVQ) to hold register values for checking. Upon a mismatch all the instructions are squashed. The leading thread waits until the trailing thread also encounters the offending instruction and then resumes the normal execution.

2. **Error recovery after register commit:** These techniques allow the register values to be committed to the architecture register file but not to caches or memory and hence they must keep checkpoints of the consistent and error free architecture state. Checkpoints can be taken periodically or whenever new values are generated or updated (i.e., incremental checkpointing).

   Incremental checkpointing used history buffer to keep a record of all the register values whenever they are generated [308, 358]. A history buffer consists of several entries containing information about program counter, old destination register value and the mapped physical register for every retired instruction. When an instruction retires but it is still waiting in the ROB for its turn to commit an entry is allocated in the history buffer.

Once the retired instruction is verified to be error free the corresponding entry from the history buffer is deallocated. Whenever a fault is detected all the speculative instructions which are not retired are flushed. And the correct architecture state is reconstructed from the existing register file and the history buffer. The architecture register file holds the state up to the last retired instruction prior to the erroneous instruction. The values must be obtained via a roll back to the state prior to the erroneous instruction which is done by finding the latest update from history buffer to the architecture register file. The system has to iterate through all the entries in the history buffer. Once found the architecture state can be restored and the history buffer is flushed.

Periodic checkpointing takes the snapshot of the processor state periodically. Unlike incremental checkpointing periodic checkpoints can accommodate longer checkpoint periods and reduces the constraint of detecting errors on every instruction for generation of clear checkpoint. However, the amount of state has to be copied to create the checkpoint [102, 103, 107, 359–361]. Fingerprinting as proposed in [305] and discussed in Section **??** of this chapter, contains the summary of the outputs of any new register values, memory values or addresses generated by executing instructions.

3. **Cache assisted Checkpointing:** More recently checkpointing schemes have been used for enabling error recovery using caches and memory. Including caches in the checkpoint can support longer checkpointing periods.

   One of the landmark papers on backward error recovery Cache-Aided Rollback Error Recovery (CARER) explores how to use the cache to hold checkpoint [228]. CARER permits committed stores to write into the cache, but it does not allow them to be written back to memory until they have been validated as being error-free. Thus, the memory and the clean lines in the cache represent the checkpoint. Dirty lines in the cache represent state that could be recovered if an error is detected. During a recovery, all dirty lines in the cache are invalidated. If the address of one of these lines is accessed after recovery, it will miss in the cache and obtain the checkpoint value for that data from memory. Any cache or memory state, including TLB entries, that is not part of the recovery point, should be flushed. Otherwise, we may use incorrect values. CARER also observes that the memory state does not

need to be restored to the same place where it had been. For example, assume that data block X had been in the data cache with the value 21 when the checkpoint was taken. The recovery process could restore block X to the value 21 in either the data cache or the memory.

While extending CARER architecture to provide backward error recovery in a multiprocessor requires a little modification and apart from the state of the cores, caches, and memories, we need to maintain the history of shared data. Consider the following example for a two-core processor that uses its caches to save part of its checkpoint state (like CARER [228]). When the checkpoint is saved, core 1 has block A in a modified coherence state, and core 2's cached copy of block A is invalid. Upon recovery, if the shared history is not maintained then both core 1 and core 2 may end up having block A in the modified state and thus both might believe they can write to block A. Cherry(-MP) [292] & others [112, 234, 281, 286, 295, 296] are popular techniques that saves the checkpoints within the cache hierarchy.

4. **Checkpointing memory and I/O:** Now we will discuss the checkpointing schemes that allow the processor to commit values in the main memory and hence these schemes along with the architecture state and caches take snapshot of the entire main memory for successful error recovery. By including the main memory in the checkpoint these checkpointing schemes can allow very long checkpointing periods. The main challenge in generating system wide checkpoint is to maintain a consistent recovery point such that in a multiprocessor system upon encountering an error all the computing nodes can be restored to a consistent error free state. SafetyNet [107] and ReVive [102] famous examples that maintain system wide checkpoints and can recover from soft errors, hard errors and system errors.

   ReVive [102] creates a system wide checkpoint by halting all the nodes and coordinating the individual checkpoint generation. It relies on distributed parity to detect faults in memory and also to guarantee the generation of error free checkpoints. ReVive incorporates a log based scheme to keep track of the order of memory writes once the checkpoint is created. It augments all the memory blocks with an additional *log bit* and this bit is set on the first write after the creation of the checkpoint. This *log bit* helps it identify modifies writes after the checkpoint which must be undone upon recovery. ReVive implements a state machine to maintain the global coordination

while creating checkpoints. The process involves flushing and writing back all the modified data in the caches to main memory.

SafetyNet [107] generates local checkpoints such that it can create a global consistent state. This global consistent state can act as the point of recovery whenever a recovery is required. A combination of local checkpoints together constitute a global consistent state. To maintain the global consistent state SafetyNet relies on the fact that coherence transactions are atomic once they are completed. In other words, the global consistent state is not created until all the outstanding transactions are completed and are error free.

Including I/O devices in the checkpoint is non trivial and can be very complex. Moreover, it is difficult to recover from some I/O operations. For instance an erroneous print command to the printer cannot be undone. A known approach to handle I/O in checkpointing systems is to delay the commit of output until the next checkpoint (output commit problem). To accomplish this, adding a "virtual" device driver layer between the kernel and the device drivers has been proposed [106, 362]. ReViveIO [103] discusses about recovering disc operations. Disk output requests are redirected to the "virtual" device driver rather than the device driver. The "virtual" device driver blocks any output-requesting process until the next checkpoint, after which the output is performed. The "virtual" device driver can be considered an extremely thin virtual machine layer for I/O checkpointing.

7.3.3 Other Recovery Schemes

Referring to Figure 7.12 once the error is detected in `S2` it is always possible to revert back to the very initial `S0` state. Reverting back to `S0` requires the system to be rebooted. For transient errors rebooting can be economical if the latency of re-execution and the amount of work lost is non-critical. Rebooting is not a valid recovery option for hard errors because the system will most likely encounter the error again. Other recovery schemes include throwing MCA which throws an exception upon encountering an error and invokes a specific system handler for recovery [363]. Another technique is popularized as *Nuke and Restart* that involves flushing the pipeline to clear the processor state (i.e., Nuke) and restarting the execution [312].

7.4 Error Detection and Recovery using Software

Software based techniques to improve the system reliability are gaining momentum due to the higher level of customization and the possibility to deploy it even in the already established systems. The primary appeal of software redundancy is that it has no hardware costs and requires no invasive design modifications. It also provides good coverage of possible errors, although it has some small coverage holes that are fundamental to all-software schemes. However, the costs of software redundancy are significant. They degrade performance more than the hardware techniques due to the overheads incur in the implementation. The dynamic energy overhead is more than 100%.

Software based checkers for error detection have been studied in [324]. Assertion based and signature based checkers have been studied and thoroughly. Assertion based checkers work by asserting or defining rules such as memory bound violation or coherence violations that can happen due to an error. These assertions can be inserted by the programmers or by a compiler or through binary translation. Signature based checkers are popular to detect faults in control flow. One such implementation is based on *Signatured Instruction Streams* (SIS). SIS performs error detection by comparing signatures that are generated statically at compile time with the ones generated dynamically at run-time [329].

There have been extensive efforts to implement RMT system entirely in software. Unlike hardware RMT the software RMT instantiation can implement redundant version of threads within the same hardware context. Software RMT techniques can provide higher error coverage than software checkers but incur huge performance degradation compared to their hardware implementations. *Error detection by duplicated instructions* (EDDI) [282], *Software implemented fault tolerance* (SWIFT) [283] and Spot [364] are popular software RMT implementations.

EDDI takes advantage of compiler to insert redundant instructions in a single thread to create two redundant execution streams. Both the streams share the existing architecture register file and memory address space. Compiler also inserts specific instructions to compare the outcomes of the redundant streams for fault detection. EDDI causes performance degradation upto 111%.

SWIFT combines the approach of achieving fault tolerance by replicating instructions at compiler level and implementing signature based physical error detectors [283]. SWIFT is very similar to EDDI in its implementation. SWIFT duplicates the instruction streams and compare the inputs to both the *load/store* instructions to make sure they receive the correct inputs. However, unlike EDDI, SWIFT does not protect the *store* instructions. For instance, *store* instruction can be corrupted in the store buffer even after receiving correct inputs. The SWIFT assumes that the memory is protected via ECC. Note that by reducing the number of duplications and comparisons SWIFT can optimize the performance over EDDI.

Unlike EDDI or SWIFT Spot does not require the source code since it operates directly on binary [364]. Spot can dynamically trade off the reliability for performance.

Compiler assisted fault tolerance (CRAFT) [365] improves the fault coverage and reduces the overhead by undertaking hybrid approach instead of pure software RMT like SWIFT. Unlike SWIFT, CRAFT introduces redundant *store* instructions. Moreover, CRAFT implements hardware buffers for checking *load/store* instructions for errors and can provide higher coverage by protecting the entire data path.

SWAT [287] observes the software anomalies induced by hardware errors to achieve low-cost error detection for cores. SWAT scans for the suspicious software anomalies such as fatal exceptions, program crashes, an unusually high amount of operating system activity, and system hangs. Such behavior can occur due to a hardware error or a software bug. SWAT focuses on the hardware errors and with the help of embedded hardware detectors all of these anomalous behaviors are easily detectable. SWAT benefits from low additional hardware and software costs, little performance overhead and no false positives. The limitation of SWAT is that not all hardware errors manifest themselves in software anomalies. For instance a hardware error in computing floating point values may not necessarily cause a software error.

Shoestring [35] uses of minimally invasive software solution to provide just enough resilience to transient faults. The key insight that Shoestring exploits is that the majority of transient faults do not ultimately propagate to user-visible corruptions

at the application level or are easily covered by light-weight symptom-based detection. Shoestring relies on symptom based error detection to supply the bulk of the fault coverage at little to no cost. Shoestring characterizes all instructions in the program and identifies symptom generating instructions such as: (i) ISA defined exceptions: these are exceptions defined by the ISA and must already be detected by any hardware implementing the ISA (e.g., page fault or overflow), (ii) Fatal exceptions: these are the subset of the ISA defined exceptions that never occur under normal user program execution (e.g., segment fault or illegal opcode) and (iii) Anomalous behavior: these events occur during normal program execution but can also be symptomatic of a fault (e.g., branch mispredict or cache miss) etc. To address the remaining faults, compiler analysis is utilized to identify hot regions of the application code that are susceptible to soft errors and causes the corruption. These hot portions of the code are then protected with instruction duplication. In essence, Shoestring intelligently selects between relying on symptoms and judiciously applying instruction duplication to optimize the coverage and performance trade-off. Shoestring transparently provides a low-cost, high-coverage solution for soft errors in processors targeted for the consumer electronics market. Shoestring provides limited opportunistic coverage.

EverRun [366] by Marathon technologies has given a full software based solution for fault tolerance, it uses redundant virtual machines like structure to implement fault detection in software. It also allows recovery in the case of one of the virtual machines crashes. It copies the entire state of one virtual machine to another and transparently restart the entire server.

SWIFT-R as proposed in [367] can also provide forward error recovery purely via implemented software RMT. SWIFT-R uses triple redundant instructions streams and a voter similar to hardware TMR. SWIFT-R also combines AN codes for error detection. Due to triplication of instructions SWIFT-R degrades the performance by $\geq$200%.

Major disadvantages of software based solutions are as following: (i) many faults are missed (i.e., transient errors) in scenarios that are worse than the real (i.e., overclocking the processor), (ii) detecting a high-level error like a program crash provides little diagnostic information which is very important for handling hard errors, (iii) relying only on high-level error detection has a longer and unbounded error detection latency. This implies that a bit flip may not result in a program crash for a very long time. To recover from a crash requires the processor to

recover to a state from before the error's occurrence. Longer detection latencies thus require the processor to keep saved recovery points from further in the past. Unbounded detection latencies imply that certain detected errors will be unrecoverable because of unavailability of a recovery point of the state prior to the error. Longer detection latency also implies that the effects of an error may propagate farther, (iv) Software based error detection complicates the recovery process and to recover from the errors these techniques requires extensive amount of checkpointing or logging. Recovering the state of a small component is often easier than recovering a larger component or an entire chip-multiprocessor system.

Chapter 8

Conclusions

The work of this thesis introduces, develops, and analyzes a novel method to detect and recover from soft errors and improve the reliability of a state of the art microprocessor. The goal of the thesis was to provide a soft error mitigation mechanism that is low cost, simple to implement and scalable to handle the increasing soft error rate. Instead of relying on some kind of redundancy, the proposed method detects the actual particle strike rather than its consequence.

Many solutions exists to provide error detection and recovery from soft errors in logic and memory components. However, providing robustness minimizing area, power and performance is extremely challenging. As Chip Multi-Processors (CMPs) become ubiquitous, it is imperative to have a robust error handling mechanism that is low cost, less complex, scalable and capable of analyzing the complex behaviors and interactions that result. Existing solutions do not scale to cope up with the increasing soft error rate and providing coverage to all the unprotected components on a processor core increases the complexity of soft error solutions. Moreover, the cost of protection is extremely high and the existing solutions have hit the point of diminishing return.

8.1 Summary of Research

In this section we will provide a brief summary of the research carried out in this dissertation:

8.1.1 Detecting Particle Strikes for Soft Error Detection

The major novel contribution of this dissertation is using the acoustic wave detectors for detecting soft errors via detecting particle strikes and use their information to locate particle strikes within processor and to protect and recover.

The impact of a high-energy particle with a silicon nucleus can be detected by detecting the sound, light or heat generated upon impact due to various quantum physical phenomenons. By detecting particle strikes we are detecting the cause of soft errors and not wait for the symptom (i.e., an actual error) like other redundancy based solutions. We detect only those particle strikes that may cause soft errors.

We observed how acoustic wave detectors are used for soft error detection. We also studied several particles strike detectors that detect voltage/current glitches, metastability, sound or deposited charge to detect the soft errors. We compared all the detectors for various trade-offs such as area, power, performance overheads.

8.1.2 Unified Error Detection for Logic & Memory

The proposed architecture uses acoustic wave detectors to detect soft errors. Acoustic wave detectors can detect the soft errors by detecting the sound the energetic particle makes upon impact on silicon. And hence, the proposed error detection architecture is not dependent on the functional or behavioral properties of the underlying component that is being protected. This eliminates the necessity of having different schemes for detecting errors in memory and logic components in a processor and hence, the proposed architecture acts as a *unified* error detection mechanism protecting the entire processor.

8.1.3 Precisely Locating the Errors

Using the acoustic wave detectors, we can only detect the particle strikes and hence avoid possible data corruption. To provide successful error correction or recovery, the system must know the precise location of the error. Once the error has been detected, a hardware or software mechanism would trigger an appropriate recovery action for error correction.

We presented an architecture to precisely locate the particle strikes using acoustic wave detectors. We demonstrated a solution based on measuring the TDOA across different detectors, generating a set of hyperbolic equations, and solving them to obtain the location of particle strike. We presented a firmware/hardware approach in which the hardware takes responsibility for TDOA measurements and generating hyperbolic equations while the firmware is responsible for solving the equations using several algorithms. We implemented algorithms to solve deterministic and non-deterministic system of equations and discuss their computational complexity, runtime, their ability to provide exact solutions and the risk of not reaching a valid solution. We also discussed in detail how design parameters like number of detectors and their location impact complexity, runtime and especially, the accuracy. Lastly, we presented a detailed case study which helped us understanding various trade-offs between design parameters (e.g., sampling frequency, location of detectors etc.) and the algorithmic properties (i.e., runtime, accuracy, complexity etc.). We concluded that for the maximum accuracy and coverage non-deterministic iterative algorithm is the best option.

8.1.4 Reducing Reliability Cost for Caches and Memory

We proposed a new solution that combines acoustic wave detectors with error correcting codes in such a way that we decrease the total cost of the protection mechanism while providing the same reliability levels. Our analysis concluded that SEC-DED combined with acoustic wave detectors can provide the same degree of protection as stand-alone DEC-TED, at a significantly low overheads. We discussed the architectural modifications for integrating error codes with acoustic wave detectors.

We specifically focused on caches closer to the core (i.e., L1 cache) that have only error detection capability. Because of higher costs of error correction designers cannot afford to provide error correction in L1 cache. Lack of error correction makes them the highest contributors to the over all DUE FIT budget. We showed that by accommodating acoustic wave detectors with bit interleaved parity codes, we can correct 98% of single bit errors in L1 cache. We then presented a mechanism to detect and correct multi-bit errors in L1 caches. We showed how adapting acoustic wave detectors and parity protected physically interleaved bits can provide error correction against 2-bit and 3-bit MBUs at very low cost.

8.1.5 Protecting Entire Processor

We proposed an architectural framework to completely eliminate the SDC and DUE related with soft errors in single and multicore processors. The architecture uses acoustic wave detectors for error detection. We tailored a novel error recovery mechanism that is less intrusive on design and highly scalable. The error recovery scheme relies on an extremely light-weight checkpointing mechanism. The proposed architecture stores checkpoints in caches. We discussed different design parameters and evaluated cost of checkpointing & recovery. We also observed the impact of error detection latency on the cost and complexity of the required amount of checkpointing. We discussed in detail different trade-offs related with complexity of detectors deployment, detection latency and complexity of recovery mechanism. The proposed error detection and recovery mechanism can eliminate SDC and DUE related with soft errors at a negligible 0.8% of performance penalty.

8.1.6 One Solution for All Computing Segments

In general, most of the reliability techniques that are applicable to high performance computing are render useless for protecting embedded processors due to the area, power and performance overheads and complexity. The design constraints for the embedded systems are different from those in the high-performance domain and hence robustness techniques specific to the embedded processors are required.

As a part of this dissertation we presented an architecture to provide reliability in high-performance multicore processors and we showed that the same architecture can be configured to provide reliability in embedded processors with little design modification. In this thesis we presented an architecture that uses acoustic wave detectors to detect and contains the error with minimal hardware overhead incurring negligible area, power and performance cost. The presented architecture provides the flexibility to configure various design parameters such as error detection latency and error containment boundary which significantly affect the cost of recovery and performance overhead. This flexibility is very important for providing robustness in an embedded processor.

We also showed that the proposed architecture can optimize the trade-off between degree of reliability and performance for non-mission critical embedded applications. We explained how we can quantify the vulnerability of processor structures

and explored the possibility to reduce the vulnerability of a structure in an architecture by protecting it using acoustic wave detectors.

8.2 Discussions

In this section, we discuss the limitation of the work as presented so far as well as the potential future applications and uses that are enabled by the use of acoustic wave detectors.

8.2.1 Future Work

The main goals of this dissertation work were as follow: (i) we wanted to analyze the possibility of detecting soft errors via particle strike detection using acoustic wave detectors, (ii) once the error detection mechanism is in place explore the mechanism to precisely locate the particle strikes and hence soft errors, (iii) once we have identified the location of the error build architecture to protect the caches and the explore the feasibility of combining acoustic wave detectors with existing solutions for protecting caches and memory and (iv) build an extremely simple, scalable and cost effective architecture that can detect, contain and recover from soft errors while protecting entire chip-multiprocessor system.

In this work, various properties such as error detection latency, sensitivity to detect only particle strikes etc. of acoustic wave detectors are entirely based on simulations. Perhaps an implementation of an actual micro-electromechanical acoustic wave detector prototype would provide the first hand insight towards these properties. By fabricating such device the experimental results would benefit from a more summarized view of the questions such as if the acoustic detector is able to determine whether the particle strikes has really caused an upset, or if it can only determine the strike? Moreover, an experimental prototype can also help to determine if it is feasible to fabricate and calibrate the acoustic wave detectors for detecting only potent particle strikes and accurately characterizing and eventually eliminating false positives.

Another aspect of the future work is to focus on the optimization of the firmware to precisely locate the particle strikes. It may be possible to always pinpoint the

exact location of error. By identifying the exact erroneous bit can simplify the error correction mechanism.

The applicability of this architecture can be shown by extending it to protect off-chip components such as DRAM, memory controller, buses, interconnects and switching fabric etc. It will be interesting to explore the architecture based on acoustic wave detectors to provide reliability to these off-chip components and studying its impact on the area, power and performance overheads while comparing with the improved system reliability and availability.

Bibliography

[1] AnandTech Ian Cutress. Intel readying 15-core xeon e7 v2. Online, February 2014. http://www.anandtech.com/show/7753/intel-readying-15core-xeon-e7-v2.

[2] Gordon E Moore et al. Cramming more components onto integrated circuits. *Proceedings of the IEEE*, 86(1):82–85, 1998.

[3] Wm A Wulf and Sally A McKee. Hitting the memory wall: implications of the obvious. *ACM SIGARCH computer architecture news*, 23(1):20–24, 1995.

[4] Shlomit S Pinter and Adi Yoaz. Tango: a hardware-based data prefetching technique for superscalar processors. In *Proceedings of the 29th annual ACM/IEEE international symposium on Microarchitecture*, pages 214–225. IEEE Computer Society, 1996.

[5] Glenn Reinman, Brad Calder, and Todd Austin. Fetch directed instruction prefetching. In *Microarchitecture, 1999. MICRO-32. Proceedings. 32nd Annual International Symposium on*, pages 16–27. IEEE, 1999.

[6] Dean M Tullsen, Susan J Eggers, and Henry M Levy. Simultaneous multithreading: Maximizing on-chip parallelism. In *ACM SIGARCH Computer Architecture News*, volume 23, pages 392–403. ACM, 1995.

[7] John L. Hennessy and David A. Patterson. *Computer Architecture: A Quantitative Approach, 4th Edition.* Elsevier Science Publishers B. V., 2007.

[8] Robert H Dennard, Fritz H Gaensslen, V Leo Rideout, Ernest Bassous, and Andre R LeBlanc. Design of ion-implanted mosfet's with very small physical dimensions. *Solid-State Circuits, IEEE Journal of*, 9(5):256–268, 1974.

[9] Kate Greene. A new and improved moore's law. MIT Technology Review, September 2011. http://www.technologyreview.com/news/425398/a-new-and-improved-moores-law/.

[10] Mark Bohr. A 30 year retrospective on dennard's mosfet scaling paper. *Solid-State Circuits Society Newsletter, IEEE*, 12(1):11–13, 2007.

[11] Stefanos Kaxiras and Margaret Martonosi. Computer architecture techniques for power-efficiency. *Synthesis Lectures on Computer Architecture*, 3 (1):1–207, 2008.

[12] Semiconductor Industry Association et al. International technology roadmap for semiconductors (itrs), 2003 edition. *Hsinchu, Taiwan, Dec*, 2003.

[13] Hadi Esmaeilzadeh, Emily Blem, Renee St Amant, Karthikeyan Sankaralingam, and Doug Burger. Dark silicon and the end of multicore scaling. In *Computer Architecture (ISCA), 2011 38th Annual International Symposium on*, pages 365–376. IEEE, 2011.

[14] Nikos Hardavellas, Michael Ferdman, Babak Falsafi, and Anastasia Ailamaki. Toward dark silicon in servers. *IEEE Micro*, 31(4):6–15, 2011.

[15] Sani R Nassif, Nikil Mehta, and Yu Cao. A resilience roadmap. In *Proceedings of the Conference on Design, Automation and Test in Europe*, pages 1011–1016. European Design and Automation Association, 2010.

[16] T. Karnik, J. Tschanz, N. Borkar, J. Howard, S. Vangal, V. De, and S. Borkar. Resiliency for many-core system on a chip. In *Design Automation Conference (ASP-DAC), 2014 19th Asia and South Pacific*, pages 388–389, Jan 2014.

[17] Robert Baumann. Soft errors in advanced computer systems. In *Proceedings of IEEE Design and Test of Computers*, pages 258–266, Los Alamitos, CA, USA, 2005. IEEE Computer Society.

[18] Douglas Bossen. Cmos soft errors and server design. *IEEE 2002 Reliability Physics Tutorial Notes, Reliability Fundamentals*, 121:07–1, 2002.

[19] James F Ziegler, Huntington W Curtis, Hans P Muhlfeld, Charles J Montrose, and B Chin. Ibm experiments in soft fails in computer electronics (1978–1994). *IBM journal of research and development*, 40(1):3–18, 1996.

[20] R. Baumann. Soft errors in advanced semiconductor devices-part i: the three radiation sources. *IEEE Transactions on Device and Materials Reliability*, 1(1):17–22, 2001. ISSN 7045-483.

[21] JF Ziegler and WA Lanford. Effect of cosmic rays on computer memories. *Science*, 206(4420):776–788, 1979.

[22] JF Ziegler and WA Lanford. The effect of sea level cosmic rays on electronic devices. *Journal of applied physics*, 52(6):4305–4312, 1981.

[23] H. Quinn and P. Graham. Terrestrial-based radiation upsets: A cautionary tale. Technical Report LA-UR-08-1643, Los Alamos National Laboratory, 2008.

[24] Australian Transport Safty Bureau. In-flight upset-airbus a330-303 vh-qpa. online. http://www.atsb.gov.au/publications/investigation_reports/2008/aair/ao-2008-070.aspx.

[25] Eugene Normand. Single-event effects in avionics. *Nuclear Science, IEEE Transactions on*, 43(2):461–474, 1996.

[26] Bianca Schroeder, Eduardo Pinheiro, and Wolf-Dietrich Weber. Dram errors in the wild: a large-scale field study. In *ACM SIGMETRICS Performance Evaluation Review*, volume 37, pages 193–204. ACM, 2009.

[27] Actel. Understanding soft and firm errors in semiconductor devices. White paper, Actel. `http://www.microsemi.com`.

[28] James F Ziegler and Helmut Puchner. *SER–history, Trends and Challenges: A Guide for Designing with Memory ICs*. Cypress, 2004.

[29] Robert Baumann. The impact of technology scaling on soft error rate performance and limits to the efficacy of error correction. In *IEDm: international electron devices meeting*, pages 329–332, 2002.

[30] Tanay Karnik and Peter Hazucha. Characterization of soft errors caused by single event upsets in cmos processes. *Dependable and Secure Computing, IEEE Transactions on*, 1(2):128–143, 2004.

[31] Scott Hareland, Jose Maiz, Mohsen Alavi, Kaizad Mistry, Steve Walsta, and Changhong Dai. Impact of cmos process scaling and soi on the soft

error rates of logic processes. In *VLSI Technology, 2001. Digest of Technical Papers. 2001 Symposium on*, pages 73–74. IEEE, 2001.

[32] Anand Dixit and Alan Wood. The impact of new technology on soft error rates. In *Proceedings of the International Reliability Physics Symposium (IRPS)*, 2011.

[33] Shekhar Borkar. Designing reliable systems from unreliable components: the challenges of transistor variability and degradation. *Micro, IEEE*, 25(6): 10–16, 2005.

[34] Premkishore Shivakumar, Michael Kistler, Stephen W Keckler, Doug Burger, and Lorenzo Alvisi. Modeling the effect of technology trends on the soft error rate of combinational logic. In *Dependable Systems and Networks, 2002. DSN 2002. Proceedings. International Conference on*, pages 389–398. IEEE, 2002.

[35] Shuguang Feng, Shantanu Gupta, Amin Ansari, and Scott Mahlke. Shoestring: probabilistic soft error reliability on the cheap. In *ACM SIGARCH Computer Architecture News*, volume 38, pages 385–396. ACM, 2010.

[36] Nicholas J Wang and Sanjay J Patel. Restore: Symptom-based soft error detection in microprocessors. *IEEE Transactions on Dependable and Secure Computing,*, 3(3):188–201, 2006.

[37] Tanay Karnik, Bradley Bloechel, K Soumyanath, Vivek De, and Shekhar Borkar. Scaling trends of cosmic ray induced soft errors in static latches beyond 0.18 u. In *Symposium on VLSI circuits digest of technical papers*, pages 61–62, 2001.

[38] Subhashish Mitra, Norbert Seifert, and Pia Sanda. Soft errors: Trends, system effects, and protection techniques. IOLTS-Tutorial Slides, December 2007.

[39] Niranjan Soundararajan, Anand Sivasubramaniam, and Vijay Narayanan. Characterizing the soft error vulnerability of multicores running multi-threaded applications. In *ACM SIGMETRICS Performance Evaluation Review*, volume 38, pages 379–380. ACM, 2010.

[40] Cristian Constantinescu. Trends and challenges in vlsi circuit reliability. *IEEE micro*, 23(4):14–19, 2003.

[41] Hang T Nguyen, Yoad Yagil, Norbert Seifert, and Mike Reitsma. Chip-level soft error estimation method. *IEEE Transactions on Device and Materials Reliability*, 5(3):365–381, 2005.

[42] Ethan H Cannon, A KleinOsowski, Rouwaida Kanj, Daniel D Reinhardt, and Rajiv V Joshi. The impact of aging effects and manufacturing variation on sram soft-error rate. *Device and Materials Reliability, IEEE Transactions on*, 8(1):145–152, 2008.

[43] Richard W Hamming. Error detecting and error correcting codes. *Bell System technical journal*, 29(2):147–160, 1950.

[44] Mu-Yue Hsiao. A class of optimal minimum odd-weight-column sec-ded codes. *IBM Journal of Research and Development*, 14(4):395–401, 1970.

[45] Chin-Long Chen and MY Hsiao. Error-correcting codes for semiconductor memory applications: A state-of-the-art review. *IBM Journal of Research and Development*, 28(2):124–134, 1984.

[46] Timothy J Dell. A white paper on the benefits of chipkill-correct ecc for pc server main memory. *IBM Microelectronics Division*, pages 1–23, 1997.

[47] Weldon E J. Peterson W W. *Error-Correcting Codes*. MIT Press, 2003.

[48] C W Slayman. Cache and memory error detection, correction, and reduction techniques for terrestrial servers and workstations. *IEEE Transactions on Device and Materials Reliability*, 5(3):397–404, 2005.

[49] Jangwoo Kim, Nikos Hardavellas, Ken Mai, Babak Falsafi, and James Hoe. Multi-bit error tolerant caches using two-dimensional error coding. In *Proceedings of International Symposium on Microarchitecture (MICRO)*, pages 197–209. Ieee, 2007.

[50] Jiri Gaisler. A portable and fault-tolerant microprocessor based on the sparc v8 architecture. In *Proceedings of International Conference on Dependable Systems and Networks, 2002. DSN 2002.*, pages 409–415, 2002.

[51] Ken Yano, Takanori Hayashida, and Toshinori Sato. Analysis of ser improvement by radiation hardened latches. In *IEEE 18th Pacific Rim International Symposium on Dependable Computing (PRDC), 2012*, pages 89–95, 2012.

[52] Liang Wang, Yuhong Li, Suge Yue, Yuanfu Zhao, Long Fan, and Liquan Liu. Single event effects on hard-by-design latches. In *Radiation and Its Effects on Components and Systems, 2007. RADECS 2007. 9th European Conference on*, pages 1–4, 2007.

[53] Sheng Lin, Yong-Bin Kim, and Fabrizio Lombardi. Design and performance evaluation of radiation hardened latches for nanoscale cmos. *Very Large Scale Integration (VLSI) Systems, IEEE Transactions on*, 19(7):1315–1319, 2011.

[54] Timothy J Slegel, Robert M Averill III, Mark A Check, Bruce C Giamei, Barry W Krumm, Christopher A Krygowski, Wen H Li, John S Liptay, John D MacDougall, Thomas J McPherson, et al. Ibm's s/390 g5 microprocessor design. *IEEE Micro*, 19(2):12–23, 1999.

[55] Subhasish Mitra, Norbert Seifert, Ming Zhang, Quan Shi, and Kee Sup Kim. Robust system design with built-in soft-error resilience. *Computer*, 38(2): 43–52, 2005.

[56] Xavier Vera, Jaume Abella, Javier Carretero, and Antonio González. Selective replication: A lightweight technique for soft errors. *ACM Transactions on Computer Systems (TOCS)*, 27:8:1–8:30, January 2010.

[57] Shubhendu S Mukherjee, Michael Kontz, and Steven K Reinhardt. Detailed design and evaluation of redundant multithreading alternatives. In *Proceedings of International Symposium on Computer Architecture (ISCA)*, 2002.

[58] Lisa Spainhower and Thomas A Gregg. IBM S/390 parallel enterprise server G5 fault tolerance: a historical perspective. *IBM Journal of Research and Development*, 43(5/6):863–873, 1999.

[59] Patrick J Meaney, Scott B Swaney, Pia N Sanda, and Lisa Spainhower. Ibm z990 soft error detection and recovery. *Device and Materials Reliability, IEEE Transactions on*, 5(3):419–427, 2005.

[60] Blaine Stackhouse, Sal Bhimji, Chris Bostak, Dave Bradley, Brian Cherkauer, Jayen Desai, Erin Francom, Mike Gowan, Paul Gronowski, Dan

Krueger, et al. A 65 nm 2-billion transistor quad-core itanium processor. *Solid-State Circuits, IEEE Journal of*, 44(1):18–31, 2009.

[61] Reid Riedlinger, Ron Arnold, Larry Biro, Bill Bowhill, Jason Crop, Kevin Duda, Eric S Fetzer, Olivier Franza, Tom Grutkowski, Casey Little, et al. A 32 nm, 3.1 billion transistor, 12 wide issue itanium® processor for mission-critical servers. *Solid-State Circuits, IEEE Journal of*, 47(1):177–193, 2012.

[62] Myron L Fair, Christopher R Conklin, Scott B Swaney, Patrick J Meaney, William J Clarke, Luiz C Alves, Indravadan N Modi, Fritz Freier, Wolfgang Fischer, and Norman E Weber. Reliability, availability, and serviceability (ras) of the ibm eserver z990. *IBM Journal of Research and Development*, 48(3.4):519–534, 2004.

[63] Alan Wood, Robert Jardine, and Wendy Bartlett. Data integrity in hp nonstop servers. In *Workshop on SELSE*, 2006.

[64] Nhon Quach. High availability and reliability in the itanium processor. *IEEE Micro*, 20(5):61–69, 2000.

[65] S.K. Reinhardt and S.S. Mukherjee. Transient fault detection via simultaneous multithreading. In *Proceedings of the 27th International Symposium on Computer Architecture (ISCA)*, New York, NY, USA, 2000. ACM Press.

[66] T.N. Vijaykumar, I. Pomeranz, and K. Cheng. Transient-fault recovery using simultaneous multithreading. In *Proceedings of the 29th International Symposium on Computer Architecture (ISCA)*, 2002.

[67] Todd M Austin. DIVA: a reliable substrate for deep submicron microarchitecture design. In *Proceedings of International Symposium on Microarchitecture (MICRO)*, 1999.

[68] Eric Rotenberg. AR-SMT: A microarchitectural approach to fault tolerance in microprocessors. In *Proceedings of International Symposium on Fault-Tolerant Computing (FTC)*, page 84, 1999. ISBN 0-7695-0213-X.

[69] J.C. Smolens, J. Kim, J.C. Hoe, and B. Falsafi. Efficient resource sharing in concurrent error detecting superscalar microarchitectures. In *Proceedings of the 37th International Symposium on Microarchitecture (MICRO)*, 2004.

[70] Joydeep Ray, James C Hoe, and Babak Falsafi. Dual use of superscalar datapath for transient-fault detection and recovery. In *Proceedings of the 34th annual ACM/IEEE international symposium on Microarchitecture*, pages 214–224. IEEE Computer Society, 2001.

[71] M.A. Gomaa and T.N. Vijaykumar. Opportunistic transient-fault detection. In *Proceedings of International Symposium on Computer Architecture (ISCA)*, 2005.

[72] Mohamed Gomaa, Chad Scarbrough, TN Vijaykumar, and Irith Pomeranz. Transient-fault recovery for chip multiprocessors. In *Proceedings of 30th Annual International Symposium on Computer Architecture, 2003*, pages 98–109. IEEE, 2003.

[73] S. Kumar and A. Aggarwal. Reducing resource redundancy for concurrent error detection techniques in high performance microprocessors. In *Proceedings of the International Symposium on High-Performance Computer Architecture (HPCA)*, 2006.

[74] M.K. Qureshi, O. Mutlu, and Y.N. Patt. Microarchitectural-based inspection: a technique for transient-fault tolerance in microprocessors. In *Proceedings of International Conference on Dependable Systems and Networks (DSN)*, 2005.

[75] Angshuman Parashar, Anand Sivasubramaniam, and Sudhanva Gurumurthi. *SlicK: slice-based locality exploitation for efficient redundant multithreading*, volume 40. ACM, 2006.

[76] D.K. Pradhan. *Fault-tolerant computer system design*. Computer Science Press, 2003.

[77] Muhammad Shafique, Siddharth Garg, Jörg Henkel, and Diana Marculescu. The eda challenges in the dark silicon era: Temperature, reliability, and variability perspectives. In *Proceedings of the The 51st Annual Design Automation Conference on Design Automation Conference*, pages 1–6. ACM, 2014.

[78] Douglas Bossen, Joel M Tendler, and Kevin Reick. Power4 system design for high reliability. *Micro, IEEE*, 22(2):16–24, 2002.

[79] Naveen Muralimanohar. *Wire Aware Cache Architecture.* PhD thesis, Citeseer, 2009.

[80] Eishi Ibe, Hitoshi Taniguchi, Yasuo Yahagi, Ken-ichi Shimbo, and Tadanobu Toba. Impact of scaling on neutron-induced soft error in srams from a 250 nm to a 22 nm design rule. *Electron Devices, IEEE Transactions on*, 57(7): 1527–1538, 2010.

[81] Joel M Tendler, J Steve Dodson, JS Fields, Hung Le, and Balaram Sinharoy. Power4 system microarchitecture. *IBM Journal of Research and Development*, 46(1):5–25, 2002.

[82] John Wuu, Don Weiss, Charles Morganti, and Michael Dreesen. The asynchronous 24mb on-chip level-3 cache for a dual-core itanium®-family processor. In *IEEE International Solid-State Circuits Conference Digest of Technical Papers*, 2005.

[83] Chetana N Keltcher, Kevin J McGrath, Ardsher Ahmed, and Pat Conway. The amd opteron processor for multiprocessor servers. *IEEE Micro*, 23(2): 66–76, 2003.

[84] Krisztián Flautner, Nam Sung Kim, Steve Martin, David Blaauw, and Trevor Mudge. Drowsy caches: simple techniques for reducing leakage power. In *Computer Architecture, 2002. Proceedings. 29th Annual International Symposium on*, pages 148–157. IEEE, 2002.

[85] Dan Ernst, Nam Sung Kim, Shidhartha Das, Sanjay Pant, Rajeev Rao, Toan Pham, Conrad Ziesler, David Blaauw, Todd Austin, Krisztian Flautner, et al. Razor: A low-power pipeline based on circuit-level timing speculation. In *Microarchitecture, 2003. MICRO-36. Proceedings. 36th Annual IEEE/ACM International Symposium on*, pages 7–18. IEEE, 2003.

[86] Lin Li, Vijay Degalahal, Narayanan Vijaykrishnan, Mahmut Kandemir, and Mary Jane Irwin. Soft error and energy consumption interactions: a data cache perspective. In *Low Power Electronics and Design, 2004. ISLPED'04. Proceedings of the 2004 International Symposium on*, pages 132–137. IEEE, 2004.

[87] Zhang K Maiz J, Hareland S. Characterization of multi-bit soft error events in advanced srams. In *IEEE International Electron Devices Meeting, 2003.*

IEDM'03 Technical Digest, pages 21–24, Los Alamitos, CA, USA, March 2003. IEEE Computer Society.

[88] N. Seifert, P. Slankard, M. Kirsch, B. Narasimham, V. Zia, B C. Brookresonand A. Voand S. Mitraand B. Gill, and J. Maiz. Radiation-induced soft error rates of advanced cmos bulk devices. In *Proceedings of International Reliability Physics Symposium*, pages 217–225, Los Alamitos, CA, USA, March 2006. IEEE Computer Society.

[89] D Costello and Shu Lin. *Error control coding*. Pearson Higher Education, 2004.

[90] Irving S Reed and Gustave Solomon. Polynomial codes over certain finite fields. *Journal of the Society for Industrial & Applied Mathematics*, 8(2): 300–304, 1960.

[91] AMD Bios. kernel developers guide for amd athlon 64 and amd opteron processors. Technical report, Technical Report Pub. 26094, AMD, 2006.

[92] A.M. Saleh, J.J. Serrano, and J.H. Patel. Reliability of scrubbing recovery techniques for memory systems. *IEEE Transactions on Reliability*, 39(1): 114–122, 1990.

[93] S.S. Mukherjee, J. Emer, T. Fossum, and S.K. Reinhardt. Cache scrubbing in microprocessor. In *Proceedings of International Symposium on Pacific Rim Dependable Computing (PRDC)*, 2004.

[94] Shuai Wang, Jie Hu, and Sotirios G Ziavras. On the characterization and optimization of on-chip cache reliability against soft errors. *Computers, IEEE Transactions on*, 58(9):1171–1184, 2009.

[95] Kazunari Ishimaru. 45nm/32nm cmos–challenge and perspective. *Solid-State Electronics*, 52(9):1266–1273, 2008.

[96] Vijay Degalahal, Lin Li, Vijaykrishnan Narayanan, Mahmut Kandemir, and Mary Jane Irwin. Soft errors issues in low-power caches. *Very Large Scale Integration (VLSI) Systems, IEEE Transactions on*, 13(10):1157–1166, 2005.

[97] S.S. Mukherjee, C. Weaver, J. Emer, S.K. Reinhardt, and T. Austin. A systematic methodology to compute the architectural vulnerability factors

for a high-performance microprocessor. In *Proceedings of the 36th International Symposium on Microarchitecture (MICRO)*, New York, NY, USA, 2003. ACM Press.

[98] Arijit Biswas, Charles Recchia, Shubhendu S Mukherjee, Vinod Ambrose, Leo Chan, Aamer Jaleel, Athanasios E Papathanasiou, Mike Plaster, and Norbert Seifert. Explaining cache ser anomaly using due avf measurement. In *High Performance Computer Architecture (HPCA), 2010 IEEE 16th International Symposium on*, pages 1–12. IEEE, 2010.

[99] Jinho Suh, Mehrtash Manoochehri, Murali Annavaram, and Michel Dubois. Soft error benchmarking of l2 caches with parma. *ACM SIGMETRICS Performance Evaluation Review*, 39(1):85–96, 2011.

[100] Ishwar Parulkar. Impact of soft errors on reliability and availability of servers in the internet computing era. online. http://www.slideshare.net/ishwardutt/vts2006softerrorimpactservers2.

[101] Vision Solutions. Assessing the financial impact of downtime. *white paper*, 2008.

[102] Milos Prvulovic, Zheng Zhang, and Josep Torrellas. Revive: cost-effective architectural support for rollback recovery in shared-memory multiprocessors. In *Computer Architecture, 2002. Proceedings. 29th Annual International Symposium on*, pages 111–122. IEEE, 2002.

[103] Jun Nakano, Pablo Montesinos, Kourosh Gharachorloo, and Josep Torrellas. Revivei/o: Efficient handling of i/o in highly-available rollback-recovery servers. In *High-Performance Computer Architecture, 2006. The Twelfth International Symposium on*, pages 200–211. IEEE, 2006.

[104] Michel Banâtre, Alain Gefflaut, Philippe Joubert, Christine Morin, and Peter A Lee. An architecture for tolerating processor failures in shared-memory multiprocessors. *Computers, IEEE Transactions on*, 45(10):1101–1115, 1996.

[105] Elmootazbellah N Elnozahy and Willy Zwaenepoel. Manetho: Transparent roll back-recovery with low overhead, limited rollback, and fast output commit. *IEEE Transactions on Computers*, 41(5):526–531, 1992.

[106] Elmootazbellah Nabil Elnozahy, Lorenzo Alvisi, Yi-Min Wang, and David B Johnson. A survey of rollback-recovery protocols in message-passing systems. *ACM Computing Surveys (CSUR)*, 34(3):375–408, 2002.

[107] Daniel J Sorin, Milo MK Martin, Mark D Hill, and David A Wood. Safetynet: improving the availability of shared memory multiprocessors with global checkpoint/recovery. In *Computer Architecture, 2002. Proceedings. 29th Annual International Symposium on*, pages 123–134. IEEE, 2002.

[108] Brian T Gold, Jangwoo Kim, Jared C Smolens, Eric S Chung, Vasileios Liaskovitis, Eriko Nurvitadhi, Babak Falsafi, James C Hoe, and Andreas G Nowatzyk. Truss: a reliable, scalable server architecture. *Micro, IEEE*, 25 (6):51–59, 2005.

[109] Daniel J Sorin, Milo MK Martin, Mark D Hill, and David A Wood. Fast checkpoint/recovery to support kilo-instruction speculation and hardware fault tolerance. *Dept. of Computer Sciences Technical Report CS-TR-2000-1420, University of Wisconsin-Madison*, 2000.

[110] James S Plank, Yuqun Chen, Kai Li, Micah Beck, and Gerry Kingsley. Memory exclusion: Optimizing the performance of checkpointing systems. *Software-Practice and Experience*, 29(2):125–142, 1999.

[111] M. Gomaa, C. Scarbrough, T.N. Vijaykumar, and I. Pomeranz. Transient-fault recovery for chip multiprocessors. In *Proceedings of the 30th International Symposium on Computer Architecture (ISCA)*, 2003.

[112] K-L Wu, W. Kent Fuchs, and Janak H. Patel. Error recovery in shared memory multiprocessors using private caches. *IEEE Transactions on Parallel and Distributed Systems,*, 1(2):231–240, 1990.

[113] David Bernick, Bill Bruckert, Paul Del Vigna, David Garcia, Robert Jardine, Jim Klecka, and Jim Smullen. Nonstop® advanced architecture. In *Proceedings. International Conference on Dependable Systems and Networks, 2005. DSN 2005.*, pages 12–21. IEEE, 2005.

[114] Wendy Bartlett and Lisa Spainhower. Commercial fault tolerance: A tale of two systems. *IEEE Transactions on Dependable and Secure Computing,*, 1(1):87–96, 2004.

[115] Karthik Sundaramoorthy, Zach Purser, and Eric Rotenberg. Slipstream processors: improving both performance and fault tolerance. In *Proceedings of the 33th International Symposium on Microarchitecture (MICRO)*, 2000.

[116] ARM. Arm926ej-s™technical reference manual. Online, February 2014. http://infocenter.arm.com/help/index.jsp?topic=/com.arm.doc.ddi0198e/index.html.

[117] Shubhendu S Mukherjee. *Architecture Design for Soft Errors.* 1st edition, 2009.

[118] Jason Blome, Scott Mahlke, Daryl Bradley, and Krisztián Flautner. A microarchitectural analysis of soft error propagation in a production-level embedded microprocessor. In *Proceedings of the 1st Workshop on Architectural Reliability, 38th International Symposium on Microarchitecture, Barcelona, Spain*, 2005.

[119] L.G. Szafaryn, B.H. Meyer, and K. Skadron. Evaluating overheads of multibit soft-error protection in the processor core. *Micro, IEEE*, 33(4):56–65, July 2013.

[120] James R Black. Electromigrationa brief survey and some recent results. *Electron Devices, IEEE Transactions on*, 16(4):338–347, 1969.

[121] JEDEC Solid State Technology Association et al. Failure mechanisms and models for semiconductor devices. *JEDEC Publication JEP122-B*, 2003.

[122] C-K Hu, R Rosenberg, HS Rathore, DB Nguyen, and B Agarwala. Scaling effect on electromigration in on-chip cu wiring. In *Interconnect Technology, 1999. IEEE International Conference*, pages 267–269. IEEE, 1999.

[123] E Wu, J Sune, W Lai, E Nowak, J McKenna, A Vayshenker, and D Harmon. Interplay of voltage and temperature acceleration of oxide breakdown for ultra-thin gate oxides. *Solid-State Electronics*, 46(11):1787–1798, 2002.

[124] Jaume Abella, Xavier Vera, and Antonio Gonzalez. Penelope: The nbti-aware processor. In *Microarchitecture, 2007. MICRO 2007. 40th Annual IEEE/ACM International Symposium on*, pages 85–96. IEEE, 2007.

[125] Taniya Siddiqua and Sudhanva Gurumurthi. Recovery boosting: A technique to enhance nbti recovery in sram arrays. In *VLSI (ISVLSI), 2010 IEEE Computer Society Annual Symposium on*, pages 393–398. IEEE, 2010.

[126] Rakesh Vattikonda, Wenping Wang, and Yu Cao. Modeling and minimization of pmos nbti effect for robust nanometer design. In *Proceedings of the 43rd annual Design Automation Conference*, pages 1047–1052. ACM, 2006.

[127] Jaume Abella, Javier Carretero, Pedro Chaparro, Xavier Vera, and Antonio González. Low vccmin fault-tolerant cache with highly predictable performance. In *Proceedings of the 42nd Annual IEEE/ACM International Symposium on Microarchitecture*, pages 111–121. ACM, 2009.

[128] Cristian Constantinescu. Neutron ser characterization of microprocessors. In *Dependable Systems and Networks, 2005. DSN 2005. Proceedings. International Conference on*, pages 754–759. IEEE, 2005.

[129] Ennis T Ogawa, Jinyoung Kim, Gad S Haase, Homi C Mogul, and Joe W McPherson. Leakage, breakdown, and tddb characteristics of porous low-k silica-based interconnect dielectrics. In *Reliability Physics Symposium Proceedings, 2003. 41st Annual. 2003 IEEE International*, pages 166–172. IEEE, 2003.

[130] Marty Agostinelli, J Hicks, J Xu, B Woolery, K Mistry, K Zhang, S Jacobs, J Jopling, W Yang, B Lee, et al. Erratic fluctuations of sram cache vmin at the 90nm process technology node. In *Electron Devices Meeting, 2005. IEDM Technical Digest. IEEE International*, pages 655–658. IEEE, 2005.

[131] Shubhendu S Mukherjee, Joel Emer, and Steven K Reinhardt. The soft error problem: An architectural perspective. In *High-Performance Computer Architecture, 2005. HPCA-11. 11th International Symposium on*, pages 243–247. IEEE, 2005.

[132] Balkaran Gill, Michael Nicolaidis, Francis Wolff, Chris Papachristou, and Steven Garverick. An efficient bics design for seus detection and correction in semiconductor memories. In *Proceedings of the conference on Design, Automation and Test in Europe-Volume 1*, pages 592–597. IEEE Computer Society, 2005.

[133] Zheng Feng Huang and Mao Xiang Yi. Biss: A built-in seu sensor for soft error mitigation. *Applied Mechanics and Materials*, 130:4228–4231, 2012.

[134] Ashay Narsale and Michael C Huang. *Variation-tolerant hierarchical voltage monitoring circuit for soft error detection.* IEEE, 2009.

[135] Gaurang Upasani, Xavier Vera, and Antonio González. Setting an error detection infrastructure with low cost acoustic wave detectors. In *Proceedings of the 39th International Symposium on Computer Architecture (ISCA)*, 2012.

[136] Timothy C May and Murray H Woods. Alpha-particle-induced soft errors in dynamic memories. *Electron Devices, IEEE Transactions on*, 26(1):2–9, 1979.

[137] Tino Heijmen. Radiation-induced soft errors in digital circuits–a literature survey. 2002.

[138] JEDEC SOLID STATE TECHNOLOGY ASSOCIATION. Measurement and reporting of alpha particle and terrestrial cosmic ray-induced soft errors in semiconductor devices. Technical Report JDEC89A, Electronic Industries Alliance, 2006.

[139] www.seutest.com. Soft error testing resources. online, September 2006. URL `http://www.seutest.com/cgi-bin/FluxCalculator.cgi`. Available online.

[140] Hajime Kobayashi, Nobutaka Kawamoto, Jun Kase, and Ken Shiraish. Alpha particle and neutron-induced soft error rates and scaling trends in sram. In *Reliability Physics Symposium, 2009 IEEE International*, pages 206–211. IEEE, 2009.

[141] Robert Baumann. Silicon amnesia: a tutorial on radiation induced soft errors. In *International Reliability Physics Symposium (IRPS)*, 2001.

[142] Eric Hannah. Cosmic ray detectors for integrated circuit chips. United States Patent Number 7309866B2, December 2007. Available online (17 pages).

[143] J.R. Letaw and E. Normand. Guidelines for predicting single-event upsets in neutron environments [ram devices]. *IEEE Transactions on Nuclear Science*, 38(6):1500–1506, 1991. ISSN 4108617.

[144] MS Gordon, P Goldhagen, KP Rodbell, TH Zabel, HHK Tang, JM Clem, and P Bailey. Measurement of the flux and energy spectrum of cosmic-ray induced neutrons on the ground. *Nuclear Science, IEEE Transactions on*, 51(6):3427–3434, 2004.

[145] James F Ziegler. Terrestrial cosmic rays. *IBM journal of research and development*, 40(1):19–39, 1996.

[146] Chang-Ming Hsieh, Philip C Murley, and Redmond R O'Brien. Collection of charge from alpha-particle tracks in silicon devices. *Electron Devices, IEEE Transactions on*, 30(6):686–693, 1983.

[147] Eric Dupont, Michael Nicolaidis, and Peter Rohr. Embedded robustness ips for transient-error-free ics. *IEEE Design & Test of Computers*, 19(3):56–70, 2002.

[148] R. Silberberg, H. Tsao Chen, and J.R. Letaw. Neutron generated single-event upsets in the atmosphere. *IEEE Transactions on Nuclear Science*, 31 (6):1183–1185, 1984. ISSN 0018-9499.

[149] H. Tsao Chen ans R. Silberberg and J.R. Letaw. A comparison of neutron induced soft error rate in si and gaas devices. *IEEE Transactions on Nuclear Science*, 35(6):1634–1637, 1988. ISSN 0018-9499.

[150] Henry HK Tang. Nuclear physics of cosmic ray interaction with semiconductor materials: particle-induced soft errors from a physicist's perspective. *IBM journal of research and development*, 40(1):91–108, 1996.

[151] Xin Li, Kai Shen, Michael C Huang, and Lingkun Chu. A memory soft error measurement on production systems. In *USENIX Annual Technical Conference*, pages 275–280, 2007.

[152] Xin Li, Michael C Huang, Kai Shen, and Lingkun Chu. A realistic evaluation of memory hardware errors and software system susceptibility. In *USENIX Annual Technical Conference*, 2010.

[153] Vilas Sridharan and Dean Liberty. A study of dram failures in the field. In *High Performance Computing, Networking, Storage and Analysis (SC), 2012 International Conference for*, pages 1–11. IEEE, 2012.

[154] Andy A Hwang, Ioan A Stefanovici, and Bianca Schroeder. Cosmic rays don't strike twice: understanding the nature of dram errors and the implications for system design. *ACM SIGPLAN Notices*, 47(4):111–122, 2012.

[155] Timothy J Dell. System ras implications of dram soft errors. *IBM Journal of Research and Development*, 52(3):307–314, 2008.

[156] Peter Hazucha and Christer Svensson. Impact of cmos technology scaling on the atmospheric neutron soft error rate. *Nuclear Science, IEEE Transactions on*, 47(6):2586–2594, 2000.

[157] Peter Hazucha, Christer Svensson, and Stephen A Wender. Cosmic-ray soft error rate characterization of a standard 0.6-/spl mu/m cmos process. *Solid-State Circuits, IEEE Journal of*, 35(10):1422–1429, 2000.

[158] C Detcheverry, C Dachs, E Lorfevre, C Sudre, G Bruguier, JM Palau, J Gasiot, and R Ecoffet. Seu critical charge and sensitive area in a submicron cmos technology. 1997.

[159] Philip C Murley and GR Srinivasan. Soft-error monte carlo modeling program, semm. *IBM Journal of Research and Development*, 40(1):109–118, 1996.

[160] ITRS. International technology roadmap for semiconductors. 2010.

[161] Vilas Sridharan and Dean Liberty. A field study of dram errors. *studies*, 3 (5):10, 2012.

[162] N. Seifert and N. Tam. Timing vulnerability factors of sequentials. *IEEE Transactions on Device and Materials Reliability*, 4(3):516–522, 2004.

[163] Premkishore Shivakumar, Michael Kistler, Stephen W Keckler, Doug Burger, and Lorenzo Alvisi. Modeling the effect of technology trends on the soft error rate of combinational logic. In *Proceedings of International Conference on Dependable Systems and Networks (DSN)*, volume 00, page 389, Los Alamitos, CA, USA, 2002. IEEE Computer Society. ISBN 0-7695-1597-5.

[164] Jordi Barrat i Esteve, Ben Goldsmith, and John Turner. International experience with e-voting. 2012.

[165] Belgian Goverment Report. Bevoting study of electronic voting systems. online. http://www.ibz.rrn.fgov.be/fileadmin/user_upload/Elections2011/fr/presentation/bevotin 1_gb.pdf.

[166] Ciscos Internet Business Solutions Group (IBSG). The internet of things. online. http://share.cisco.com/internet-of-things.html.

[167] Larry D Edmonds. Electric currents through ion tracks in silicon devices. *Nuclear Science, IEEE Transactions on*, 45(6):3153–3164, 1998.

[168] Larry D Edmonds. A time-dependent charge-collection efficiency for diffusion. *Nuclear Science, IEEE Transactions on*, 48(5):1609–1622, 2001.

[169] Paul E Dodd. Device simulation of charge collection and single-event upset. *Nuclear Science, IEEE Transactions on*, 43(2):561–575, 1996.

[170] PE Dodd and FW Sexton. Critical charge concepts for cmos srams. *Nuclear Science, IEEE Transactions on*, 42(6):1764–1771, 1995.

[171] PE Dodd, FW Sexton, GL Hash, MR Shaneyfelt, BL Draper, AJ Farino, and RS Flores. Impact of technology trends on seu in cmos srams. *Nuclear Science, IEEE Transactions on*, 43(6):2797–2804, 1996.

[172] PE Dodd, MR Shaneyfelt, E Fuller, JC Pickel, FW Sexton, and PS Winokur. Impact of substrate thickness on single-event effects in integrated circuits. *Nuclear Science, IEEE Transactions on*, 48(6):1865–1871, 2001.

[173] Norbet Seifert, David Moyer, Norman Leland, and Ray Hokinson. Historical trend in alpha-particle induced soft error rates of the alpha tm microprocessor. In *Reliability Physics Symposium, 2001. Proceedings. 39th Annual. 2001 IEEE International*, pages 259–265. IEEE, 2001.

[174] Norbert Seifert, Xiaowei Zhu, D Moyer, R Mueller, R Hokinson, N Leland, M Shade, and L Massengill. Frequency dependence of soft error rates for sub-micron cmos technologies. In *Electron Devices Meeting, 2001. IEDM'01. Technical Digest. International*, pages 14–4. IEEE, 2001.

[175] Matthew J Gadlage, Jonathan R Ahlbin, Vishwanath Ramachandran, Pascale Gouker, Cody A Dinkins, Bharat L Bhuva, Balaji Narasimham, Ronald D Schrimpf, Michael W McCurdy, Michael L Alles, et al. Temperature dependence of digital single-event transients in bulk and fully-depleted soi technologies. Institute of Electrical and Electronics Engineers, 2009.

[176] S Jagannathan, Z Diggins, N Mahatme, TD Loveless, BL Bhuva, S-J Wen, R Wong, and LW Massengill. Temperature dependence of soft error rate in flip-flop designs. In *Reliability Physics Symposium (IRPS), 2012 IEEE International*, pages SE–2. IEEE, 2012.

[177] Guillaume Hubert, Nadine Buard, Cécile Weulersse, Thierry Carrière, Marie-Catherine Palau, Jean-Marie Palau, Damien Lambert, Jacques Baggio, Frederic Wrobel, Frédéric Saigné, et al. A review of dasie code family: Contribution to seu/mbu understanding. In *IOLTS*, pages 87–94, 2005.

[178] Yukiya Kawakami, Masami Hane, Hideyuki Nakamura, Takashi Yamada, and Kouichi Kumagai. Investigation of soft error rate including multi-bit upsets in advanced sram using neutron irradiation test and 3d mixed-mode device simulation. In *International Electron Devices Meeting*, pages 945–948, 2004.

[179] Kenichi Osada, Ken Yamaguchi, Yoshikazu Saitoh, and Takayuki Kawahara. Sram immunity to cosmic-ray-induced multierrors based on analysis of an induced parasitic bipolar effect. *Solid-State Circuits, IEEE Journal of*, 39 (5):827–833, 2004.

[180] Ludger Borucki, Guenter Schindlbeck, and Charles Slayman. Comparison of accelerated dram soft error rates measured at component and system level. In *Reliability Physics Symposium, 2008. IRPS 2008. IEEE International*, pages 482–487. IEEE, 2008.

[181] Charles Slayman. Soft error trends and mitigation techniques in memory devices. In *Reliability and Maintainability Symposium (RAMS), 2011 Proceedings-Annual*, pages 1–5. IEEE, 2011.

[182] S Satoh, Y Tosaka, and SA Wender. Geometric effect of multiple-bit soft errors induced by cosmic ray neutrons on dram's. *Electron Device Letters, IEEE*, 21(6):310–312, 2000.

[183] Timothy J O'Gorman. The effect of cosmic rays on the soft error rate of a dram at ground level. *Electron Devices, IEEE Transactions on*, 41(4): 553–557, 1994.

[184] Ethan H Cannon, Daniel D Reinhardt, Michael S Gordon, and Paul S Makowenskyj. Sram ser in 90, 130 and 180 nm bulk and soi technologies. In *IEEE international reliability physics symposium*, pages 300–304, 2004.

[185] P Oldiges, K Bernstein, D Heidel, B Klaasen, E Cannon, R Dennard, H Tang, M Ieong, and H-SP Wong. Soft error rate scaling for emerging soi technology options. In *VLSI Technology, 2002. Digest of Technical Papers. 2002 Symposium on*, pages 46–47. IEEE, 2002.

[186] Eric Karl, Yih Wang, Yong-Gee Ng, Zheng Guo, Fatih Hamzaoglu, Uddalak Bhattacharya, Kevin Zhang, Kaizad Mistry, and Mark Bohr. A 4.6 ghz 162mb sram design in 22nm tri-gate cmos technology with integrated active v min-enhancing assist circuitry. In *Solid-State Circuits Conference Digest of Technical Papers (ISSCC), 2012 IEEE International*, pages 230–232. IEEE, 2012.

[187] ITRS. International technology roadmap for semiconductors. Online, 2006. http://www.itrs.net/Links/2006Update/FinalToPost/04_PIDS2006Update.pdf.

[188] Jon Cartwright. Intel enters the third dimension. *nature news*, 2011.

[189] Matthew Murray. Intel's new tri-gate ivy bridge transistors: 9 things you need to know. *Retrieved March*, 13:2012, 2011.

[190] Y-P Fang and Anthony S Oates. Neutron-induced charge collection simulation of bulk finfet srams compared with conventional planar srams. *Device and Materials Reliability, IEEE Transactions on*, 11(4):551–554, 2011.

[191] F El-Mamouni, EX Zhang, ND Pate, N Hooten, RD Schrimpf, RA Reed, KF Galloway, D McMorrow, J Warner, E Simoen, et al. Laser-and heavy ion-induced charge collection in bulk finfets. *Nuclear Science, IEEE Transactions on*, 58(6):2563–2569, 2011.

[192] Norbert Seifert, Balkaran Gill, Shah Jahinuzzaman, Joseph Basile, Vinod Ambrose, Quan Shi, Randy Allmon, and Arkady Bramnik. Soft error susceptibilities of 22 nm tri-gate devices. *Nuclear Science, IEEE Transactions on*, 59(6):2666–2673, 2012.

[193] Kinam Kim. Technology for sub-50nm dram and nand flash manufacturing. In *Electron Devices Meeting, 2005. IEDM Technical Digest. IEEE International*, pages 323–326. IEEE, 2005.

[194] Tokyo Electron TEL. Emerging research devices. *Special Focus*, page 29.

[195] Nak Hee Seong, Sungkap Yeo, and Hsien-Hsin S Lee. Tri-level-cell phase change memory: Toward an efficient and reliable memory system. In *Proceedings of the 40th Annual International Symposium on Computer Architecture*, pages 440–451. ACM, 2013.

[196] Sungkap Yeo, Nak Hee Seong, and Hsien-Hsin S Lee. Can multi-level cell pcm be reliable and usable? analyzing the impact of resistance drift. In *the 10th Ann. Workshop on Duplicating, Deconstructing and Debunking (WDDD)*, 2012.

[197] Doe Hyun Yoon, Naveen Muralimanohar, Jichuan Chang, Parthasarathy Ranganathan, Norman P Jouppi, and Mattan Erez. Free-p: Protecting non-volatile memory against both hard and soft errors. In *High Performance Computer Architecture (HPCA), 2011 IEEE 17th International Symposium on*, pages 466–477. IEEE, 2011.

[198] Stuart Schechter, Gabriel H Loh, Karin Straus, and Doug Burger. Use ecp, not ecc, for hard failures in resistive memories. In *ACM SIGARCH Computer Architecture News*, volume 38, pages 141–152. ACM, 2010.

[199] N. Wang, A. Mahesri, and S.J. Patel. Examining ace analysis reliability estimates using fault-injection. In *Proceedings of International Symposium on Computer Architecture (ISCA)*, 2007.

[200] Shubhendu S Mukherjee, Christopher Weaver, Joel Emer, Steven K Reinhardt, and Todd Austin. A systematic methodology to compute the architectural vulnerability factors for a high-performance microprocessor. In *Proceedings of the 36th annual IEEE/ACM International Symposium on Microarchitecture*, page 29. IEEE Computer Society, 2003.

[201] K. Walcott, G. Humphreysand, and S. Gurumurthi. Dynamic prediction of architectural vulnerability from microarchitectural state. In *Proceedings of 34th International Symposium on Computer Architecture (ISCA)*, 2007.

[202] A. Biswas, N. Soundararajan, S. Mukherjee, and S. Gurumurthi. Quantized avf: A means of capturing vulnerability variations over small windows of time. In *Proceedings of Workshop on Silicon Errors in Logic -System Effects (SELSE)*, 2009.

[203] A. Biswas, P. Racunas, R. Cheveresan, J. Emer, S.S. Mukherjee, and R. Rangan. Computing architectural vulnerability factors for address-based structures. In *Proceedings of the 32nd International Symposium on Computer Architecture (ISCA)*, 2005.

[204] L. Duan, B. Li, and L. Peng. Versatile prediction and fast estimation of architectural vulnerability factor from processor performance metrics. In

Proceedings of International Symposium on High Performance Computer Architecture (HPCA), 2009.

[205] X. Fu, J. Poe, T. Li, and J. Fortes. Characterizing microarchitecture soft error vulnerability phase behavior. In *Proceedings of International Symposium on Modeling, Analysis, and Simulation of Computer and Telecommunication Systems (MASCOTS)*, 2006.

[206] Egas Henes Neto, Ivandro Ribeiro, Michele Vieira, Gilson Wirth, and Fernanda Lima Kastensmidt. Using bulk built-in current sensors to detect soft errors. *Micro, IEEE*, 26(5):10–18, 2006.

[207] Patrick Ndai, Amit Agarwal, Qikai Chen, and Kaushik Roy. A soft error monitor using switching current detection. In *Computer Design: VLSI in Computers and Processors, 2005. ICCD 2005. Proceedings. 2005 IEEE International Conference on*, pages 185–190. IEEE, 2005.

[208] Gaurang Upasani, Xavier Vera, and Antonio González. Reducing due-fit of caches by exploiting acoustic wave detectors for error recovery. In *IOLTS*, pages 85–91, 2013.

[209] I Abt. Silicon detectors: Technology and applications. Max Planck Institut for Physics, Munich.

[210] Nicolas Wyrsch, S Dunand, C Miazza, A Shah, G Anelli, M Despeisse, A Garrigos, P Jarron, J Kaplon, D Moraes, et al. Thin-film silicon detectors for particle detection. *physica status solidi (c)*, 1(5):1284–1291, 2004.

[211] P S. Marrocchesi, O Adriani, C Avanzini, M G. Bagliesi, A Basti, K Batkov, G Bigongiari, L Bonechi, R Cecchi, M Y. Kim, et al. A silicon array for cosmic-ray composition measurements in calet. *Journal of the Physical Society of Japan*, 78(Suppl. A):181–183, 2009.

[212] Howard H Chen, John A Fifield, Louis L Hsu, and Henry HK Tang. Programmable heavy-ion sensing device for accelerated dram soft error detection, 2009. US Patent 7,499,308.

[213] B. C. Daly, T. B. Norris, J. Chen, and J. B. Khurgin. Picosecond acoustic phonon pulse propagation in silicon. *Phys. Rev. B*, 70:214307, Dec 2004.

[214] M. Hammig. The design and construction of a mechanical radiation detector. In *Proceedings of IEEE Nuclear Science Symposium*, pages 803–805, Dept. of Nucl. Eng., Michigan Univ., Ann Arbor, MI, 1998. IEEE.

[215] M. Hammig. Nuclear radiation detection via the detection of pliable microstructures. In *Proceedings of Nuclear Instruments and Methods in Physics Research*, pages 278–281, Los Alamitos, CA, USA, 1999. Elsevier Science.

[216] Robert W Keyes. Semiconductor surface acoustic wave device, November 1982. US Patent 4,358,745.

[217] Larry K. Baxter. *Capacitive Sensors: Design and Applications*. John Wiley and Sons, 1996.

[218] Scott Whitney. Vibrations of cantilever beams: Deflection, frequency, and research uses. *Website: Apr*, 23:10, 1999.

[219] M. William, O. Roger, and M. Daniel. Capacitance bar sensor. United States Patent US4947131, August 1990.

[220] Intel Corporation. *Intel's Nehalem data sheet*. Intel Corporation'.

[221] Mark D Hammig, David K Wehe, and John A Nees. The measurement of sub-brownian lever deflections. *Nuclear Science, IEEE Transactions on*, 52 (6):3005–3011, 2005.

[222] N Blanc, J Brugger, NF De Rooij, and U Durig. Scanning force microscopy in the dynamic mode using microfabricated capacitive sensors. *Journal of Vacuum Science & Technology B: Microelectronics and Nanometer Structures*, 14(2):901–905, 1996.

[223] Moussa Hoummady, Andrew Campitelli, and Wojtek Wlodarski. Acoustic wave sensors: design, sensing mechanisms and applications. *Smart materials and structures*, 6(6):647, 1997.

[224] Sandia National Laboratories. Microsensors and sensor microsystems. Online, June 2013. http://www.sandia.gov/mstc/MsensorSensorMsystems/technical-information/SH-SAW-biosensors.html.

[225] Roberto Raiteri, Massimo Grattarola, Hans-Jürgen Butt, and Petr Skládal. Micromechanical cantilever-based biosensors. *Sensors and Actuators B: Chemical*, 79(2):115–126, 2001.

[226] Philip A. Bernstein. Sequoia: A fault-tolerant tightly coupled multiprocessor for transaction processing. *Computer*, 21(2):37–45, 1988.

[227] Radu Teodorescu, Jun Nakano, and Josep Torrellas. Swich: A prototype for efficient cache-level checkpointing and rollback. *IEEE Micro*, 26(5):28–40, 2006.

[228] Douglas B Hunt and Peter N Marinos. A general purpose cache-aided rollback error recovery (carer) technique. In *Proceedings of the 17th International Symposium on Fault-Tolerant Computing Systems*, pages 170–175, 1987.

[229] Hisashige Ando, Yuuji Yoshida, Aiichiro Inoue, Itsumi Sugiyama, Takeo Asakawa, Kuniki Morita, Toshiyuki Muta, Tsuyoshi Motokurumada, Seishi Okada, Hideo Yamashita, et al. A 1.3-ghz fifth-generation sparc64 microprocessor. *Solid-State Circuits, IEEE Journal of*, 38(11):1896–1905, 2003.

[230] Shuguang Feng, Shantanu Gupta, Amin Ansari, Scott A Mahlke, and David I August. Encore: low-cost, fine-grained transient fault recovery. In *Proceedings of the 44th Annual IEEE/ACM International Symposium on Microarchitecture*, pages 398–409. ACM, 2011.

[231] N.J. Wang and S.J. Patel. Restore: Symptom based soft error detection in microprocessors. In *Proceedings of International Conference on Dependable Systems and Networks (DSN)*, 2005.

[232] Harish Naik, Rinku Gupta, and Pete Beckman. Analyzing checkpointing trends for applications on the ibm blue gene/p system. In *Parallel Processing Workshops, 2009. ICPPW'09. International Conference on*, pages 81–88. IEEE, 2009.

[233] Jason Duell. The design and implementation of berkeley lab's linux checkpoint/restart. *Lawrence Berkeley National Laboratory*, 2005.

[234] Rana E Ahmed, Robert C Frazier, and Peter N Marinos. Cache-aided rollback error recovery (carer) algorithm for shared-memory multiprocessor systems. In *Digest of Papers., 20th International Symposium Fault-Tolerant Computing, 1990. FTCS-20.*, pages 82–88. IEEE, 1990.

[235] Xiangyu Dong, Yuan Xie, Naveen Muralimanohar, and Norman P Jouppi. A case study of incremental and background hybrid in-memory checkpointing. In *Proc. of the 2010 Exascale Evaluation and Research Techniques Workshop*, volume 115, pages 119–147, 2010.

[236] G. Shen, R. Zetik, and R.S. Thoma. Performance comparison of toa and tdoa based location estimation algorithms in los environment. *Proceedings of Workshop on Positioning, Navigation and Communication(WPNC)*, pages 71–78, 2008. ISSN 1001-3454.

[237] W. Foy. Position-Location Solutions by Taylor-Series Estimation. *IEEE Transactions on Aerospace Electronic Systems*, 12:187–194, March 1976.

[238] B. T. Fang. Simple solutions for hyperbolic and related position fixes. *IEEE Transactions on Aerospace Electronic Systems*, 26:748–753, September 1990.

[239] YT Chan and KC Ho. A simple and efficient estimator for hyperbolic location. *Signal Processing, IEEE Transactions on*, 42(8):1905–1915, 1994.

[240] KC Ho. Bias reduction for an explicit solution of source localization using tdoa. *Signal Processing, IEEE Transactions on*, 60(5):2101–2114, 2012.

[241] Christopher C. Paige and Michael A. Saunders. Lsqr: An algorithm for sparse linear equations and sparse least squares. *ACM Trans. Math. Softw.*, 8:43–71, March 1982. ISSN 0098-3500.

[242] C. McMillan and P. McMillan. Characterizing rifle performance using circular error probable measured via a flatbed scanner. Creative Commons Attribution-Noncommercial-No Derivative Works, December 2008.

[243] L. Li, V. Degalahal, N. Vijaykrishnan, M. Kandemir, and M.J. Irwin. Soft error and energy consumption interactions: a data cache perspective. In *Proceedings of the International Symposium on Low Power Electronics and Design (ISLPED)*, 2004.

[244] Hisashige Ando, Ken Seki, Satoru Sakashita, Masatosh Aihara, Ryuji Kan, Kenji Imada, Masaru Itoh, Masamichi Nagai, Yoshiharu Tosaka, Keiji Takahisa, et al. Accelerated testing of a 90nm sparc64 v microprocessor for neutron ser. In *The Third Workshop on System Effects on Logic Soft Errors*, 2007.

[245] COMPAQ. Alpha 21264 microprocessor hardware reference manual. July 1999.

[246] Poonacha Kongetira, Kathirgamar Aingaran, and Kunle Olukotun. Niagara: A 32-way multithreaded sparc processor. *Micro, IEEE*, 25(2):21–29, 2005.

[247] Davide Bertozzi, Luca Benini, and Giovanni De Micheli. Error control schemes for on-chip communication links: the energy-reliability tradeoff. *Computer-Aided Design of Integrated Circuits and Systems, IEEE Transactions on*, 24(6):818–831, 2005.

[248] Doe Hyun Yoon and Mattan Erez. Memory mapped ecc: low-cost error protection for last level caches. In *Proceedings of the 36th annual international symposium on Computer architecture(ISCA)*, 2009.

[249] Mehrtash Manoochehri, Murali Annavaram, and Michel Dubois. Cppc: correctable parity protected cache. In *Proceedings of the 38th annual international symposium on Computer architecture(ISCA)*, 2011.

[250] ARM ARM. Cortex-a15 mpcore processor technical reference manual, 2013.

[251] Paul Genua and Freescale Semiconductor. Error correction and error handling on powerquicc iii processors. *DOI= http://www. freescale. com/-files/32bit/doc/app_note/AN3532. pdf*, 2004.

[252] Sakai S. Hung L D, Goshima M. Zigzag-hvp: A cost-effective technique to mitigate soft errors in caches with word-based access. In *IPSJ Digital Courier*, Washington, DC, USA, 2006. IEEE Computer Society.

[253] Mai K Kim J, Hardavellas N. Multi-bit error tolerant caches using two-dimensional error coding. In *Proceedings of International Symposium on Microarchitecture (MICRO)*, Washington, DC, USA, 2007. IEEE Computer Society.

[254] Calingaert P. Two-dimensional parity checking. In *Proceedings of International Symposium on Microarchitecture (MICRO)*, Washington, DC, USA, 1961. IEEE Computer Society.

[255] Jack Huynh. The amd athlon xp processor with 512kb l2 cache. *AMD White Paper (Feb.)*, 2003.

[256] Stefan Rusu, Harry Muljono, and Brian Cherkauer. Itanium 2 processor 6m: higher frequency and larger l3 cache. *Micro, IEEE*, 24(2):10–18, 2004.

[257] Harry Muljono, Stefan Rusu, Brian Cherkauer, and Jason Stinson. New 130nm itanium 2 processors for 2003. In *Hot Chips*, pages 1–22, 2003.

[258] Alaa R Alameldeen, Ilya Wagner, Zeshan Chishti, Wei Wu, Chris Wilkerson, and Shih-Lien Lu. Energy-efficient cache design using variable-strength error-correcting codes. In *Computer Architecture (ISCA), 2011 38th Annual International Symposium on*, pages 461–471. IEEE, 2011.

[259] Sai-Wai Fu, Amr M Mohsen, and Tim C May. Alpha-particle-induced charge collection measurements and the effectiveness of a novel p-well protection barrier on vlsi memories. *Electron Devices, IEEE Transactions on*, 32(1): 49–54, 1985.

[260] D Lage Burnett and A C Bormann. Soft-error-rate improvement in advanced bicmos srams. Reliability Physics Symposium, 1993. 31st Annual Proceedings., International, 1993.

[261] G-H Asadi, Vilas Sridharan, Mehdi Baradaran Tahoori, and David Kaeli. Balancing performance and reliability in the memory hierarchy. In *Performance Analysis of Systems and Software, 2005. ISPASS 2005. IEEE International Symposium on*, pages 269–279. IEEE, 2005.

[262] H-H.S. Lee, G.S. Tyson, and M.K. Farrens. Improving bandwidth utilization using eager writeback. *Journal of Instruction Level Parallelism*, 3:1–22, 2001.

[263] S. Kaxiras, Z. Hu, and M. Martonosi. Cache decay: exploiting generational behavior to reduce cache leakage power. In *Proceedings of 28th International Symposium on Computer Architecture (ISCA)*, 2001.

[264] T Calin, M Nicolaidis, and R Velazco. Upset hardened memory design for submicron cmos technology. *IEEE Transactions on Nuclear Science*, 43, 1996.

[265] Peter Hazucha, Tanay Karnik, Steven Walstra, Bradley A Bloechel, James W Tschanz, Jose Maiz, Krishnamurthy Soumyanath, Gregory E Dermer, Siva Narendra, Vivek De, et al. Measurements and analysis of ser-tolerant latch in a 90-nm dual-v t cmos process. *Solid-State Circuits, IEEE Journal of*, 39(9):1536–1543, 2004.

[266] F Ootsuka, M Nakamura, T Miyake, S Iwahashi, Y Ohira, T Tamaru, K Kikushima, and K Yamaguchi. A novel 0.20/spl mu/m full cmos sram cell using stacked cross couple with enhanced soft error immunity. In *Electron Devices Meeting, 1998. IEDM'98. Technical Digest., International*, pages 205–208. IEEE, 1998.

[267] Philippe Roche, Francois Jacquet, Christian Caillat, and J-P Schoellkopf. An alpha immune and ultra low neutron ser high density sram. In *Reliability Physics Symposium Proceedings, 2004. 42nd Annual. 2004 IEEE International*, pages 671–672. IEEE, 2004.

[268] Tanay Karnik, Sriram Vangal, V Veeramachaneni, Peter Hazucha, Vasantha Erraguntla, and Shekhar Borkar. Selective node engineering for chip-level soft error rate improvement [in cmos]. In *VLSI Circuits Digest of Technical Papers, 2002. Symposium on*, pages 204–205. IEEE, 2002.

[269] Leonard R Rockett Jr. An seu-hardened cmos data latch design. *IEEE Transactions on Nuclear Science*, 35:1682–1687, 1988.

[270] N Derhacobian, Valery A Vardanian, and Yervant Zorian. Embedded memory reliability: The ser challenge. In *Memory Technology, Design and Testing, 2004. Records of the 2004 International Workshop on*, pages 104–110. IEEE, 2004.

[271] Hossein Asadi, Vilas Sridharan, Mehdi B Tahoori, and David Kaeli. Reliability tradeoffs in design of cache memories. In *1st Workshop on Architectural Reliability (WAR-1)*, 2005.

[272] Bharadwaj S Amrutur and Mark A Horowitz. Speed and power scaling of sram's. *Solid-State Circuits, IEEE Journal of*, 35(2):175–185, 2000.

[273] Soontae Kim. Reducing area overhead for error-protecting large l2/l3 caches. *Computers, IEEE Transactions on*, 58(3):300–310, 2009.

[274] Arun K. Somani Seongwoo Kim. Area efficient architectures for information integrity in cache memories. *International Symposium on Computer Architecure*, 1999.

[275] Koustav Bhattacharya, Nagarajan Ranganathan, and Soontae Kim. A framework for correction of multi-bit soft errors in l2 caches based on redundancy. *Very Large Scale Integration (VLSI) Systems, IEEE Transactions on*, 17(2):194–206, 2009.

[276] Zeshan Chishti, Alaa R Alameldeen, Chris Wilkerson, Wei Wu, and Shih-Lien Lu. Improving cache lifetime reliability at ultra-low voltages. In *Proceedings of the 42nd Annual IEEE/ACM International Symposium on Microarchitecture*, pages 89–99. ACM, 2009.

[277] Soontae Kim. Area-efficient error protection for caches. In *Proceedings of the conference on Design, automation and test in Europe: Proceedings*, pages 1282–1287. European Design and Automation Association, 2006.

[278] Wei Zhang, Sudhanva Gurumurthi, Mahmut T Kandemir, and Anand Sivasubramaniam. Icr: In-cache replication for enhancing data cache reliability. In *DSN*, pages 291–300, 2003.

[279] Wei Zhang. Replication cache: a small fully associative cache to improve data cache reliability. *Computers, IEEE Transactions on*, 54(12):1547–1555, 2005.

[280] Nidhi Aggarwal, Parthasarathy Ranganathan, Norman P Jouppi, and James E Smith. Configurable isolation: building high availability systems with commodity multi-core processors. *ACM SIGARCH Computer Architecture News*, 35(2):470–481, 2007.

[281] Christopher LaFrieda, Engin Ipek, Jose F Martinez, and Rajit Manohar. Utilizing dynamically coupled cores to form a resilient chip multiprocessor. In *37th Annual IEEE/IFIP International Conference on Dependable Systems and Networks, 2007. DSN'07.*, pages 317–326. IEEE, 2007.

[282] Nahmsuk Oh, Philip P Shirvani, and Edward J McCluskey. Error detection by duplicated instructions in super-scalar processors. *Reliability, IEEE Transactions on*, 51(1):63–75, 2002.

[283] George A Reis, Jonathan Chang, Neil Vachharajani, Ram Rangan, and David I August. Swift: Software implemented fault tolerance. In *Proceedings of the International Symposium on Code Generation and Optimization*, pages 243–254. IEEE Computer Society, 2005.

[284] George A Reis, Jonathan Chang, Neil Vachharajani, Shubhendu S Mukherjee, R Rangan, and DI August. Design and evaluation of hybrid fault-detection systems. In *Proceedings of 32nd International Symposium on Computer Architecture, 2005. ISCA'05.*, pages 148–159. IEEE, 2005.

[285] K Constantinides, S Shyam, S Phadke, V Bertacco, and T Austin. Ultra low-cost defect protection for microprocessor pipelines. In *Proc. of ASPLOS*, 2006.

[286] Kypros Constantinides, Stephen Plaza, Jason Blome, Bin Zhang, Valeria Bertacco, Scott Mahlke, Todd Austin, and Michael Orshansky. Bulletproof: A defect-tolerant cmp switch architecture. In *The Twelfth International Symposium on High-Performance Computer Architecture, 2006.*, pages 5–16. IEEE, 2006.

[287] Man-Lap Li, Pradeep Ramachandran, Swarup Kumar Sahoo, Sarita V Adve, Vikram S Adve, and Yuanyuan Zhou. Understanding the propagation of hard errors to software and implications for resilient system design. *ACM Sigplan Notices*, 43(3):265–276, 2008.

[288] Paul Racunas, Kypros Constantinides, Srilatha Manne, and Shubhendu S Mukherjee. Perturbation-based fault screening. In *IEEE 13th International Symposium on High Performance Computer Architecture, 2007. HPCA 2007.*, pages 169–180. IEEE, 2007.

[289] Albert Meixner, Michael E Bauer, and Daniel J Sorin. Argus: Low-cost, comprehensive error detection in simple cores. In *40th Annual IEEE/ACM International Symposium on Microarchitecture, 2007. MICRO 2007.*, pages 210–222. IEEE, 2007.

[290] Rajeev Balasubramonian, Naveen Muralimanohar, Karthik Ramani, and Venkatanand Venkatachalapathy. Microarchitectural wire management for performance and power in partitioned architectures. In *11th International Symposium on High-Performance Computer Architecture, 2005. HPCA-11.*, pages 28–39. IEEE, 2005.

[291] Naveen Muralimanohar, Rajeev Balasubramonian, and Norman P Jouppi. Architecting efficient interconnects for large caches with cacti 6.0. *IEEE Micro,*, 28(1):69–79, 2008.

[292] José F Martínez, Jose Renau, Michael C Huang, and Milos Prvulovic. Cherry: Checkpointed early resource recycling in out-of-order microprocessors. In *Proceedings. 35th Annual IEEE/ACM International Symposium on Microarchitecture, 2002.(MICRO-35).*, pages 3–14. IEEE, 2002.

[293] Oguz Ergin, Deniz Balkan, Dmitry Ponomarev, and Kanad Ghose. Early register deallocation mechanisms using checkpointed register files. *IEEE Transactions on Computers,*, 55(9):1153–1166, 2006.

[294] Edson Borin, Youfeng Wu, Mauricio Breternitz, and Cheng Wang. Lar-cc: Large atomic regions with conditional commits. In *Proceedings of the 2011 9th Annual IEEE/ACM International Symposium on Code Generation and Optimization*, pages 54–63. IEEE Computer Society, 2011.

[295] Meyrem Kyrman, Nevin Kyrman, and Jose F Martynez. Cherry-mp: Correctly integrating checkpointed early resource recycling in chip multiprocessors. In *Proceedings of the 38th annual IEEE/ACM International Symposium on Microarchitecture*, pages 245–256. IEEE Computer Society, 2005.

[296] M Wasiur Rashid and Michael C Huang. Supporting highly-decoupled thread-level redundancy for parallel programs. In *IEEE 14th International Symposium on High Performance Computer Architecture, 2008. HPCA 2008.*, pages 393–404. IEEE, 2008.

[297] Steven K Reinhardt, Shubhendu S Mukherjee, Joel S Emer, et al. Periodic checkpointing in a redundantly multi-threaded architecture, December 11 2007. US Patent 7,308,607.

[298] Milo MK Martin, Daniel J Sorin, Bradford M Beckmann, Michael R Marty, Min Xu, Alaa R Alameldeen, Kevin E Moore, Mark D Hill, and David A Wood. Multifacet's general execution-driven multiprocessor simulator (gems) toolset. *ACM SIGARCH Computer Architecture News*, 33(4): 92–99, 2005.

[299] J. Somers. *Stratus ftServer - Intel Fault Tolerant Platform.* Intel Corporation.

[300] C. Webb. *z6 - The Next-generation Mainframe Microprocessor*. Hot Chips.

[301] Ravi Nair and James E Smith. Method and apparatus for fault-tolerance via dual thread crosschecking, March 21 2006. US Patent 7,017,073.

[302] Thomas D Bissett, Paul A Leveille, Erik Muench, and Glenn A Tremblay. Loosely-coupled, synchronized execution, April 20 1999. US Patent 5,896,523.

[303] D.M. Tullsen, S.J. Eggers, J.S. Emer, H.M. Levy, J.L. Lo, and R.L. Stamm. Exploiting choice: instruction fetch and issue on an implementable simultaneous multithreading processor. In *Proceedings of the 23rd International Symposium on Computer Architecture (ISCA)*, pages 191–202, New York, NY, USA, 1996. ACM Press.

[304] Darrell Boggs, Aravindh Baktha, Jason Hawkins, Deborah T Marr, J Alan Miller, Patrice Roussel, Ronak Singhal, Bret Toll, and KS Venkatraman. The microarchitecture of the intel pentium 4 processor on 90nm technology. *Intel Technology Journal*, 8(1), 2004.

[305] Jared C Smolens, Brian T Gold, Jangwoo Kim, Babak Falsafi, James C Hoe, and Andreas G Nowatzyk. Fingerprinting: bounding soft-error detection latency and bandwidth. In *ACM SIGPLAN Notices*, volume 39, pages 224–234. ACM, 2004.

[306] Javier Carretero, Xavier Vera, Jaume Abella, Tanausu Ramirez, Matteo Monchiero, and Antonio Gonzalez. Hardware/software-based diagnosis of load-store queues using expandable activity logs. In *High Performance Computer Architecture (HPCA), 2011 IEEE 17th International Symposium on*, pages 321–331. IEEE, 2011.

[307] Vimal K Reddy, Eric Rotenberg, and Sailashri Parthasarathy. Understanding prediction-based partial redundant threading for low-overhead, high-coverage fault tolerance. In *ACM SIGARCH Computer Architecture News*, volume 34, pages 83–94. ACM, 2006.

[308] James E. Smith and Andrew R. Pleszkun. Implementing precise interrupts in pipelined processors. *Computers, IEEE Transactions on*, 37(5):562–573, 1988.

[309] ARM. *ARM11 Technical Reference Manual.* ARM, . http://infocenter.arm.com/help/topic/com.arm.doc.ddi0360e/DDI0360E_arm11_mpcore_r1p0_trm.pdf.

[310] Doug Burger and Todd M Austin. The simplescalar tool set, version 2.0. *ACM SIGARCH Computer Architecture News*, 25(3):13–25, 1997.

[311] Matthew R Guthaus, Jeffrey S Ringenberg, Dan Ernst, Todd M Austin, Trevor Mudge, and Richard B Brown. Mibench: A free, commercially representative embedded benchmark suite. In *Workload Characterization, 2001. WWC-4. 2001 IEEE International Workshop on*, pages 3–14. IEEE, 2001.

[312] S Dion Rodgers and Lawrence O Smith. Method and apparatus for processing events in a multithreaded processor, February 15 2005. US Patent 6,857,064.

[313] ARM. *ARM Cortex A5 Technical Reference Manual.* ARM, . http://infocenter.arm.com/help/topic/com.arm.doc.ddi0433b/DDI0433B_cortex_a5_r0p1_trm.pdf.

[314] Seongwoo Kim and Arun K Somani. Soft error sensitivity characterization for microprocessor dependability enhancement strategy. In *Dependable Systems and Networks, 2002. DSN 2002. Proceedings. International Conference on*, pages 416–425. IEEE, 2002.

[315] Giacinto Paolo Saggese, Anoop Vetteth, Zbigniew Kalbarczyk, and Ravishankar Iyer. Microprocessor sensitivity to failures: control vs. execution and combinational vs. sequential logic. In *Dependable Systems and Networks, 2005. DSN 2005. Proceedings. International Conference on*, pages 760–769. IEEE, 2005.

[316] Daya Shanker Khudia, Griffin Wright, and Scott Mahlke. Efficient soft error protection for commodity embedded microprocessors using profile information. In *ACM SIGPLAN Notices*, volume 47, pages 99–108. ACM, 2012.

[317] Tuo Li, Roshan Ragel, and Sri Parameswaran. Reli: Hardware/software checkpoint and recovery scheme for embedded processors. In *Design, Automation & Test in Europe Conference & Exhibition (DATE), 2012*, pages 875–880. IEEE, 2012.

[318] E.S. Fetzer, D. Dahle, C. Little, and K. Safford. The parity protected, multithreaded register files on the 90-nm Itanium microprocessors. *IEEE Journal of Solid-State Circuits*, 41(1), January 2006.

[319] Ruchir Puri, Tanay Karnik, and Rajiv Joshi. Technology impacts on sub-90nm cmos circuit design & design methodologies. In *VLSI Design, 2006. Held jointly with 5th International Conference on Embedded Systems and Design., 19th International Conference on*, pages 3–pp. IEEE, 2006.

[320] Kartik Mohanram and Nur A Touba. Cost-effective approach for reducing soft error failure rate in logic circuits. In *2013 IEEE International Test Conference (ITC)*, pages 893–893. IEEE Computer Society, 2003.

[321] Chuanjun Zhang, Frank Vahid, and Walid Najjar. A highly configurable cache architecture for embedded systems. In *Computer Architecture, 2003. Proceedings. 30th Annual International Symposium on*, pages 136–146. IEEE, 2003.

[322] Subhasish Mitra, Ming Zhang, Norbert Seifert, TM Mak, and Kee Sup Kim. Built-in soft error resilience for robust system design. In *Integrated Circuit Design and Technology, 2007. ICICDT'07. IEEE International Conference on*, pages 1–6. IEEE, 2007.

[323] Shidhartha Das, Carlos Tokunaga, Sanjay Pant, Wei-Hsiang Ma, Sudherssen Kalaiselvan, Kevin Lai, David M Bull, and David T Blaauw. Razorii: In situ error detection and correction for pvt and ser tolerance. *Solid-State Circuits, IEEE Journal of*, 44(1):32–48, 2009.

[324] Aamer Mahmood and Edward J McCluskey. Concurrent error detection using watchdog processors-a survey. *Computers, IEEE Transactions on*, 37 (2):160–174, 1988.

[325] Seongwoo Kim and Arun K Somani. On-line integrity monitoring of microprocessor control logic. *Microelectronics journal*, 32(12):999–1007, 2001.

[326] Vimal Reddy and Eric Rotenberg. Coverage of a microarchitecture-level fault check regimen in a superscalar processor. In *Dependable Systems and Networks With FTCS and DCC, 2008. DSN 2008. IEEE International Conference on*, pages 1–10. IEEE, 2008.

[327] X Delord and Gabriele Saucier. Formalizing signature analysis for control flow checking of pipelined risc microprocessors. In *Test Conference, 1991, Proceedings., International*, page 936. IEEE, 1991.

[328] Nirmal R Saxena and Edward J McCluskey. Control-flow checking using watchdog assists and extended-precision checksums. *Computers, IEEE Transactions on*, 39(4):554–559, 1990.

[329] Michael A. Schuette and John Paul Shen. Processor control flow monitoring using signatured instruction streams. *Computers, IEEE Transactions on*, 100(3):264–276, 1987.

[330] Nancy J Warter and W-MW Hwu. A software based approach to achieving optimal performance for signature control flow checking. In *Fault-Tolerant Computing, 1990. FTCS-20. Digest of Papers., 20th International Symposium*, pages 442–449. IEEE, 1990.

[331] Kent Wilken and John Paul Shen. Continuous signature monitoring: low-cost concurrent detection of processor control errors. *Computer-Aided Design of Integrated Circuits and Systems, IEEE Transactions on*, 9(6):629–641, 1990.

[332] Albert Meixner and Daniel J Sorin. Error detection using dynamic dataflow verification. In *Parallel Architecture and Compilation Techniques, 2007. PACT 2007. 16th International Conference on*, pages 104–118. IEEE, 2007.

[333] V.K. Reddy, A.S. Al-Zawawi, and E. Rotenberg. Assertion-based microarchitecture design for improved fault tolerance. In *Proceedings of International Conference on Computer Design (ICCD)*, pages 362–369, 2007.

[334] Nithin Nakka, Zbigniew Kalbarczyk, Ravishankar K Iyer, and Jun Xu. An architectural framework for providing reliability and security support. In *Dependable Systems and Networks, 2004 International Conference on*, pages 585–594. IEEE, 2004.

[335] Karthik Pattabiraman, Giacinto Paolo Saggese, Daniel Chen, Zbigniew Kalbarczyk, and Ravishankar K Iyer. Dynamic derivation of application-specific error detectors and their implementation in hardware. In *Dependable Computing Conference, 2006. EDCC'06. Sixth European*, pages 97–108. IEEE, 2006.

[336] Sam Gat-Shang Chu, Daniel R Knebel, and Stephen V Kosonocky. Register file cell with soft error detection and circuits and methods using the cell, July 14 2009. US Patent 7,562,273.

[337] Pablo Montesinos, Wei Liu, and Josep Torrellas. Using register lifetime predictions to protect register files against soft errors. In *Dependable Systems and Networks, 2007. DSN'07. 37th Annual IEEE/IFIP International Conference on*, pages 286–296. IEEE, 2007.

[338] Pablo Montesinos, Wei Liu, and Josep Torrellas. Shield: Cost-effective soft-error protection for register files. In *Third IBM TJ Watson Conference on Interaction between Architecture, Circuits and Compilers (PAC206)*, 2006.

[339] Sorin Iacobovici. Residue-based error detection for a shift operation, June 2 2009. US Patent 7,543,007.

[340] J-C Lo. Reliable floating-point arithmetic algorithms for error-coded operands. *Computers, IEEE Transactions on*, 43(4):400–412, 1994.

[341] C Webb. z6-the next-generation mainframe micropro cessor. In *Hot Chips*, pages 19–21, 2007.

[342] Michael Nicolaidis. Carry checking/parity prediction adders and alus. *Very Large Scale Integration (VLSI) Systems, IEEE Transactions on*, 11(1):121–128, 2003.

[343] Michael Nicolaidis. Efficient implementations of self-checking adders and alus. In *Fault-Tolerant Computing, 1993. FTCS-23. Digest of Papers., The Twenty-Third International Symposium on*, pages 586–595. IEEE, 1993.

[344] I Alzaher Noufal and Michael Nicolaidis. A cad framework for generating self-checking multipliers based on residue codes. In *Proceedings of the conference on Design, automation and test in Europe*, page 29. ACM, 1999.

[345] Michael Nicolaidis and Ricardo O Duarte. Fault-secure parity prediction booth multipliers. *IEEE design & test of computers*, 16(3):90–101, 1999.

[346] Michael Nicolaidis, Ricardo O Duarte, Salvador Manich, and Joan Figueras. Fault-secure parity prediction arithmetic operators. *IEEE Design & Test of computers*, 14(2):60–71, 1997.

[347] C. Weaver, J. Emer, S.S. Mukherjee, and S.K. Reinhardt. Techniques to reduce the soft error rate of a high-performance microprocessor. In *Proceedings of the 31st International Symposium on Computer Architecture (ISCA)*, Washington, DC, USA, 2004. IEEE Computer Society.

[348] Javier Carretero, Pedro Chaparro, Xavier Vera, Jaume Abella, and Antonio González. End-to-end register data-flow continuous self-test. In *ACM SIGARCH Computer Architecture News*, volume 37, pages 105–115. ACM, 2009.

[349] Smitha Shyam, Kypros Constantinides, Sujay Phadke, Valeria Bertacco, and Todd Austin. Ultra low-cost defect protection for microprocessor pipelines. In *ACM Sigplan Notices*, volume 41, pages 73–82. ACM, 2006.

[350] W.Bartlett A.Wood, R.Jardine. Data integrity in hp nonstop servers. In *In the Proceedings of the IEEE workshop on Silicon Errors in Logic and System Effects (SELSE)*, Los Alamitos, CA, USA, 2006.

[351] Jared C Smolens, Brian T Gold, Babak Falsafi, and James C Hoe. Reunion: Complexity-effective multicore redundancy. In *Proceedings of the 39th Annual IEEE/ACM International Symposium on Microarchitecture*, pages 223–234. IEEE Computer Society, 2006.

[352] Janak H. Patel and Leona Y. Fung. Concurrent error detection in alu's by recomputing with shifted operands. *Computers, IEEE Transactions on*, 100 (7):589–595, 1982.

[353] John Von Neumann. Probabilistic logics and the synthesis of reliable organisms from unreliable components. *Automata studies*, 34:43–98, 1956.

[354] Antonin Svoboda. From mechanical linkages to electronic computers: Recollections from czechoslovakia. *Metropolis, N., J. Howlett, and Gian-Carlo Rota, A History of Computing in the Twentieth Century, Academic Press, New York*, pages 579–586, 1980.

[355] YC Yeh. Triple-triple redundant 777 primary flight computer. In *Aerospace Applications Conference, 1996. Proceedings., 1996 IEEE*, volume 1, pages 293–307. IEEE, 1996.

[356] Brian T Gold, Jared C Smolens, Babak Falsafi, and James C Hoe. The granularity of soft-error containment in shared memory multiprocessors.

In *Proceedings of The Workshop on Silicon Errors in Logic-System Effects (SELSE)*, 2006.

[357] Michael J Mack, WM Sauer, Scott B Swaney, and Bruce G Mealey. Ibm power6 reliability. *IBM Journal of Research and Development*, 51(6):763–774, 2007.

[358] Joel S Emer, Shubhendu S Mukherjee, and Steven K Reinhardt. Incremental checkpointing in a multi-threaded architecture, July 10 2007. US Patent 7,243,262.

[359] Haitham Akkary, Ravi Rajwar, and Srikanth T Srinivasan. Checkpoint processing and recovery: Towards scalable large instruction window processors. In *Microarchitecture, 2003. MICRO-36. Proceedings. 36th Annual IEEE/ACM International Symposium on*, pages 423–434. IEEE, 2003.

[360] Chris Gniady and Babak Falsafi. Speculative sequential consistency with little custom storage. In *Parallel Architectures and Compilation Techniques, 2002. Proceedings. 2002 International Conference on*, pages 179–188. IEEE, 2002.

[361] Avinash C Palaniswamy and Philip A Wilsey. An analytical comparison of periodic checkpointing and incremental state saving. In *ACM SIGSIM Simulation Digest*, volume 23, pages 127–134. ACM, 1993.

[362] Yoshio Masubuchi, Satoshi Hoshina, Tomofumi Shimada, B Hirayama, and Nobuhiro Kato. Fault recovery mechanism for multiprocessor servers. In *Fault-Tolerant Computing, 1997. FTCS-27. Digest of Papers., Twenty-Seventh Annual International Symposium on*, pages 184–193. IEEE, 1997.

[363] Douglas C Bossen, Alongkorn Kitamorn, Kevin F Reick, and Michael S Floyd. Fault-tolerant design of the ibm pseries 690 system using power4 processor technology. *IBM Journal of Research and Development*, 46(1):77–86, 2002.

[364] Steven K Reinhardt and Shubhendu S Mukherjee. *Transient fault detection via simultaneous multithreading*, volume 28. ACM, 2000.

[365] G.A. Reis, J. Chang, N. Vachharajani, R. Rangan, D.I. August, and S.S. Mukherjee. Design and evaluation of hybrid fault-detection systems. In

Proceedings of the 32nd International Symposium on Computer Architecture (ISCA), 2005.

[366] D.P. Siewiorek and R.S. Swarz. *Reliable Computer Systems: Design and Evaluation.* A. K. Peters, Ltd., Natick, MA, USA, 1998. ISBN 1-56881-092-X.

[367] George A Reis, Jonathan Chang, and David I August. Automatic instruction-level software-only recovery. *IEEE micro*, 27(1):36–47, 2007.